SYSTEMIC COORDINATION OF INVERTEBRATE HOMEOSTASIS

EDITED BY: Fabio Gomes, Jose Luis Ramirez and Isabela Ramos
PUBLISHED IN: Frontiers in Physiology

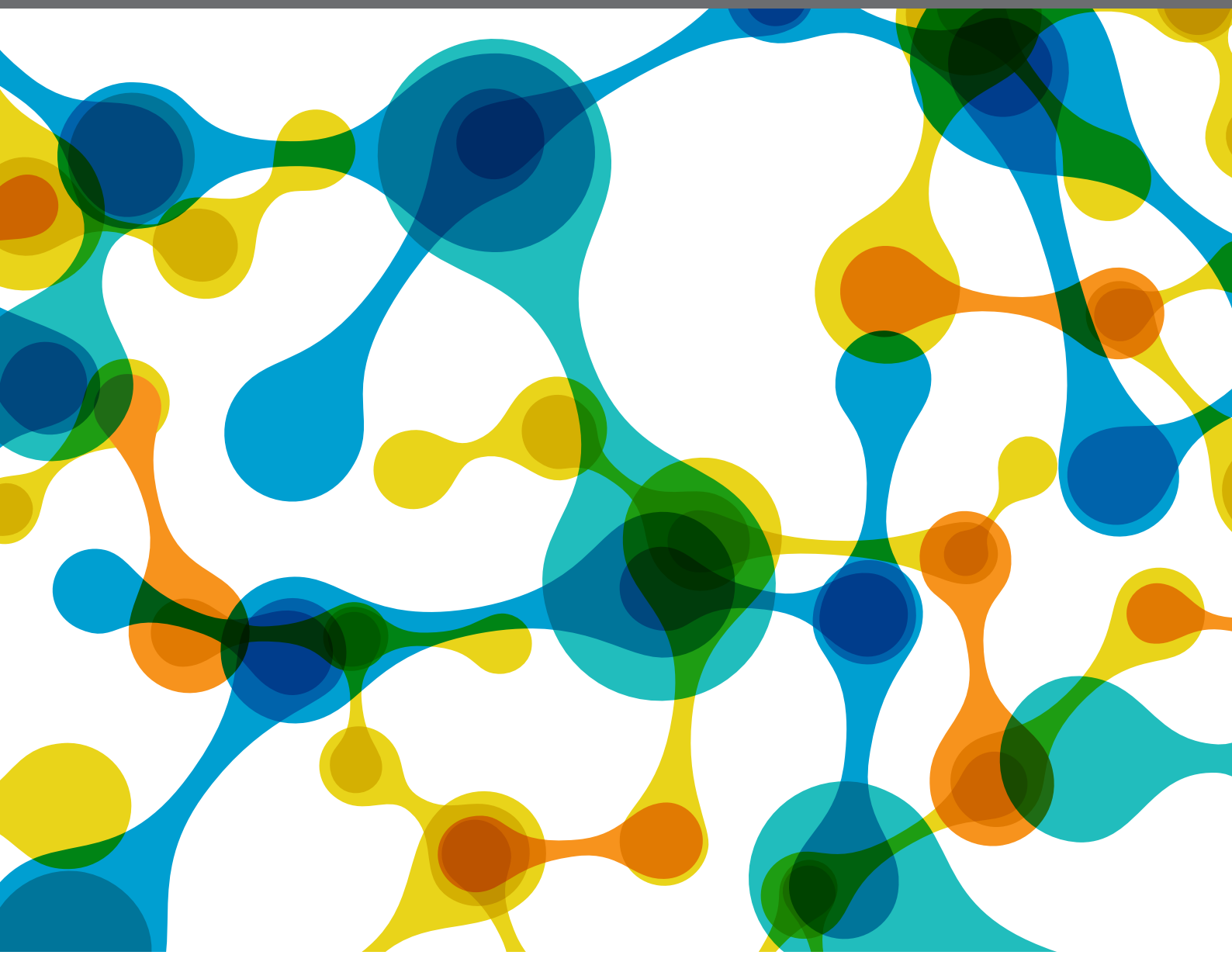

frontiers Research Topics

frontiers

ISSN 1664-8714
ISBN 978-2-88971-531-2
DOI 10.3389/978-2-88971-531-2

About Frontiers

Frontiers is more than just an open-access publisher of scholarly articles: it is a pioneering approach to the world of academia, radically improving the way scholarly research is managed. The grand vision of Frontiers is a world where all people have an equal opportunity to seek, share and generate knowledge. Frontiers provides immediate and permanent online open access to all its publications, but this alone is not enough to realize our grand goals.

Frontiers Journal Series

The Frontiers Journal Series is a multi-tier and interdisciplinary set of open-access, online journals, promising a paradigm shift from the current review, selection and dissemination processes in academic publishing. All Frontiers journals are driven by researchers for researchers; therefore, they constitute a service to the scholarly community. At the same time, the Frontiers Journal Series operates on a revolutionary invention, the tiered publishing system, initially addressing specific communities of scholars, and gradually climbing up to broader public understanding, thus serving the interests of the lay society, too.

Dedication to Quality

Each Frontiers article is a landmark of the highest quality, thanks to genuinely collaborative interactions between authors and review editors, who include some of the world's best academicians. Research must be certified by peers before entering a stream of knowledge that may eventually reach the public - and shape society; therefore, Frontiers only applies the most rigorous and unbiased reviews.
Frontiers revolutionizes research publishing by freely delivering the most outstanding research, evaluated with no bias from both the academic and social point of view. By applying the most advanced information technologies, Frontiers is catapulting scholarly publishing into a new generation.

What are Frontiers Research Topics?

Frontiers Research Topics are very popular trademarks of the Frontiers Journals Series: they are collections of at least ten articles, all centered on a particular subject. With their unique mix of varied contributions from Original Research to Review Articles, Frontiers Research Topics unify the most influential researchers, the latest key findings and historical advances in a hot research area! Find out more on how to host your own Frontiers Research Topic or contribute to one as an author by contacting the Frontiers Editorial Office: frontiersin.org/about/contact

SYSTEMIC COORDINATION OF INVERTEBRATE HOMEOSTASIS

Topic Editors:
Fabio Gomes, Federal University of Rio de Janeiro, Brazil
Jose Luis Ramirez, United States Department of Agriculture (USDA), United States
Isabela Ramos, Federal University of Rio de Janeiro, Brazil

Citation: Gomes, F., Ramirez, J. L., Ramos, I., eds. (2021). Systemic Coordination of Invertebrate Homeostasis. Lausanne: Frontiers Media SA.
doi: 10.3389/978-2-88971-531-2

Table of Contents

frontiers in Physiology

EDITORIAL
published: 07 September 2021
doi: 10.3389/fphys.2021.736185

Editorial: Systemic Coordination of Invertebrate Homeostasis

José Luis Ramirez[1], *Isabela Ramos*[2] *and Fabio M. Gomes*[3]*

[1] Crop Bioprotection Research Unit, United States Department of Agriculture, National Center for Agricultural Utilization Research, Agricultural Research Service, Peoria, IL, United States, [2] Instituto de Bioquímica Médica Leopoldo de Meis, Universidade Federal do Rio de Janeiro, Rio de Janeiro, Brazil, [3] Instituto de Biofísica Carlos Chagas Filho, Universidade Federal do Rio de Janeiro, Rio de Janeiro, Brazil

Keywords: homeostasis, microbiome, immunity, hormonal regulation, lipid transport, oogenesis, blood digestion

Editorial on the Research Topic

Systemic Coordination of Invertebrate Homeostasis

Multicellularity has allowed highly specialized cells to organize in tissues and organs in order to develop specific functions. While this resulted in an unsurpassable level of efficiency, it became necessary for organs and cells to coordinate their metabolism. In this Research Topic, several new contributing articles provide much-needed new information in this area of research. Overall, these articles highlight how invertebrate organisms have found solutions that allowed them to integrate their physiology to achieve a highly complex systemic coordination of homeostasis.

OPEN ACCESS

Edited by:
Graziano Fiorito, Zoological Station Anton Dohrn, Italy

Reviewed by:
Eleonora Maria Pieroni, Associazione Cefalopodo Ricerca (CephRes), Italy

***Correspondence:**
Fabio M. Gomes
fabiomg@biof.ufrj.br

Specialty section:
This article was submitted to Invertebrate Physiology, a section of the journal Frontiers in Physiology

Received: *04 July 2021*
Accepted: *12 August 2021*
Published: *07 September 2021*

Citation:
Ramirez JL, Ramos I and Gomes FM (2021) Editorial: Systemic Coordination of Invertebrate Homeostasis. Front. Physiol. 12:736185. doi: 10.3389/fphys.2021.736185

THE COORDINATION OF NUTRIENT UPTAKE AND EGG FORMATION

While several metabolites can be synthesized *de novo* by anabolic reactions, some others can only be obtained through feeding or as by-products from their microbiota's metabolism. To sustain their development, invertebrates must not only obtain a proper level of nutrients; but also have to metabolize and coordinate their storage and distribution to remaining organs (Karasov and Douglas, 2013). In this Research Topic, Entringer et al. studied the fate of cholesterol in the kissing bug *Rhodnius prolixus*. Unlike mammals, insects are not able to convert acetate into cholesterol. The authors investigated the coordination between cholesterol intake and storage by different organs (Entringer et al.). Their results showed that multiple gut epithelia segments can absorb cholesterol, which transiently accumulates in the fat body, with very small levels of cholesterol being found available in the hemolymph. They have also observed that nutrients are later used for the maturation of ovaries and the build-up of vitellogenic oocytes, where cholesterol progressively accumulates.

The coordination of such events must rely on signaling molecules that coordinate interorgan and cell-cell communication. For example, insulin-like peptides (ILPs—analogous to vertebrate insulin) and their counterpart adipokinetic hormone (AKH—analogous to vertebrate glucagon) have a major role in regulating nutrient homeostasis by coordinating nutrient-sensing pathways, such as the PI3K-AKT-TOR pathways (Nässel and Vanden Broeck, 2016). Also working with *R. prolixus*, Leyria et al. showed that trehalose stores follow a pattern of accumulation during vitellogenesis due to the transcription of the trehalose-specific facilitated transporter gene (Rhopr-TRET) in the ovaries. The authors also showed that ILPs and the adipokinetic hormone (AKH) mediate Rhopr-TRET expression, providing a link between blood-feeding, insulin signaling, and trehalose accumulation and mobilization during vitellogenesis.

Choriogenesis is the last stage of oocyte maturation before fertilization. At this stage, the follicle cells assemble the chorion layers, which will allow gas exchange and provide protection, while impairing desiccation for the developing embryo. Follicle cells can coordinate the assembly of a set of proteins generating an intricate network of macromolecules on the chorion. However, the exact mechanisms by which this is accomplished are only partially understood. Santos and Ramos studied *R. prolixus* choriogenesis and provided evidence that ATG3 (autophagy-related gene 3) is highly expressed in the ovaries during vitellogenesis. They further showed that parental deficiency in ATG3 impairs autophagosome formation and proper chorion biogenesis by the follicle cells, resulting in altered chorion ultrastructure and protein composition. Further studies will allow a finer understanding of the triggering signals and the signaling pathways that regulate ATG3 function during choriogenesis.

INTERORGAN COMMUNICATION OF TISSUE HOMEOSTASIS

Coordination of physiology and behavior is highly dependent on interorgan communication, which is provided for the most part by hormonal regulation. In insects, the molting hormone 20-hydroxyecdysone (20E) is an ecdysteroid derived from cholesterol metabolism. During larval development, 20E is synthesized in the prothoracic gland and coordinates insect molt by interacting with the ecdysteroid receptor, a heterodimer composed by ecdysone receptor (EcR) and ultraspiracle (USP) (Yao et al., 1993). Shi et al. used video recording to identify the phases of cocoon-spinning in the diamondback moth *Plutella xylostella*. The authors identified three successive phases (selection of a pupation site, spinning a loose cocoon, and padding the scaffold cocoon). Furthermore, they demonstrated that 20E plays an important role in cocoon-spinning behavior via the modulation of silk gland fibroin genes.

Apart from lipid hormones, several other components participate in systemic coordination of invertebrate physiology. Wound healing is a key aspect of tissue homeostasis. During this process, cells must be driven to the site of injury in order to rapidly repair the injured tissue and prevent pathogen invasion. In the leech *Hirudo verbana,* the T2 ribonuclease HvRNASET2 (rHvRNASET2) stimulates the production of collagen and is involved in the extracellular matrix remodeling, by acting as chemoattractants for macrophages (Baranzini et al., 2019). Through a series of morphological studies coupled with molecular bioassays, Baranzini et al. demonstrated the remarkable complexity of tissue homeostasis maintenance during the wound healing process. Leeches injected with rHvRNASET2 induced macrophage recruitment, collagen synthesis, and participated in muscle tissue regeneration. The authors also described the homeostatic role of rHvRNASET2 in vasculogenesis and angiogenesis during the recruitment of myoendothelial vessel-associated precursor cells.

THE COORDINATION OF HEMATOPHAGY AND VECTOR COMPETENCE

In hematophagous insects, blood is a key source of nutrients for egg production. Gandara et al. studied the role of NADPH oxidases and xanthine dehydrogenases (XDH) in *R. prolixus* digestive physiology. They show that superoxide produced by NADPH oxidase 5 (NOX5) and urate produced by XDH coordinate midgut peristalsis and are key to blood digestion. Blood ingestion is correlated with an increase in midgut microbial load, which facilitates blood digestion and regulates host immunological status (Oliveira et al., 2011). As many species developed a preference for human blood, hematophagy also allowed several invertebrate species to act as vectors of human diseases. Talyuli et al. presented a thorough review of how blood-feeding triggers several aspects of vector competence that are not canonical components of the invertebrate immune system.

Indeed, it has now become clear that tissue homeostasis and vector immunity coordinate invertebrate responses to infections. Redox homeostasis during blood digestion is a key component of this coordination (Talyuli et al.). During *Plasmodium* invasion of the midgut of *Anopheles gambiae*, the activation of nitric oxide synthase (NOS) drives the accumulation of nitric oxide (NO). As a result, reactive oxygen species (ROS) detoxifying enzymes, such as heme-peroxidases are produced under the control of c-Jun N-terminal kinases (JNK) signaling and ultimately nitrify the parasite, targeting it for killing by mosquito humoral factors (Oliveira et al., 2012). In this Research Topic, Kakani et al. provided evidence of an additional role for heme-peroxidase 2 in the Asian malaria vector *Anopheles stephensi* in regulating the gut microbiota. They propose that enterocyte-produced heme-peroxidase 2 (AsHPX2) regulates the levels of ROS at the gut lumen and that a reduction of AsHPX2 following blood-feeding creates proper physicochemical conditions for the expansion of the gut microbiota, which is essential for blood digestion.

THE INTERPLAY BETWEEN HOST AND HOST MICROBIOTA REGULATING VECTOR COMPETENCE

Manipulation of microbiota is a promising strategy to manipulate vector competence and diminish transmission of vector-borne pathogens. For example, the release of *Wolbachia*-infected mosquitoes has become one of the most promising strategies for arbovirus control. Upon *Wolbachia* infection, natural populations of *Aedes aegypti* become refractory to dengue (DENV) and Zika (ZIVK) viruses. More recently, field studies using this approach have shown a strong effect in the reduction of dengue fever cases (Utarini et al., 2021). However, the molecular mechanisms underlying *Wolbachia*-Aedes-arbovirus regulation of vector competence remain uncertain. Martins et al. performed quantitative mass spectrometry-based proteomics in sections of heads and salivary glands of ZIKV and *Wolbachia*-infected *Ae. aegypti*. Their study provides a panel of proteins and pathways belonging to diverse biological processes and physiological pathways that are under modulation by Zika

and *Wolbachia* including the *Wolbachia*-induced effects on ROS production and the modulation of immune pathways. Such datasets can provide invaluable data for the refinement of the interaction models between *Wolbachia* and *Aedes* in future studies.

AUTHOR CONTRIBUTIONS

JR and IR contributed to the idealization, development of the Research Topics and editorial, and reviewed this manuscript. FG contributed to the idealization, development of the Research Topics and editorial, and prepared the draft and final version of this manuscript. All authors contributed to the article and approved the submitted version.

FUNDING

This work was supported by the Serrapilheira Institute (Grant number R-1912-32058).

REFERENCES

Baranzini, N., Monti, L., Vanotti, M., Orlandi, V. T., Bolognese, F., Scaldaferri, D., et al. (2019). AIF-1 and RNASET2 Play complementary roles in the innate immune response of medicinal leech. *J. Innate Immun.* 11, 150–167. doi: 10.1159/000493804

Karasov, W. H., and Douglas, A. E. (2013). Comparative digestive physiology. *Compr. Physiol.* 3, 741–783. doi: 10.1002/cphy.c110054

Nässel, D. R., and Vanden Broeck, J. (2016). Insulin/IGF signaling in Drosophila and other insects: factors that regulate production, release and post-release action of the insulin-like peptides. *Cell. Mol. Life Sci.* 73, 271–290. doi: 10.1007/s00018-015-2063-3

Oliveira, G., de, A., Lieberman, J., and Barillas-Mury, C. (2012). Epithelial nitration by a peroxidase/NOX5 system mediates mosquito antiplasmodial immunity. *Science* 335, 856–859. doi: 10.1126/science.1209678

Oliveira, J. H. M., Gonçalves, R. L. S., Lara, F. A., Dias, F. A., Gandara, A. C. P., Menna-Barreto, R. F. S., et al. (2011). Blood meal-derived heme decreases ROS levels in the midgut of Aedes aegypti and allows proliferation of intestinal microbiota. *PLoS Pathog.* 7:e1001320. doi: 10.1371/journal.ppat.1001320

Utarini, A., Indriani, C., Ahmad, R. A., Tantowijoyo, W., Arguni, E., Ansari, M. R., et al. (2021). Efficacy of wolbachia-infected mosquito deployments for the control of dengue. *N. Engl. J. Med.* 384, 2177–2186. doi: 10.1056/NEJMoa2030243

Yao, T. P., Forman, B. M., Jiang, Z., Cherbas, L., Chen, J. D., McKeown, M., et al. (1993). Functional ecdysone receptor is the product of EcR and Ultraspiracle genes. *Nature* 366, 476–479. doi: 10.1038/366476a0

Conflict of Interest: The authors declare that the research was conducted in the absence of any commercial or financial relationships that could be construed as a potential conflict of interest.

Publisher's Note: All claims expressed in this article are solely those of the authors and do not necessarily represent those of their affiliated organizations, or those of the publisher, the editors and the reviewers. Any product that may be evaluated in this article, or claim that may be made by its manufacturer, is not guaranteed or endorsed by the publisher.

frontiers in Physiology

ORIGINAL RESEARCH
published: 08 September 2020
doi: 10.3389/fphys.2020.572340

Heme-Peroxidase 2, a Peroxinectin-Like Gene, Regulates Bacterial Homeostasis in *Anopheles stephensi* Midgut

Parik Kakani[1,2], *Lalita Gupta*[1,3] *and Sanjeev Kumar*[1,4]*

[1] Molecular Parasitology and Vector Biology Laboratory, Department of Biological Sciences, Birla Institute of Technology and Science (BITS), Pilani, India, [2] Department of Biological Sciences, Indian Institute of Science Education and Research (IISER), Bhopal, India, [3] Department of Zoology, Chaudhary Bansi Lal University, Bhiwani, India, [4] Department of Biotechnology, Chaudhary Bansi Lal University, Bhiwani, India

The dynamic nature of mosquito gut microbiome is associated with different stages of development and feeding behaviors. Therefore, mosquito gut harbors a wide range of endogenous microbes that promote numerous life processes such as, nutrition, reproduction and immunity. In addition, gut microbiota also play an important role in the regulation of *Plasmodium* (malaria parasite) development. Thus, understanding the mechanism of microbial homeostasis in mosquito gut might be one of the strategies to manipulate malaria parasite development. In the present study, we characterized a 692 amino acids long secreted midgut heme-peroxidase 2 (AsHPX2) in *Anopheles stephensi*, the major Indian malaria vector. The presence of putative integrin binding motifs, LDV (Leu–Asp–Val), indicated its peroxinectin-like nature. Our phylogenetic analysis revealed that AsHPX2 is a Culicinae lineage-specific gene. RNA interference (RNAi)-mediated silencing of AsHPX2 gene significantly enhanced the growth of midgut bacteria in sugar-fed mosquitoes against sham-treated controls. Interestingly, blood-feeding drastically reduced AsHPX2 gene expression and enhanced the growth of midgut bacteria. These results revealed a negative correlation between the expression of AsHPX2 gene and gut bacterial growth. We proposed that AsHPX2, being a mosquito-specific gene, might serve as a "potent target" to manipulate midgut microbiota and vector competence.

Keywords: ***Anopheles stephensi*, midgut, bacteria, heme-peroxidase, homeostasis, vector competence**

OPEN ACCESS

Edited by:
Isabela Ramos, Federal University of Rio de Janeiro, Brazil

Reviewed by:
Ana Cristina Bahia, Federal University of Rio de Janeiro, Brazil
Daniele Pereira Castro, Oswaldo Cruz Foundation (Fiocruz), Brazil

***Correspondence:**
Sanjeev Kumar
sanjeevnih@gmail.com

Specialty section:
This article was submitted to Invertebrate Physiology, a section of the journal Frontiers in Physiology

Received: *13 June 2020*
Accepted: *17 August 2020*
Published: *08 September 2020*

Citation:
Kakani P, Gupta L and Kumar S (2020) Heme-Peroxidase 2, a Peroxinectin-Like Gene, Regulates Bacterial Homeostasis in Anopheles stephensi Midgut. Front. Physiol. 11:572340. doi: 10.3389/fphys.2020.572340

INTRODUCTION

Newly emerged mosquitoes are born with a limited energy reserve and therefore, they start feeding the nectar to replenish energy in order to power the flight for swarming, mating and blood-seeking activities. The initial feeding behavior contributes to the establishment of the microbial community in the mosquito midgut. The midgut microbes facilitate food digestion, metabolism, detoxification and the development of immunity (Gusmão et al., 2007; Minard et al., 2013; Kajla et al., 2015).

Interestingly, the dynamic nature of gut microbiota is also associated with different stages of mosquito development as well as their nutritional conditions. For example, in sugar-fed mosquito

midguts cellulose degrading bacteria predominate, however, the bacteria facilitating blood digestion are more common in blood-fed midguts (de Gaio et al., 2011; Wang et al., 2011; Minard et al., 2013). In addition, the microbial interaction with mosquito midgut immunity also plays a pivotal role in the biological outcome of this symbiotic association. Thus, microbial homeostasis is managed by numerous immune mechanisms such as the production of lysozyme, reactive oxygen species (ROS), reactive nitrogen species (RNS), and antimicrobial peptides (AMPs) (Luckhart et al., 1998; Graca-Souza et al., 2006; Peterson and Luckhart, 2006; Brennan et al., 2008; Nishikori et al., 2009; Login et al., 2011; Wang et al., 2011).

It is also noteworthy to mention that the midgut microbiota also regulates *Plasmodium* development (Dong et al., 2009; Cirimotich et al., 2011). It was evident from numerous studies where co-feedings of either live or heat-killed bacteria decreased parasites number (Dong et al., 2009). Moreover, the parasite load also increased in antibiotics fed mosquitoes. Interestingly, the bacteria-induced ROS in mosquito midgut suppressed *Plasmodium* development (Beier et al., 1994; Dong et al., 2009; Cirimotich et al., 2011). Thus, we believe that the manipulation of midgut bacteria or mechanisms regulating bacterial homeostasis might be promising to alter the vectorial capacity (the property to support parasite development) of mosquito.

Heme-peroxidases regulate antibacterial pathways in mammals and insects. They catalyze H_2O_2-dependent oxidation of halides that, in turn, inhibit microbial metabolism and growth (Ha et al., 2005a; Klebanoff, 2005; Kumar et al., 2010; Kajla et al., 2016a). In addition, heme-peroxidases also catalyze the crosslinking of mucins layer over the midgut epithelium to block the interaction of lumen bacteria with mosquito immunity. This cross-linked barrier-based mechanism creates a low immunity zone in midgut to support the growth of microbial community (Kumar et al., 2010; Kajla et al., 2016a). Thus, mosquito peroxidases play a dramatic role in bacteria homeostasis and immunity.

Our analyses of *Anopheles stephensi* genome revealed the presence of 18 heme-peroxidases that participate in important biological functions (Kajla et al., 2016b; Choudhury et al., 2019; Kakani et al., 2019). In this study, we characterized *An. stephensi* midgut heme-peroxidase 2 (AsHPX2) and explored its role in the regulation of bacterial homeostasis. Our findings will open new opportunities to exploit the peroxidase-mediated immunemodulatory mechanism in mosquito for manipulating malaria parasite development.

MATERIALS AND METHODS

Ethics Statement

The use of experimental animals in this study was approved by the BITS, Pilani Institutional Animal Ethical Committee (Approval number IAEC/RES/18/02). Animal maintenance and experiments were performed in accordance with guidelines of the Committee for the Purpose of Control and Supervision of Experiments on Animals (CPCSEA), Government of India.

Rearing of Mosquitoes

Anopheles stephensi mosquitoes were reared in an insectary at Birla Institute of Technology and Science, Pilani, Rajasthan. The insectary was maintained at 28°C, 80% relative humidity (RH) and 12 h light:dark cycle as described before (Dhawan et al., 2017; Kajla et al., 2017). Adult mosquitoes were regularly fed on 10% sucrose solution. For colony propagation, 4- to 5-day-old females were fed on anesthetized mice and their eggs were collected in moist conditions. The hatched larvae were floated in water to continue the life cycle and fed on a 1:1 mixture of dog food (Pet Lover's crunch milk biscuit, India) and fish food (Gold Tokyo, India) (Gupta et al., 2017; Choudhury et al., 2019; Kakani et al., 2019).

Retrieval of Heme Peroxidase AsHPX2 Gene From *An. stephensi* Genome

Anopheles gambiae AgHPX2 gene (AGAP009033) was blast searched against the partially annotated genome of *An. stephensi* (taxid: 30069) to retrieve its ortholog. The best matching *An. stephensi* contig 7145 (SuperContig KB664566 and Ensembl identifier ASTE003848) was analyzed using Augustus software to identify the full-length putative AsHPX2 gene as before (Stanke et al., 2008; Choudhury et al., 2019; Kakani et al., 2019). AsHPX2 and AgHPX2 gene sequences were aligned to design gene-specific primers. The list of these primers is provided in **Supplementary Table S1**.

Cloning, Sequencing and Phylogenetic Analysis of AsHPX2

Full-length AsHPX2 gene was PCR amplified from *An. stephensi* midgut cDNA template using Phusion High-Fidelity DNA Polymerase (Thermo scientific, #F-530S) and F4R5 primers. PCR was initiated at 98°C for 30 s followed by 35 cycles at 98°C for 10 s, 62°C for 30 s and 72°C for 2 min. The final extension was carried at 72°C for 10 min. The amplified product was purified and sequenced at Eurofins genomics. The sequence identity of full-length AsHPX2 cDNA was confirmed through general BLAST and submitted to NCBI Genbank (accession numbers: KY363390).

The 5′ upstream region of AsHPX2 gene was analyzed by Augustus and JASPAR/MatInspector software to mark the putative promoter and regulatory sequences, respectively as before (Cartharius et al., 2005; Stanke et al., 2008; Mathelier et al., 2014; Kajla et al., 2016b; Kakani et al., 2019). The search criteria for these analyses were restricted to the transcription factors from insect family with minimum 80% similarity.

To analyze the evolutionary relationship of AsHPX2 protein, phylogenetic tree was constructed using the neighbor-joining (NJ) method implemented in MEGA 5.2 program as before (Saitou and Nei, 1987). The sequences of different animal heme peroxidases, implemented to construct the tree, were downloaded from NCBI and listed in **Supplementary Table S2**. The branching pattern reliability of the phylogenetic tree was tested by 1,000 bootstrap replicates.

In Silico Analysis of AsHPX2 Protein

Conserved domains in AsHPX2 protein were identified with the help of Conserved Domain Database (CDD) as well as SMART database (Letunic et al., 2014; Marchler-Bauer et al., 2015). The putative signal peptide in AsHPX2 protein was analyzed using SignalP and Phobius software (Käll et al., 2007; Petersen et al., 2011). The putative active sites and 3D structure of AsHPX2 protein was analyzed using Phyre^2 and TASSER software (Kelley et al., 2015; Yang et al., 2015). The quality of the predicted AsHPX2 model was assessed by TM-score (Zhang, 2008).

Collection of Different Mosquito Development Stages and Tissues

Different developmental stages of *An. stephensi* such as, eggs, first to fourth instar larvae, pupae, adult males or females were pooled and collected separately in RNAlater (Qiagen) and stored at −80°C. The midguts or carcasses (rest of the body parts after removing midguts) from sugar- or blood-fed females were also collected in a similar way. In some experiments, mosquitoes, as well as dissected midguts, were surface sterilized by rinsing them thrice, each for 5 s, in absolute ethanol and stored in RNAlater at −80°C (Gupta et al., 2009; Kumar et al., 2010; Wang et al., 2011).

RNA Isolation, cDNA Preparation and Analysis of Gene Expression

Total RNA was isolated from mosquito tissues by RNAeasy mini kit (Qiagen) and the first-strand cDNA was synthesized using Quantitect reverse transcription kit (Qiagen) that included a genomic wipeout treatment step to remove genomic DNA contamination. Since, the central gene of interest in this study is intronless, therefore, to insure no gDNA contamination in RNA preparations we included a negative RT control (i.e., a cDNA preparation using DNase-treated RNA and all reaction components except the RT enzyme) in the qPCR analyses. The IQ5 multicolor real-time PCR detection system (Bio-Rad) was used to analyze the relative mRNA expressions of AsHPX2 gene and the bacterial load was determined by the amplification of 16S rRNA gene. The sequences of all the mosquito gene primers and universal 16S primers are listed in **Supplementary Table S1**. The ribosomal protein subunit S7 mRNA was used as an internal loading control as before (Kumar et al., 2010; Dixit et al., 2011; Kakani et al., 2019). PCR cycle parameters were following: 95°C for 5 min, 40 cycles each at 94°C for 20 s, 55°C for 30 s, and 72°C for 50 s. Fluorescence was read at 72°C after each cycle. The final extension was carried at 72°C for 10 min and then subjected to a melting curve to confirm the identity of PCR product. The end product was run on a gel to confirm the specificity of primers. Relative mRNA levels of various genes were calculated using $^{\Delta\Delta}$Ct method as before (Livak and Schmittgen, 2001; Kumar et al., 2010; Kakani et al., 2019). The PCR amplification efficiency was determined with LinRegPCR as described elsewhere (Ramakers et al., 2003).

dsRNA Synthesis and Gene Silencing

A 450-bp fragment of AsHPX2 cDNA was amplified using F1R1 primers (**Supplementary Table S1**) and cloned into the pCRII-TOPO vector. Similarly, a 218-bp fragment of LacZ gene was amplified and cloned using the primers (5′ to 3′) F-GAGTCAGTGAGCGAGGAAGC and R-TATCCGCTCACAATTCCACA (Gupta et al., 2009; Kajla et al., 2017). These clones already have a T7 promoter site at one end thus, another T7 promoter was incorporated at the other end of the fragment by amplifying the insert with the primers: M13F-GTAAAACGACGGCCAGT and T7-M13R-CTCGAGTAATACGACTCACTATAGGGCAGGAAACAGCTATGAC. PCR cycle parameters were following: 94°C for 5 min followed by 40 cycles each with 94°C for 30 s, 55°C for 30 s, and 72°C for 30 s. The final extension was carried at 72°C for 10 min. Amplicons were extracted from the gel with QIAquick Gel Extraction Kit (Qiagen) and used to synthesize dsRNA as per the instructions of MEGAscript RNAi kit (Ambion). dsRNA was purified with the help of Microcon YM-100 filter (Millipore) and finally concentrated to 3 μg/μl in DNase- and RNase-free water (Dhawan et al., 2017; Kajla et al., 2017; Kakani et al., 2019).

For gene silencing, 2-day-old female mosquitoes were injected with 69 nl of 3 μg/μl dsAsHPX2 (silenced) or dsLacZ (control) RNA into their thorax using a nanojector (Drummond). Four days after the injection, mosquitos were surface sterilized and their midguts were dissected as before (Gupta et al., 2009; Kumar et al., 2010; Wang et al., 2011).

Statistical Analysis of the Data

All the data were expressed as a mean ± standard deviation. GraphPad Prism 5.0 software was used to analyze statistical significance between test and respective controls by performing Student's *t*-test or one-way ANOVA (Motulsky, 1999). The data were considered significant if $p < 0.05$. Each experiment was performed at least thrice to validate the findings.

RESULTS

Cloning and Characterization of AsHPX2 Gene

Putative AsHPX2 gene was identified in contig 7,145 of un-annotated *An. stephensi* genome as described in the Materials and Methods. Analysis of this contig by Augustus software predicted 2,868 bp full-length AsHPX2 gene containing 2,079 bp open reading frame (ORF), which encodes for a 692 amino acids long protein. The 5′-untranslated region (5′-UTR) and 3′-UTR of AsHPX2 gene were found to be 438 and 351 bp, respectively. The polyadenylation signal AATAAA was identified 331 bp downstream from the stop codon (**Supplementary Figure S1**).

Furthermore, the 5′ upstream region of AsHPX2 gene was analyzed by JASPAR and MatInspector software to identify putative transcription factor binding motifs (TFBM) in its promoter region. Our analyses indicated the binding sites for some major transcription factors such as, GATA (pnr), Rel1, AP-1 (a Jun/Fos dimer) and Broad complex (Br-C) (**Supplementary Figure S1**) that indicated a tissue-specific immune role of AsHPX2 in a way similar to other insect genes (Senger et al., 2006; Zhu et al., 2007; Garver et al., 2013; Kajla et al., 2016b; Zakovic and Levashina, 2017; Kakani et al., 2019).

The predicted AsHPX2 cDNA sequence was aligned with *An. gambiae* AgHPX2 (AGAP009033) gene to design gene-specific primers (**Supplementary Table S1**) and F4R5 primers set amplified ∼2 kb full-length gene from *An. stephensi* cDNA (**Figure 1**). The PCR product was sequenced and blast search revealed its 80% identity with AgHPX2 gene (*e* value $3e^{-107}$). This sequence was submitted to NCBI (GenBank accession number: KY363390) and its alignment with the predicted *An. stephensi* genomic DNA revealed that AsHPX2 is an intron-less gene (**Figure 1**) in a way similar to its ortholog AgHPX2 (Giraldo-Calderón et al., 2015).

Sequence and Domain Analysis of AsHPX2 Protein

Analyses of 76.9 kDa AsHPX2 protein by SMART program revealed that it is an animal heme-peroxidase (**Figure 2**). The presence of a 21 amino acids long signal peptide and signal peptidase cleavage site between Gly_{21} and Arg_{22} residues at *N*-terminal suggested that AsHPX2 is a secreted protein (**Figure 2B**). Phyre[2] software analyses revealed the presence of 47% alpha helices in the secondary structure of AsHPX2 protein (**Supplementary Figure S2**) indicating that it is a globular protein as suggested by others (Pace and Scholtz, 1998; Kajla et al., 2016b). In addition, this protein also contains 10 heme-binding sites, 13 substrate-binding sites, three calcium-binding sites, and three homodimer interface sites (**Supplementary Figure S2**) in a way similar to other insect heme-peroxidases (Soudi et al., 2012; Kajla et al., 2016b; Bailey et al., 2017; Choudhury et al., 2019; Kakani et al., 2019). Three-dimensional structure of AsHPX2 protein (TM-score 0.70 ± 0.12) revealed the presence of catalytic quartet (Thr_{212}, Ala_{430}, Gly_{602}, and Arg_{669}), which is positioned toward the protein surface. Interestingly, the presence of a surface oriented triplet of Leu_{530}, Asp_{531}, and Val_{532} (LDV), which constitutes an integrin binding motif, indicated that AsHPX2 is a peroxinectin-like protein (**Figures 2B,C**) and might participate in cell adhesion as suggested by others (Johansson et al., 1995; Ruoslahti, 1996; Johanssen et al., 1999).

Sequence Homology and Phylogenetic Analysis of AsHPX2 Protein

The sequence of AsHPX2 protein was aligned with heme-peroxidases from other organisms as listed in **Supplementary Table S2** to analyze their sequence conservation. AsHPX2 shared 79 and 73% identity with *An. gambiae* AgHPX2 and *An. sinensis* AsnHPX2, respectively (**Supplementary Table S2**). On the other hand, it shared 57, 59, and 58% identity with *Aedes aegypti* AeHPX2, *Ae. albopictus* AaHPX2, and *Culex quinquefasciatus* CqHPX2, respectively. Interestingly, AsHPX2 protein shared only 34% identity with *Drosophila melanogaster* immune-related catalase (IRC), a heme-peroxidase that performs catalase cycle (Ha et al., 2005a,b). In addition, it shared less than 30% identity with human peroxidases (**Supplementary Table S2**). Evolutionary relationship of AsHPX2 protein with heme-peroxidases from other organisms

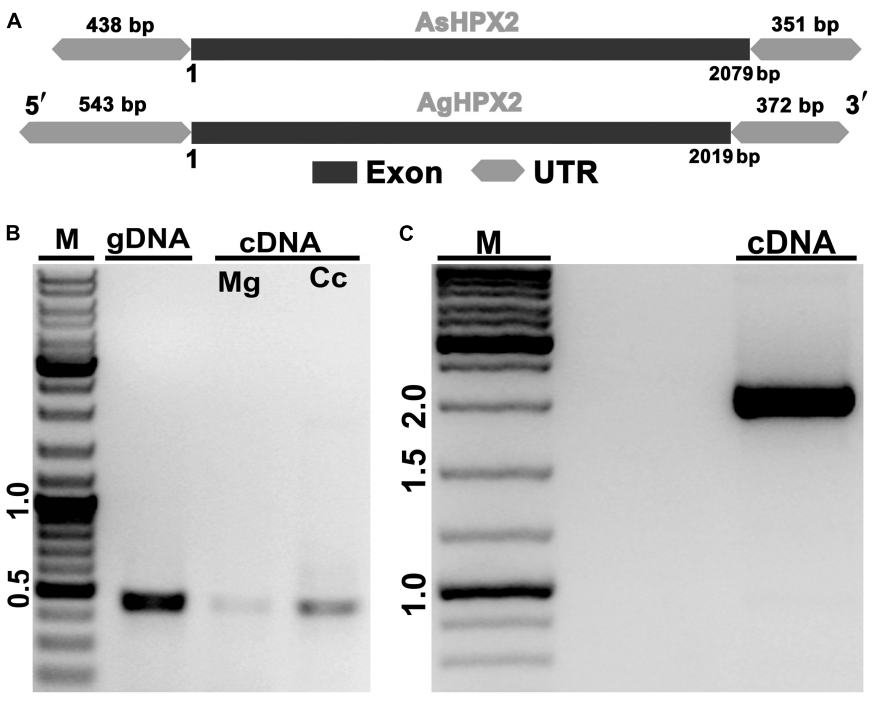

FIGURE 1 | Molecular identification of AsHPX2 gene. **(A)** Genomic organization of AsHPX2 gene: both AgHPX2 (2,019 bp) and AsHPX2 (2,079 bp) genes have single exon. The 5′ and 3′ UTRs of AsHPX2 gene are 438 and 351 bp, respectively. However, 5′ and 3′ UTRs of AgHPX2 gene are 543 and 372 bp, respectively. **(B)** PCR amplification of 450 bp partial segment of AsHPX2 gene using F1R1 primers from genomic DNA (gDNA), midgut (Mg) or carcass (Cc) cDNA template. **(C)** PCR amplification of full-length AsHPX2 gene from cDNA template using F4R5 primers. M represents the DNA ladder in kb.

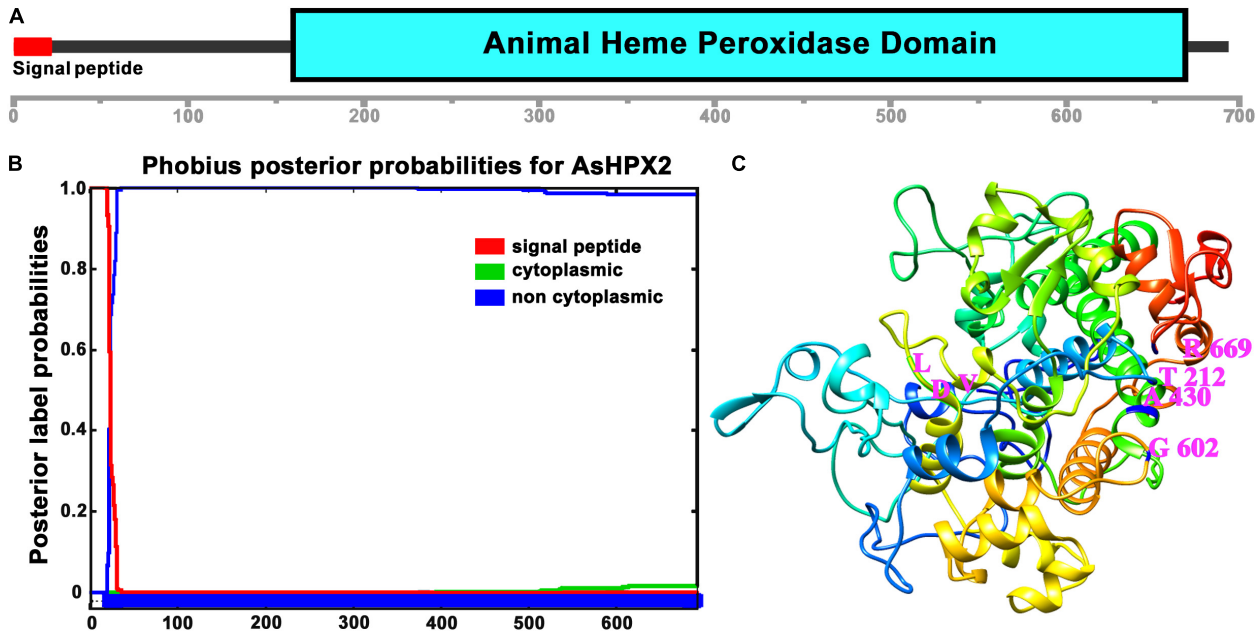

FIGURE 2 | Domain organization of AsHPX2 protein. **(A)** The amino acid sequence of AsHPX2 protein was analyzed with the help of SMART program that revealed the presence of an animal heme peroxidase domain and *N*-terminal signal peptide. **(B)** The AsHPX2 protein sequence was analyzed using Phobius software that also revealed the presence of a signal peptide. **(C)** Three-dimensional structure of AsHPX2 protein was constructed by TASSER program that depicted the amino acids at active site (represented by letter symbols and numbers indicate their position). The integrin binding motif, LDV is oriented toward the surface of AsHPX2 protein.

(as mentioned in **Supplementary Table S2**) also revealed that mosquito HPX2s appeared in a single cluster and are diverged from *D. melanogaster* IRC (**Supplementary Figure S3**). Human peroxidases appeared in a separate cluster far away from mosquito HPX2 peroxidases.

AsHPX2 Is Distinctively Expressed in Different Developmental Stages of Mosquito

The expression of AsHPX2 gene in different developmental stages of *An. stephensi* was analyzed by qRT-PCR. AsHPX2 gene is expressed throughout all developmental stages of *An. stephensi* namely, eggs, first to fourth instar larvae, pupae, adult males or females (**Figure 3**). The relative mRNA levels of AsHPX2 gene were 6-fold, 4-fold, 2.5-fold, and 0.65-fold in first, second, third, and fourth instar larvae, respectively when compared to the eggs (p = 0.0087, p = 0.0024, p = 0.0030, and p = 0.0148, respectively). Furthermore, the relative AsHPX2 mRNA levels were 2-fold, 26-fold and 84-fold in pupae, adult males and females, respectively, against eggs (p = 0.0012, p = 0.0008, and p = 0.0005, respectively) (**Figure 3**).

Blood-Feeding Down Regulates the Expression of AsHPX2 Gene

The relative mRNA levels of AsHPX2 gene were analyzed in sugar- or 24 h post blood-fed midguts or carcasses to decipher its tissue-specific expression. The results presented in **Figure 4** showed that AsHPX2 mRNA levels were 33-fold higher in sugar-fed carcasses than midguts (p = 0.0017). Moreover, its mRNA levels were reduced twofold (p = 0.0367) and 10-fold (p = 0.0020) in 24 h post blood-fed midguts and carcasses, respectively against their sugar-fed controls. In addition, the time kinetics also revealed that the midgut expression of AsHPX2 gene is down regulated after blood-feeding when compared to the sugar-fed controls (**Figure 5**).

The downregulation of AsHPX2 gene expression in blood-fed midguts might be explained by the presence of Z3 isoform of Br-C TFBM in its regulatory region (**Supplementary Figure S1**), which restricts tissue- and condition-specific expression of the gene (Von Kalm et al., 1994; Bayer et al., 1996; Chen et al., 2004; Zhu et al., 2007).

AsHPX2 Regulates the Bacterial Homeostasis in Midgut

The domain analyses revealed that AsHPX2 exhibits peroxinectin-like nature (has cell adhesive property and role in immunity) (**Figure 2C** and **Supplementary Figure S2**). Thus, we hypothesized that AsHPX2 gene might regulating bacterial homeostasis in mosquito midguts. To demonstrate this, AsHPX2 gene was silenced in the midguts of sugar-fed mosquitoes as described in Materials and Methods and its effect was evaluated on the levels of endogenous bacteria. Our analyses of AsHPX2 mRNA levels in controls and silenced midguts revealed 90% silencing of this gene (p = 0.0006, **Figure 6**). Furthermore, the analyses of 16S rRNA levels of endogenous bacteria in these samples indicated that their levels increased ∼4-fold in silenced

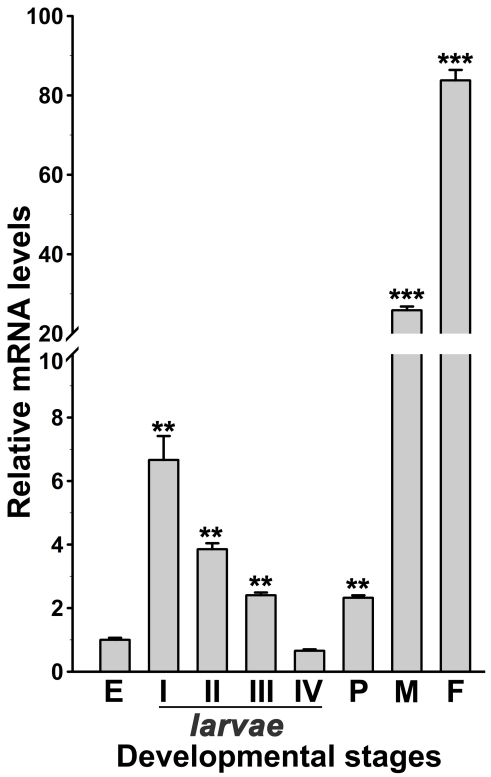

FIGURE 3 | Analysis of AsHPX2 gene expression in different development stages of *An. stephensi*. Relative mRNA levels of AsHPX2 gene were analyzed in different stages of mosquito development against the mRNA levels of eggs, which were considered as 1.0. Significant differences ($p < 0.001$ or 0.01) are indicated by three or two asterisks, respectively. E, eggs; I–IV indicate different stages of instar larvae; *P*, pupae; *M*, males; *F*, females.

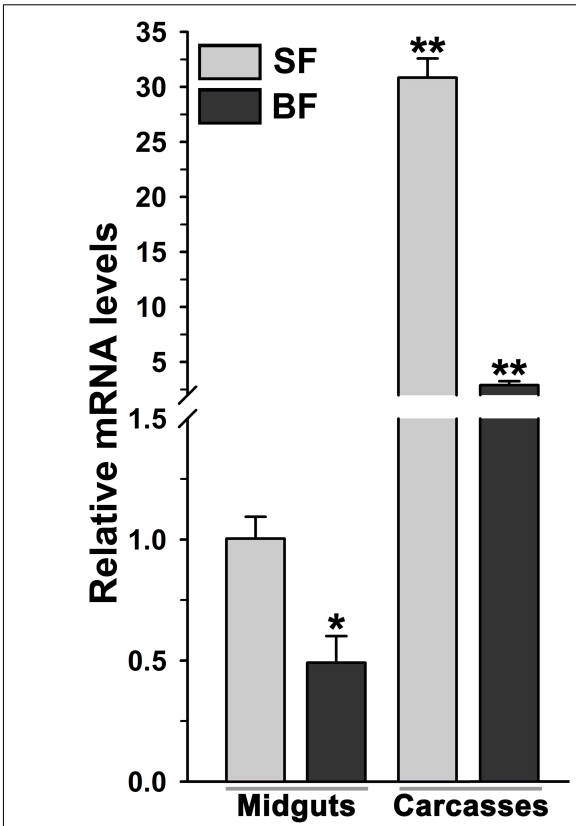

FIGURE 4 | Analysis of mosquito body compartment-specific expression of AsHPX2 gene. Relative mRNA levels of AsHPX2 gene were analyzed in sugar-fed or 24 h post blood-fed mosquito midguts or carcasses. The relative levels of AsHPX2 were calculated against mRNA levels of sugar-fed midguts, which were considered as 1.0. Significant differences $p < 0.01$ or <0.05 are indicated by two or one asterisk, respectively.

midguts against controls ($p = 0.0012$, **Figure 6**). These results established the antibacterial role of AsHPX2 gene.

The silencing of AsHPX2 gene increased bacterial load in the midguts of sugar fed mosquitoes (**Figure 6**). Interestingly, our time kinetics study revealed that blood-feeding induced the growth of midgut bacteria (**Figure 5**) in a similar way as reported in our previous publications as well as by others (Kumar et al., 2010; Oliveira et al., 2011; Habtewold et al., 2016; Kajla et al., 2016a). However, on the other hand, there is an inverse correlation between the increased growth of bacteria and expression of AsHPX2 gene in blood-fed midguts (**Figure 5**). Thus, we believe that the down regulation of AsHPX2 gene in blood fed midguts (**Figures 4**, **5**) augments the growth of midgut bacteria to support blood digestion.

Together, we proposed a putative model that describes the role of AsHPX2 gene in maintaining gut microbiome homeostasis as depicted in **Figure 7**. In brief, AsHPX2, a peroxinectin-like peroxidase limits the growth of bacteria in sugar-fed midguts most probable through the formation of hypochlorous acid (HOCl) produced from H_2O_2 and halides via halogenation cycle (Klebanoff, 1968; Klebanoff, 2005; Allen and Stephens, 2011). After a blood meal, AsHPX2 gene down-regulation (**Figure 5**) and up-regulation of another heme-peroxidase AsHPX15 that catalyzes the crosslinking of mucins barrier over the immune reactive midgut epithelium (Kumar et al., 2010; Kajla et al., 2015, 2016b) collectively promote the growth of endogenous bacteria to support various life processes such as digestion and reproduction (Oliveira et al., 2011; Kajla et al., 2015; Habtewold et al., 2016).

DISCUSSION

In this study, we characterized AsHPX2 gene from *An. stephensi* mosquito that encodes for a 692 amino acid long secreted protein. Interestingly, the intronless nature of AsHPX2 gene indicates that it has a tissue-specific expression with a high rate of evolution in a way similar to other intronless genes such as calmodulin-like gene NB1 and Poly(A) polymerase in human (Le et al., 2001; Shabalina et al., 2010). AsHPX2 has >70 and <60% amino acid identity with anopheline and Culicinae HPX2s, respectively. However, it shares <35% identity with human peroxidases and *D. melanogaster* IRC, a heme-peroxidase that performs catalase cycle (Ha et al., 2005a,b). In conclusion,

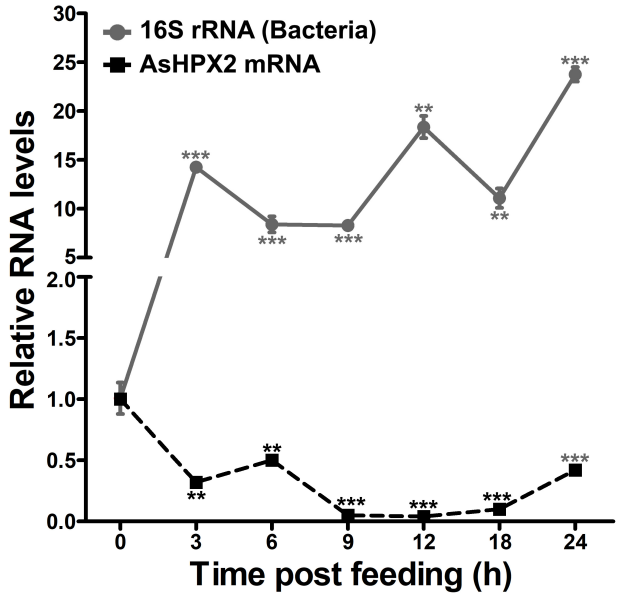

FIGURE 5 | Expression kinetics of AsHPX2 gene in blood-fed midguts. Relative mRNA levels of AsHPX2 gene or 16S rRNA were analyzed in midguts collected at different time points after blood-feeding. The relative levels of AsHPX2 mRNA and 16S rRNA were calculated against the respective sugar-fed midguts, which were considered as 1.0. Significant differences ($p < 0.001$ or 0.01) are indicated by three or two asterisks, respectively.

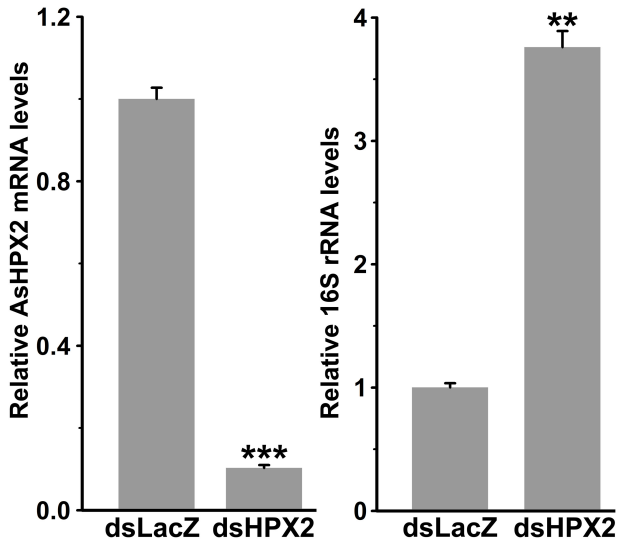

FIGURE 6 | Relative levels of 16S rRNA in AsHPX2 silenced midguts. Mosquitoes were injected with dsLacZ (controls) or dsAsHPX2 (silenced) RNA and relative levels of AsHPX2 mRNA or 16S rRNA were analyzed in their midguts 4 days post-injection. Significant differences ($p < 0.001$ or 0.01) are shown by three or two asterisks, respectively.

these data indicated that AsHPX2 is a mosquito-specific gene. The presence of different TFBM in the regulatory region of AsHPX2 gene signifies its importance in mosquito biology. For example, GATA (pnr) and Br-C binding might explain its tissue-specific expression and down-regulation in blood-fed midguts, respectively in a way similar to other insect genes (Von Kalm et al., 1994; Bayer et al., 1996; Chen et al., 2004; Senger et al., 2006; Zhu et al., 2007; Kajla et al., 2016b; Kakani et al., 2019). It is noteworthy to mention that Br-C isoforms are activated in response to the blood-feeding induced ecdysone. Interestingly, out of four different isoforms of Br-C (Z1 to Z4), any one of them can circumstantially either induce or suppress a target gene (Von Kalm et al., 1994; Edgar, 2006; Zhu et al., 2007). For example, a robust expression of vitellogen gene is induced by Z2 isoform of Br-C in mosquito fat body within 24 h of blood-feeding. However, Z1 and Z4 isoforms of Br-C ensure the termination of vitellogen gene expression after 24 h post blood meal (Zhu et al., 2007). In summary, Br-C isoforms participate in the regulation of specific gene(s) in a coordinated and well-orchestrated way.

The presence of integrin binding motif (LDV) in AsHPX2 protein suggested its peroxinectin-like nature. Peroxinectins are invertebrate peroxidases that are involved in cell adhesion (Liu et al., 2004; Vizzini et al., 2013; Shanthi et al., 2014). Interestingly, the surface orientation of LDV motif in AsHPX2 protein seems to be facilitating its adhesion in a way similar to other adhesion molecules (Johanssen et al., 1999; Liu et al., 2005). Peroxinectins selectively bind to the bacteria and catalyze the formation of HOCl, an anti-bacterial molecule, through halogenation cycle (Klebanoff, 1968, 2005; Allen and Stephens, 2011). Interestingly, peroxinectins also bind superoxide dismutase (SOD), an enzyme that catalyzes the formation of H_2O_2 from superoxide anions, which, in turn, promotes the continuity of halogenation cycle (Holmblad and Soderhall, 1999; Johanssen et al., 1999; Choudhury et al., 2019).

Differential expression of AsHPX2 gene in different stages of mosquito development corroborates with the expression profile of some peroxidases (Mdes000915, Mdes001004, Mdes009520, and Mdes015930) across the developmental stages of Hessian fly *Mayetiola destructor* (Chen et al., 2016). Because peroxidases catalyze the crosslinking of biological matrices and regulate immune functions thus, their expression might reveal a direct association to the immune status and/or bacterial homeostasis during insect development. Direct evidence for this belief was reported in *An. gambiae* where a dynamic mosquito gut microbiome is associated with transitions in developmental stages and alteration of feeding behavior from the sugar diet to blood meal (Wang et al., 2011).

AsHPX2 gene silencing significantly enhanced the growth of midgut bacteria that revealed its antibacterial role in sugar fed mosquitoes. Therefore, the downregulation of AsHPX2 gene expression in blood-fed midguts is an important event and it is inversely correlated to the growth of bacteria. Because the bacteria play an important role in blood digestion thus, down-regulation of AsHPX2 gene creates a physiological condition in blood-fed midguts to facilitate digestion (Kumar et al., 2010; de Gaio et al., 2011; Kajla et al., 2015). Our results indicated that AsHPX2 is one of the important regulators that maintain homeostasis of endogenous bacteria in sugar- or

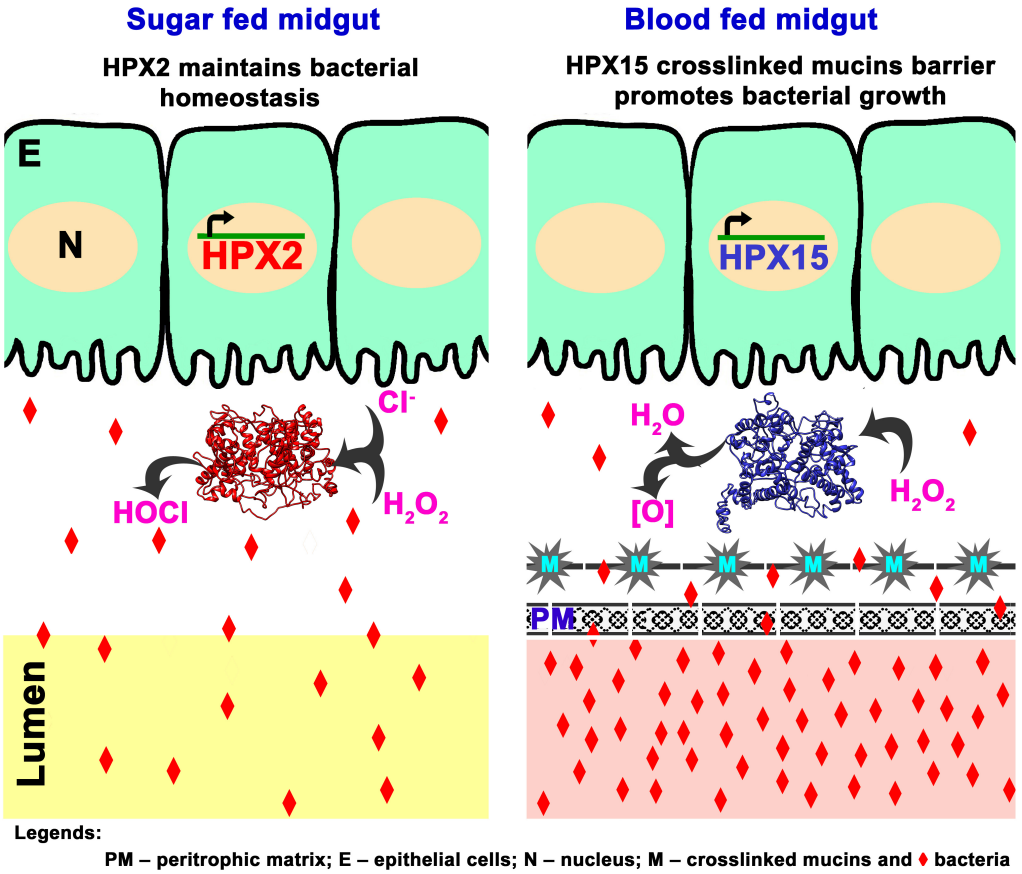

FIGURE 7 | Proposed mechanism of AsHPX2 mediated bacterial homeostasis in *An. stephensi* midgut. In sugar-fed midguts, AsHPX2 catalyzes the halogenation cycle and produces hypochlorous acid (HOCl) to maintain the bacterial homeostasis. Blood-feeding suppresses the expression of AsHPX2 gene (**Figure 5**) and induces another heme-peroxidase AsHPX15 (Kumar et al., 2010; Kajla et al., 2016b), which catalyzes mucins crosslinking at the surface of midgut epithelium. Cross-linked mucins act like a barrier that blocks the recognition of bacteria by the immune-reactive epithelium. This mechanism creates a "low immunity zone" in this body compartment to promote the growth of bacteria that, in turn, facilitate blood digestion (Kumar et al., 2010; Kajla et al., 2015). Collectively, the reduced AsHPX2 expression and induced expression of HPX15 in blood-fed midguts create a fine-tuned balance between blood digestion and immunity.

blood-fed midguts. Interestingly, blood-feeding up-regulates the expression of another heme-peroxidase, AsHPX15 that catalyzes the crosslinking of mucins barrier over the immune reactive midgut epithelium to protect the growing bacteria (Kumar et al., 2010; Kajla et al., 2015, 2016b).

Thus, the systematic regulation of bacterial antagonistic (AsHPX2) and agonistic (AsHPX15) peroxidases create a low immunity zone in midgut for promoting the growth of bacteria, facilitating blood digestion and maintaining a fine balance between food digestion and immunity. Hence, the regulated expression of heme-peroxidases is one of the mechanisms that actively maintain bacterial homeostasis in mosquito midgut during distinctive nutritional conditions.

In conclusion, the identification of *Anopheles* genes that maintain microbial homeostasis in the midgut are of great value as they can be exploited to achieve dysbiosis of the mosquito gut ecosystem and hence, the vector competence. Overall, from the present study, it is clear that AsHPX2 is a mosquito-specific gene that plays an important role in midgut physiology and immunity. Hence, this gene can be a potent target to alter the bacterial community and regulating *Plasmodium* development.

DATA AVAILABILITY STATEMENT

The raw data supporting the conclusions of this article will be made available by the authors, without undue reservation.

ETHICS STATEMENT

The animal study was reviewed and approved by BITS, Pilani Institutional Animal Ethical Committee.

AUTHOR CONTRIBUTIONS

PK, LG, and SK designed the experiments, performed expression kinetics of AsHPX2 and silencing experiments, analyzed the

data, and wrote the manuscript. PK and SK collected samples to perform experiments. All authors approved the manuscript.

FUNDING

This work was funded by the research grants from the Department of Science and Technology (DST), Government of India (grant number SR/SO/HS-0131/2010) and Department of Biotechnology (DBT), Government of India (grant number BT/PR8758/AGR/36/744/2013). The fellowship for PK was supported by the DST, Government of India.

ACKNOWLEDGMENTS

We wish to thank Institute administration for providing all other facilities to accomplish the research and central animal facilities (CAF) for providing the study animals.

SUPPLEMENTARY MATERIAL

The Supplementary Material for this article can be found online at: https://www.frontiersin.org/articles/10.3389/fphys.2020.572340/full#supplementary-material

REFERENCES

Allen, R. C., and Stephens, J. T. Jr. (2011). Myeloperoxidase selectively binds and selectively kills microbes. *Infect. Immun.* 79, 474–485. doi: 10.1128/iai.00910-09

Bailey, D., Basar, M. A., Nag, S., Bondhu, N., Teng, S., and Duttaroy, A. (2017). The essential requirement of an animal heme peroxidase protein during the wing maturation process in Drosophila. *BMC Dev. Biol.* 17:1. doi: 10.1186/s12861-016-0143-8

Bayer, C. A., Holley, B., and Fristrom, J. W. (1996). A switch in broad-complex zinc-finger isoform expression is regulated posttranscriptionally during the metamorphosis of *Drosophila* imaginal discs. *Dev. Biol.* 177, 1–14. doi: 10.1006/dbio.1996.0140

Beier, M. S., Pumpuni, C. B., Beier, J. C., and Davis, J. R. (1994). Effects of para-aminobenzoic acid, insulin, and gentamycin on *Plasmodium falciparum* development in Anopheline mosquitoes (Diptera: Culicidae). *J. Med. Entomol.* 31, 561–565. doi: 10.1093/jmedent/31.4.561

Brennan, L. J., Keddie, B. A., Braig, H. R., and Harris, H. L. (2008). The endosymbiont *Wolbachia pipientis* induces the expression of host antioxidant. *PLoS One* 3:e2083. doi: 10.1371/journal.pone.0002083

Cartharius, K., Frech, K., Grote, K., Klocke, B., Haltmeier, M., Klingenhoff, A., et al. (2005). MatInspector and beyond: promoter analysis based on transcription factor binding sites. *Bioinformatics* 21, 2933–2942. doi: 10.1093/bioinformatics/bti473

Chen, L., Zhu, J., Sun, G., and Raikhel, A. S. (2004). The early gene broad is involved in the ecdysteroid hierarchy governing vitellogenesis of the mosquito *Aedes aegypti*. *J. Mol. Endocrinol.* 33, 743–761. doi: 10.1677/jme.1.01531

Chen, M.-S., Liu, S., Wang, H., Cheng, X., El Bouhssini, M., and Whitworth, R. J. (2016). Massive shift in gene expression during transitions between developmental stages of the gall midge, *Mayetiola Destructor*. *PLoS One* 11:e0155616. doi: 10.1371/journal.pone.0155616

Choudhury, T. P., Gupta, L., and Kumar, S. (2019). Identification, characterization and expression analysis of *Anopheles stephensi* double peroxidase. *Acta Trop.* 190, 210–219. doi: 10.1016/j.actatropica.2018.10.008

Cirimotich, C. M., Dong, Y., Clayton, A. M., Sandiford, S. L., Souza-Neto, J. A., Mulenga, M., et al. (2011). Natural microbe-mediated refractoriness to *Plasmodium* infection in *Anopheles gambiae*. *Science* 332, 855–858. doi: 10.1126/science.1201618

de Gaio, A., Gusmão, D. S., Santos, A. V., Berbert-Molina, M. A., Pimenta, P. F., and Lemos, F. J. (2011). Contribution of midgut bacteria to blood digestion and egg production in *Aedes aegypti* (diptera: culicidae) (L.). *Parasit Vect.* 4:105. doi: 10.1186/1756-3305-4-105

Dhawan, R., Gupta, K., Kajla, M., Kakani, P., Choudhury, T. P., Kumar, S., et al. (2017). Apolipophorin-III acts as a positive regulator of *plasmodium* development in *Anopheles stephensi*. *Front. Physiol.* 8:185. doi: 10.3389/fphys.2017.00185

Dixit, R., Rawat, M., Kumar, S., Pandey, K. C., Adak, T., and Sharma, A. (2011). Salivary gland transcriptome analysis in response to sugar feeding in malaria vector *Anopheles stephensi*. *J. Insect Physiol.* 57, 1399–1406. doi: 10.1016/j.jinsphys.2011.07.007

Dong, Y., Manfredini, F., and Dimopoulos, G. (2009). Implication of the mosquito midgut microbiota in the defense against malaria parasites. *PLoS Pathog.* 5:e1000423. doi: 10.1371/journal.ppat.1000423

Edgar, B. A. (2006). How flies get their size: genetics meets physiology. *Nat. Rev. Genet.* 7, 907–916. doi: 10.1038/nrg1989

Garver, L. S., de Almeida Oliveira, G., and Barillas-Mury, C. (2013). The JNK pathway is a key mediator of *Anopheles gambiae* antiplasmodial immunity. *PLoS Pathog.* 9:e1003622. doi: 10.1371/journal.ppat.1003622

Giraldo-Calderón, G. I., Emrich, S. J., MacCallum, R. M., Maslen, G., Dialynas, E., Topalis, P., et al. (2015). . VectorBase: an updated bioinformatics resource for invertebrate vectors and other organisms related with human diseases. *Nucl. Acids Res.* 43, D707–D713. doi: 10.1093/nar/gku1117

Graca-Souza, A. V., Maya-Monteiro, C., Paiva-Silva, G. O., Braz, G. R., and Paes, M. C. (2006). Adaptations against heme toxicity in blood-feeding arthropods. *Insect Biochem. Mol. Biol.* 36, 322–335. doi: 10.1016/j.ibmb.2006.01.009

Gupta, K., Dhawan, R., Kajla, M., Misra, T., Kumar, S., and Gupta, L. (2017). The evolutionary divergence of STAT transcription factor in different *Anopheles* species. *Gene* 596, 89–97. doi: 10.1016/j.gene.2016.09.022

Gupta, L., Molina-Cruz, A., Kumar, S., Rodrigues, J., Dixit, R., Zamora, R. E., et al. (2009). The STAT pathway mediates late-phase immunity against *Plasmodium* in the mosquito *Anopheles gambiae*. *Cell Host Microbe* 5, 498–507. doi: 10.1016/j.chom.2009.04.003

Gusmão, D. S., Santos, A. V., Marini, D. C., Russo, Ede, S., Peixoto, A. M., et al. (2007). First isolation of microorganisms from the gut diverticulum of *Aedes aegypti* (Diptera: Culicidae): new perspectives for an insect-bacteria association. *Mem. Inst. Oswaldo Cruz* 102, 919–924. doi: 10.1590/s0074-02762007000800005

Ha, E. M., Oh, C. T., Bae, Y. S., and Lee, W. J. (2005a). A direct role for dual oxidase in *Drosophila* gut immunity. *Science* 310, 847–850. doi: 10.1126/science.1117311

Ha, E. M., Oh, C. T., Ryu, J. H., Bae, Y. S., Kang, S. W., Jang, I. H., et al. (2005b). An antioxidant system required for host protection against gut infection in *Drosophila*. *Dev. Cell.* 8, 125–132. doi: 10.1016/j.devcel.2004.11.007

Habtewold, T., Duchateau, L., and Christophides, G. K. (2016). Flow cytometry analysis of the microbiota associated with the midguts of vector mosquitoes. *Parasit Vect.* 9:167. doi: 10.1186/s13071-016-1438-0

Holmblad, T., and Soderhall, K. (1999). Cell adhesion molecules and antioxidative enzymes in a crustacean, possible role in immunity. *Aquaculture* 172, 111–123. doi: 10.1016/s0044-8486(98)00446-3

Johanssen, M. W., Holmblad, T., ThoÈrnqvist, P.-O., Cammarata, M., Parrinello, N., and SoÈderhall, K. (1999). A cell-surface superoxide dismutase is a binding protein for peroxinectin, a cell-adhesive peroxidase in crayfish. *J. Cell. Sci.* 112, 917–925.

Johansson, M. W., Lind, M. I., Holmblad, T., Thörnqvist, P. O., and Söderhäll, K. (1995). Peroxinectin, a novel cell adhesion protein from crayfish, blood. *Biochem. Biophys. Res. Commun.* 216, 1079-1087.

Kajla, M., Choudhury, T. P., Kakani, P., Gupta, K., Dhawan, R., Gupta, L., et al. (2016b). Silencing of *Anopheles stephensi* heme peroxidase HPX15 activates diverse immune pathways to regulate the growth of midgut bacteria. *Front. Microbiol.* 7:1351. doi: 10.3389/fmicb.2016.01351

Kajla, M., Gupta, K., Gupta, L., and Kumar, S. (2015). A fine-tuned management between physiology and immunity maintains the gut microbiota in insects. *Biochem. Physiol.* 4:182. doi: 10.4172/2168-9652.1000182

Kajla, M., Kakani, P., Choudhury, T. P., Kumar, V., Gupta, K., Dhawan, R., et al. (2017). *Anopheles stephensi* heme peroxidase HPX15 suppresses midgut immunity to support *Plasmodium* development. *Front. Immunol.* 8:249. doi: 10.3389/fimmu.2017.00249

Kajla, M., Kakani, P., Gupta, K., Choudhury, T. P., Gupta, L., and Kumar, S. (2016a). Characterization and expression analysis of gene encoding heme peroxidase HPX15 in major Indian malaria vector *Anopheles stephensi* (Diptera: Culicidae). *Acta Trop.* 158, 107–116. doi: 10.1016/j.actatropica.2016.02.028

Kakani, P., Kajla, M., Choudhury, T. P., Gupta, L., and Kumar, S. (2019). *Anopheles stephensi* dual oxidase silencing activates the thioester-containing protein 1 pathway to suppress *Plasmodium* development. *J. Innate Immun.* 11, 496–505. doi: 10.1159/000497417

Käll, L., Krogh, A., and Sonnhammer, E. L. (2007). Advantages of combined transmembrane topology and signal peptide prediction–the Phobius web server. *Nucleic Acids Res.* 35, W429–W432.

Kelley, L. A., Mezulis, S., Yates, C. M., Wass, M. N., and Sternberg, M. J. (2015). The Phyre2 web portal for protein modelling, prediction and analysis. *Nat. protocols* 10, 845–858. doi: 10.1038/nprot.2015.053

Klebanoff, S. J. (1968). Myeloperoxidase-halide-hydrogen peroxide antibacterial system. *J. Bacteriol.* 95, 2131–2138. doi: 10.1128/jb.95.6.2131-2138.1968

Klebanoff, S. J. (2005). Myeloperoxidase: friend and foe. *J. Leukoc. Biol.* 77, 598–625. doi: 10.1189/jlb.1204697

Kumar, S., Molina-Cruz, A., Gupta, L., Rodrigues, J., and Barillas-Mury, C. (2010). A peroxidase/dual oxidase system modulates midgut epithelial immunity in *Anopheles gambiae*. *Science* 327, 1644–1648. doi: 10.1126/science.1184008

Le, Y. J., Kim, H., Chung, J. H., and Lee, Y. (2001). Testis-specific expression of an intronless gene encoding a human poly(A) polymerase. *Mol. Cells* 11, 379–385.

Letunic, I., Doerks, T., and Bork, P. (2014). SMART: recent updates, new developments and status in 2015. *Nucleic Acids Res.* 43, D257–D260.

Liu, C. H., Chen, W., Kuo, C. M., and Chen, J. C. (2004). Molecular cloning and characterisation of a cell adhesion molecule, peroxinectin from the white shrimp *Litopenaeus vannamei*. *Fish Shellfish Immunol.* 17, 13–26. doi: 10.1016/j.fsi.2003.11.002

Liu, C. H., Cheng, W., and Chen, J. C. (2005). The peroxinectin of white shrimp *Litopenaeus vannamei* is synthesised in the semi-granular and granular cells, and its transcription is up-regulated with *Vibrio alginolyticus* infection. *Fish Shellfish Immunol.* 18, 431–444. doi: 10.1016/j.fsi.2004.10.005

Livak, K. J., and Schmittgen, T. D. (2001). Analysis of relative gene expression data using real-time quantitative PCR and the 2(-Delta Delta C(T)) Method. *Methods* 25, 402–408. doi: 10.1006/meth.2001.1262

Login, F. H., Balmand, S., Vallier, A., Vincent-Monégat, C., Vigneron, A., Weiss-Gayet, M., et al. (2011). Antimicrobial peptides keep insect endosymbionts under control. *Science* 334, 362–365. doi: 10.1126/science.1209728

Luckhart, S., Vodovotz, Y., Cui, L., and Rosenberg, R. (1998). The mosquito *Anopheles stephensi* limits malaria parasite development with inducible synthesis of nitric oxide. *Proc. Natl. Acad. Sci. U.S.A.* 95, 5700–5705. doi: 10.1073/pnas.95.10.5700

Magnusson, K., Mendes, A. M., Windbichler, N., Papathanos, P. A., Nolan, T., Dottorini, T., et al. (2011). Transcription Regulation of Sex-Biased Genes during Ontogeny in the Malaria Vector *Anopheles gambiae*. *PLoS One* 6:e21572. doi: 10.1371/journal.pone.0021572

Marchler-Bauer, A., Derbyshire, M. K., Gonzales, N. R., Lu, S., Chitsaz, F., Geer, L. Y., et al. (2015). CDD: NCBI's conserved domain database. *Nucleic Acids Res.* 43, D222–D226.

Mathelier, A., Zhao, X., Zhang, A. W., Parcy, F., Worsley-Hunt, R., Arenillas, D. J., et al. (2014). JASPAR 2014: an extensively expanded and updated open-access database of transcription factor binding profiles. *Nucl. Acids Res.* 42, D142–D147.

Minard, G., Mavingui, P., and Moro, C. V. (2013). Diversity and function of bacterial microbiota in the mosquito holobiont. *Parasit Vect.* 6:146. doi: 10.1186/1756-3305-6-146

Motulsky, H. J. (1999). *Analyzing Data with GraphPad Prism*. San Diego, CA: GraphPad Software Inc.

Nishikori, K., Morioka, K., Kubo, T., and Morioka, M. (2009). Age- and morph-dependent activation of the lysosomal system and Buchnera degradation in aphid endosymbiosis. *J. Insect Physiol.* 55, 351–357. doi: 10.1016/j.jinsphys.2009.01.001

Oliveira, J. H., Gonçalves, R. L., Lara, F. A., Dias, F. A., Gandara, A. C., Menna-Barreto, R. F., et al. (2011). Blood meal-derived heme decreases ROS levels in the midgut of *Aedes aegypti* and allows proliferation of intestinal microbiota. *PLoS Pathog.* 7:e1001320. doi: 10.1371/journal.ppat.1001320

Pace, C. N., and Scholtz, J. M. (1998). A helix propensity scale based on experimental studies of peptides and proteins. *Biophys. J.* 75, 422–427. doi: 10.1016/s0006-3495(98)77529-0

Petersen, T. N., Brunak, S., von Heijne, G., and Nielsen, H. (2011). SignalP 4.0: discriminating signal peptides from transmembrane regions. *Nat. Methods* 8, 785–786. doi: 10.1038/nmeth.1701

Peterson, T. M., and Luckhart, S. (2006). A mosquito 2-Cys peroxiredoxin protects against nitrosative and oxidative stresses associated with malaria parasite infection. *Free Radic. Biol. Med.* 40, 1067–1082. doi: 10.1016/j.freeradbiomed.2005.10.059

Ramakers, C., Ruijter, J. M., Lekanne Deprez, R. H., and Moorman, A. F. (2003). Assumption-free analysis of quantitative real-time polymerase chain reaction (PCR) data. *Neurosci. Lett.* 339, 62–66. doi: 10.1016/s0304-3940(02)01423-4

Ruoslahti, E. (1996). RGD and other recognition sequences for integrins. *Annu. Rev. Cell. Dev. Biol.* 12:697e715. doi: 10.1146/annurev.cellbio.12.1.697

Saitou, N., and Nei, M. (1987). The neighbor-joining method: a new method for reconstructing phylogenetic trees. *Mol. Biol. Evol.* 4, 406–425.

Senger, K., Harris, K., and Levine, M. (2006). GATA factors participate in tissue-specific immune responses in *Drosophila* larvae. *Proc. Natl. Acad. Sci. U.S.A.* 103, 15957–15962. doi: 10.1073/pnas.0607608103

Shabalina, S. A., Ogurtsov, A. Y., Spiridonov, A. N., Novichkov, P. S., Spiridonov, N. A., and Koonin, E. V. (2010). Distinct patterns of expression and evolution of intronless and intron-containing mammalian genes. *Mol. Biol. Evol.* 27, 1745–1749. doi: 10.1093/molbev/msq086

Shanthi, S., Manju, S., Rajakumaran, P., and Vaseeharan, B. (2014). Molecular cloning of peroxinectin gene and its expression in response to peptidoglycan and *Vibrio harveyi* in Indian white shrimp *Fenneropenaeus indicus*. *Cell Commun. Adhes.* 21, 281–289. doi: 10.3109/15419061.2014.943396

Soudi, M., Zamocky, M., Jakopitsch, C., Furtmüller, P. G., and Obinger, C. (2012). Molecular evolution, structure, and function of peroxidasins. *Chem. Biodivers.* 9, 1776–1793. doi: 10.1002/cbdv.201100438

Stanke, M., Diekhans, M., Baertsch, R., and Haussler, D. (2008). Using native and syntenically mapped cDNA alignments to improve de novo gene finding. *Bioinformatics* 24, 637–644. doi: 10.1093/bioinformatics/btn013

Vizzini, A., Parrinello, D., Sanfratello, M. A., Mangano, V., Parrinello, N., and Cammarata, M. (2013). *Ciona intestinalis* peroxinectin is a novel component of the peroxidase-cyclooxygenase gene superfamily upregulated by LPS. *Dev. Comp. Immunol.* 41, 59–67. doi: 10.1016/j.dci.2013.03.015

Von Kalm, L., Crossgrove, K., Von Seggern, D., Guild, G. M., and Beckendorf, S. K. (1994). The broad-complex directly controls a tissue-specific response to the steroid hormone ecdysone at the onset of *Drosophila* metamorphosis. *EMBO J.* 13, 3505–3516. doi: 10.1002/j.1460-2075.1994.tb06657.x

Wang, Y., Gilbreath, T. M. I. I. I., Kukutla, P., Yan, G., and Xu, J. (2011). Dynamic gut microbiome across life history of the malaria mosquito *Anopheles gambiae* in Kenya. *PLoS One* 6:e24767. doi: 10.1371/journal.pone.0024767

Yang, J., Yan, R., Roy, A., Xu, D., Poisson, J., and Zhang, Y. (2015). The I-TASSER Suite: protein structure and function prediction. *Nat. Methods* 12, 7–8. doi: 10.1038/nmeth.3213

Zakovic, S., and Levashina, E. A. (2017). NF-κB-like signaling pathway REL2 in immune defenses of the malaria vector *Anopheles gambiae*. *Front. Cell Infect. Microbiol.* 7:258. doi: 10.3389/fcimb.2017.00258

Zhang, Y. (2008). I-TASSER server for protein 3D structure prediction. *BMC Bioinformatics* 9:40. doi: 10.1186/1471-2105-9-40

Zhu, J., Chen, L., and Raikhel, A. S. (2007). Distinct roles of broad isoforms in regulation of the 20-hydroxyecdysone effector gene, Vitellogenin, in the mosquito *Aedes aegypti*. *Mol. Cell. Endocrinol.* 267, 97–105. doi: 10.1016/j.mce.2007.01.006

Conflict of Interest: The authors declare that the research was conducted in the absence of any commercial or financial relationships that could be construed as a potential conflict of interest.

frontiers in Physiology

ORIGINAL RESEARCH
published: 15 December 2020
doi: 10.3389/fphys.2020.574800

Cocoon-Spinning Behavior and 20-Hydroxyecdysone Regulation of Fibroin Genes in *Plutella xylostella*

Yan Shi[1], *Gan-Lin Lin*[1], *Xiu-Lian Fu*[1], *Mike Keller*[1,2], *Guy Smagghe*[3]* *and Tong-Xian Liu*[1]*

[1] Key Lab of Integrated Crop Pest Management of Shandong Province, College of Plant Health and Medicine, Qingdao Agricultural University, Qingdao, China, [2] School of Agriculture, Food and Wine, University of Adelaide, Glen Osmond, SA, Australia, [3] Department of Plants and Crops, Faculty of Bioscience Engineering, Ghent University, Ghent, Belgium

The diamondback moth *Plutella xylostella* is a serious pest of crucifers. It has high reproductive potential and is resistant to many insecticides. Typically, the last-instar larvae of *P. xylostella*, before pupation, move to the lower or outer plant leaves to make a loose silk cocoon and pupate inside for adult formation. To better understand this pivotal stage we studied the cocoon-spinning behavior of *P. xylostella* and measured three successive phases by video-recording, namely the selection of a pupation site, spinning a loose cocoon and padding the scaffold cocoon. Subsequently, we cloned three fibroin genes related to cocoon production, i.e., fibroin light chain (Fib-L), fibroin heavy chain (Fib-H), and glycoprotein P25. A spatio-temporal study of these three fibroin genes confirmed a high expression in the silk glands during the final larval instar silk-producing stage. In parallel, we did an exogenous treatment of the insect molting hormone 20-hydroxyecdysone (20E), and this suppressed fibroin gene expression, reduced the normal time needed for cocoon spinning, and we also observed a looser cocoon structure under the scanning electron microscope. Hence, we demonstrated that the expression levels of key genes related to the synthesis of 20E [the three Halloween genes *Spook (Spo)*, *Shadow* (*Sad),* and *Shade* (*Shd*)] decreased significantly during spinning, the expression of the 20E receptor (*EcR* and *USP*) was significantly lower during spinning than before spinning, and that the expression levels of *CYP18-A1* related to 20E degradation were significantly up-regulated during spinning. The significance of the cocoon and the effects of 20E on the cocoon-spinning behavior of *P. xylostella* are discussed.

Keywords: *Plutella xylostella*, diamondback moth, cocoon-spinning behavior, 20E, fibroin genes

OPEN ACCESS

Edited by:
Jose Luis Ramirez, United States Department of Agriculture (USDA), United States

Reviewed by:
Youjun Zhang, Chinese Academy of Agricultural Sciences, China
Xiaofeng Xia, Fujian Agriculture and Forestry University, China

***Correspondence:**
Tong-Xian Liu
txliu@qau.edu.cn
Guy Smagghe
guy.smagghe@ugent.be

Specialty section:
This article was submitted to Invertebrate Physiology, a section of the journal Frontiers in Physiology

Received: *21 June 2020*
Accepted: *23 October 2020*
Published: *15 December 2020*

Citation:
Shi Y, Lin G-L, Fu X-L, Keller M, Smagghe G and Liu T-X (2020) Cocoon-Spinning Behavior and 20-Hydroxyecdysone Regulation of Fibroin Genes in Plutella xylostella. Front. Physiol. 11:574800. doi: 10.3389/fphys.2020.574800

INTRODUCTION

Cocoon spinning behaviors have been described in many insect species before like, the domesticated silkworm *Bombyx mori* (Yokoyama, 1951; Kiyosawa et al., 1999; Chen et al., 2012a,b; Guo et al., 2016), the giant silkworm *Hyalophora cecropia* (Van der Kloot and Williams, 1953), and the Chinese oak silkworm *Antheraea pernyi* (Lounibos, 1975, 1976). These authors described the major features of the stereotyped spinning movements and the effects of environmental conditions on the morphology, structure and mechanical properties. Yagi (1926) classified cocoons into four types by their formation of the exit hole of the adults and the modes of attachment. They were: (1) stalked and closed, (2) stalkless

and closed, (3) stalkless and open, and (4) stalked and open. The cocoon of *P. xylostella* belongs to the third type.

The fibrous silk core is generally comprised of a three-protein complex, including fibroin light chain (Fib-L), fibroin heavy chain (Fib-H) and glycoprotein P25 (Sehnal and Zurovec, 2004; Sutherland et al., 2010). The development and function of the silk gland are under hormone control (Chaitanya and Aparna, 2010; Boulet-Audet et al., 2016). Ecdysone is the fundamental steroid hormone, released from the prothoracic glands in insects. The dormant state of ecdysone is discharged into the hemolymph and converted into 20-hydroxyecdysone (20E) in the peripheral tissues (Li et al., 2019). Most hormonal studies on *Fib-H*, *Fib-L* and *P25* are limited to *B. mori, Corcyra cephalonica* and *Sylepta derogate* (Miao et al., 2004; Chaitanya and Aparna, 2010; Su et al., 2015). In *B. mori*, the ecdysteroids are essential for appropriate function of silk gland. In *C. cephalonica*, studies revealed that 20E modulates the expression of the *Fib-L*, *Fib-H,* and *P25* genes at the mRNA level. These reports indicated that larval development and silk gland function in these insects are regulated by 20E. Although the synthesis and secretion of silk fibroin have been studied in detail in model insects like *B. mori*, the cocoon behavior, these silk genes and the hormonal regulation have not been uncleared in the diamondback moth, which is an agricultural pest that causes high damage to cruciferous vegetables. It has a high reproductive potential, a wide distribution in the world, and is resistant to many insecticides.

In this study, we therefore studied the cocoon-spinning behavior of *P. xylostella* larvae by video-recording, and subsequently we examined the silk genes *Fib-L*, *Fib-H,* and *P25* by cloning and a spatio-temporal molecular characterization, and tested the effect of an exogenous treatment of 20E on their expression and the cocoon formation under the scanning electron microscope (SEM). Finally, we measured the expression of three 20E-related genes for synthesis [namely the Halloween genes *Spook* (*Spo*), *Shadow* (*Sad*), and *Shade* (*Shd*)], its receptor (the ecdysone receptor *EcR* and Ultraspiracle *USP*) and degradation (*CYP18-A1*) at the moments of before, during and after the spinning behavior. We selected *Spo* (Cyp307a1) and *Sad* (Cyp315a1) encoding cytochrome P450 enzyme needed for 20E biosynthesis (Namiki et al., 2005; Gilbert, 2008). *Shd* (Cyp314a1) is the final step in the biosynthetic pathway for an ecdysone 20-monooxygenase enzyme responsible (Petryk et al., 2003). On EcR and USP, they form the functional nuclear heterodimer receptor for 20E, which modulates insect molting and metamorphosis (reviewed in Fahrbach et al., 2012). Finally, CYP18-A1 encodes a P450 enzyme ecdysteroid 26-hydroxylase that is a major 20E hormone inactivation enzyme (Guittard et al., 2011; Li et al., 2014). We believe these data should allow to better understand the significance of the cocoon, the effects of 20E on cocoon spinning behavior of *P. xylostella*, and the possible use of cocoon manipulation for pest management.

MATERIALS AND METHODS

Insect Rearing and Cocoon Collection

The *P. xylostella* used for this works were collected from a cabbage (*Brassica rapa* L. ssp. *pekinensis*) field in Jiaozhou, Qingdao (36°16′39″N, 120°00′41″E) in 2018, and has since been reared in laboratory at the Qingdao Agriculture University. *Plutella xylostella* were rearing in a 16:8 h (L: D) photoperiod maintained insectary cages at 20–25°C and 50–70% relative humidity (RH). Adults were fed 10% honey solution, and larvae were fed with fresh Chinese cabbage (*Brassica rapa* L. ssp. *pekinensis*) leaves until they started to spin cocoons. For collecting cocoon, we used dissecting scissors to gently peel off the pupa from the cocoon to observe using electron microscope.

Observation of Cocoon-Spinning Behavior

The cocoon-spinning behavior of *P. xylostella* larvae was recorded using a Canon video camera (HFR86, Canon, Tokyo, Japan) and analyzed by playing the video recordings back on a computer. Each larval cocoon-spinning behavior was recorded from the time when the larva started selection of its pupation site and scaffolding until the completion of the inner cocoon. For the observation and recording of cocoon, we totally recoded 15 larvae cocooning.

Sequence Alignment and Phylogenetic Analysis

DNAMAN 6.0 software was used to predict the open reading frame (ORF). NCBI CDD database was applied to identify the conserved domains. The amino acid sequences of homologous Halloween genes and ecdysone receptor genes were aligned with Clustal W2.0. Phylogenetic tree was constructed using the method of neighbor-joining (NJ) with a bootstrap value of 1000 replicates.

Cloning and Real-Time Quantitative PCR (RT-qPCR)

Using the genome database and transcriptome of *P. xylostella* (Tang et al., 2014) and identified gene sequence in *B. mori*, the partial gene of fibroin-H and the open reading frame of the fibroin-L, P25, the three 20E-biosynthesis Halloween genes *Spo* (Cyp307a1), *Sad* (Cyp315a1), and *Shd* (Cyp314a1), and the ecdysone receptor (*EcR*), Ultraspiracle (*USP*) and the 20E-catabolizing *CYP18-A1* genes were identified by performing a homologous search. RNA was extracted from the final instar larvae using Trizol reagent (Promega, Beijing, China). Single-strand cDNA was prepared using the PrimeScript first-strand synthesis system (Promega, Beijing, China). Primers were designed based on the genome data of *P. xylostella* (**Supplementary Table 1**). Using high-fidelity DNA polymerase PrimeSTAR (Takara, Dalian, Liaoning, China), the partial of *fib-H* and the open reading frame of *fib-L* and *P25* were amplified. We refer to Shi et al. (2017) for the setting of the amplified PCR program. Subsequently, PCR products were purified and cloned into vector and sequenced (TsingKe, Qingdao, China). Total RNA of four replicates was obtained for the 20E treatment and the control. Single-strand cDNA was prepared using the PrimeScript first-strand synthesis system (Takara). We performed the RT-qPCR with the protocol as described by Shi et al. (2017), and *Actin* and *rpl32* were used as reference genes (Sun et al., 2013). Four biological replicates and each replicate including 3 individuals were performed for each developmental

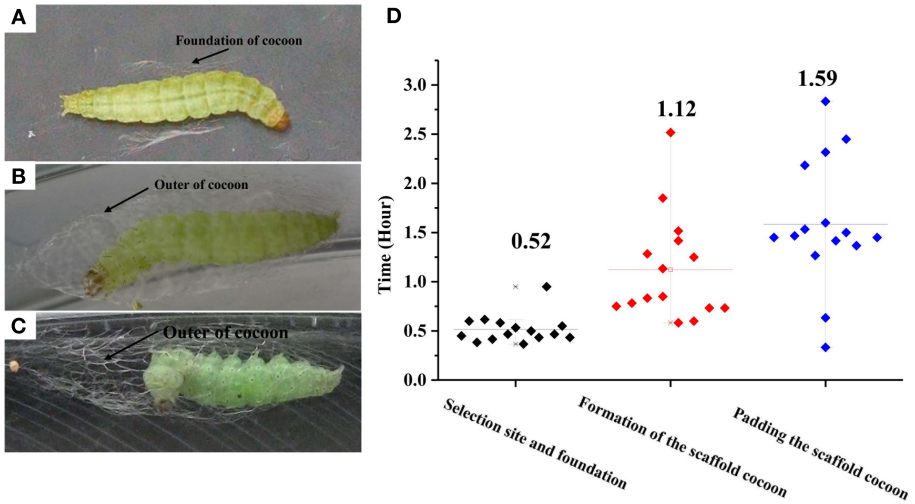

FIGURE 1 | Photographs of the three successive phases for cocoon construction by *Plutella xylostella* larvae. **(A)** Selecting a pupation site and building a foundation. **(B)** Formation of the scaffold cocoon; **(C)** Padding the scaffold cocoon; and durations **(D)**. Different letters indicate statistical differences. The left y-axis indicates the time spent in each phases of cocooning; the x-axis shows three phases of cocooning.

stage (egg, larva, pupa, and adult), larval tissue (midgut, central nervous system, silk gland, cuticle, and Malpighian tubules), before and after spinning, and the data were analyzed with the $2^{-\Delta\Delta Ct}$ method (Pfaffl, 2001).

Effect of 20E on the Expression of Fibroin-H, Fibroin-L, and P25

A 5 μg/μL solution of 20E (Sigma-Aldrich, St. Louis, MO, USA) was dissolved in 95% ethanol. Each 3th instar larva in the 20E-treatment group was injected with a dose of 500 ng 20E solution by micro 4 injector (World precision instruments). Each larva in the control group was injected with an equal volume of ethanol. Four injected larvae were randomly taken at 3, 6, and 12 h after injection, and the RNA of the silk gland (four biological replicates per treatment and each replicate included 20 silk glands) was separated to check the relative expression levels using qPCR, as described above.

SEM Observation of Cocoon

A cocoon was removed from the leaf surface, pasted on superconducting tape and sputter coated, and a hole (3.5 mm in diameter) was punched in each cocoon with a steel punching device. Then, the fibers were put into fine tubes and crushed perpendicular to the fiber lengths. The tubes with fibers were pasted on tape and sputter coated. Then the coated samples were observed in a SEM (Jeol Neoscope JCM-5000, Nikon, Tokyo, Japan) at 15 kV voltage. Both the 20E-treated cocoons and the control cocoons were observed with four replications each.

Data Analysis

To analyze the significance of time spent in each steps, the gene expression profile in different tissues and the relative transcripts of key genes related to 20E in three steps of spinning, we used the one-way ANOVA followed by a Tukey's honest significant difference multiple comparison test ($P < 0.05$). Other data in the treatment and control groups with four replications were analyzed using a Student's *t*-test ($^*P < 0.05$) to determine the significant differences by SPSS 20.0 (SPSS, Chicago, IL, USA), and data are presented as means ± SD.

RESULTS

The construction of a cocoon by a final instar larva of *P. xylostella* can be divided into three phases separable by their movement patterns: (1) selection of a pupation site and construction of a cocoon foundation, (2) formation of a scaffold cocoon, and (3) internal padding the scaffold cocoon. Before the *P. xylostella* larva begins cocoon construction it evacuates its gut, wanders for a period of time, and then precedes to pupate. It first makes a foundation for the cocoon by spinning a small amount of silk on the leaf surface. By strengthening interconnecting strands with applications of silk, the larva produces a fibrous network which forms the foundation for the incipient cocoon. The larva remains attached in this location until the spinning process is completed. Under laboratory conditions, each larva spent an average of 0.52 h in this initial phase of cocoon construction. More than half of the cocoon construction time was used to create the foundation (**Figures 1A,D**). The mature larva first spins a wide foundation of silk, and then gradually concentrates its spinning area to a size that is similar to the final cocoon. The larva spins a thin outer cocoon layer after completion of the foundation. Once the larva begins spinning, it continues without stopping and this process lasts an average of 3.23 h. During this time, it repeats the fixation and movement of the posterior half of the larval body with abdominal and caudal legs. The larva fixes the posterior half of the body, and spins by moving the anterior half of the body. The larva spends an average of 1.12 h for the construction of the outer cocoon (**Figures 1B,D**, **Supplementary Video 1**). In the final spinning cycle, the larva frequently interrupts its extension-recovery sequence and remains motionless. The

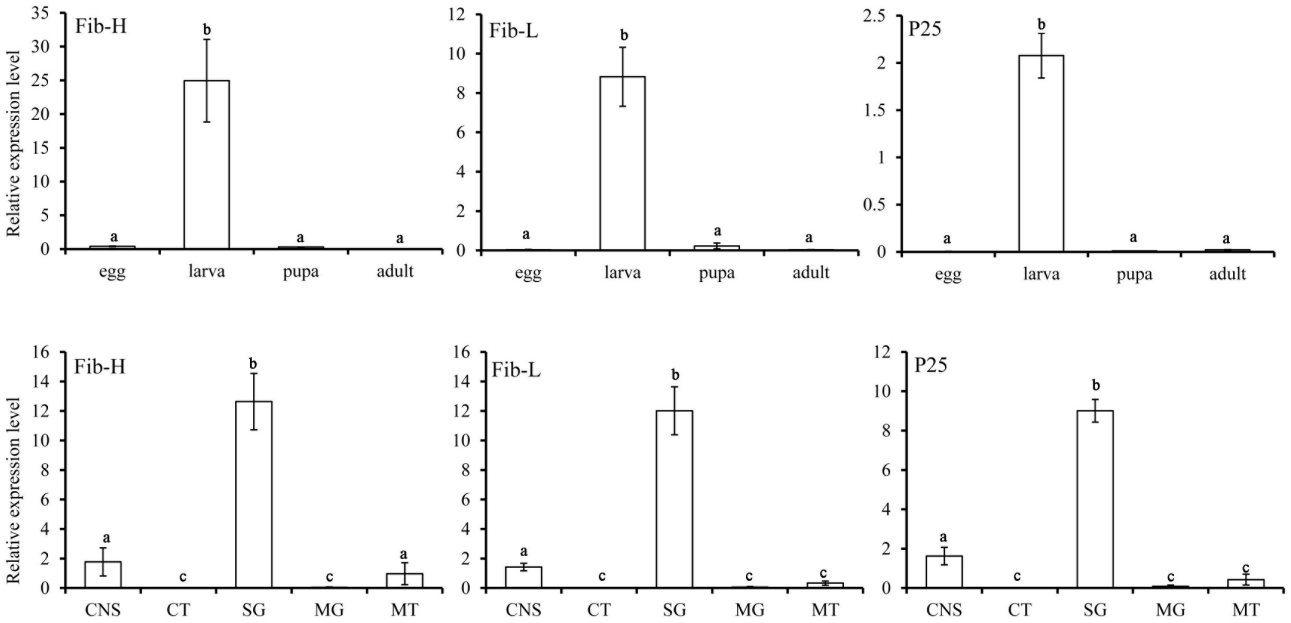

FIGURE 2 | Relative transcripts of *Fib-L, P25*, and *Fib-H* detected by qPCR indifferent developmental stages (egg, larva, pupa, and adult) and different larval tissues of *Plutella xylostella*. Abbreviations used on X-axis: MG, midgut; CNS, central nervous system including brain and ventral nerve cord; SG, silk gland; CT, cuticle; MT, Malpighian tubules.

intervals between the motionless periods gradually use greater proportions of successive, head-up cycles until the spinning behavior ends. At the time, the larva remains still in the head-up position. Padding the scaffold cocoon requires a longer time than the first two phases ($t = 11.14$; df = 1, 441; $P < 0.01$; **Figures 1C,D**).

Cloning Genes and Expression Profiling

P. xylostella Fib-L, *P25,* and the 5′end of *Fib-H*, *EcR, USP,* and *CYP18-A1* consisted of 252, 221, 106, 546, 415, and 532 amino acids, respectively (**Supplementary Figure 2**). These nucleotide sequences of *P. xylostella* were expressed as in GenBank, respectively (**Supplementary Table 1**). *Fib-L, P25,* and *Fib-H* genes are regulated in specific developmental stages and in specific tissues (**Figure 2**). Expression of the *Fib-L, P25,* and *Fib-H* genes occurs mainly in the final instar larvae but not in pupae. The maximum expression of *Fib-L, P25,* and *Fib-H* genes was observed in the silk gland tissue but none is expressed in other tissues (**Figure 2**). On *EcR*, *USP,* and *CYP18-A1* of *P. xylostella*, they were cloned and the phylogenetic analysis confirmed that *PxEcR*, *PxUSP,* and *PxCYP18-A1* are closely related to *EcR*, *USP,* and *CYP18-A1* from other lepidopteran insects, such as *B. mori*, *Manduca sexta*, *Spodoptera exigua* (**Supplementary Figure 1**).

Effect of 20E on Fibroin mRNA Expression and Cocoon Spinning Behavior

The effects of 20E and ethanol on the expression of *Fib-L*, *Fib-H,* and *P25* genes in silk glands are shown in **Figures 3A–C**. The transcript levels at the same time points (3, 6, and 12 h after treatment) and the expression levels of *Fib-L, Fib-H,* and *P25* genes were unaltered at 3 and 6 h after treatment. At 12 h after treatment, there was a decline in the expression levels of *Fib-L, Fib-H,* and *P25* genes in the 20E treatment compared with the control (**Figures 3A–C**). Hence, the 20E-treated group had significantly less spinning time than the control ($t = 13.11$; df = 1, 44; $P < 0.01$; **Figure 4A**), and also the 20E-treated larvae spun cocoons that were looser and the resulting pupae were smaller than the controls ($t = 11.54$; df = 1, 40; $P < 0.01$; **Figure 4B**). At same times, the 20E-treatment group showed that the cocoon became thinner leaving only some scaffold silks, while some of the filled silk disappeared (**Figure 5**).

In order to better understand the relationship between the spinning behavior and the 20E treatment (**Figures 6A–C**), we measured the expression levels of three key genes in the biosynthesis of 20E (the Halloween genes *Spo, Sad,* and *Shd*), its signaling pathway (*EcR* and *USP*) and the degradation of 20E (*CYP18-A1*) in the three periods of before, during and after spinning. The results showed that the expression level of three key genes related to 20E synthesis (*Spo, Sad,* and *Shd*) decreased significantly from high before spinning to low during spinning (**Figures 6D–F**). For the 20E receptor (*EcR* and *USP*), the expression level also decreased between before and during spinning (**Figures 6G,H**). In contrast, the expression of the key gene *CYP18-A1* related to degrading 20E, its expression levels were significantly higher during spinning and after spinning as compared to before spinning (**Figure 6I**).

DISCUSSION

Cocoons are a pivotal stage in the survival and reproduction of many arthropods. Most researches have focused on the cocoon

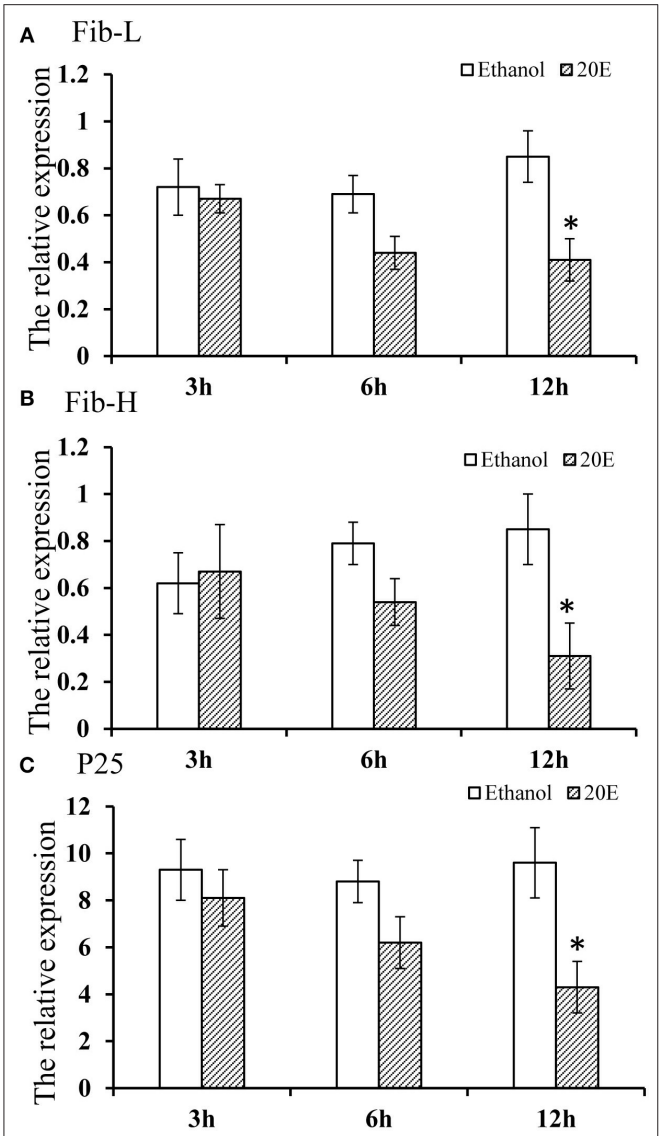

FIGURE 3 | (A–C) Effect of 20E on *Fib-L, P25*, and *Fib-H* expression of larval silk glands of *Plutella xylostella* larvae at 3, 6, and 12 h time points in the control (ethanol treated) and 20E-treated groups. Data are means SD. Significant differences were checked using Students *t*-test (*$P < 0.05$).

silk of silkworms and the dragline silk of spiders (Offord et al., 2016; Xu et al., 2018). However, many insect species produce cocoons using a wide variety of spinning behaviors. The spinning behavior of many insects has been described (Lounibos, 1975; Giebultowicz et al., 1980; Stuart and Hunter, 1995; Kiyosawa et al., 1999). The cocoon-spinning behavior of *P. xylostella* consists of three phases. The first phase begins with gut purging behavior. This is distinct, physiologically important and similar to the behavior of *B. mori* (Lounibos, 1975; Stuart and Hunter, 1995; Kiyosawa et al., 1999).

Silk cocoons are composed of fiber proteins (fibroins) and adhesive glue proteins (sericins), which provide a physical barrier that protects the pupa (Chen et al., 2012a,b, 2013). The cocoon silk fibroins consist of a large protein, named as the heavy chain fibroin (Fib-H), and two smaller proteins, named the light chain fibroin (Fib-L) and P25 (Chen et al., 2012b). Insects characterized three forms of silk fibroin structures. These are the Fib-H, Fib-L, and P25 in *B. mori* and *C. cephalonica* (Shimizu et al., 2007; Chaitanya and Aparna, 2010). Our study confirmed the presence of *Fib-L*, *P25,* and *Fib-H* in *P. xylostella*. We also cloned the *Fib-L*, *P25,* and a partial *Fib-H* cDNA from *P. xylostella*. Tissue-specific and developmental stage expression of *Fib-L, P25,* and *Fib-H* genes revealed that they are highly expressed in the silk gland only and this during the final larval stage (**Figure 2**). This indicates that the transcription of *Fib-L, P25,* and *Fib-H* genes is developmental and tissue-specific regulated (**Figure 2**). These results in *P. xylostella* are consistent with studies in *B. mori, S. derogate,* and *C. cephalonica* (Sehnal and Zurovec, 2004; Chaitanya and Aparna, 2010; Su et al., 2015). Molting occurs mainly in the larval stage, and 20E is the main hormone that regulates the molting process (Li et al., 2019). Based on our current findings and previous studies, the larval stage of *P. xylostella* was selected to study the effects of an exogenous treatment of 20E on these genes and the cocoon behavior and structure. We measured the effect of 20E on the expression of these genes in the larval silk glands. Ecdysteroids cause silk gland degeneration during the larva-pupa molt of *B. mori* (Shimizu et al., 2007). The larva-pupa molt is associated with ecdysteroids. The developmental pattern of *Fib-L, P25,* and *Fib-H* genes in *P. xylostella* showed that their expression dropped when 20E was used to treat the mature larva (**Figure 3**). Therefore, we speculated that 20E may regulate the spinning behavior of *P. xylostella.* Further, more evidence was obtained when we measured the expression levels of key genes related to 20E, including its biosynthesis, signaling and degradation, in three periods of spinning, namely before, during and after spinning (**Figures 6A–C**). The results showed that they changed significantly in the three different periods of spinning (**Figures 6D–I**). Specifically, the three 20E-biosynthesis Halloween genes *Spo*, *Sad,* and *Shd* decreased from high to low with the appearance of the spinning behavior (**Figures 6D–F**). Based on the results of Niwa and Niwa (2014), Niwa and Niwa (2016), and Peng et al. (2019) we believe that the expression profile of *Spo*, *Sad* and *Shd* corresponds with the 20E hormone titer, where an increase in expression corresponds to 20E biosynthesis and a hormone peak rise (Iga and Smagghe, 2010). Hence, Peng et al. (2019) reported on the role of *Shd* in *P. xylostella* where RNAi of Shd significantly reduced the 20E titer and resulted in a longer developmental duration and lower pupation of *P. xylostella* fourth-instar larvae. For *EcR* and *USP*, forming the nuclear ecdysone receptor heterodimer, their expression profile followed that of the 3 Halloween genes, where there was a strong drop from before to during the spinning (**Figures 6G,H**). This is according to our expectations as before it has been reported by different authors in multiple insects that the presence hormone receptor follows its hormone titer (reviewed in Fahrbach et al., 2012). In contrast, the expression of the 20E-degrading 26-hydroxylase enzyme CYP18-A1, which follows after a peak of 20E to reduce the hormone titer, was strongly increased with the appearance of the spinning behavior. Before it has been reported that 20E hormone was degraded and

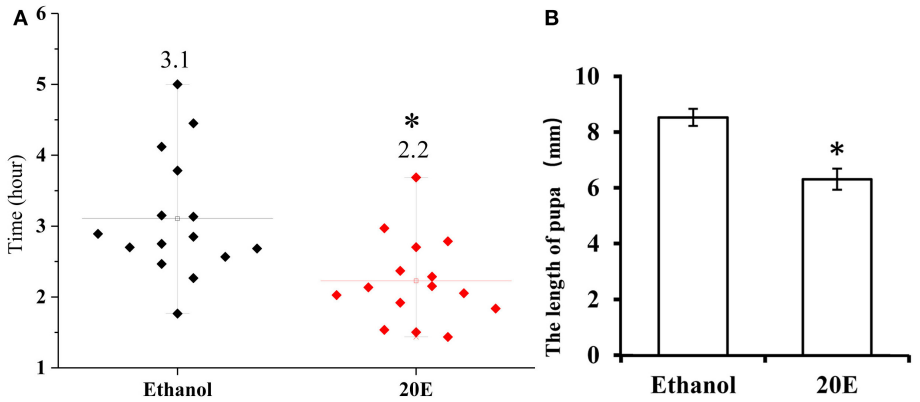

FIGURE 4 | (A) Cocoon-spinning times *Plutella xylostella* larvae in the control and the 20E-treated groups. **(B)** The pupa sizes in the control and the 20E-treatedgroups. Data are expressed as means SD. Significant differences were calculated using Students *t*-test (*$P < 0.05$). The left y-axis indicates the time spent of cocooning; the x-axis shows control and the 20E treated groups.

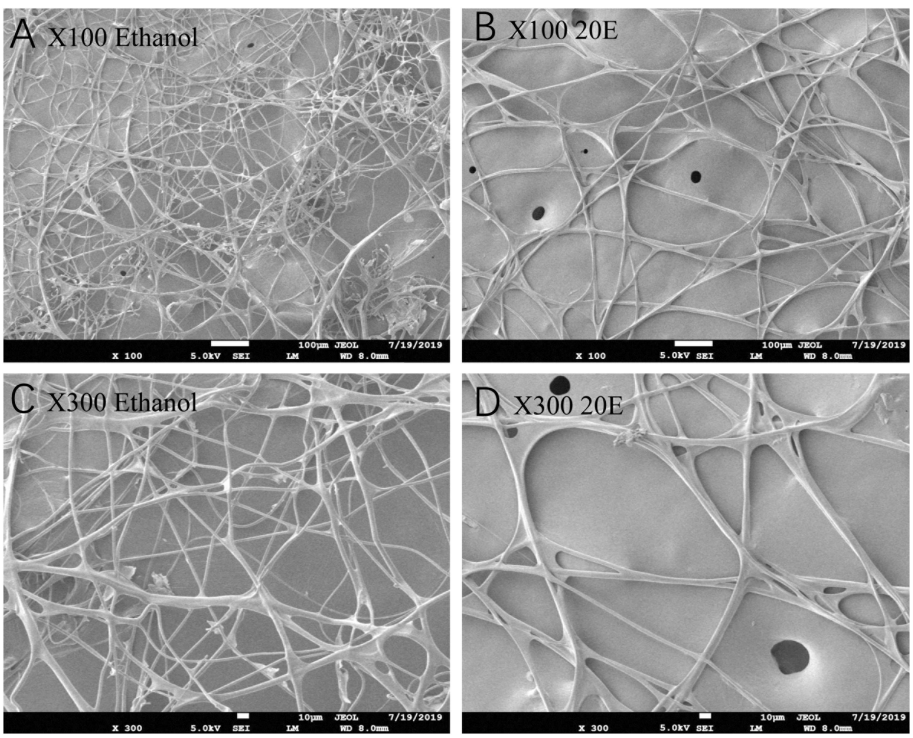

FIGURE 5 | Scanning electron microscopy micrographs of the cocoon looseness of *Plutella xylostella* in the control **(A,C)** and the 20E-treated groups **(B,D)** with 100 and 300 magnification.

cleared out of the insect body by CYP18-A1 enzyme and this is required for successful development, specifically post-apolysial processes as ecdysial behavior (Guittard et al., 2011; Li et al., 2014). Indeed this event is consistent with our expectation that the expression level of CYP18-A1 was significantly increased with the spinning behavior of *P. xylostella* (**Figure 6I**). All these research data demonstrated that the presence of 20E inhibits the cocoon spinning of diamondback moth. Therefore, the treatment of the final instar larvae with exogenous 20E significantly downregulated the expression of these genes in the silk gland and led to the construction of looser cocoons as we saw in the SEM (**Figure 5**). We also found that 20E reduced the spinning time (**Figure 4**) and this may be related to the acceleration of pupation. Hence, we note here that a series of studies has reported that 20E and ecdysteroid-mimicking compounds, which can be used as insect growth-regulatory insecticides to control pest insects (irac-online-org), can accelerate larval metamorphosis (Smagghe and Degheele, 1994; Smagghe et al., 2013; Scieuzo et al., 2018; Lin et al., 2019). Sometimes pupation occurs before the larva is mature, resulting in a smaller pupa than normal.

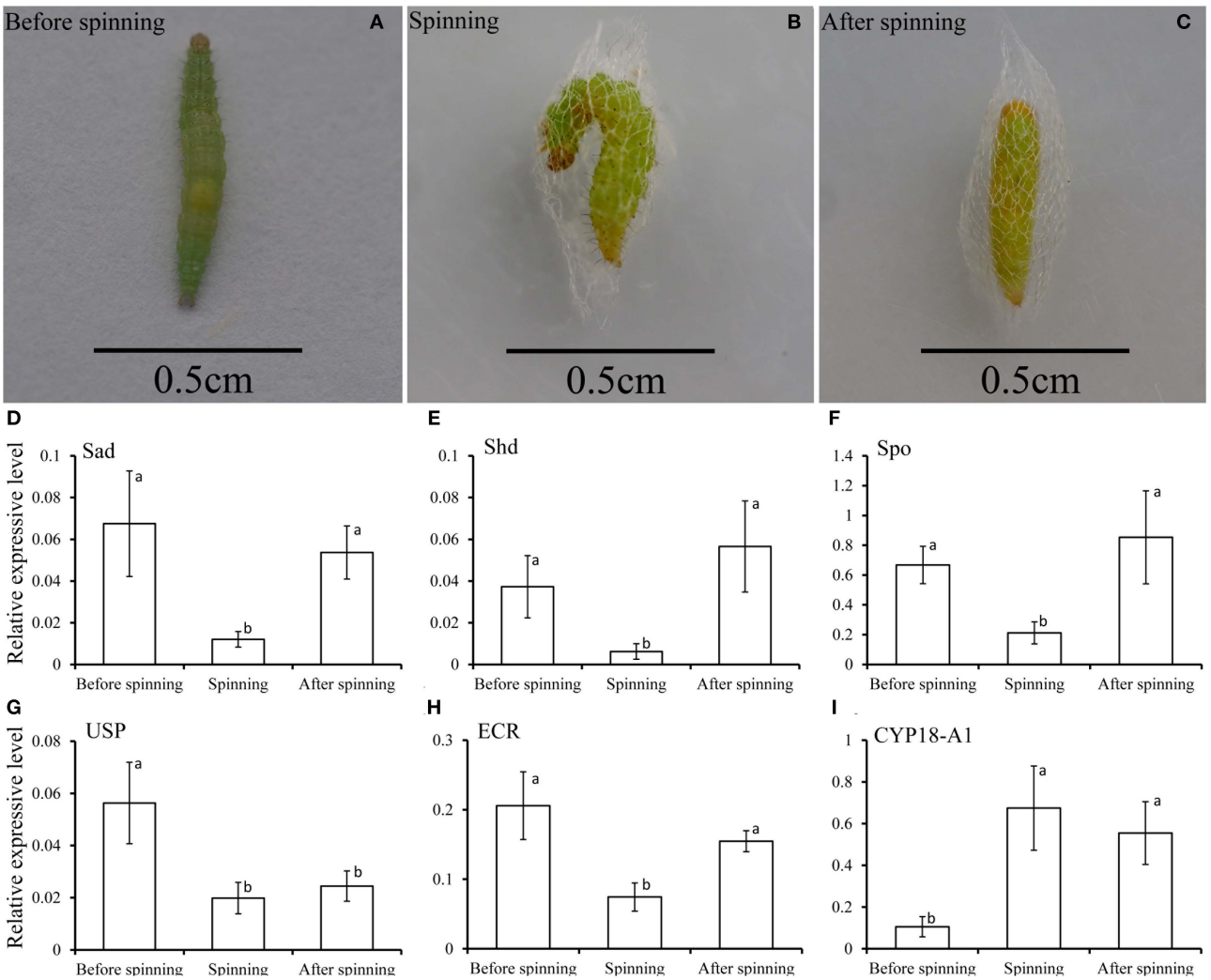

FIGURE 6 | (A–C) Respectively represent the before spinning, spinning, and after spinning of the diamondback moth larvae. **(D–I)** Relative transcripts of the key genes related to 20E, including 20E-biosynthesis (*Spo, Sad*, and *Shd*), signaling (*EcR* and *USP*), and degradation *(CYP18-A1)*, detected by qPCR at before, during and after spinning of *Plutella xylostella* mature larvae.

In summary, we described the entire cocoon-spinning process by video-recording and the exact steps and movement, as well as the duration of the process. We also found 20E affected the cocoon-spinning and the structure of the cocoon through modulation of *Fib-L, P25,* and *Fib-H* at the mRNA level in the final instar *P. xylostella* larvae. More studies on cocoon silk-producing insect pests, the function of the cocoon, and the possible use of cocoon manipulation for pest management are needed.

DATA AVAILABILITY STATEMENT

The raw data supporting the conclusions of this article will be made available by the authors, without undue reservation.

AUTHOR CONTRIBUTIONS

YS, GS, and T-XL designed research. YS performed all of the experiments with the help of G-LL and X-LF provided the materials. YS, G-LL, X-LF, and MK analyzed data. YS, MK, GS, and T-XL wrote the paper. All authors contributed to the article and approved the submitted version.

FUNDING

This study was supported by National Natural Science Foundation of China Youth Fund (32001907) and Qingdao Agricultural University High-level Talent Fund (665-1117002; 663-1119002).

SUPPLEMENTARY MATERIAL

The Supplementary Material for this article can be found online at: https://www.frontiersin.org/articles/10.3389/fphys.2020.574800/full#supplementary-material

Supplementary Figure 1 | Phylogenetic analysis of ECR, USP, and CYP18-A1 homologs from different insect species based on amino acid sequences.

Supplementary Figure 2 | Multiple alignments of Fib-L, P25, and a partial of Fib-H in *Bombyx mori, Corcyra cephalonica*, and *Plutella xylostella*.

Supplementary Video 1 | The video of diamondback moth larvae spinning and cocooning.

Supplementary Table 1 | Primer sequences used in this study.

REFERENCES

Boulet-Audet, M., Holland, C., Gheysens, T., and Vollrath, F. (2016). Dry-spun silk produces native-like fibroin solutions. *Biomacromolecules* 17, 3198–3204. doi: 10.1021/acs.biomac.6b00887

Chaitanya, R. K., and Aparna, D. G. (2010). Light chain fibroin and P25 genes of *Corcyra cephalonica*: molecular cloning, characterization, tissue-specific expression, synchronous developmental and 20-hydroxyecdysone regulation during the last instar larval development. *Gen. Comp. Endocr.* 167, 113–121. doi: 10.1016/j.ygcen.2010.02.007

Chen, F., Hesselberg, T., Porter, D., and Vollrath, F. (2013). The impact behaviour of silk cocoons. *J. Exp. Biol.* 216, 2648–2657. doi: 10.1242/jeb.082545

Chen, F., Porter, D., and Vollrath, F. (2012a). Silk cocoon (*Bombyx mori*): Multi-layer structure and mechanical properties. *Acta Biomater.* 8, 2620–2627. doi: 10.1016/j.actbio.2012.03.043

Chen, F., Porter, D., and Vollrath, F. (2012b). Morphology and structure of silkworm cocoons. *Mat. Sci. Eng. C-Mater.* 32, 772–778. doi: 10.1016/j.msec.2012.01.023

Fahrbach, S. E., Smagghe, G., and Velarde, R. A. (2012). Insect nuclear receptors. *Annu. Rev. Entomol.* 57, 83–106. doi: 10.1146/annurev-ento-120710-100607

Giebultowicz, J. M., and Zdarek, J. U., Chróścikowska. (1980). Cocoon spinning behaviour in *Ephestia kuehniella*: Correlation with endocrine events. *J. Insect. Physiol.* 26, 0–464. doi: 10.1016/0022-1910(80)90116-X

Gilbert, L. (2008). *Drosophila* is an inclusive model for human diseases, growth and development. *Mol. Cell. Endocrinol.* 293, 25–31. doi: 10.1016/j.mce.2008.02.009

Guittard, E., Blais, C., Maria, A., Parvy, J. -P., Pasricha, S., Lumb, C., et al. (2011). CYP18A1, a key enzyme of Drosophila steroid hormone inactivation, is essential for metamorphosis. *Dev. Biol.* 349, 35–45. doi: 10.1016/j.ydbio.2010.09.023

Guo, X., Dong, Z., Zhang, Y., Li, Y., and Zhao, P. (2016). Proteins in the cocoon of silkworm inhibit the growth of *Beauveria bassiana*. *PLoS ONE* 11:e0151764. doi: 10.1371/journal.pone.0151764

Iga, M., and Smagghe, G. (2010). Identification and expression profile of Halloween genes involved in ecdysteroid biosynthesis in *Spodoptera littoralis*. *Peptides* 31, 456–467. doi: 10.1016/j.peptides.2009.08.002

Kiyosawa, M., Shirai, I. E., Kanekatsu, R., Miura, M., and Kiguchi, K. (1999). Cocoon spinning behavior in the silkworm, *Bombyx mori*: comparison of three strains constructing different cocoons in shape. *Zool. Sci.* 16, 215–223. doi: 10.2108/zsj.16.215

Li, S., Yu, X. Q., and Feng, Q. L. (2019). Fat body biology in the last decade. *Annu. Rev. Entomol.* 64, 315–333. doi: 10.1146/annurev-ento-011118-112007

Li, Z., Ge, X., Ling, L., Zeng, B., Xu, J., Asla, A. F., You, L., Palli, S. R., Huang, Y. P., and Tan, A. J. (2014). Cyp18a1 regulates tissue-specific steroid hormone inactivation in *Bombyx mori*. *Insect Biochem. Molec. Biol.* 54, 33–41. doi: 10.1016/j.ibmb.2014.08.007

Lin, X. Y., Schutter, K. D., Chafino, S., Franch-Marro, X., Martin, D., and Smagghe, G. (2019). Target of rapamycin (TOR) determines appendage size during pupa formation of the red flour beetle *Tribolium castaneum*. *J. Insect Physiol.* 117, 0022–1910. doi: 10.1016/j.jinsphys.2019.103902

Lounibos, L. P. (1975). The cocoon spinning behaviour of the Chinese oak silkworm, *Antheraea pernyi*. *Anim. Behav.* 23, 843–853. doi: 10.1016/0003-3472(75)90109-8

Lounibos, L. P. (1976). Initiation and maintenance of cocoon spinning behaviour by saturniid silkworms. *Physiol. Entomol.* 1, 195–206. doi: 10.1111/j.1365-3032.1976.tb00961.x

Miao, Y. G., Shi, L. G., and Nair, K. S. (2004). Ecdysteroid as a mediator in the regulation of silk protein synthesis and its influence on silkworm (Lepidoptera) genome. *J. Appl. Entomol.* 128, 348–353. doi: 10.1111/j.1439-0418.2004.00854.x

Namiki, T., Niwa, R., Sakudoh, T., Shirai, K., Takeuchi, H., and Kataoka, H. (2005). Cytochrome 450 CYP307A1/Spook: A regulator for ecdysone synthesis in insects. *Biochem. Bioph. Res. Co.* 337, 367–374. doi: 10.1016/j.bbrc.2005.09.043

Niwa, Y., and Niwa, R. S. (2014). Neural control of steroid hormone biosynthesis during development in the fruit fly *Drosophila melanogaster*. *Genes Genet. Syst.* 89, 27–34. doi: 10.1266/ggs.89.27

Niwa, Y. S., and Niwa, R. (2016). Transcriptional regulation of insect steroid hormone biosynthesis and its role in controlling timing of molting and metamorphosis. *Dev. Growth Differ.* 58, 94–105. doi: 10.1111/dgd.12248

Offord, C., Vollrath, F., and Holland, C. (2016). Environmental effects on the construction and physical properties of *Bombyx mori* cocoons. *J. Mate. Sci.* 51, 10863–10872. doi: 10.1007/s10853-016-0298-5

Peng, L., Wang, L., and Zou, M. M. (2019). Identification of halloween genes and RNA interference-mediated functional characterization of a Halloween gene Shadow in *Plutella xylostella*. *Front. Physiol.* 10:1120. doi: 10.3389/fphys.2019.01120

Petryk, A., Warren, J. T., Marques, G., Jarcho, M. P., Gilbert, L. I., Kahler, J., et al. (2003). Shade is the *Drosophila* P450 enzyme that mediates the hydroxylation of ecdysone to the steroid insect molting hormone 20-hydroxyecdysone. *Proc. Natl. Acad. Sci. U.S.A.* 100, 13773–13778. doi: 10.1073/pnas.2336088100

Pfaffl, M. W. (2001). A new mathematical model for relative quantification in real-time RT–PCR. *Nucleic Acids Res.* 29:e45. doi: 10.1093/nar/29.9.e45

Scieuzo, C., Nardiello, M., and Salvia, R. (2018). Ecdysteroidogenesis and development in, *Heliothis virescens*, (Lepidoptera: Noctuidae): focus on PTTH-stimulated pathways. *J. Insect Physiol.* 107, 57–67. doi: 10.1016/j.jinsphys.2018.02.008

Sehnal, F., and Zurovec, M. (2004). Construction of silk fiber core in Lepidoptera. *Biomacromolecules* 5, 666–674. doi: 10.1021/bm0344046

Shi, Y., Jiang, H. B., Gui, S. H., Liu, X. Q., Pei, Y. X., Li, X., et al. (2017). Ecdysis triggering hormone signaling (ETH/ETHR-a) is required for the larva-larva ecdysis in *Bactrocera dorsalis* (Diptera: Tephritidae). *Front. Physiol.* 8:587. doi: 10.3389/fphys.2017.00587

Shimizu, K., Ogawa, S., Hino, R., Adachi, T., Tomita, M., and Yoshizato, K. (2007). Structure and function of 5'-flanking regions of *Bombyx mori* fibroin heavy chain gene: Identification of a novel transcription enhancing element with a homeodomain protein-binding motif. *Insect Biochem. Mole. Biol.* 37, 713–725. doi: 10.1016/j.ibmb.2007.03.016

Smagghe, G., and Degheele, D. (1994). Effects of the ecdysteroid agonists RH 5849 and RH 5992, alone and in combination with a juvenile hormone analogue, pyriproxyfen, on larvae of *Spodoptera exigua*. *Entomol. Exp. Appl.* 72,115–123. doi: 10.1111/j.1570-7458.1994.tb01809.x

Smagghe, G., Gomez, L. E., and Dhadialla, T. S. (2013). The bisacylhydrazine insecticides for selective pest control. *Adv. Insect Physiol.* 43,163–249. doi: 10.1016/B978-0-12-391500-9.00002-4

Stuart, A. E., and Hunter, F. F. (1995). A re-description of the cocoon-spinning behaviour of *Simulium vittatum* (Diptera: Simuliidae). *Ital. J. Zool.* 7, 363–377. doi: 10.1080/08927014.1995.9522944

Su, H., Cheng, Y., Wang, Z., Li, Z., Stanley, D., and Yang, Y. (2015). Silk gland gene expression during larval-pupal transition in the cotton leaf roller *Sylepta derogata* (Lepidoptera: Pyralidae). *PLoS ONE* 10:e0136868. doi: 10.1371/journal.pone.0136868

Sun, M. J., Liu, Y., Walker, W. B., Liu, C. C., Lin, K. J., Gu, S. H., Zhang, Y. J., Zhou, J. J., and Wang, G. R. (2013). Identification and characterization of

pheromone receptors and interplay between receptors and pheromone binding proteins in the diamondback moth, *Plutella xylostella*. *PLoS ONE* 8:e62098. doi: 10.1371/journal.pone.0062098

Sutherland, T. D., Young, J. H., Weisman, S., Hayashi, C. Y., and Merritt, D. J. (2010). Insect silk: one name, many materials. *Annu. Rev. Entomol.* 55, 171–188. doi: 10.1146/annurev-ento-112408-085401

Tang, W. Q., Yu, L. Y., He, W. Y., Yang, G., Ke, F. S., Baxter, S. W., et al. (2014). DBM-DB: the diamondback moth genome database. *Database* 2014:bat087. doi: 10.1093/database/bat087

Van der Kloot, W. G., and Williams, C. M. (1953). Cocoon construction by the *Cecropia* silkworm. I. the role of the external environment. *Behaviour* 5, 141–156. doi: 10.1163/156853953X 00087

Xu, J., Dong, Q. L., Yu, Y., Niu, B. L., Ji, D. F., Li, M. W., Huang, Y. P., Chen, X., and Tan, A. J. (2018). Mass spider silk production through targeted gene replacement in *Bombyx mori*. *Proc. Natl. Acad. Sci. U.S.A.* 115, 8757–8762. doi: 10.1073/pnas.1806805115

Yagi, N. (1926). The cocooning behavior of a *saturnian caterpillar* (*Dictyoploca japonica*); a problem in analysis of insect conduct. *J. Exp. Zool.* 46, 245–259. doi: 10.1002/jez.1400460205

Yokoyama, T. (1951). Studies on the cocoon-formation of the silkworm, *Bombyx mori*. *Bull. Seri. Exp. Stat.* 13, 183–260.

Conflict of Interest: The authors declare that the research was conducted in the absence of any commercial or financial relationships that could be construed as a potential conflict of interest.

frontiers in Physiology

ORIGINAL RESEARCH
published: 03 February 2021
doi: 10.3389/fphys.2021.638026

ATG3 Is Important for the Chorion Ultrastructure During Oogenesis in the Insect Vector *Rhodnius prolixus*

Anna Santos[1] *and Isabela Ramos*[1,2]*

[1] *Laboratório de Bioquímica de Insetos, Instituto de Bioquímica Médica Leopoldo de Meis, Universidade Federal do Rio de Janeiro, Paraná, Brazil,* [2] *Instituto Nacional de Ciência e Tecnologia em Entomologia Molecular – INCT-EM/CNPq, Rio de Janeiro, Brazil*

In insects, the last stage of the oogenesis is the choriogenesis, a process where the multiple layers of the chorion are synthesized, secreted, and deposited in the surface of the oocytes by the follicle cells. The chorion is an extracellular matrix that serves as a highly specialized protective shield for the embryo, being crucial to impair water loss and to allow gas exchange throughout development. The E2-like enzyme ATG3 (autophagy related gene 3) is known for its canonical function in the autophagy pathway, in the conjugation of the ubiquitin-like ATG8/LC3 to the membranes of autophagosomes. Although the ATGs were originally described and annotated as genes related to autophagy, additional functions have been attributed to various of these genes. Here, we found that *Rhodnius prolixus* ATG3 is highly expressed in the ovaries of the adult vitellogenic females. Parental RNAi depletion of ATG3 resulted in a 15% decrease in the oviposition rates of depleted females and in the generation of unviable eggs. ATG3-depleted eggs are small and present one specific phenotype of altered chorion ultrastructure, observed by high resolution scanning electron microscopy. The amounts of the major chorion proteins Rp30, Rp45, Rp100, and Rp200 were decreased in the ATG3-depleted chorions, as well as the readings for dityrosine cross-linking and sulfur, detected by fluorescence emission under ultraviolet excitation and X-ray elemental detection and mapping. Altogether, we found that ATG3 is important for the proper chorion biogenesis and, therefore, crucial for this vector reproduction.

Keywords: ATG3, choriogenesis, *Rhodnius prolixus*, vector biology, autophagy related 3

OPEN ACCESS

Edited by:
Xanthe Vafopoulou,
York University, Canada

Reviewed by:
Sheila Ons,
National University of La Plata, Argentina
Maria-Dolors Piulachs,
Consejo Superior de Investigaciones Científicas (CSIC), Spain

****Correspondence:***
Isabela Ramos
isabela@bioqmed.ufrj.br

Specialty section:
This article was submitted to Invertebrate Physiology, a section of the journal Frontiers in Physiology

Received: *04 December 2020*
Accepted: *12 January 2021*
Published: *03 February 2021*

Citation:
Santos A and Ramos I (2021) ATG3 Is Important for the Chorion Ultrastructure During Oogenesis in the Insect Vector Rhodnius prolixus. Front. Physiol. 12:638026. doi: 10.3389/fphys.2021.638026

INTRODUCTION

The ability of insects to produce a large number of eggs in a short period of time is one of the characteristics that contributes to their remarkable adaptive success in inhabiting many different habitats and acting as vectors of human diseases. Exploring the specific mechanisms of egg formation and embryo development should be of great importance to further understand the reproductive biology of various vectors and to elaborate new strategies for vector population control (Pereira et al., 2020). This is especially important for the neglected, vector borne tropical diseases, which are endemic to developing countries such as dengue fever and Chagas Disease[1].

[1] www.who.int/neglected_diseases/en/

In oviparous animals, including insects, the female germline cells enter meiosis, while they differentiate into a highly specialized cell designed to support embryo development after fertilization. The cytoplasm of a mature oocyte is characterized by the presence of accumulated maternal mRNAs, ribosomes and mitochondria, as well as set of endocytic-originated vesicles named yolk organelles that usually occupy most of the oocyte volume (Kerkut and Gilbert, 1985; Kunkel and Nordin, 1985; Alberts et al., 2002). In the latest stage of oogenesis, the follicle cells (a single layered tissue of professional secretory cells that surround the oocytes during oogenesis) go through the major metabolic challenge of rapidly synthesizing and secreting the chorion layers (Huebner and Anderson, 1972; Wu et al., 2008). After choriogenesis the mature oocyte is ready to be fertilized and laid in the environment. In species that colonize land, the chorion layers allow gas exchange and serve as a shielding barrier to impair water loss during embryogenesis (Kerkut and Gilbert, 1985; Bomfim et al., 2017). The process of chorion formation and its complex ultrastructure represent a remarkable model for *in vivo* studies of biogenesis and assembly of the network of macromolecules in an extracellular matrix. In *Drosophila*, studies about choriogenesis focus mostly on the programed gene-specific transcriptional activation of chorion genes (Tootle et al., 2011; Velentzas et al., 2018) and on the biochemical characterization of chorion proteins, mainly by mass spectrometry (Fakhouri et al., 2006). In *Rhodnius prolixus*, the chorion ultrastructure and permeability properties were previously explored (Beament, 1948; Dias et al., 2013; Bomfim et al., 2017; Bomfim and Ramos, 2020) and the identification of the specific chorion proteins Rp30 and Rp45, the latter associated to an antifungal activity, were also described (Bouts et al., 2007).

Autophagy is an intracellular degradation pathway in which target organelles or complexes are sequestered by an expanded double membrane vesicle generating an organelle named autophagosome. After fusion of the autophagosome with the lysosome, the degradation products of autophagy are reutilized by the cell as a source of building blocks for the synthesis of new macromolecules (Klionsky et al., 2016). Autophagy is a well-conserved mechanism throughout evolution in eukaryotic cells and it is carried out by a set of conserved autophagy related genes (ATGs) that can be found from yeast to mammals. The autophagy pathway includes two essential ubiquitin-like conjugation systems (Mizushima et al., 1998; Ichimura et al., 2000; Ohsumi, 2001). In one of them, the ubiquitin-like molecule ATG12 is activated by the E1-like enzyme ATG7, transferred to the E2-like conjugating enzyme ATG10, and in the end attached to ATG5 (Mizushima et al., 1998; Tanida et al., 1999; Nemoto et al., 2003). In the other, ATG7 and the E2-like enzyme ATG3 conjugate the ubiquitin-like ATG8/LC3 to the lipid phosphatidylethanolamine in the autophagosomes (Tanida et al., 1999, 2002; Ichimura et al., 2000; Ohsumi, 2001). Although the ATGs have been used for the study of autophagy since their discovery in 1993 in *Saccharomyces cerevisiae* (Tsukada and Ohsumi, 1993), additional non-autophagic functions have been assigned to these genes (Subramani and Malhotra, 2013; Galluzzi and Green, 2019). It was recently identified that ATG3 also regulates late endosomal trafficking, cell proliferation, LC3-associated phagocytosis and exosome release (Sanjuan et al., 2007; Martinez et al., 2015; Murrow and Debnath, 2015, 2018; O'Sullivan et al., 2016).

Here, we found that *R. prolixus* ATG3 is highly expressed in the ovaries of vitellogenic females. RNAi depletion of ATG3 resulted in a small decrease in the oviposition rates and the generation of unviable eggs. ATG3-depleted eggs were small and presented a specific phenotype of altered chorion ultrastructure as seen by high resolution scanning electron microscopy. Although the major chorion proteins Rp30, Rp45, Rp100, and Rp200 were detected in the ATG3-depleted chorions, their levels were reduced. The readings for cross-linking of chorion proteins, as seen by the reduced fluorescence emission under ultraviolet excitation, which indicates lower levels of dityrosine crosslinking were also reduced. Finally, ATG3-depleted chorions were also deficient in sulfur, a marker for protein presence and potential cysteine protein cross-linking, as detected by X-ray elemental detection and mapping. Altogether, we found that ATG3 is important for the proper chorion biogenesis and, therefore, crucial for this vector reproduction.

MATERIALS AND METHODS

Ethics Statement

All animal care and experimental protocols were approved by guidelines of the institutional care and use committee (Committee for Evaluation of Animal Use for Research from the Federal University of Rio de Janeiro, CEUA-UFRJ #01200.001568/2013-87, order number 155/13), under the regulation of the national council of animal experimentation control (CONCEA). Technicians dedicated to the animal facility conducted all aspects related to animal care under strict guidelines to ensure careful and consistent animal handling.

Insects

Insects were maintained at a 28 ± 2°C controlled temperature and relative humidity of 70–80%. Mated females are fed for the first time (as adult insects) in live-rabbit blood 14 to 21 days after the 5th instar nymph to adult ecdysis. After the first blood feeding, all adult insects in our insectarium are fed every 21 days. For all experiments, mated females of the second or third blood feeding were used. All animal care and experimental protocols were approved by the guidelines previously described in the ethics statement.

Gene Identification

The sequence of the *R. prolixus* ATG3 transcript was identified as one single isoform of the gene *RpATG3* (RPRC008742) corresponding to the transcript RPRC008742-RA in the *R. prolixus* genome assembly (RproC3.4) available at Vector Base[2]. The identification was accessed by similarity to the *Drosophila melanogaster* ATG3 sequence (Gene ID 40044) using tBlastn under default settings. Conserved domains were detected

[2]https://www.vectorbase.org/

using PFAM. Alignments of the ATG3 protein sequence to the ATG3 sequences from different species were performed using Clustal Omega.

Extraction of RNA and cDNA Synthesis

All organs were dissected 7 days after blood meal and homogenized in Trizol reagent (Invitrogen) for total RNA extraction. Reverse transcription reaction was carried out using the High Capacity cDNA Reverse Transcription Kit (Applied Biosystems), using 1 μg of total RNA after RNase-free DNase I (Invitrogen) treatment, all according to the manufacturer's protocol.

PCR/RT-qPCR

Specific primers for *R. prolixus* ATG3 sequence were designed to amplify a 203 bp fragment in a PCR using the following cycling parameters: 5 min at 95°C, followed by 35 cycles of 30 s at 95°C, 30 s at 52°C and 30 s at 72°C and a final extension of 15 min at 72°C. Amplifications were observed in 2% agarose gels. Quantitative PCR (RT-qPCR) was performed in a StepOne Real-Time PCR System (Applied Biosystems) using SYBR Green PCR Master Mix (Applied Biosystems) under the following conditions: 10 min at 95°C, followed by 40 cycles of 30 s at 95°C and 30 s at 60°C. RT-qPCR amplification was performed using the specific primers listed on **Supplementary Table S1**. The relative expressions were calculated using the delta C_t (cycle threshold) obtained using the reference gene 18S (RPRC017412) and calculated 2^{-dCt}. For all RT-qPCRs the samples for each biological replicate were dissected from a pool of three insects.

RNAi Depletion

dsRNA was synthesized by MEGAScript RNAi Kit (Ambion Inc.) using primers for *R. prolixus ATG3* specific gene amplification with the T7 promoter sequence designed to target a region of 647 bp. Unfed adult females were injected between the second and third thoracic segments using a 10 μL Hamilton syringe with 1 μg dsRNA (in a volume of 1 μL) and fed 2 days later. Seven days after the blood feeding, the knockdown efficiency was confirmed by RT-qPCR. A fragment of 808 bp of the Escherichia *coli MalE* gene (Gene ID: 948538) included in the control plasmid LITMUS 28iMal obtained from the HiScribe RNAi Transcription kit (New England BioLabs) was amplified by PCR using a T7 promoter-specific primer, targeting the opposing T7 promoters of the vector. The cycling conditions were: 10 min at 95°C, followed by 35 cycles of 30 s at 95°C, 30 s at 52°C and 60 s at 72°C and a final extension of 15 min at 72°C. The amplified fragment was used as a template for the synthesis of the control dsRNA (dsMal). Adult females injected with dsRNAs were fed and transferred to individual vials.

Evaluation of Survival and Egg Laying

All groups injected with dsRNAs (10 insects per batch, 3–4 batches per treatment) were kept separately in transparent plastic jars. Mortality was recorded daily. Egg laying was recorded weekly. Additional measurements are described below. Three experiments were performed, each of them containing at least 10 insects per treatment.

Chorion Protein Extraction and SDS-PAGE

A total of 0 to 72 h eggs were collected and their chorions were carefully washed in 0.01 M Tris/HCl pH 8.4 several times. Following, the chorions from five control and ATG3-depleted eggs were treated as previously described by Bouts et al. (2007). Briefly, the chorions were homogenized in 8 M urea, 360 mM Tris/HCl (pH 8.4) and 30 mM dithiothreitol using a glass/teflon potter Elvehjem homogenizer and solubilized at room temperature for 10 min. The samples were centrifuged at 12,000 *g* for 10 min, and the supernatant was collected and stored at −20°C for further use. The small precipitate obtained during centrifugation was discarded. 10 μl of the urea-extracted proteins were applied to a 10% SDS-PAGE and stained with silver nitrate (Merril et al., 1981). Densitometry was performed using ImageJ.

Field Emission Scanning Electron Microscopy (SEM)

Freshly laid eggs were carefully collected and fixed by immersion in 2.5% glutaraldehyde (Grade I) and 4% freshly prepared formaldehyde in 0.1 M cacodylate buffer, pH 7.3. Samples were washed in cacodylate buffer, dehydrated in an ethanol series, critical point dried and coated with a thin layer of gold. Models were observed in a FEI Quanta 250 field emission scanning electron microscope operating at 15 kV.

Dityrosine Chorion Fluorescence

Eggs were photographed using a Zeiss Axiozoom V.16 stereomicroscope using a DAPI filter set for dityrosine fluorescence detection, as previously described by Dias et al. (2013). Comparison of fluorescence levels was performed using the same objectives and exposure times. For fluorescence quantification, images of eight eggs each from control and depleted females were analyzed with ImageJ software. To calculate the approximate chorion fluorescence (CF), we used the following formula: CF = integrated density − (area of selected egg × mean fluorescence of background readings).

Energy Dispersive X-Ray Microanalysis and Elemental Mapping

For X-ray microanalysis, the eggs were collected at times ranging from 0 to 24 h after oviposition and were directly examined in a Hitachi TM4000Plus scanning electron microscope operating at 15 kV. For spectra and elemental mapping, X-rays were collected for 100 s using a Silicon drift detector (SDD) on a 0 to 10 KeV energy range with a resolution of 158 eV.

RESULTS

R. prolixus ATG3 Is Highly Expressed in the Ovaries and Oocytes During Vitellogenesis

Rhodnius prolixus ATG3 encodes a predicted protein with 309 amino acid residues and 76/64% similarity/identity with

the human ATG3. All the expected ATG3 conserved domains (PF03986, Autophagy_N; PF03987, Autophagy_act_C; PF10381, Autophagy_C) were detected (**Supplementary Figure S1**). Using quantitative PCR (RT-qPCR) we found that the ovary of vitellogenic females express an average of 3× more ATG3 than the midgut and fat body (**Figure 1A**). Within the ovary, ATG3 mRNA was detected in the tropharium (structure where the germ cell cluster and the nurse cells are located) and in all stages of the developing follicles (pre-vitellogenic, vitellogenic, and chorionated) (**Figure 1B**).

RNAi Depletion of ATG3 Results in Decreased Oviposition and Altered Chorion Ultrastructure

To investigate the role of ATG3 in the ovary, we synthesized one specific double-stranded RNA designed to target the sequence of *R. prolixus* ATG3 and injected it directly into the females hemocoel, 2 days before the blood meal. RT-qPCR showed that the ATG3 knockdown was efficient, with an average of 95% mRNA silencing in the ovaries of vitellogenic females. The bacterial *MalE* gene was used as a control dsRNA (dsMal) (**Figure 2A**). Because ATG3 is one of the enzymes responsible for the conjugation of ATG8/LC3 to the autophagosome membrane, we performed immunoblottings to address the ATG8 lipidation status in control and depleted ovaries. We found that depletion of ATG3 resulted in decreased levels of ATG8/LC3 lipidation (ATG8-II), as expected (**Figure 2B**), suggesting that autophagosomes were not properly formed in the ovaries of ATG3-depleted females. The depletion of ATG3 did not result in alterations in the main physiological characteristics of the adult female such as digestion, as measured by the weight of the insects (**Figure 3A**), and longevity (median survival of 28 days for control females and 27 days for depleted females, $p > 0.05$) (**Figure 3B**). To investigate the role of ATG3 during oogenesis, we quantified the oviposition in control and ATG3-depleted females and maintained the collected eggs under control conditions to ensure embryo development. Our results show a 18% decrease in the total number of eggs laid by ATG3-depleted females (**Figure 3C**). In addition to the reduced oviposition, we observed that the ATG3-depleted females laid eggs presenting two main types of abnormal phenotypes, shown in **Figure 4A**. Per female, an average of four eggs (10% of the total number of eggs) were smaller than controls but showed no apparent defects in the chorion structure (phenotype 1), and 5 eggs (12% of the total number of eggs) were smaller than controls and showed evident defects in the chorion structure (phenotype 2) (**Figures 4A,B**). In total, we observed a 70% decrease in the embryo viability of ATG3-depleted females when compared to control females. All the eggs that presented one of the phenotypes described above were unviable and only 30% of the eggs that presented an apparent normal morphology were viable (**Figure 4C**).

To further examine the ATG3 chorion defects (phenotype 2), control and ATG3-depleted eggs were processed for high resolution SEM and the ultrastructure of the external surface of the chorion was observed. We found that ATG3-depleted eggs presented major alterations in the structure of the operculum at the anterior pole of the egg (**Figures 5A** and **D**, arrowheads) (Tuft, 1950). Also, as shown in **Figures 5A** and **D**, the malformations in the chorion of the ATG3-depleted eggs result in leaking of internal contents out of the operculum (**Figure 5D**, arrow), and the embryo to dry out within a few hours after oviposition (not shown). As for the rest of the egg surface, control eggs are covered by a stiff chorion marked by the presence of irregular pentagonal or hexagonal depressions, which are demarcated by the spaces where the follicle cells were placed during oogenesis. In contrast ATG3-depleted eggs present regions where this general outline of the chorion structure is strongly altered (**Figures 5B–F**, red asterisks).

The Altered Chorion Ultrastructure Is Due to Altered Protein Levels and Reduced Protein-Crosslinking

To further investigate the nature of the defects in the chorion ultrastructure in ATG3-depleted eggs, we performed urea extractions of the main chorion proteins from control and ATG3-depleted insects, as previously described by Bouts et al. (2007). We found that ATG3-depleted chorions possess reduced levels of all the major chorion proteins detected by SDS-PAGE (**Figures 6A,B**). Rp30 and Rp100 are 90% decreased in ATG3-depleted eggs, whereas Rp45 and Rp200 are reduced only by approximately 50% (**Figure 6B**). Additionally, it is known that the hardening and waterproofing properties of the chorion in *R. prolixus* involve protein cross-linking through peroxidase-mediated oxidation of tyrosine residues (Li et al., 1996; Dias et al., 2013). To investigate the cross-linking properties in the chorion defective eggs, we measured the level of fluorescence of the ATG3-depleted chorions under ultraviolet excitation, a property of dityrosine formed by oxidative protein cross-linking (Neff et al., 2000; Andersen and Roepstorff, 2005). We found that the ATG3 defective chorions showed an average of 60% decrease in fluorescence emission under ultraviolet excitation (**Figures 6C,D**). Furthermore, X-ray microanalysis showed that the chorion possesses significant amounts of carbon, oxygen, and sulfur. The latter is a commonly used element-marker for the presence of proteins (**Figures 7A,B**). Elemental mapping of the image shown in **Figure 7A**, showed that these elements are evenly distributed over the chorion surface (**Figures 7A–C**). For the ATG3-depleted eggs, the content of sulfur in the chorion was generally reduced (**Figures 7D,E**), and the elemental mapping of the image in **Figure 7D**, showed that sulfur is mostly absent in the regions of the chorion that are present in the most altered ultrastructure (**Figures 7D–F**), indicating that the ATG3 abnormal ultrastructure is likely the result of both reduced protein levels and crosslinking.

DISCUSSION

In 2005, the WHO created the department of the neglected tropical diseases (NTDs), recognizing their importance and with the objective of managing their incidence. *R. prolixus* is a vector of Chagas disease, an important NTD in endemic regions of Latin American countries. Currently 7 million people are estimated to

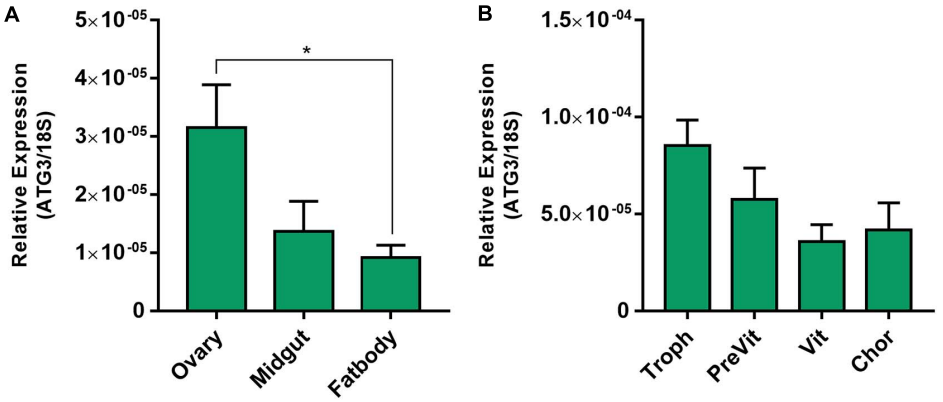

FIGURE 1 | ATG3 is highly expressed in the ovaries and developing follicles of vitellogenic females. **(A)** RT-qPCR showing the ATG3 mRNA quantification in the different organs of vitellogenic females dissected 7 days after the blood meal. **(B)** RT-qPCR showing the ATG3 mRNA quantification in the different components of the ovariole: Tropharium, pre-vitellogenic oocytes, vitellogenic oocytes and chorionated oocytes. The relative expression was quantified using the ΔCT method. Graphs show mean ± SEM (n = 4). *$p < 0.05$, one-way ANOVA.

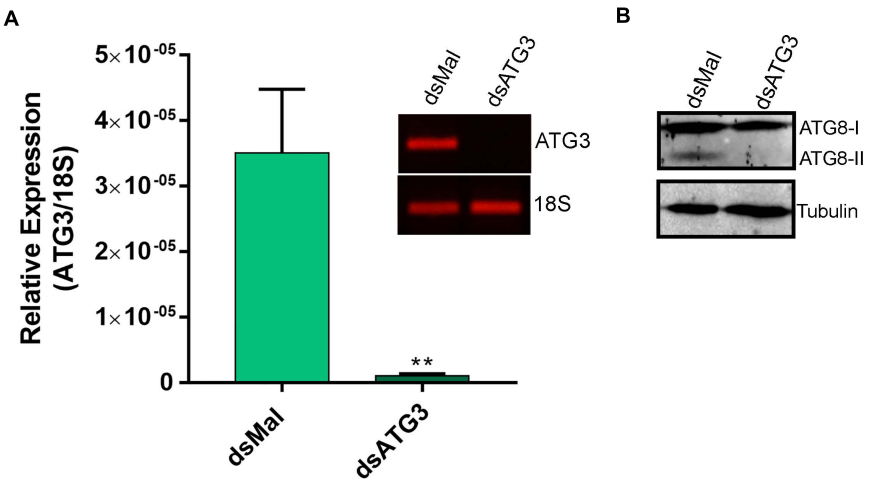

FIGURE 2 | ATG3 is depleted in the ovary of vitellogenic females. **(A)** RT-qPCR showing the levels of ATG3 mRNA in control (dsMal) and ATG3-depleted (dsATG3) ovaries dissected 7 days after the blood meal. Graph shows mean ± SEM (n = 5). ***$p < 0.001$, Student's t test. Inset: 25-cycle PCR fragments showing the amplification of ATG3 and 18S in control and depleted ovaries 7 days after the blood meal. **(B)** ATG8/LC3 Immunoblotting on dsMal and dsATG3 ovary samples. ATG8-I, non-lipidated ATG8; ATG8-II, ATG8 conjugated to the phosphatidylethanolamine.

be infected by Chagas, and vector control is still the most useful method to prevent this illness (Nunes-da-fonseca et al., 2017; WHO, 2019). Here, we found that ATG3, a known component of the autophagy machinery, is essential for the chorion biogenesis and embryo viability in *R. prolixus*. We consider these findings significant because they provide knowledge on the biology of egg production of an important vector. Exploring and identifying the molecular machinery essential for egg formation is of crucial importance to further understand the reproductive biology of various vectors and might contribute to the development of new strategies for vector population control and the prevention of vector borne diseases such as Chagas Disease.

The participation of the autophagy machinery in different contexts of oogenesis and embryo development has been observed before in different models. The clearance of maternal mRNAs during the maternal to zygotic transition and the degradation of paternal mitochondria after fertilization were associated to an increase in the autophagic flux in mice and *Caenorhabditis elegans*, respectively (Al Rawi et al., 2011; Yamamoto et al., 2014). In Drosophila, different ATG mutants present varied phenotypes of impaired embryogenesis (McPhee and Baehrecke, 2010; Kuhn et al., 2015). In *R. prolixus*, members of the autophagy machinery, such as ATG6/Beclin1, ATG8/LC3, and ATG1/ULK1 are also highly expressed in the ovary and oocytes throughout vitellogenesis, and, like ATG3, their knockdown result in various oogenesis and impaired embryo phenotypes (Vieira et al., 2018; Bomfim and Ramos, 2020; Pereira et al., 2020).

The process of chorion formation represents a remarkable model system for studying *in vivo* the biogenesis of complex

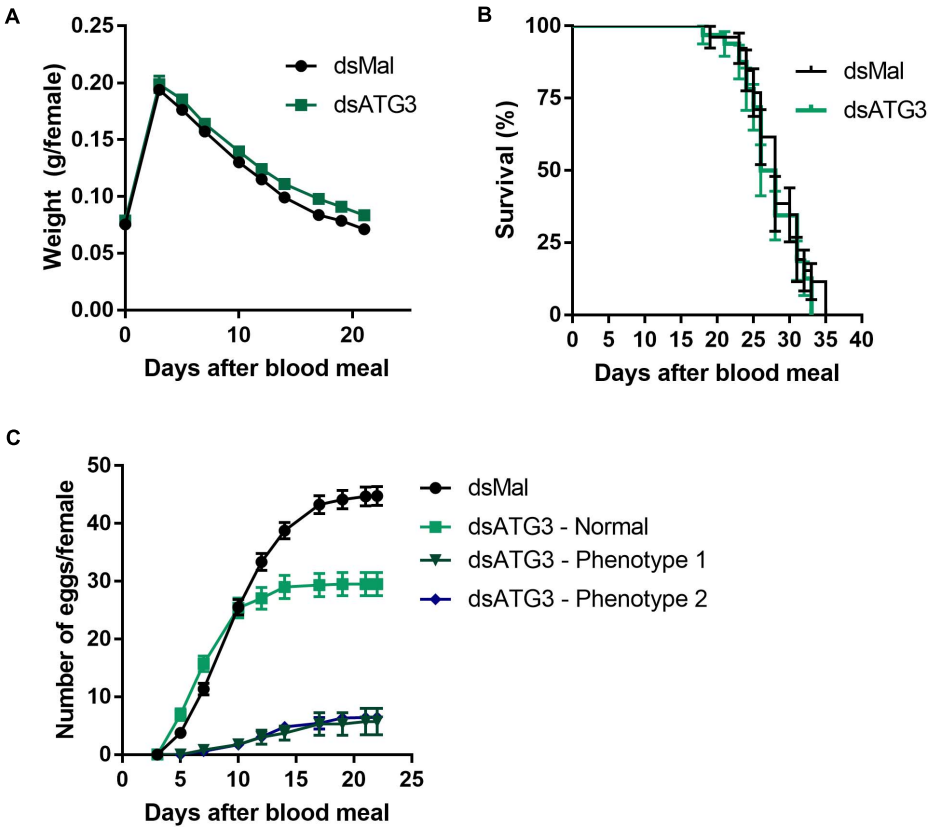

FIGURE 3 | Depletion of ATG3 does not affect digestion and longevity of the vitellogenic females. **(A)** Control and ATG3-depleted females were weighted for different days after the blood meal. **(B)** Survival rates of control and ATG3-depleted females. **(C)** Oviposition rates of control and depleted females over the gonotrophic cycle. All graphs show mean ± SEM (n = 30).

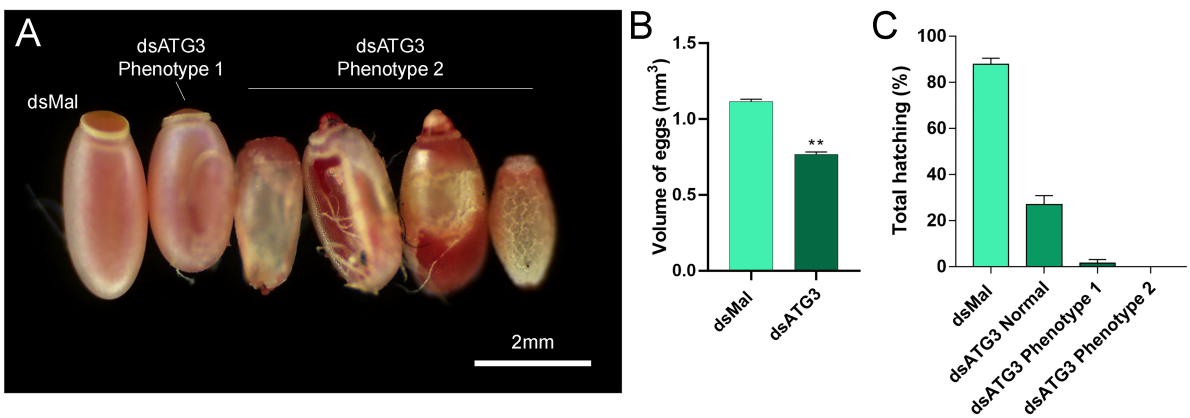

FIGURE 4 | Parental depletion of ATG3 results in small, chorion-defective, and unviable eggs. **(A)** Representative images of control and ATG3-depleted eggs. The two types of observed phenotypes are indicated. **(B)** Approximated calculated volume of control and ATG3-depleted eggs (n = 12). **(C)** Hatching rates of the embryos from control and ATG3-depleted females (n = 24). Graphs show mean ± SEM. *$p < 0.05$, **$p < 0.01$, one-way ANOVA.

extracellular matrix architectures. In *Drosophila*, studies about choriogenesis focus mostly on the programed gene-specific transcriptional activation of chorion genes (Tootle et al., 2011; Velentzas et al., 2018), and on the biochemical characterization of chorion proteins by mass spectrometry (Fakhouri et al., 2006). The fact that LC3-lipidation was reduced in ATG3-depleted samples indicates that the autophagic canonical function of ATG3 was indeed altered in the oocytes. Thus, it is probable that, at least at some level, an autophagy impairment contributed to the altered chorion secretion/deposition ATG3 phenotype.

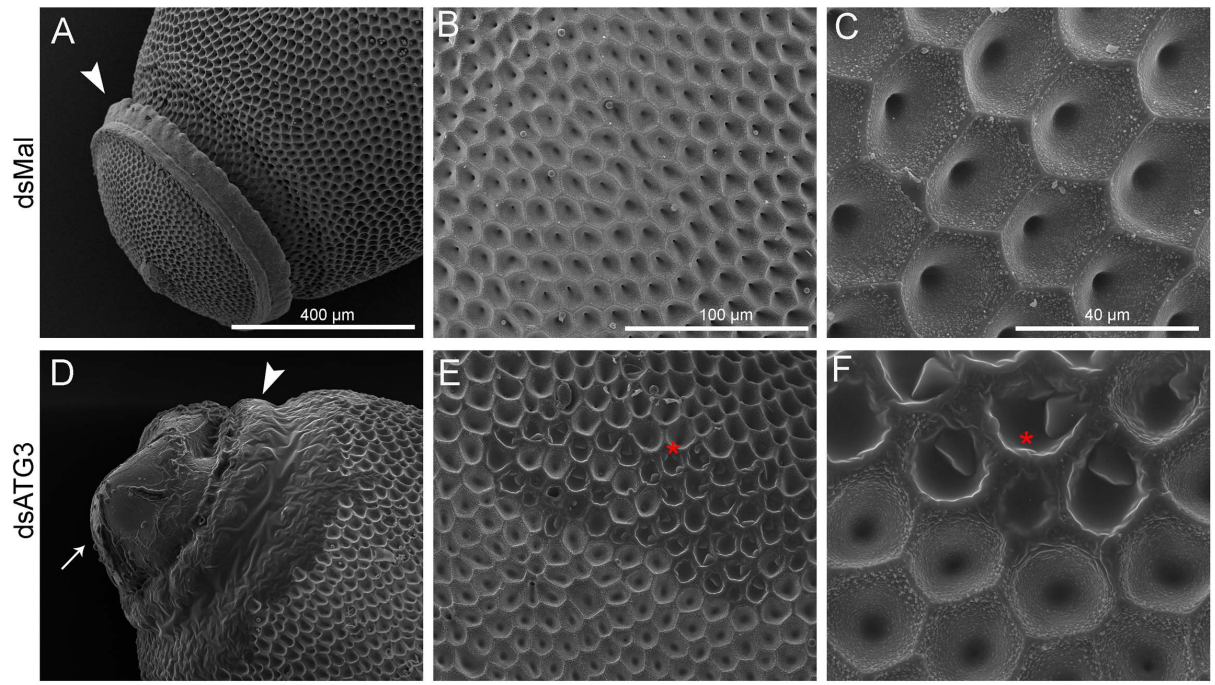

FIGURE 5 | Depletion of ATG3 results in defective chorion ultrastructure. Freshly laid eggs were processed for scanning electron microscopy (SEM). **(A–C)** SEM images of the chorion of control (dsMal) eggs in increasing magnifications. **(A)** Detail of the anterior pole of the egg. Arrowhead: operculum. **(B)** Transitional magnification image of the exochorion surface. **(C)** High magnification image of the exochorion surface showing the typical hexagonal patterns of the chorion in *R. prolixus*. **(D–F)** SEM images of the chorion of ATG3-depleted eggs in increasing magnifications. **(D)** Detail of the anterior pole of the ATG3-depleted egg sowing the altered structure of the operculum (arrowhead), and the leaking of the egg internal contents from the defective operculum (arrow). **(E)** Transitional magnification image of the exochorion surface of depleted eggs. **(C)** High magnification image of the exochorion surface showing the typical hexagonal patterns of the chorion in *R. prolixus* and the altered ultrastructure regions (asterisk). All images are representative of five eggs laid by at least five control and ATG3-depleted females ($n = 5$).

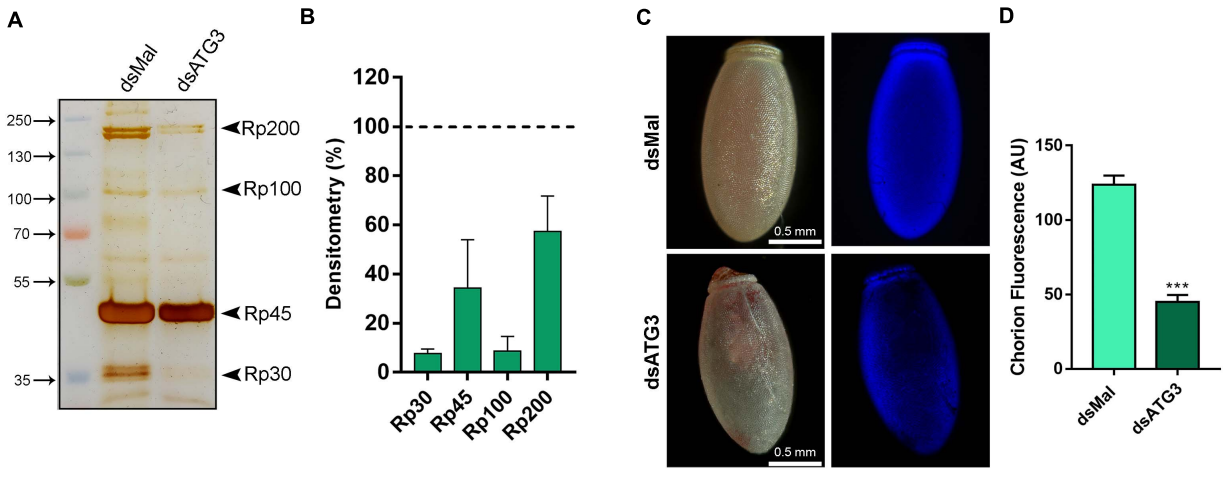

FIGURE 6 | ATG3-depleted eggs present reduced levels of all the major chorion proteins and lower levels of dityrosine crosslinking. **(A)** 10% SDS-PAGE of the urea-extracted proteins from control and ATG3-depleted chorions, collected 0–24 h after oviposition. Arrowheads show Rp30, Rp45, Rp100, and Rp200. **(B)** Densitometry measurements of the chorion proteins indicated in **(A)** was performed using Image J. Graph shows mean ± SEM ($n = 4$). **(C)** Representative images of the dityrosine fluorescence in control and ATG3-depleted egg chorions. The fluorescence images were taken using a filter set for intrinsic dityrosine fluorescence. **(D)** Total chorion fluorescence was quantified using ImageJ software. Graph shows mean ± SEM ($n = 10$). ***$p < 0.0001$, Student's t test. *AU*, arbitrary units.

However, because ATG3 has been implicated in various other cellular functions, such as endosomal trafficking, phagocytosis, cell proliferation, and exosome release (Murrow and Debnath, 2015, 2018), it is difficult to interpret the contribution of all those potential functions to the compromised secretion/exocytosis of the chorion proteins. Furthermore, although we tested

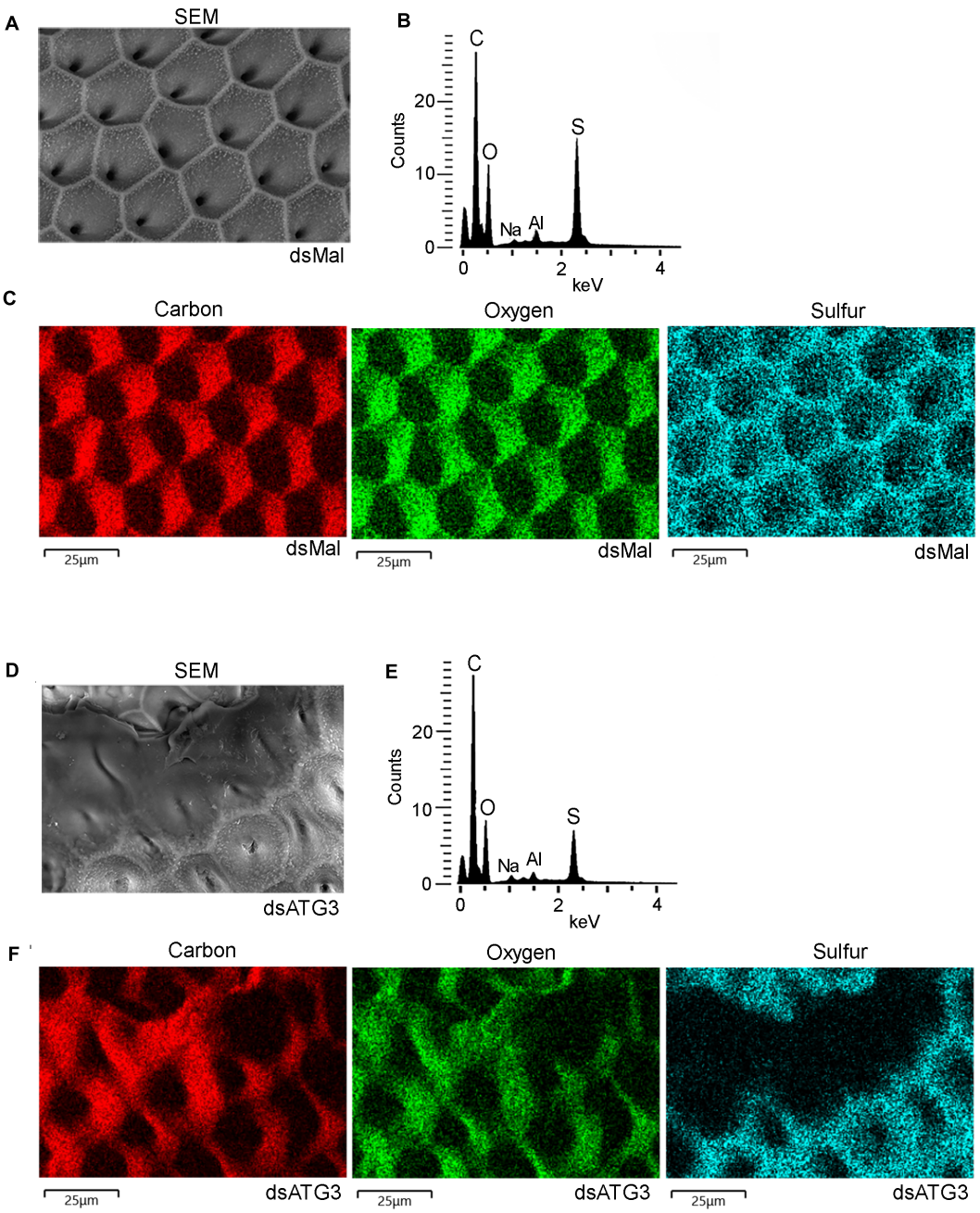

FIGURE 7 | ATG3-depleted chorions present lower levels of sulfur, a marker of protein cross-linking. Control and ATG3-depleted chorions were analyzed by electron probe X-ray microanalysis. **(A)** Scanning electron microscopy image of the chorion from whole and unfixed control eggs. **(B)** X-ray spectrum corresponding to image in panel A. Aluminum (Al) peak in the spectrum came from the stub. **(C)** Elemental mapping of the chorion image shown in **(A)** reveals the co-localization of carbon (C), oxygen (O), sodium (Na) and sulfur (S). **(D)** Scanning electron microscopy image of the chorion from whole and unfixed ATG3-depleted egg. **(E)** X-ray spectrum corresponding to image in panel D. Aluminum (Al) peak in the spectrum came from the stub. **(F)** Elemental mapping of the chorion shown in **(D)** reveals sulfur is absent from the regions where the chorion shows the most severe abnormal ultrastructure. The images are representative of X-ray detections from three control and ATG3-depleted eggs. Bars: 25 µm.

in silico for predicted off targets using our dsRNA fragment against the *R. prolixus* transcriptome database and found no significate results, it is not possible to rule out potential off target effects of RNAi silencing. Despite the fact that the chorion biogenesis is essential for reproduction in oviparous animals, the machinery and signals encompassing the chorion proteins synthesis, sorting, and secretion by the follicle cells, are still largely unexplored. In *R. prolixus*, transcriptome analysis demonstrated that the follicle cells are highly committed to transcription, translation, protein turnover and vesicular traffic,

as those functions accounted for more than two-thirds of all transcripts identified. Measurements of the expression of six transcripts involved in the unfolded protein response (UPR), a signaling network that coordinates the recovery of ER function in conditions of protein-folding stress, showed their expression to be increased during early stages of oogenesis and repressed at late stages, especially in the choriogenic follicles (Medeiros et al., 2011). Thus, it seems reasonable to assume that any molecular perturbation that somehow affect the follicle cells biosynthetic secretory pathway will result in some type of altered chorion structure. In fact, in previous work, our group has shown that parental RNAi depletion of ULK1/ATG1 in *R. prolixus* also resulted in oocytes with abnormal chorion ultrastructure. Unlike ATG3, the lipidation of LC3 was not affected, and it was shown that the ATG1/ULK1 depleted follicle cells displayed expanded rough ER membranes as well as increased expression of the ER chaperone BiP3, both indicatives of ER-stress. Plus, the knockdown of SEC16A, a known partner of the non-canonical ULK1/ATG1 function in the ER exit sites, phenocopied the depletion of ULK1/ATG1 (Bomfim and Ramos, 2020).

The stable biding of proteins through intermolecular covalent bonds is commonly referred to as protein cross-linking. It generates new macromolecular assemblies with different physicochemical properties and functions. The formation of specific disulfide bonds occurs as the protein folds in the ER where the linking of proper cysteines is coordinated by the action of a system of ER chaperones. For the maturation of extracellular proteins, correct cysteine crosslinking is essential to stabilize the protein as well to bind them to other proteins that will form the matrix network (Wilkinson and Gilbert, 2004; Heck et al., 2013). In this context, our findings that not all of the control chorion proteins are detected in the depleted samples, and that sulfur is decreased in the chorion layers of ATG3-depleted insects, indicates that specific proteins were not properly delivered to the chorion, either because they were not properly synthesized or folded or because they were not correctly secreted by the follicle cells. In addition, the mechanical rigidity and waterproofing properties of the chorion in *R. prolixus* has been attributed to protein cross-linking by peroxidases (Beament, 1946; Li et al., 1996; Konstandi et al., 2005; Li and Li, 2006; Dias et al., 2013) and the fact that we detected reduced dityrosine fluorescence signals provides additional evidence that the protein networks that are likely to form in the chorion layers were not properly formed in ATG3-depleted insects.

Most interestingly, the findings that ATG3 also participates in exosome release (Murrow and Debnath, 2015, 2018) raises the speculation that exosomes might be a part of the general chorion biogenesis. It has been shown that late endosomes can fuse with the plasma membrane leading to secretion of intralumenal vesicles as exosomes (Théry et al., 2002). Because the chorion is a highly specialized extracellular matrix, it is possible that some of the components are delivered to the eggshell packed in extracellular vesicles, such as exosomes. Experiments focusing on the follicle cells ultrastructure and *in vitro* secretion patterns, including the investigation of extracellular vesicles, are currently under investigation in our laboratory.

DATA AVAILABILITY STATEMENT

The original contributions presented in the study are included in the article/**Supplementary Material**, further inquiries can be directed to the corresponding author/s.

ETHICS STATEMENT

The animal study was reviewed and approved by all animal care and experimental protocols were approved by guidelines of the institutional care and use committee (Committee for Evaluation of Animal Use for Research from the Federal University of Rio de Janeiro, CEUA-UFRJ #01200.001568/2013-87, order number 155/13), under the regulation of the national council of animal experimentation control (CONCEA).

AUTHOR CONTRIBUTIONS

AS designed and conducted the experiments and revised the manuscript. IR designed the experiments and wrote the manuscript. Both authors contributed to the article and approved the submitted version.

FUNDING

This work was funded by the following grants: JCNE-FAPERJ (www.faperj.br/), INCT-EM-CNPq/FAPERJ (http://cnpq.br/), and CAPES (www.capes.gov.br/).

ACKNOWLEDGMENTS

We thank Yasmin Gutierrez and Yan Mendonça for the careful care of our lab *insectarium* and HITACHI, dpUNION, and CENABIO-UFRJ for providing electron microscopy equipment and facilities.

SUPPLEMENTARY MATERIAL

The Supplementary Material for this article can be found online at: https://www.frontiersin.org/articles/10.3389/fphys.2021.638026/full#supplementary-material

Supplementary Figure 1 | *R. prolixus* ATG3 sequence. **(A)** Representation of ATG3 protein conserved domains in different species. Sequence information was obtained from Vector Base (https://www.vectorbase.org/). Conserved domains were obtained from the NCBI Conserved Domains Database. PF03986 (Autophagy_N); PF03987 (Autophagy_act_C); PF10381 (Autophagy_C). **(B)** Matrix of similarity and identity of ATG3 protein sequences from different species (SIAS Server). Reference sequences: *Rp, Rhodnius prolixus*; HsAtg3, *Homo sapiens* (Gene ID: 64422); DmAtg3, *Drosophila melanogaster* (Gene ID: 40044); BmAtg3, *Bombyx mori* (Gene ID: 100216351); ScAtg3, *Saccharomyces cerevisiae* (Gene ID: 855741).

Supplementary Table 1 | Primers sequences. All sequences were obtained from *Vector Base* (https://www.vectorbase.org/) and primers were synthesized by Macrogen or IDT technologies. The T7 sequence is underlined.

REFERENCES

Al Rawi, S., Louvet-Vallée, S., Djeddi, A., Sachse, M., Culetto, E., Hajjar, C., et al. (2011). Postfertilization autophagy of sperm organelles prevents paternal mitochondrial DNA transmission. *Science* 334, 1144–1147. doi: 10.1126/science.1211878

Alberts, B., Johnson, A., Lewis, J., Raff, M., Roberts, K., and Walter, P. (2002). *Molecular Biology of the Cell*, 4th Edn. New York, NY: Garland science.

Andersen, S. O., and Roepstorff, P. (2005). The extensible alloscutal cuticle of the tick, *Ixodes ricinus*. *Insect Biochem. Mol. Biol.* 35, 1181–1188. doi: 10.1016/j.ibmb.2005.05.009

Beament, J. W. (1946). The Formation and Structure of the Chorion of the Egg in an Hemipteran, *Rhodnius prolixus*. *Q. J. Microsc. Sci.* 87, 393–439.

Beament, J. W. L. (1948). The penetration of the insect egg-shells; penetration of the chorion of *Rhodnius prol*ixus. Stal. *Bull. Entomol. Res.* 39, 359–383. doi: 10.1017/s0007485300022471

Bomfim, L., and Ramos, I. (2020). Deficiency of ULK1/ATG1 in the follicle cells disturbs ER homeostasis and causes defective chorion deposition in the vector *Rhodnius prolixus*. *FASEB J. Off. Publ. Fed. Am. Soc. Exp. Biol.* 34, 13561–13572. doi: 10.1096/fj.202001396R

Bomfim, L., Vieira, P., Fonseca, A., and Ramos, I. (2017). Eggshell ultrastructure and delivery of pharmacological inhibitors to the early embryo of *R. prolixus* by ethanol permeabilization of the extraembryonic layers. *PLoS One* 12:e0185770. doi: 10.1371/journal.pone.0185770

Bouts, D. M. D., Melo, A. C., do, A., Andrade, A. L. H., Silva-Neto, M. A. C., Paiva-Silva, G., et al. (2007). Biochemical properties of the major proteins from *Rhodnius prolixus* eggshell. *Insect Biochem. Mol. Biol.* 37, 1207–1221. doi: 10.1016/j.ibmb.2007.07.010

Dias, F. A., Gandara, A. C., Queiroz-Barros, F. G., Oliveira, R. L. L., Sorgine, M. H. F., Braz, G. R. C., et al. (2013). Ovarian dual oxidase (Duox) activity is essential for insect eggshell hardening and waterproofing. *J. Biol. Chem.* 288, 35058–35067. doi: 10.1074/jbc.M113.522201

Fakhouri, M., Elalayli, M., Sherling, D., Hall, J. D., Miller, E., Sun, X., et al. (2006). Minor proteins and enzymes of the *Drosophila* eggshell matrix. *Dev. Biol.* 293, 127–141. doi: 10.1016/j.ydbio.2006.01.028

Galluzzi, L., and Green, D. R. (2019). Autophagy-Independent functions of the autophagy machinery. *Cell* 177, 1682–1699. doi: 10.1016/j.cell.2019.05.026

Heck, T., Faccio, G., Richter, M., and Thöny-Meyer, L. (2013). Enzyme-catalyzed protein crosslinking. *Appl. Microbiol. Biotechnol.* 97, 461–475. doi: 10.1007/s00253-012-4569-z

Huebner, E., and Anderson, E. (1972). A cytological study of the ovary of *Rhodnius prolixus*. III. Cytoarchitecture and development of the trophic chamber. *J. Morphol.* 138, 1–39. doi: 10.1002/jmor.1051380102

Ichimura, Y., Kirisako, T., Takao, T., Satomi, Y., Shimonishi, Y., Ishihara, N., et al. (2000). A ubiquitin-like system mediates protein lipidation. *Nature* 408, 488–492. doi: 10.1038/35044114

Kerkut, G. A., and Gilbert, L. I. (1985). *Comprehensive Insect Physiology,Biochemistry and Pharmacology*. Oxford: Pergamon Press.

Klionsky, D. J., Abdelmohsen, K., Abe, A., Abedin, M. J., Abeliovich, H., Arozena, A. A., et al. (2016). Guidelines for the use and interpretation of assays for monitoring autophagy (3rd edition). *Autophagy* 12, 1–222. doi: 10.1080/15548627.2015.1100356

Konstandi, O. A., Papassideri, I. S., Stravopodis, D. J., Kenoutis, C. A., Hasan, Z., Katsorchis, T., et al. (2005). The enzymatic component of *Drosophila melanogaster* chorion is the Pxd peroxidase. *Insect Biochem. Mol. Biol.* 35, 1043–1057. doi: 10.1016/j.ibmb.2005.04.005

Kuhn, H., Sopko, R., Coughlin, M., Perrimon, N., and Mitchison, T. (2015). The Atg1-Tor pathway regulates yolk catabolism in *Drosophila* embryos. *Development* 142, 3869–3878. doi: 10.1242/dev.125419

Kunkel, J. G., and Nordin, J. H. (1985). *Yolk Proteins: Comprehensive Insect Physiology, Biochemistry and Pharmacology*. Oxford: Pergamon Press.

Li, J., Hodgeman, B. A., and Christensen, B. M. (1996). Involvement of peroxidase in chorion hardening in *Aedes aegypti*. *Insect Biochem. Mol. Biol.* 26, 309–317. doi: 10.1016/0965-1748(95)00099-2

Li, J. S., and Li, J. (2006). Major chorion proteins and their crosslinking during chorion hardening in *Aedes aegypti* mosquitoes. *Insect Biochem. Mol. Biol.* 36, 954–964. doi: 10.1016/j.ibmb.2006.09.006

Majerowicz, D., Alves-Bezerra, M., Logullo, R., Fonseca-De-Souza, A. L., Meyer-Fernandes, J. R., Braz, G. R. C., et al. (2011). Looking for reference genes for real-time quantitative PCR experiments in *Rhodnius prolixus* (Hemiptera: reduviidae). *Insect Mol. Biol.* 20, 713–722. doi: 10.1111/j.1365-2583.2011.01101.x

Martinez, J., Malireddi, R. K. S., Lu, Q., Cunha, L. D., Pelletier, S., Gingras, S., et al. (2015). Molecular characterization of LC3-associated phagocytosis reveals distinct roles for Rubicon, NOX2 and autophagy proteins. *Nat. Cell Biol.* 17, 893–906. doi: 10.1038/ncb3192

McPhee, C. K., and Baehrecke, E. H. (2010). Autophagy in *Drosophila melanogaster* Christina. *Biochim Biophys Acta* 1793, 1452–1460. doi: 10.1016/j.bbamcr.2009.02.009.Autophagy

Medeiros, M. N., Logullo, R., Ramos, I. B., Sorgine, M. H. F., Paiva-Silva, G. O., Mesquita, R. D., et al. (2011). Transcriptome and gene expression profile of ovarian follicle tissue of the triatomine bug *Rhodnius prolixus*. *Insect Biochem. Mol. Biol.* 41, 823–831. doi: 10.1016/j.ibmb.2011.06.004

Merril, C. R., Dunau, M. L., and Goldman, D. (1981). A rapid sensitive silver stain for polypeptides in polyacrylamide gels. *Anal. Biochem.* 110, 201–207. doi: 10.1016/0003-2697(81)90136-6

Mizushima, N., Noda, T., Yoshimori, T., Tanaka, Y., Ishii, T., George, M. D., et al. (1998). A protein conjugation system essential for autophagy. *Nature* 395, 395–398. doi: 10.1038/26506

Murrow, L., and Debnath, J. (2015). ATG12-ATG3 connects basal autophagy and late endosome function. *Autophagy* 11, 961–962. doi: 10.1080/15548627.2015.1040976

Murrow, L., and Debnath, J. (2018). Atg12–Atg3 Coordinates Basal Autophagy, Endolysosomal Trafficking, and Exosome Release. *Mol. Cell. Oncol.* 5, 1–3. doi: 10.1080/23723556.2015.1039191

Neff, D., Frazier, S. F., Quimby, L., Wang, R. T., and Zill, S. (2000). Identification of resilin in the leg of cockroach, *Periplaneta americana*: confirmation by a simple method using pH dependence of UV fluorescence. *Arthropod Struct. Dev.* 29, 75–83. doi: 10.1016/S1467-8039(00)00014-1

Nemoto, T., Tanida, I., Tanida-Miyake, E., Minematsu-Ikeguchi, N., Yokota, M., Ohsumi, M., et al. (2003). The mouse APG10 homologue, an E2-like enzyme for Apg12p conjugation, facilitates MAP-LC3 modification. *J. Biol. Chem.* 278, 39517–39526. doi: 10.1074/jbc.M300550200

Nunes-da-fonseca, R., Berni, M., Tobias-Santos, V., Pane, A., and Araujo, H. M. (2017). *Rhodnius prolixus*: from classical physiology to modern developmental biology. *Genesis* 55, e22995. doi: 10.1002/dvg.22995

Ohsumi, Y. (2001). Molecular dissection of autophagy: two ubiquitin-like systems. *Nat. Rev. Mol. Cell Biol.* 2, 211–216. doi: 10.1038/35056522

O'Sullivan, T. E., Geary, C. D., Weizman, O., El Geiger, T. L., Rapp, M., Dorn, G. W., et al. (2016). Atg5 is essential for the development and survival of innate lymphocytes. *Cell Rep.* 15, 1910–1919. doi: 10.1016/j.celrep.2016.04.082

Pereira, J., Diogo, C., Fonseca, A., Bomfim, L., Cardoso, P., Santos, A., et al. (2020). Silencing of RpATG8 impairs the biogenesis of maternal autophagosomes in vitellogenic oocytes, but does not interrupt follicular atresia in the insect vector *Rhodnius prolixus*. *PLoS Negl. Trop. Dis.* 14:e0008012. doi: 10.1371/journal.pntd.0008012

Sanjuan, M. A., Dillon, C. P., Tait, S. W. G., Moshiach, S., Dorsey, F., Connell, S., et al. (2007). Toll-like receptor signalling in macrophages links the autophagy pathway to phagocytosis. *Nature* 450, 1253–1257. doi: 10.1038/nature06421

Subramani, S., and Malhotra, V. (2013). Non-autophagic roles of autophagy-related proteins. *EMBO Rep.* 14, 143–151. doi: 10.1038/embor.2012.220

Tanida, I., Mizushima, N., Kiyooka, M., Ohsumi, M., Ueno, T., Ohsumi, Y., et al. (1999). Apg7p/Cvt2p: a novel protein-activating enzyme essential for autophagy. *Mol. Biol. Cell* 10, 1367–1379. doi: 10.1091/mbc.10.5.1367

Tanida, I., Tanida-Miyake, E., Komatsu, M., Ueno, T., and Kominami, E. (2002). Human Apg3p/Aut1p homologue is an authentic E2 enzyme for multiple substrates, GATE-16, GABARAP, and MAP-LC3, and facilitates the conjugation of hApg12p to hApg5p. *J. Biol. Chem.* 277, 13739–13744. doi: 10.1074/jbc.M200385200

Théry, C., Zitvogel, L., and Amigorena, S. (2002). Exosomes: composition, biogenesis and function. *Nat. Rev. Immunol.* 2, 569–579. doi: 10.1038/nri855

Tootle, T. L., Williams, D., Hubb, A., Frederick, R., and Spradling, A. (2011). *Drosophila* eggshell production: identification of new genes and

coordination by Pxt. *PLoS One* 6:e19943. doi: 10.1371/journal.pone.0019943

Tsukada, M., and Ohsumi, Y. (1993). Isolation and characterization of autophagy-defective mutants of *Saccharomyces cerevisiae*. *FEBS Lett.* 333, 169–174. doi: 10.1016/0014-5793(93)80398-e

Tuft, P. H. (1950). The structure of the insect egg -Shell in relation to the respiration of the embryo. *J. Exp. Biol.* 26, 327–334.

Velentzas, A. D., Velentzas, P. D., Katarachia, S. A., Anagnostopoulos, A. K., Sagioglou, N. E., Thanou, E. V., et al. (2018). The indispensable contribution of s38 protein to ovarian-eggshell morphogenesis in *Drosophila melanogaster*. *Sci. Rep.* 8:16103. doi: 10.1038/s41598-018-34532-2

Vieira, P. H., Bomfim, L., Atella, G. C., Masuda, H., and Ramos, I. (2018). Silencing of RpATG6 impaired the yolk accumulation and the biogenesis of the yolk organelles in the insect vector *R. prolixus*. *PLoS Negl. Trop. Dis.* 12:e0006507. doi: 10.1371/journal.pntd.0006507

WHO (2019). Available online at: https://www.who.int/en/news-room/fact-sheets/detail/chagas-disease-(american-trypanosomiasis)(accessed December 4, 2020).

Wilkinson, B., and Gilbert, H. F. (2004). Protein disulfide isomerase. *Biochim. Biophys. Acta Proteins Proteomics* 1699, 35–44. doi: 10.1016/j.bbapap.2004.02.017

Wu, X., Tanwar, P. S., and Raftery, L. A. (2008). *Drosophila* follicle cells: morphogenesis in an eggshell. *Semin. Cell Dev. Biol.* 19, 271–282. doi: 10.1016/j.semcdb.2008.01.004

Yamamoto, A., Mizushima, N., and Tsukamoto, S. (2014). Fertilization-Induced Autophagy in Mouse Embryos is Independent of mTORC11. *Biol. Reprod.* 91, 1–7. doi: 10.1095/biolreprod.113.115816

Conflict of Interest: The authors declare that the research was conducted in the absence of any commercial or financial relationships that could be construed as a potential conflict of interest.

frontiers in Physiology

ORIGINAL RESEARCH
published: 10 February 2021
doi: 10.3389/fphys.2021.624165

Regulation of a Trehalose-Specific Facilitated Transporter (TRET) by Insulin and Adipokinetic Hormone in *Rhodnius prolixus*, a Vector of Chagas Disease

Jimena Leyria, Hanine El-Mawed, Ian Orchard and Angela B. Lange*

Department of Biology, University of Toronto Mississauga, Mississauga, ON, Canada

OPEN ACCESS

Edited by:
Isabela Ramos, Federal University of Rio de Janeiro, Brazil

Reviewed by:
Sheila Ons, National University of La Plata, Argentina
Gerd Gäde, University of Cape Town, South Africa
David Majerowicz, Federal University of Rio de Janeiro, Brazil

***Correspondence:**
Jimena Leyria
jimenal.leyria@utoronto.ca

Specialty section:
This article was submitted to Invertebrate Physiology, a section of the journal Frontiers in Physiology

Received: *30 October 2020*
Accepted: *18 January 2021*
Published: *10 February 2021*

Citation:
Leyria J, El-Mawed H, Orchard I and Lange AB (2021) Regulation of a Trehalose-Specific Facilitated Transporter (TRET) by Insulin and Adipokinetic Hormone in Rhodnius prolixus, a Vector of Chagas Disease. Front. Physiol. 12:624165. doi: 10.3389/fphys.2021.624165

Using the blood-sucking kissing bug, *Rhodnius prolixus* as an experimental model, we have studied the involvement of insulin-like peptides (ILPs) and adipokinetic hormone (AKH) signaling in carbohydrate metabolism, focusing on the regulation of the trehalose-specific facilitated transporter (Rhopr-TRET), particularly in the ovaries. We find that trehalose stores in ovaries increase after feeding, synchronously with the beginning of vitellogenesis, but that the transcript expression of enzymes involved in trehalose synthesis show no changes between unfed and blood-fed animals. However, an eightfold increase in *Rhopr-TRET* transcript expression is observed in the ovaries post-blood meal. *In vivo* and *ex vivo* assays using exogenous insulins and Rhopr-AKH, reveal that *Rhopr-TRET* is up-regulated in ovaries by both peptide families. In accordance with these results, when ILP and AKH signaling cascades are impaired using RNA interference, *Rhopr-TRET* transcript is down-regulated. In addition, trehalose injection induces an up-regulation of *Rhopr-TRET* transcript expression and suggests an activation of insulin signaling. Overall, the results support the hypothesis of a direct trehalose uptake by ovaries from the hemolymph through Rhopr-TRET, regulated by ILP and/or AKH. We also show that Rhopr-TRET may work cooperatively with AKH signaling to support the release of trehalose from the ovaries into the hemolymph during the unfed (starved) condition. In conclusion, the results indicate that in females of *R. prolixus,* trehalose metabolism and its hormonal regulation by ILP and AKH play critical roles in adapting to different nutritional conditions and physiological states.

Keywords: reproduction, starvation, triatominae, carbohydrate metabolism, hormonal regulation

INTRODUCTION

Carbohydrates represent one of the main energy reserves in animal cells, which is why they participate as essential factors in various biological processes of all multicellular organisms (Brosnan, 1999). In insects, glucose is stored in its polymeric form, glycogen, which is synthesized mainly from dietary carbohydrates or amino acids by the fat body, a multifunctional organ analogous to vertebrate adipose tissue and liver (Arrese and Soulages, 2010). Glycogen can be

readily degraded on demand to be used as a glycolytic fuel, or mobilized from the fat body as trehalose for uptake by other tissues. Trehalose is a non-reducing disaccharide that consists of two glucose molecules and is non-toxic at the high levels that are found in insect hemolymph (Elbein et al., 2003). Trehalose biosynthesis depends mainly on two enzymatic reactions involving trehalose-6-phosphate synthase (TPS) and trehalose-6-phosphate phosphatase (Thompson, 2003). However, to be used in cell metabolism, trehalose must be converted into glucose by enzymes called trehalases (Shukla et al., 2015). A trehalose-specific facilitated transporter (TRET) leads to both the transfer of newly synthesized trehalose from the fat body into the circulating hemolymph and its uptake by other tissues, working in a reversible bidirectional way depending on the concentration gradient of trehalose and physiological needs (Thompson, 2003).

In insects, carbohydrate homeostasis is under strict hormonal regulation (Toprak, 2020) led mainly by insulin-like peptides (ILPs) and/or insulin-like growth factors (IGFs), and adipokinetic hormones (AKHs). The release and circulating levels of these peptide hormones are mainly regulated by feeding and starvation. In this context, the elevated circulating carbohydrate level after feeding is reduced by take-up into the fat body or ovaries through the actions of ILPs or IGFs to regulate anabolic processes, e.g., glycogen synthesis; whereas during starvation, defined as a prolonged unfed condition, catabolic processes are enhanced, e.g., glycogen breakdown and gluconeogenesis led mainly through AKH signaling (Arrese and Soulages, 2010; Badisco et al., 2013; Toprak, 2020).

Blood-sucking insects usually need to process a large amount of blood in a short time to provide energy to support the optimal progress of physiological events related to growth, development, and reproduction. They also often have to overcome long periods of starvation between successful gorging (Millen and Beckel, 1970; Foster, 1995). Insect reproduction is a process that places high demand on female metabolism for the provision of nutrients and other components for egg formation (Roy et al., 2018). Reproduction is therefore intimately associated with nutrition and metabolic state. While juvenile hormones (JHs) and ecdysteroids are the key players involved in the hormonal regulation of vitellogenesis to promote egg growth, insulin and AKH signaling have a critical role in controlling nutrient signaling and generating the energy necessary for those events to occur successfully (Roy et al., 2018; Lenaerts et al., 2019).

Triatomines (Hemiptera: Reduviidae) are a subfamily of blood-sucking insects with relevance in public health since they are vectors of *Trypanosoma cruzi*, the causal agent of Chagas disease. This illness is endemic in Latin American countries, but with globalization, this disease has spread throughout the world, and according to the World Health Organization, affects 6-7 million people worldwide (World Health Organization [WHO], 2020). Furthermore, due to climatic suitability, areas throughout the world have been identified as being at risk of becoming suitable habitats for the development of triatomines, thereby expanding endemic areas (Eberhard et al., 2020). In this context, research focusing on the physiology of triatomines can provide novel tools with potential for use in vector control strategies. *Rhodnius prolixus*, one of the most important vectors of Chagas disease, has been a classical model in insect physiology since the origins of the pioneering work of Wigglesworth (1936). *R. prolixus* blood-gorge only once in each instar and may remain for long periods of time in an unfed (starved) condition depending on availability of a blood-donating host.

In ***R. prolixus***, AKH-signaling plays a critical role in modulating lipid levels (Marco et al., 2013; Patel et al., 2014; Zandawala et al., 2015; Alves-Bezerra et al., 2016), and the ILP/IGF cascade participates in lipid metabolism, carbohydrate mobilization and reproductive performance (Defferrari et al., 2016b, 2018; Leyria et al., 2020a). The presence of the AKH receptor (***AKHR***) transcript and ILP/IGF signaling activation in ovaries of ***R. prolixus*** has been reported (Zandawala et al., 2015; Alves-Bezerra et al., 2016; Leyria et al., 2020a), suggesting that both peptide hormones may also have a role in controlling aspects of reproductive physiology in ovaries. In addition, a transcriptome analysis of ovaries from fed females of ***R. prolixus*** suggests that the trehalose which is taken up by that tissue comes from extra-ovarian sources (Leyria et al., 2020b). Although in the ovaries of ***R. prolixus*** females, the percentage of carbohydrates stored during vitellogenesis is lower (around 6–10%) compared to those found for other nutrients, such as lipids and proteins (Santos et al., 2008, 2012; Leyria et al., 2020b), the use of glycogen has been related to successful embryonic development, revealing the importance of carbohydrate accumulation by oocytes. Here, we present results supporting the hypothesis that a direct trehalose uptake through the ***R. prolixus*** TRET (Rhopr-TRET), regulated by insulin and/or AKH-signaling, is important for the storage of carbohydrates by the ovaries. Also, we demonstrate that Rhopr-TRET could work cooperatively with the ***R. prolixus*** AKH (Rhopr-AKH) signaling pathway to promote the release of trehalose from the fat body and ovaries to the hemolymph during starvation. Overall, these results show that in ***R. prolixus***, carbohydrate metabolism and its hormonal regulation may play critical roles in adapting to different physiological conditions, including reproduction and starvation.

MATERIALS AND METHODS

Insects

Experiments were carried out with adults of *R. prolixus* taken from an established colony at the University of Toronto Mississauga. Insects were reared in incubators at 25°C under high humidity (∼50%). Standardized conditions of insect rearing were previously described (Leyria et al., 2020a). It is important to note that under our standardized conditions, female insects can only lay eggs after a blood meal (Leyria et al., 2020a,b). Thus, some experiments required females to take a blood meal in order to promote egg growth. For these experiments, females at 10 days post-ecdysis were fed through an artificial feeding membrane on defibrinated rabbit blood (Cedarlane Laboratories Inc., Burlington, ON, Canada). All insects used in this work have

a similar feeding and body weight history. Tissues or hemolymph were sampled from adult females on representative days of the unfed and fed conditions, specified below for each experiment.

Trehalose Quantification

Adult female insects were dissected 10, 20, and 30 days post-ecdysis (representing the unfed condition, i.e., unfed as adults). One group of adult insects were fed and the tissues collected at 1, 2, 3, 4, and 5 days post-blood meal (representing the fed condition). Ovaries and ventral and dorsal fat bodies were dissected under cold *R. prolixus* saline (150 mM NaCl, 8.6 mM KCl, 2.0 mM $CaCl_2$, 8.5 mM $MgCl_2$, 4.0 mM $NaHCO_3$, 5.0 mM HEPES, pH 7.0) and then homogenized in 1.5 ml microtubes containing 200 μl of cold phosphate-buffered saline (20 mM Na_2HPO_4/KH_2PO_4, 150 mM NaCl, pH 6). The homogenates were centrifuged at 2,500 × *g* for 5 min at 4°C and pellets containing tissue debris were discarded. The resulting material was re-centrifuged at 12,000 × *g* for 10 min at 4°C and the supernatants collected for trehalose quantification. After immobilizing the insects on a slide using masking tape, 10 μL of hemolymph was collected using a Hamilton syringe (Hamilton Company, Reno, NV, United States) from cut ends of the legs while pressing gently on the abdomen. The hemolymph was placed in ice-cold microtubes and then diluted in cold anticoagulant solution (10 mM Na_2EDTA, 100 mM glucose, 62 mM NaCl, 30 mM sodium citrate, 26 mM citric acid, pH 4.6) at a ratio of 1:5 (anticoagulant: hemolymph) (de Azambuja et al., 1991). Samples were then centrifuged at 10,000 × *g* for 10 min at 4°C to remove hemocytes and the supernatants used for determination of trehalose concentration. Trehalose content in tissues and hemolymph was determined by the method of Parrou and François (1997) with slight modifications (Huang and Lee, 2011). In order to inactivate endogenous enzymes and to convert glucose into its reduced form, 50 μl of tissue extract or 12.5 μl of hemolymph (hemolymph + anticoagulant) were transferred to a new tube containing 50 μl or 87.5 μl, respectively, of 0.25 M Na_2CO_3 buffer solution and incubated at 95°C for 10 min. Once the tubes were cool, 80 μl of 0.25 M sodium acetate (pH 5.2) plus 20 μl of 1 M acetic acid were added, mixed and then centrifuged at 12,000 × *g* for 10 min at room temperature. The supernatants obtained were used to measure trehalose levels. One-hundred μl of each supernatant was incubated overnight at 37°C with 1 μl porcine kidney trehalase (Millipore-Sigma, Oakville, ON, Canada) to catalyze the conversion of trehalose into glucose, or with *R. prolixus* saline to determine the endogenous glucose content of the samples. Glucose contained in all the samples was determined using the glucose assay kit [Glucose (GO) Assay Kit, Millipore-Aldrich, Oakville, ON, Canada] according to the manufacturer's protocol (30 μl of sample was added to 100 μl of glucose reagent solution). A standard curve using a 0–0.6 μg range of glucose was run in parallel with the experimental samples. The samples were quantified at 540 nm using a plate reader spectrophotometer (Synergy HTX Multi-Mode Microplate Reader by Biotek, Winooski, VT, United States). The trehalose concentration was then corrected for the amount of glucose present in the samples (trehalose concentration = (glucose measured in samples treated with trehalase − glucose measured in samples untreated)/2). The final trehalose concentration in each tissue or hemolymph sample was obtained by taking into consideration all dilutions used throughout the protocol. The results are shown as the mean ± standard error of the mean (SEM) (n = 6, where each n represents an individual tissue from 1 insect or a hemolymph pool from 2-3 insects).

Identification and Cloning of cDNA Sequence Encoding the *R. prolixus* Trehalose-Specific Facilitated Transporter (Rhopr-TRET)

By BLAST (Basic Local Alignment Search Tool) algorithm, the gene annotation from the RproC1.3 gene set (Mesquita et al., 2015) and using the trehalose transporter sequences from *Nilaparvata lugens* (XP_022183984.1) and *Cimex lectularius* (XP_024085685.1), we obtained the putative *Rhopr-TRET*. To successfully amplify and confirm the 5′ and 3′ regions of *Rhopr-TRET*, 5′ and 3′ rapid amplification of cDNA ends (RACE) assays were performed using the SMARTer RACE 5′/3′ Kit (Takara Bio USA, Mountain View, CA, United States). Briefly, fat bodies from fed females were dissected and placed in cold autoclaved phosphate buffered saline (PBS, 6.6 mM Na_2HPO_4/KH_2PO_4, 150 mM NaCl, pH 7.4). Total RNA extraction was performed with Trizol reagent (Invitrogen by Thermo Fisher Scientific, MA, United States) according to the manufacturer's recommendations. The final concentration and A260/280 ratio of purified RNA was measured using a DS-11 + spectrophotometer (DeNovix Inc., Wilmington, DE, United States). All samples had a ratio between 1.9 and 2.0. RNA integrity, including potential degradation products and DNA contamination, was evaluated by electrophoresis in a 1% agarose gel (FroggaBio Inc., Concord, ON, Canada). RNA was considered intact when the 18S rRNA band was observed. 5′- and 3′-RACE-ready cDNA were synthesized using the SMARTScribe Reverse Transcriptase, provided in the kit. Three specific pairs of primers were used in order to ensure specificity of the amplified sequence. The manufacturer-supplied protocol was followed to perform RACE reactions. The final products of the RACE reactions were later subjected to 2% agarose gel electrophoresis and the single products obtained of the expected sizes were sent for Sanger sequencing by Macrogen USA (Macrogen, Brooklyn, NY, United States). The gene-specific primers utilized are shown in **Supplementary Table 1**. All reactions were performed using an s1000 thermal cycler (Bio-Rad Laboratories, Mississauga, ON, Canada).

Sequence Analysis of Rhopr-TRET

Following sequencing of *Rhopr-TRET*, the predicted structural and biochemical features of the transporter were analyzed using online tools. To predict the exon–intron boundaries within the sequence, nucleotide BLAST (BLASTn) was performed using the *R. prolixus* genome deposited in VectorBase. Exon–Intron

Graphic Maker was the tool used to make the exon map of *Rhopr-TRET* with the ORF[1]. The deduced amino acid sequence and molecular mass prediction were assessed using tools available on ExPASy[2] (SIB Bioinformatics Resource Portal) (Artimo et al., 2012). The transmembrane domains were predicted by TMHMM Server v.2.0[3]. NetPhos 3.1 server was used to predict the potential intracellular phosphorylation sites[4], NetNGlyc 1.0 server for predicting the potential N-linked glycosylation sites[5], and GPS-lipid for predicting lipid modifications[6] (Blom et al., 1999; Sigrist et al., 2013; Xie et al., 2016). In order to provide insights into *Rhopr-TRET* function, the identification of potential domains was analyzed by Pfam 33.1 server[7] (El-Gebali et al., 2019). In addition, using VectorBase and orthoMCL DB (Li et al., 2003), potential orthologs were identified. RNA-seq data, available from the National Center for Biotechnology Information (NCBI) database (accession numbers PRJNA624187 and PRJNA624904 BioProjects) (Leyria et al., 2020a,b), was used to analyze the transcript expression of putative orthologs in the fat body and ovaries of unfed and fed *R. prolixus* females. Maxima structural model was built based on crystallographic data from proteins with similar secondary structure arrangements, using Phyre2 server (Kelley et al., 2015). The structure was visualized and analyzed using EZmol software (Reynolds et al., 2018).

Phylogenetic Analysis of Rhopr-TRET

Alignment of Rhopr-TRET was performed with TRET sequences from several invertebrate species, a bacterium and various glucose transporters from mammals, using the MUSCLE alignment tool[8] and later imported into the BOXSHADE 3.21 server[9]. Thirty-six amino acid sequences (**Supplementary File 1**) were imported into MEGA X (Molecular Evolutionary Genetics Analysis) (Pennsylvania, United States) (Kumar et al., 2018). To determine the relationship between insect sequences, a phylogenetic tree was constructed using the maximum likelihood method [based on the Jones–Thornton–Taylor (JTT) matrix-based model] (Jones et al., 1992). Bootstrap analysis was carried out using 1,000 replicates to determine confidence statistics (Felsenstein, 1985). In addition, a phylogenetic analysis of Rhopr-TRET and putative orthologs was performed as described above.

RNA Extraction and Reverse Transcription/Quantitative PCR (RT-qPCR)

mRNA levels of *TPS* (VectorBase: RPRC003010), *Rhopr-TRET* and 2 trehalases, membrane-bound (*m-Tre*) and soluble (*s-Tre*) enzymes (VectorBase: RPRC004614 and RPRC012647, respectively), were assessed in the fat body and ovaries of females throughout different time points of the unfed and fed states. In addition, the *Rhopr-AKH* precursor (VectorBase: RPRC000416) and its receptor, *Rhopr-AKHR* (GenBank: KF534791), were analyzed throughout different time points of the unfed condition in fat body, ovaries and central nervous system [CNS, composed of the brain, the suboesophageal ganglion, the prothoracic ganglion and the mesothoracic ganglionic mass, and also including the *corpora cardiaca/corpora allata* complex (CC/CA)]. The spatial distribution of the *Rhopr-TRET* transcript in different tissues (CNS, ovaries, oviducts, fat body, foregut, anterior midgut, posterior midgut, salivary glands, accessory reproductive glands, hemocytes, hindgut, Malpighian tubules and dorsal vessel) was evaluated during the unfed condition (baseline stage). Tissue dissection was performed as previously reported (Leyria et al., 2020a,b). Briefly, the tissues were dissected from females during different time points of unfed and fed states, in cold autoclaved PBS. For hemocyte collection, hemolymph samples were obtained as stated in Section "Trehalose Quantification" and then the hemocytes were pelleted by centrifugation at 10,000 × *g* for 10 min at 4°C. Total RNA extractions were performed with Trizol reagent, as described above. cDNA synthesis was performed from 1 μg of total RNA by reverse transcription reaction using random primers and 50 U of MultiScribe MuLV reverse transcriptase (High Capacity cDNA Reverse Transcription Kit, Applied-Biosystems, by Fisher Scientific, ON, Canada). The conditions of the thermal cycler were: 10 min at 25°C, 120 min at 37°C, and 5 min at 85°C. qPCR assays were performed using an advanced master mix with super green low rox reagent (Wisent Bioproducts Inc., QC, Canada), according to the manufacturer's recommendations, using 4 pmol of sense and antisense primers in a final volume of 10 μl. The qPCR temperature-cycling profile was: initial denaturation 3 min at 95°C, followed by 39 cycles of 30 s at 94°C, 30 s at 58–60°C (depending on the pair of primers used), and 1 min at 72°C, followed by a final extension at 72°C for 10 min. Each reaction contained 3 technical replicates as well as a no template control and a no reverse transcriptase control. The reactions were carried out using a CFX384 Touch Real-Time PCR Detection System (Bio-Rad Laboratories Ltd., ON, Canada). Quantitative validation was analyzed by the $2^{-\Delta\Delta}$Ct method (Livak and Schmittgen, 2011). 18S ribosomal RNA subunit and β-actin were used as reference genes (Majerowicz et al., 2011; Leyria et al., 2020a) and the transcript expressions were normalized via geometric mean. Primers (by Sigma-Aldrich, ON, Canada) are listed in **Supplementary Table 1**. Primers were designed at the exon–exon junction (i.e., over two different exons) in order to ensure that the primers only amplify transcripts. For each pair of primers, the efficiency ranged from 88 to 116%, with linear correlation coefficients (r^2) ranging from 0.8 to 1, and the dissociation curves always showed a single peak, indicating that a single cDNA product was amplified and excluding the possibility or tendency of the primers to form dimers. Specific target amplification was confirmed by automated DNA sequencing, as described above. The results are shown as the mean ± SEM (n = 3–4, where each n represents a pool of tissues from 3 insects).

[1] http://wormweb.org/exonintron
[2] www.expasy.org
[3] http://www.cbs.dtu.dk/services/TMHMM/
[4] http://www.cbs.dtu.dk/services/NetPhos/
[5] http://www.cbs.dtu.dk/services/NetNGlyc/
[6] http://lipid.biocuckoo.org/
[7] http://pfam.xfam.org/
[8] https://www.ebi.ac.uk/Tools/msa/muscle/
[9] https://embnet.vital-it.ch/software/BOX_form.html

Ex vivo and *in vivo* Insulin and AKH Signaling Stimulation

For *ex vivo* assays, ovaries of unfed females at 10 days post-ecdysis were incubated with human insulin (Millipore-Sigma, Oakville, ON, Canada), porcine insulin (Millipore-Sigma, Oakville, ON, Canada), *R. prolixus* ILP1 (Rhopr-ILP1, chemically synthesized by DGpeptidesCo., Ltd., Zhejiang, China) or with of the mammalian insulin receptor-specific activator bpV (phen) (Millipore-Sigma, Milwaukee, WI, United States). Insulin stock solutions were solubilized in pH 3 with HCl and bpV (phen) in dimethyl sulfoxide (DMSO), according to the manufacturer protocol. To make working solutions, all the drugs were diluted in *R. prolixus* saline. The incubations were performed for 3 h or 12 h, as indicated, in 200 ml of Grace's Insect Medium (Millipore-Sigma, Oakville, ON, Canada), at 30°C in the dark, as previously described (Cruz et al., 2006). The final concentration of human insulin, porcine insulin and Rhopr-ILP1 in the incubation medium was 1 mM, and for bpV(phen) was 0.1 mM. The stimulatory effects of mammalian insulins and bpV (phen) on the insulin receptor pathway in *R. prolixus* were previously reported (Defferrari et al., 2018; Leyria et al., 2020a). In parallel, ovaries of unfed females at 10 days post-ecdysis were incubated under the same condition with 0.1 μM *R. prolixus* AKH (Rhopr-AKH, pQLTFSTDWamide, chemically synthesized by Genscript Laboratories, Piscataway, NJ, United States). Stock solutions of Rhopr-AKH were dissolved in 50% 1-Methyl-2-Pyrrolidinone (Millipore-Sigma, Oakville, ON, Canada) and then stored at −20°C (Zandawala et al., 2015; Hamoudi et al., 2016). Rhopr-AKH was diluted with *R. prolixus* saline prior to performing the experiments. The solvent in the working dilution represents only 0.001% of the final volume; previously we demonstrated that this concentration does not interfere with experiments (Zandawala et al., 2015). After incubation, all tissues were immediately placed in Trizol and processed for RNA extraction and subsequent RT-qPCR to assess *Rhopr-TRET* and *TPS* mRNA levels. For both *ex vivo* assays, the results are shown as the mean ± SEM (n = 3–4, where each n represents a pool of tissues from 2 insects).

For *in vivo* assays, unfed insects (10 days post-ecdysis) were injected into the hemocoel with 5 μl of 0.1 μg/μl porcine insulin (Defferrari et al., 2018; Leyria et al., 2020a) or 0.01 μg/μl Rhopr-AKH (Zandawala et al., 2015). As control, a group of insects was injected with 5 μl of *R. prolixus* saline. Ovaries were removed under autoclaved PBS at 3 h post-injection and processed for RNA extraction and subsequent RT-qPCR to assess *Rhopr-TRET* and *TPS* mRNA levels. We used females at 10 days post-ecdysis for *in vivo* assays because (a) we previously demonstrated that unfed females of *R. prolixus* are in a sensitized state to respond to an increase of ILP levels by rapidly activating ILP signaling (Leyria et al., 2020a), and (b) food deprivation is the main stimulus for the release of AKH, which works as a metabolic stimulator leading to both carbohydrate and lipid mobilization (Bednáøová et al., 2013; Alves-Bezerra et al., 2016) and, thus the tissues should be also sensitized to respond rapidly to AKH stimulation. For both *in vivo* assays, the results are shown as the mean ± SEM (n = 3–4, where each n represents a pool of tissues from 2 insects).

Double-Stranded RNA (dsRNA) Design and Synthesis

In order to downregulate insulin and AKH signaling, the specific receptors involved in the activation of their respective cascades were interfered with using dsRNA. Gene specific primers were combined with the T7 RNA polymerase promoter sequence (**Supplementary Table 1**). Briefly, the following temperature-cycling profile was used for all PCRs: initial denaturation at 94°C for 3 min, followed by 30 cycles of 94°C for 30 s, 58°C for 30 s and 72°C for 90 s, and a final extension at 72°C for 10 min. The final PCR product was purified and used as template to synthesize dsRNA with T7 Ribomax Express RNAi System (Promega, Madison, WI, United States), according to the manufacturer's recommendations. As control, a dsRNA molecule based on the Ampicillin Resistance Gene (dsARG) from the pGEM-T Easy Vector system (Promega, Madison, WI, United States) was used throughout the study (Leyria et al., 2020a). The dsRNAs obtained were subjected to 2% agarose gel electrophoresis. A single product of the expected size was obtained for each dsRNA, which was sequenced, as described above, to confirm specificity. The sequences obtained were subjected to BLAST analysis in order to search for possible targets on VectorBase, where the *R. prolixus* genome is deposited. Alignments with the best-matching sequences are shown and scored in **Supplementary Figure 1**. Only 1 high confidence hit, i.e., genomic regions identified with high similarity with our sequence, was obtained. In addition, the specificity of dsRhopr-IR1 and dsRhopr-AKHR to downregulate *Rhopr-IR1* (Vectorbase: RPRC006251) and *Rhopr-AKHR* (GenBank: KF534791), respectively, was previously demonstrated (Zandawala et al., 2015; Defferrari et al., 2018).

Knockdown of Transcript Expression Using Double Stranded RNA

To evaluate the potential regulation of insulin signaling on *Rhopr-TRET* expression in ovaries, we used insects from a fed state, a condition where we previously demonstrated that the insulin cascade is activated (Leyria et al., 2020a). In brief, females at 10 days post-ecdysis were injected into the hemocoel with 5 μL of 2 μg/μL of dsRhopr-IR or dsARG and 3 h later the animals were given a blood meal. Insects were dissected 3 days post-injection and the transcriptional expression to *Rhopr-IR* and *Rhopr-TRET* were measured in the tissues by RT-qPCR, as described above. To evaluate the role of AKH signaling on *Rhopr-TRET* transcriptional expression, we used insects from an unfed state, a condition where AKH signaling should be increased. In brief, females 10 days post-ecdysis were injected into the hemocoel with 5 μL of 2 μg/μL of dsRhopr-AKHR or dsARG. Insects were dissected 1 or 2 days post-injection and the transcriptional expression of *Rhopr-AKHR* and *Rhopr-TRET* were measured in tissues by RT-qPCR, as described above. Groups of dsRhopr-IR1, dsRhopr-AKHR and dsARG treated insects (unfed females) were separated and injected (1 day after dsRNA treatment) into the hemocoel with 5 μl of 0.1 μg/μl porcine insulin, 0.01 μg/μl Rhopr-AKH or *R. prolixus* saline (control). Ovaries were removed under autoclaved PBS at 3 h after hormone injection and processed to RNA extraction and

subsequent RT-qPCR to assess *Rhopr-IR1*, *Rhopr-AKHR* and *Rhopr-TRET* mRNA levels, as indicated. In all cases, the results are shown as the mean ± SEM (n = 4–5, where each n represents an individual tissue from 1 insect). In addition, the percent survival of dsRhopr-AKHR injected insects during the unfed condition was analyzed (n = 15).

In vivo Trehalose Injection

In order to evaluate the effect of an increase in circulating trehalose on insulin and AKH signaling, unfed females (10 days post-ecdysis) were injected into the hemocoel with 5 μl of 70 μg/μl trehalose solution (Millipore-Sigma, Oakville, ON, Canada) diluted in *R. prolixus* saline, or 5 μl of *R. prolixus* saline (control). Insects were dissected 3 h post-injection and the expression of *Rhopr-TRET* and of the peptides *Rhopr-ILP1* (GenBank: KT896507.1), *Rhopr-IGF* (*R. prolixus* insulin growth factor, GenBank: KX185519.1) and *Rhopr-AKH* were measured in the ovaries, fat bodies or CNS, as indicated, by RT-qPCR. In addition, groups of dsRhopr-IR1 and dsARG treated insects were injected (1 day after dsRNA treatment) into the hemocoel with 5 μl of 70 μg/μl trehalose solution or 5 μl of *R. prolixus* saline (control). Fat bodies were removed under autoclaved PBS at 3 h post-injection and processed for RNA extraction and subsequent RT-qPCR to assess *Rhopr-IR1* and *Rhopr-TRET* mRNA levels. In all cases, the results are shown as the mean ± SEM (n = 4–5, where each n represents an individual tissue from 1 insect).

Statistical Analyses

All graphs were created using GraphPad Prism 9 (GraphPad Software, San Diego, CA, United States[10]). Before performing statistical analysis, we evaluated the data for normality and homogeneity of variance using the Shapiro–Wilk test, which showed that no transformations were needed, all datasets passed normality and homoscedasticity tests. Multiple group analysis was conducted by one-way ANOVA and Tukey's test as *post hoc* test, and statistically significant difference between two groups were inferred using T-test. Differences in the survival curve were analyzed using the Log-Rank test. In all the cases, a p-value < 0.05 was considered statistically significant.

[10]www.graphpad.com

RESULTS

Trehalose Quantification in Fat Body, Ovaries, and Hemolymph in Response to a Blood Meal

Trehalose content in key tissues involved in reproduction, namely the fat body (**Figure 1A**) and ovaries (**Figure 1B**), as well as circulating titers in the hemolymph (**Figure 1C**), was measured at representative days during the unfed and fed conditions. Under our experimental conditions, no trehalose is detected in the fat body or the ovaries at 10 and 20 days post-ecdysis; indeed, it remains undetectable in the ovaries until feeding. Following the blood meal, there is an overall increase in trehalose content in both tissues as well as in the hemolymph. While the trehalose content in the fat body and ovaries is highest at 5 days post-blood meal, the highest hemolymph content is seen on the fourth day and remains at this high level on the fifth day after feeding.

Rhopr-TRET cDNA Sequence, Characterization, and Modeling

Recently, by transcriptome analysis we showed that *Rhopr-TRET* is more than six and threefold up-regulated in ovaries and fat body of fed insects, respectively (Leyria et al., 2020b), supporting the hypothesis that a direct trehalose uptake from the hemolymph via Rhopr-TRET could be an important process

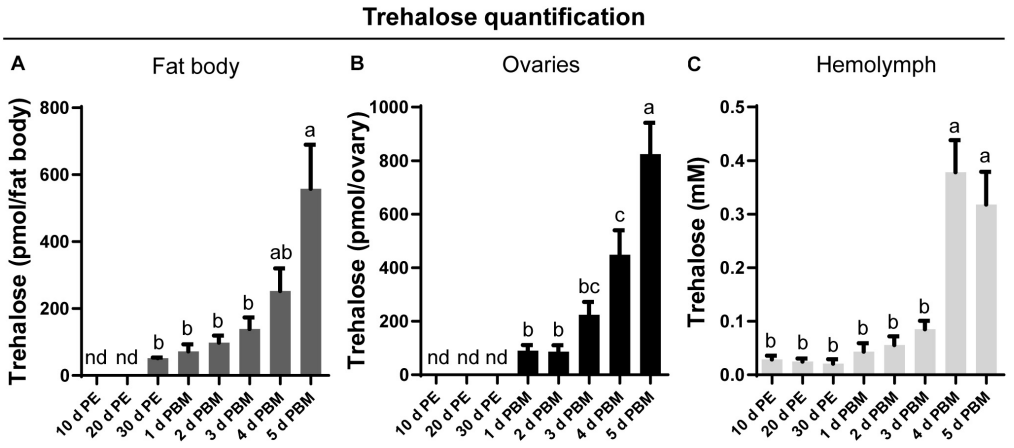

FIGURE 1 | Trehalose content in the fat body, ovary, and hemolymph of unfed and fed *R. prolixus* females. The trehalose content of fat body **(A)**, ovaries **(B),** and hemolymph **(C)** was quantified in unfed adult females [10, 20, and 30 days post-ecdysis (PE)] and in fed adult females at 1, 2, 3, 4, and 5 days post blood meal (PBM). Trehalose content increases significantly in both tissues and hemolymph following a blood-meal. The results are shown as the mean ± SEM (n = 6, where each n represents an individual tissue from 1 insect or a hemolymph pool from 2 to 3 insects). Statistically significant differences were determined by a one-way ANOVA and a Tukey's test as the *post hoc* test. Different letters indicate significant difference at $P < 0.05$. nd, not detected.

involved in the storage of carbohydrates in ovaries. The *Rhopr-TRET* candidate sequence was identified within the *R. prolixus* genome under the reference RPRC007957 and annotated as a partial sequence. We used this partial predicted sequence to design primers for RACE in order to confirm and obtain the complete sequence (GenBank: MW196439.1). Our results by RACE show an open reading frame (ORF) to *Rhopr-TRET* of 1,461 bp, which encodes a 51.58-kDa protein of 477 amino acids (**Supplementary Figure 2**). The ORF spans 6 exons, separated by 5 introns (**Figure 2A**). The domain prediction analysis revealed that *Rhopr-TRET* belongs to the sugar-transporter superfamily, including in its sequence the major facilitator superfamily domain, (MFS: CL0015) (**Supplementary Figure 3**). The RPRC007957 protein was previously annotated on the UniprotKB database (T1HV87_RHOPR) under the general classification of MFS. In addition, 12 sequences deposited on VectorBase were identified with the same conserved MFS domain, all of them belonging to the sugar transporter family (PF00083). Using BLASTp algorithm, 6 of them were classified as putative glucose transporters (RPRC002241, RPRC004616, RPRC010167, RPRC010168, RPRC011096, and RPRC014535), 1 was classified as a ribonuclease P protein subunit p25-like protein (RPRC011469), and 5 as putative trehalose transporters (RPRC002688, RPRC002833, RPRC005613, RPRC011385, and RPRC015169) (**Supplementary File 2**). Indeed, the phylogenetic tree groups Rhopr-TRET with the other putative trehalose transporters, suggesting the existence of a close relationship between them. In addition, all of the putative glucose transporters form a separate monophyletic group (**Supplementary Figure 4**). The alignment of the Rhopr-TRET amino acid sequence (via the online tool MUSCLE) with all of these sequences is shown in **Supplementary File 3**. RNA-seq data analysis shows that the putative trehalose transporters are, in general, more highly expressed in both tissues than are the glucose transporters, with *Rhopr-TRET* (RPRC007957) having the highest fold changes between fed and unfed insects (**Supplementary File 2**); and so subsequently this transcript was chosen to analyze in depth in this work. The putative transmembrane domains were predicted and suggest that Rhopr-TRET forms a 12-transmembrane structure, with a long loop connecting the transmembrane domain 6 (TM6) and TM7 on the cytosolic side of the membrane, and an intracellular *N*- and *C*-terminus, which are typical characteristics for the MFS (**Figure 2B**). Furthermore, residues conserved across all MFS members, with functional significance, are observed and highlighted (**Figure 2B**) (Kanamori et al., 2010; Price et al., 2010): tryptophan (W) and proline (P) residues in TM10, which are involved in substrate selectivity and conformational flexibility, respectively; QLS motif in TM7, involved in transport activity; glycine (G) residues conserved in the TM 1, 4, 5, 7, 8, and 10, critical to stabilize the structure; GRR/K motif in the second loop, a position characteristic of members of MFS, and a tryptophan residue in TM11, essential for transport activity (Kanamori et al., 2010), among others. By homology modeling, we can correctly predict the target structure of Rhopr-TRET (**Figure 2C**). In general, we note that polar residues form a central aqueous channel through which trehalose could be translocated through the membrane, and the hydrophobic residues would be those that participate in the anchoring of the transporter to the membrane since they are observed in a greater density on the side facing the membrane, outside of the channel (**Figure 2C**). Also, we observe post-translational modifications to Rhopr-TRET which would ensure complete functionality (**Figure 2D**): *N*-glycosylation is predicted to occur at Asn135, and Asn265 and Asp317, phosphorylation sites are predicted on 14 Thr residues, 6 Tyr residues, and 28 Ser residues, and palmitoylation predicted to occur on Cys149. Interestingly, we were unable to find the typical motif of most MFS sequences, an *N*-glycosylation site in the first extracellular loop (between TM1 and TM2).

As part of the characterization of Rhopr-TRET, we evaluated the spatial transcript expression of this transporter using various tissues from unfed adult females (baseline condition) using RT-qPCR. In accordance with the premise that the fat body is the main tissue involved in nutrient and energy metabolism, the highest expression of the *Rhopr-TRET* transcript is observed in this tissue (**Figure 2E**). The Rhopr-TRET amino acid sequence was aligned via the online tool MUSCLE with a number of sequenced orthologs from other species, including those for glucose transporters of mammals and a TRET sequence from a bacterium (**Supplementary File 1**). The results highlight the high degree of conservation in TRET sequences from insects. Indeed, the phylogenetic tree groups Rhopr-TRET with other hemipterans (**Supplementary Figure 3**), suggesting the existence of a close relationship to both the bed bug (*C. lectularius*) and the brown marmorated stink bug (*Halyomorpha halys*). In addition, all the glucose transporters form a separate monophyletic group and the TRET from *Escherichia coli* (WP_077788896.1) forms the out group.

Transcript Expression in Response to a Blood Meal

In order to obtain a general view on the dynamics of trehalose metabolism, it is essential to evaluate the expression of transcripts involved in the control of trehalose homeostasis. We examined the profiles of transcript expression of *TPS*, *m-Tre* and *s-Tre* as well as of *Rhopr-TRET* in the fat body and ovaries. Except for *TPS*, the transcript expression pattern in both tissues is quite similar throughout the different time points of the unfed and fed condition. In the fat body, *TPS* transcript levels are lower during the unfed condition but rise significantly post-blood meal when vitellogenesis begins, with maximum seen 1 day after feeding (**Figure 3A**). *Rhopr-TRET* transcript levels are also lower in the unfed condition but increase significantly (∼10-fold) by day 1 after blood feeding and remain high over the 5 days analyzed (**Figure 3B**). *m-Tre* transcript expression has a non-specific pattern of expression with regard to blood feeding, with fluctuating levels throughout all the time points (**Figure 3C**). However, *s-Tre* transcript expression is higher at day 20 and 30 of the unfed condition and remains low after the blood meal but with a slight non-statistical increase as the days post-feeding advance (**Figure 3D**).

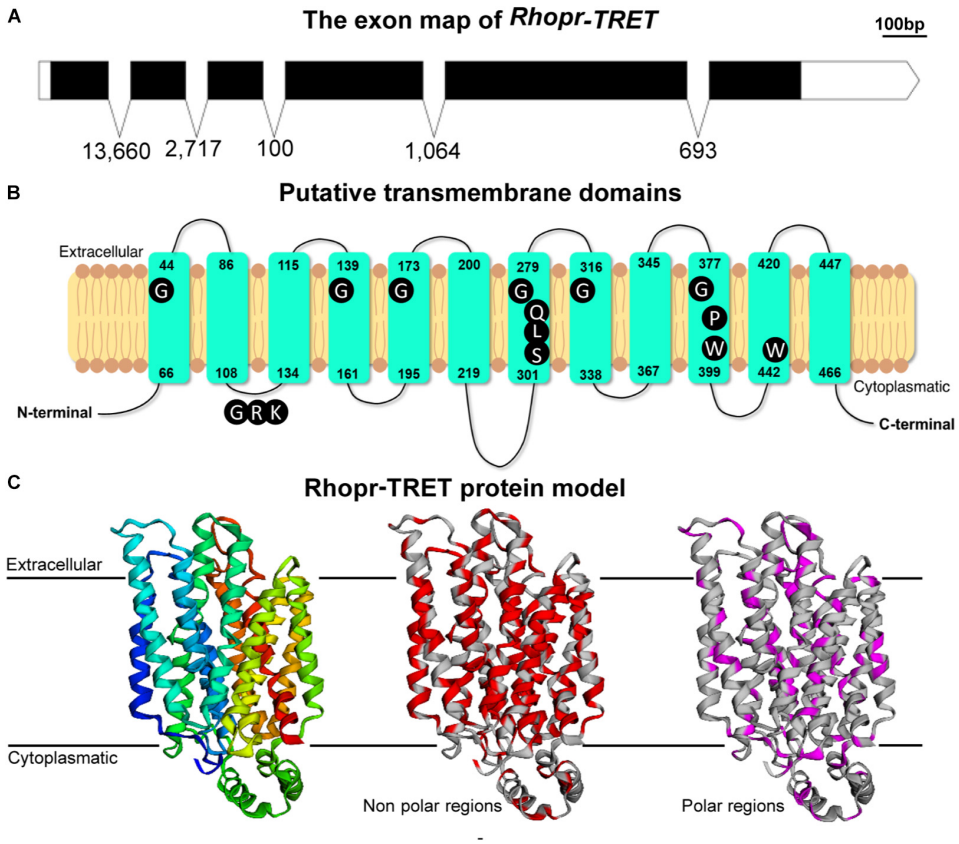

D **Putative post-translational modifications**

Prediction/position
S-Palmitoylation site/ 149
N-linked glycosylation sites/ 135, 265, 317
2, 20, 23, 35, 49, 60, 65, 70, 76, 86, 90, 95,
Y-phosphorylation sites/ 40, 63, 366, 377, 388, 435
S-phosphorylation sites/ 126, 137, 144, 154, 237, 253, 258, 267, 268, 312, 319, 370, 415, 418, 458, 473
T-phosphorylation sites/ 109, 115, 119, 172, 178, 221, 259, 303, 313, 363, 375, 428, 469, 470

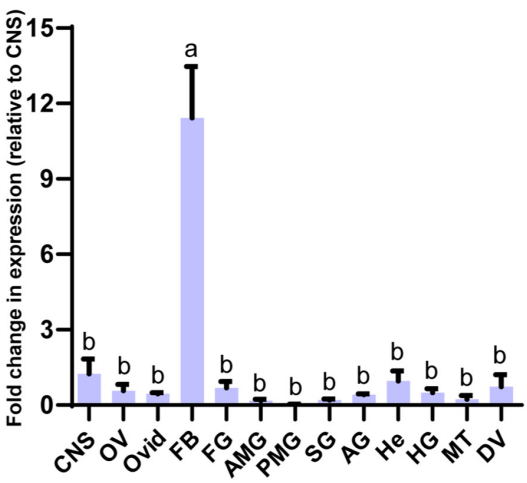

FIGURE 2 | Rhopr-TRET characterization and modeling. **(A)** Exon map of Rhopr-TRET of the open reading frame (ORF) and exons/introns. The ORF of Rhopr-TRET is denoted by the solid black box spanning the exons. The length of each box is representative of the nucleotide number (bar = 100 bp) and the numbers below represent the intron length as base pairs (bp). **(B)** Schematic diagram of *Rhopr-TRET*. The 12 transmembrane domains within the cell membrane and the position of the amino acids indicating the start and end of each transmembrane regions are shown. Conserved motifs among Rhopr-TRET sequences are highlighted in dark in their typical positions. **(C)** Molecular model of Rhopr-TRET. Cartoon representation of Rhopr-TRET illustrating the folds of the transporter; the putative non-polar and polar regions are also displayed. **(D)** Putative post-translational modifications, including *N*-glycosylation, phosphorylation and palmitoylation sites. **(E)** Distribution of *Rhopr-TRET* transcript in unfed adult female *R. prolixus*; central nervous system (CNS), ovaries (OV), oviducts (Ovid), fat body (FB), foregut (FG), anterior midgut (AMG), posterior midgut (PMG), salivary glands (SG), accessory glands (AG) (spermatheca and cement gland), hemocytes (He), hindgut (HG), Malpighian tubules (MT) and dorsal vessel (DV). The expression of transcripts in each tissue was quantified by RT-qPCR. The *y*-axis represents the fold change in expression relative to CNS (value ∼ 1). The results are shown as the mean ± SEM (n = 3–4, where each n represents a pool of tissues from 3 insects). Statistically significant differences were determined by a one-way ANOVA and a Tukey's test as the *post hoc* test. Different letters indicate significant difference at $P < 0.05$.

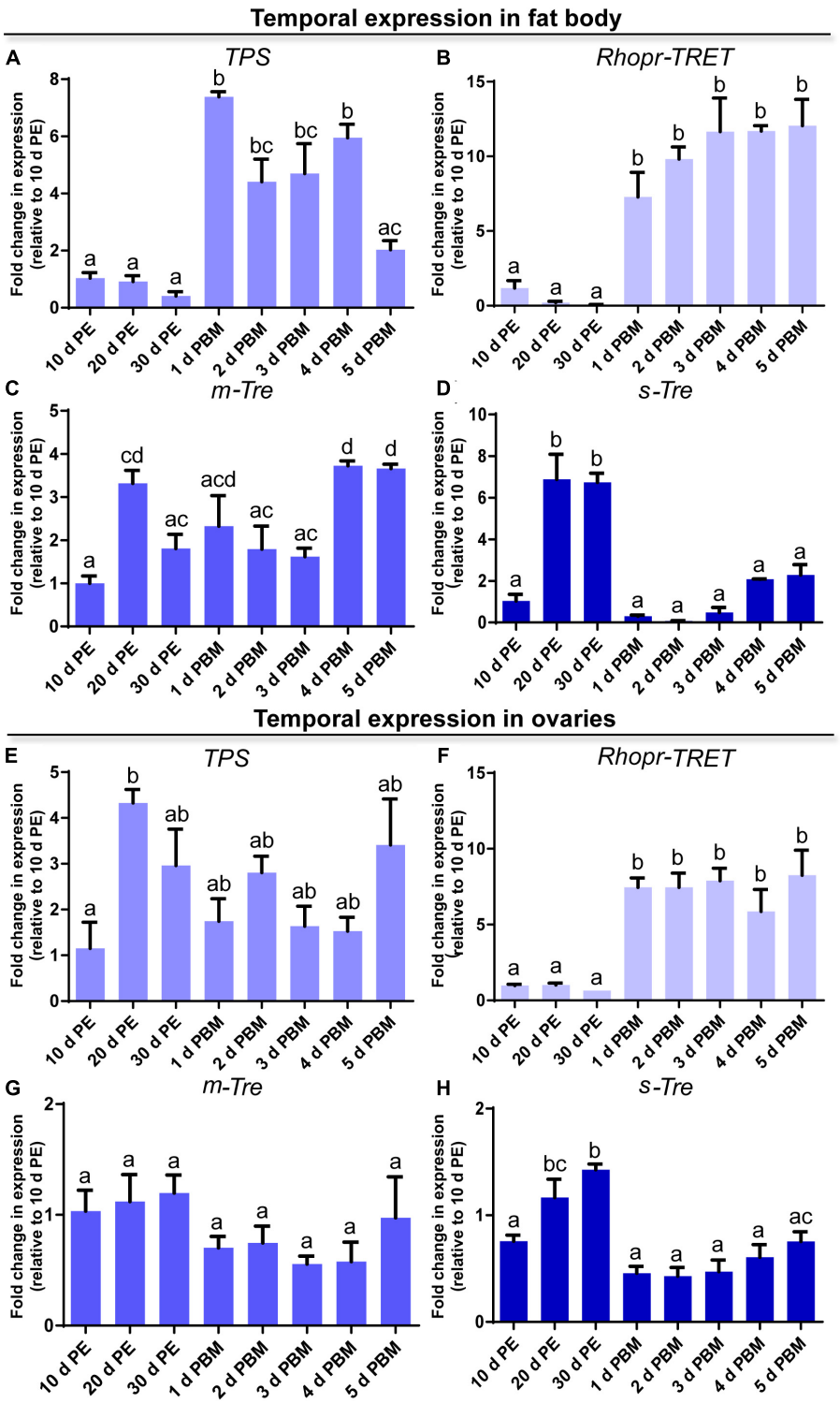

FIGURE 3 | Temporal expression of *trehalose synthase* (*TPS*), *Rhopr-TRET*, membrane-bound trehalase (*m-Tre*), and soluble trehalase (*s-Tre*) in the fat body and ovaries of *R. prolixus* under different nutritional conditions. Transcript expression of *TPS*, *Rhopr-TRET*, *m-Tre*, and *s-Tre* was quantified by RT-qPCR in the fat body (**A–D**, respectively) and ovaries (**E–H**, respectively) of adult females at varying days post-ecdysis (d PE), representing unfed conditions, and various days post-blood meal (d PBM), representing the fed condition. Results were analyzed by the $\Delta\Delta Ct$ method. The *y*-axis represents the fold change in expression relative to 10 days PE (value ~ 1). The results are shown as the mean ± SEM (n = 3–4, where each n represents a pool of tissues from 3 insects). Statistically significant differences were determined by a one-way ANOVA and a Tukey's test as the *post hoc* test. Different letters indicate significant difference at $P < 0.05$.

In the ovaries, the transcript for *TPS* after a blood meal shows levels similar to those during the unfed condition, i.e., 10, 20, and 30 days post-ecdysis (**Figure 3E**). However, a significant up-regulation of *Rhopr-TRET* transcript expression occurs after a blood meal when vitellogenesis has begun (**Figure 3F**). As seen in the fat body, *m-Tre* transcript expression has a fluctuating pattern throughout all the days analyzed (**Figure 3G**) and *s-Tre* transcript expression is up-regulated in unfed females (**Figure 3H**).

The Effects of Exogenous Insulins and Rhopr-AKH on *Rhopr-TRET* Transcript Expression in Ovaries From Unfed Females

Since insulin and AKH families are known to regulate carbohydrate metabolism in insects, we performed *ex vivo* and *in vivo* experiments using exogenous hormones and unfed female adults, where *Rhopr-TRET* transcript expression in the ovaries is low. For the *ex vivo* experiments, ovaries were incubated with insulin from 3 different sources, human insulin (H_In), porcine insulin (P_In), and *R. prolixus* ILP1 (Rhopr-ILP1), and an insulin receptor kinase activator, bpV (phen). RT-qPCR reveals that after 3 h of incubation, only the treatment with bpV (phen) is able to induce a significant increase in *Rhopr-TRET* expression ($p < 0.05$ vs. saline, by one-way ANOVA, $n = 3–4$) (**Figure 4A**). However, after 12 h of incubation, P_In and Rhopr-ILP1 also induce a statistical increase in *Rhopr-TRET* transcript expression ($p < 0.05$, by one-way ANOVA, $n = 3–4$) (**Figure 4B**). Rhopr-AKH is also able to promote an up-regulation of *Rhopr-TRET* transcript expression in ovaries with 3 h of incubation ($p = 0.019$ vs. saline, by Student's *t*-test, $n = 3–4$) (**Figure 4D**), suggesting that *Rhopr-TRET* transcript expression is regulated by hormones and that the ovaries of unfed females are more sensitized to respond rapidly to Rhopr-AKH than to insulins. In the same

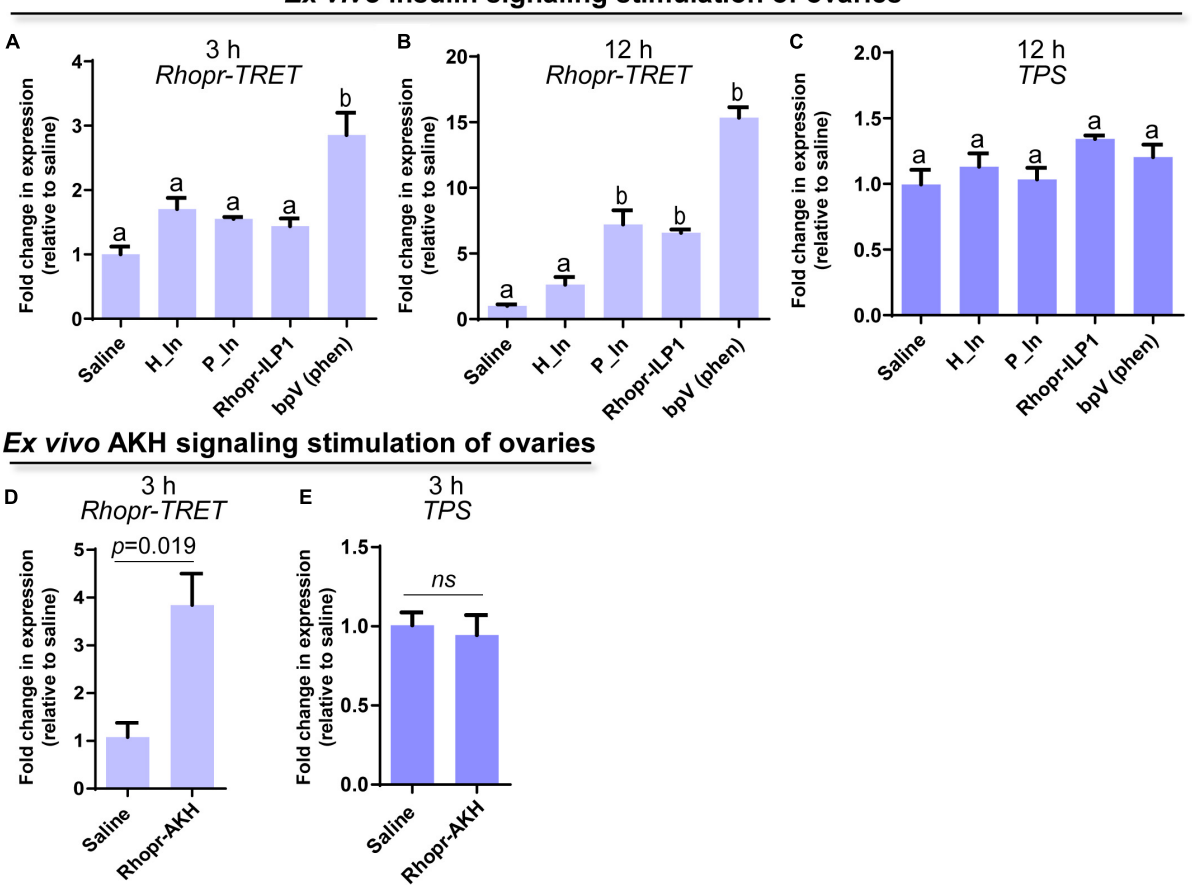

FIGURE 4 | Participation of insulin and AKH signaling in *Rhopr-TRET* mRNA expression using *ex vivo* assays. Ovaries from unfed adult females were incubated with human insulin (H_In), porcine insulin (P_In), *R. prolixus* ILP1 (Rhopr-ILP1), bpV (phen) or *R. prolixus* AKH (Rhopr-AKH). A control group of ovaries was incubated with only *R. prolixus* saline (saline). The effects of these stimulators on *Rhopr-TRET* and *TPS* transcript expression were tested by RT-qPCR. The *y*-axis represents the fold change in expression relative to control (saline, value ∼ 1). **(A)** *Rhopr-TRET* transcript expression after incubation with the insulin signaling activators for 3 h and **(B)** 12 h. **(C)** *TPS* transcript expression after incubation with the insulin signaling activators for 3 h. **(D)** *Rhopr-TRET* transcript expression after incubation with Rhopr-AKH for 3 h. **(E)** *TPS* transcript expression after incubation with Rhopr-AKH for 3 h. The results are shown as the mean ± SEM ($n = 3–4$, where each n represents a pool of tissues from 2 insects). For **(A–C)**, statistically significant differences were determined by one-way ANOVA and Tukey's test as *post hoc* test (different letters indicate significant difference at $P < 0.05$), and for **(D,E)** a Student's *t*-test was used.

ovaries, *TPS* expression was measured in order to assess the specificity of the transcript stimulation. The results show that under these experimental conditions, the transcript levels of the enzyme involved in trehalose synthesis is not altered after incubation of the ovaries with insulins, bpV (phen) or Rhopr-AKH (**Figures 4C,E**, respectively). To better understand the role of Rhopr-AKH and insulin signaling on the expression of *Rhopr-TRET* in the ovaries, we upregulated AKH (using Rhopr-AKH) and insulin (using P_In) signaling in unfed females by injection of these hormones into females at 10 days post-ecdysis, when *Rhopr-TRET* expression in the ovaries is low (**Figure 5A**). At 3 h post-injection, both hormones significantly increased the expression of *Rhopr-TRET* mRNA in ovaries (**Figures 5B,D**). As with the *ex vivo* assays, neither Rhopr-AKH nor P_In injections altered *TPS* transcript expression in the ovaries at our experimental times (**Figures 5C,E**).

Knockdown of *Rhopr-IR1* and *Rhopr-AKHR* Transcripts and Effects on *Rhopr-TRET* mRNA Expression in Ovaries

To further confirm the involvement of insulin and AKH signaling in regulating *Rhopr-TRET* transcript expression, we knocked down the receptors *Rhopr-IR1* and *Rhopr-AKHR,* using RNAi in fed or unfed females (**Figure 6A**). The dsRhopr-IR1 treatment did not influence the survival of the insects over the time course of the experiments (data not shown). However, after 2 days post-treatment, the percent survival in dsRhopr-AKHR treated insects decreased by 80% with respect to controls (**Figure 7D**); as a consequence, the tissue collection was performed 1 or 2 days post-treatment. The live insects treated with dsRhopr-AKHR showed behaviors, i.e., walking and movement of legs and proboscis when immobilized, comparable to controls at 2 days post-injection. In addition, to investigate the effects of dsRhopr-IR1 knockdown on the amount of blood ingested, the insects were weighed before and after feeding and no significant difference between treated and control females was observed (data not shown). RT-qPCR reveals that transcript levels for *Rhopr-IR1* and *Rhopr-AKHR* are reduced by 55 and 90%, respectively, in ovaries, at 3 and 2 days, respectively, following RNAi treatment (**Figures 6B,D**). Knocking down either *Rhopr-IR1* or *Rhopr-AKHR* transcripts reduced *Rhopr-TRET* transcript expression (**Figures 6C,E**). In addition, *TPS* transcript expression in the ovaries of these insects is not altered (data not shown). To confirm the potential regulation of *Rhopr-TRET* by hormones, we down-regulated Rhopr-IR1 and Rhopr-AKHR transcripts in unfed females and 1 day after dsRNA treatment, we injected porcine insulin (P_In) or Rhopr-AKH, as indicated (**Figure 6F**). Insects with down-regulated receptors (**Figures 6G,I**) are not able to increase *Rhopr-TRET* expression in ovaries after P_In (dsRhopr-IR1/P_In) or Rhopr-AKH (dsRhopr-AKHR/Rhopr-AKH) stimulation to the same levels as those of control insects [dsARG/P_In and dsARG/Rhopr-AKH (**Figures 6H,J**)]. Interestingly, dsRhopr-IR1 treated unfed insects (dsRhopr-IR1/S), are not able to down-regulate *Rhopr*-TRET (**Figure 6H**) as occurs in dsRhopr-IR1 treated insects 3 days post-feeding (**Figure 6C**). This finding shows that the blood meal is an important signal to control *Rhopr-TRET* mRNA levels via insulin signaling.

The Effects of Trehalose Injection in Unfed Females on *Rhopr-TRET* Transcript Expression in Fat Body and Ovaries

The previous results suggest that AKH and insulin signaling could contribute substantially to trehalose homeostasis through the regulation of *Rhopr-TRET* transcript expression. We therefore questioned if injection of trehalose into unfed females could modify the transcripts involved in such signaling (**Figure 8A**). In our experimental condition, trehalose injection significantly increases *Rhopr-TRET* transcript expression in the fat body ($p = 0.031$, by the Student's *t*-test, $n = 5$) at 3 h post-injection, but not in the ovaries (**Figures 8B,C**). In addition, we examined transcripts involved with the insulin and AKH signaling pathway after trehalose injection. **Figures 8D,F** show that following trehalose injection *Rhopr-IGF* and *Rhopr-ILP1* transcript levels significantly increase in the fat body and CNS, respectively, demonstrating a potential stimulatory effect on insulin signaling, which is not observed in ovaries (**Figure 8E**). In contrast, *Rhopr-AKH* transcript expression tends to decrease in the CNS ($p > 0.05$, by Student's *t*-test, $n = 4$) (**Figure 8G**). To confirm the possible regulation of *Rhopr-TRET* by insulin signaling, we down-regulated *Rhopr-IR1* in unfed females (as described above) and 1 day after dsRNA treatment, we injected trehalose (**Figure 8H**). Insects with down-regulated *Rhopr-IR1* are not able to increase *Rhopr-TRET* expression in the fat body after trehalose injection (dsRhopr-IR1/T) to the same levels as those of control insects (dsARG/T) (**Figures 8I,J**). This finding shows that trehalose seems to be an important signal for controlling *Rhopr-TRET* mRNA levels via insulin signaling at least in the fat body.

Taking into account the premise that AKH signaling has been widely studied as a catabolic cascade involved in energy production under unfavorable conditions, we evaluated the abundance of transcripts involved in AKH signaling during the unfed state on the 3 key tissues implicated in reproductive performance. As can be seen in **Figures 7A,B**, expression of *Rhopr-AKHR* transcript in the fat body and ovaries increases as the unfed condition advances, with higher levels at 30 days post-ecdysis. Accordingly, the *Rhopr-AKH* transcript expression in CNS also increases at 30 days post-ecdysis (**Figure 7C**). Interestingly, the survival of unfed insects with knock down for *Rhopr-AKHR* significantly decreases with respect to controls (dsARG) (**Figure 7D**) 2 days post dsRNA treatment. Overall, these results suggest that AKH signaling could play a leading role during starvation.

DISCUSSION

Hematophagous insects, like triatomines, feed on blood that is rich in proteins but relatively poor in lipids and carbohydrates. However, the accumulation of carbohydrate

by the eggs of *R. prolixus* is of some importance to support successful embryogenesis (Santos et al., 2008). Taking this into consideration, we show here the potential control by ILPs and AKH signaling cascades over trehalose uptake by ovaries. In addition, we suggest that Rhopr-TRET may work cooperatively with AKH signaling to support the release of trehalose from tissues into the hemolymph to be used as a source of fuel during stressful situations such as starvation.

Glycogen represents an important energy reserve in all animal cells, including the oocytes of insects (Arrese and Soulages, 2010), since glycogen, along with lipids, are primarily utilized in the metabolic production of ATP and carbon sources. While proteins

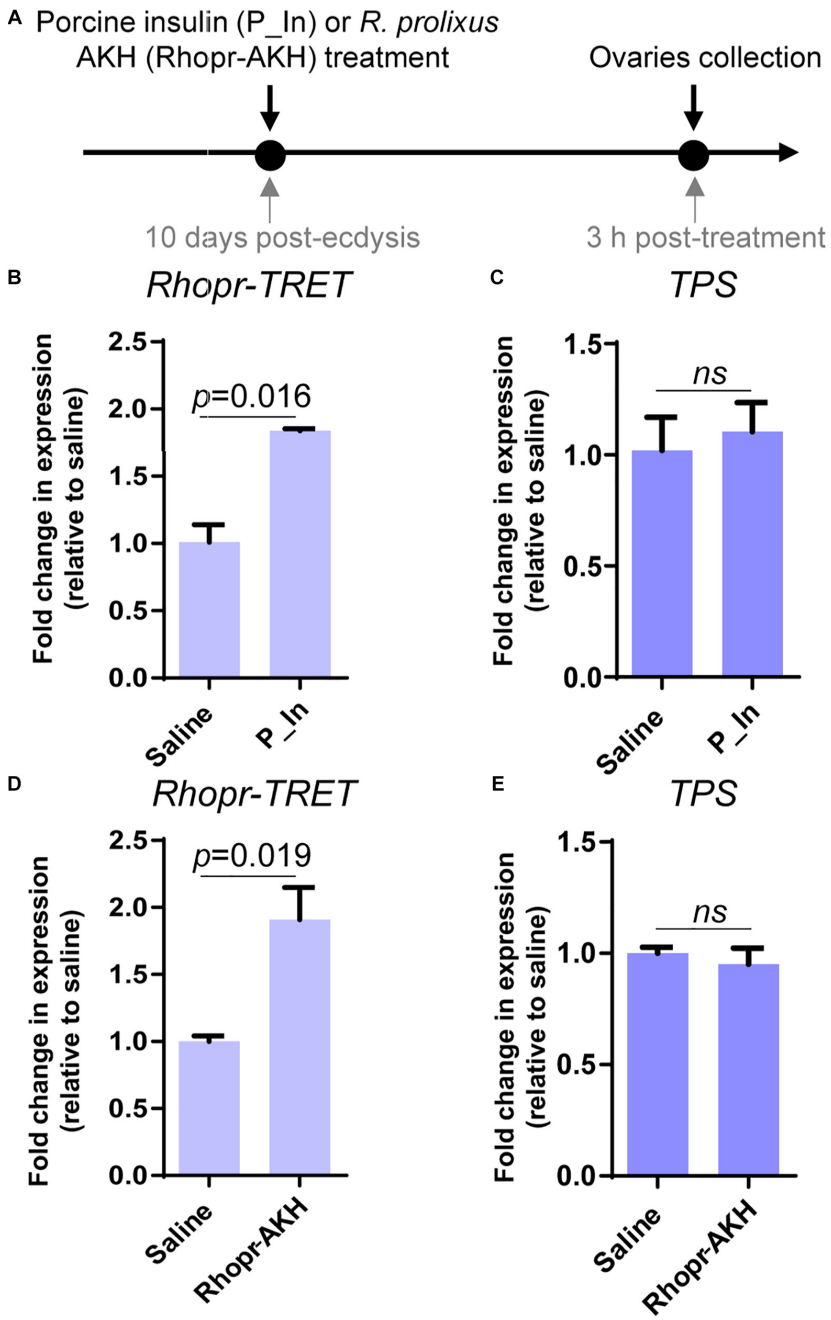

FIGURE 5 | Participation of insulin and AKH signaling in *Rhopr-TRET* mRNA expression using *in vivo* assays. **(A)** Experimental scheme for **(B–E)**. **(B)** *Rhopr-TRET* transcript expression after P_In injection; **(C)** *TPS* transcript expression after P_In injection; **(D)** *Rhopr-TRET* transcript expression after Rhopr-AKH injection. **(E)** *TPS* transcript expression after Rhopr-AKH injection. *Rhopr-TRET* and *TPS* transcript expression in ovaries of unfed adult females was tested by RT-qPCR. The *y*-axis represents the fold change in expression relative to control (saline, value ∼ 1). The results are shown as the mean ± SEM (n = 3–4, where each n represents a pool of tissues from 2 insects). Statistically significant differences were determined by the Student's *t*-test.

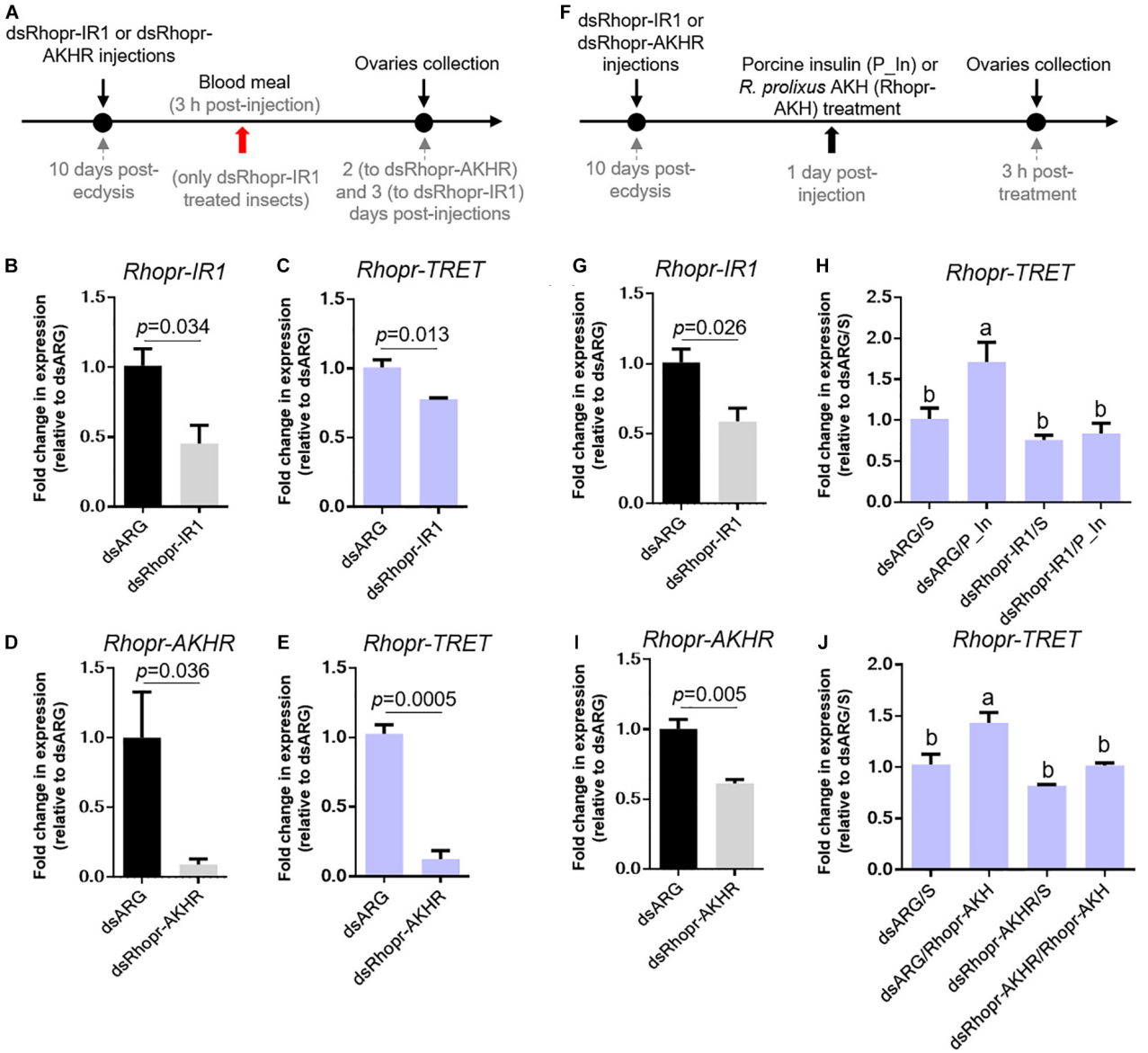

FIGURE 6 | Effect of dsRNA treatment on *Rhopr-TRET* mRNA expression. **(A)** Experimental scheme for **(B–E)**. Panels **(B,D)** show the knockdown efficiency of dsRhopr-IR1 and dsRhopr-AKHR treatments, respectively.Panels **(C,E)** show the effects of down-regulation of *Rhopr-IR1* and *Rhopr-AKHR* transcripts on *Rhopr-TRET* expression. **(F)** Experimental scheme for **(G–J)**. Panels **(G,I)** show the knockdown efficiency of dsRhopr-IR1 and dsRhopr-AKHR treatments, respectively. Panels **(H,J)** show the effects of down-regulation of *Rhopr-IR1* and *Rhopr-AKHR* transcripts on *Rhopr-TRET* mRNA expression following P_In **(H)**, Rhopr-AKH **(J)** or saline stimulation. Transcript expression was tested by RT-qPCR. The *y*-axis represents the fold change in expression relative to dsARG injection after saline treatment (dsARG/S, value ∼ 1) obtained viageometric averaging using 18S ribosomal RNA subunit and β-actin as reference genes. The results are shown as the mean ± SEM (n = 4–5, where each n represents an individual tissue from 1 insect). Statistically significant differences were determined by Student's *t*-test in all graphs except for **(H,J)** in which a one-way ANOVA and Tukey's test as *post hoc* test was used (different letters indicate significant difference at $P < 0.05$). dsARG/S: dsARG insects with saline injection; dsARG/P_In: dsARG insects with porcine insulin injection: dsARG/Rhopr-AKH: dsARG insects with Rhopr-AKH injection; dsRhopr-IR1/S: dsRhopr/IR1 insects with saline injection; dsRhopr-IR1/P_In: dsRhopr-IR1 insects with porcine insulin injection; dsRhopr-AKHR/S: dsRhopr-AKHR insects with saline injection; dsRhopr-AKHR/Rhopr-AKH: dsRhopr-AKHR insects with Rhopr-AKH injection.

and lipids are sequestered by the developing oocyte from extra-ovarian tissues (Raikhel and Dhadialla, 1992; Canavoso et al., 2001), glycogen is synthesized in the ovary itself. The fat body is the major site of synthesis of trehalose in insects, with the trehalose capable of being released into the circulation for use by other tissues, including ovaries, depending on the specific physiological state (Tang et al., 2018). Here, we show that before a blood meal, the amount of trehalose in the fat body and ovaries is very low or not detectable. This is to be expected since trehalose is not used for carbohydrate accumulation, but rather as an intermediary between what is stored as glycogen and what is transferred to other tissues. Unfed or starved insects tend to

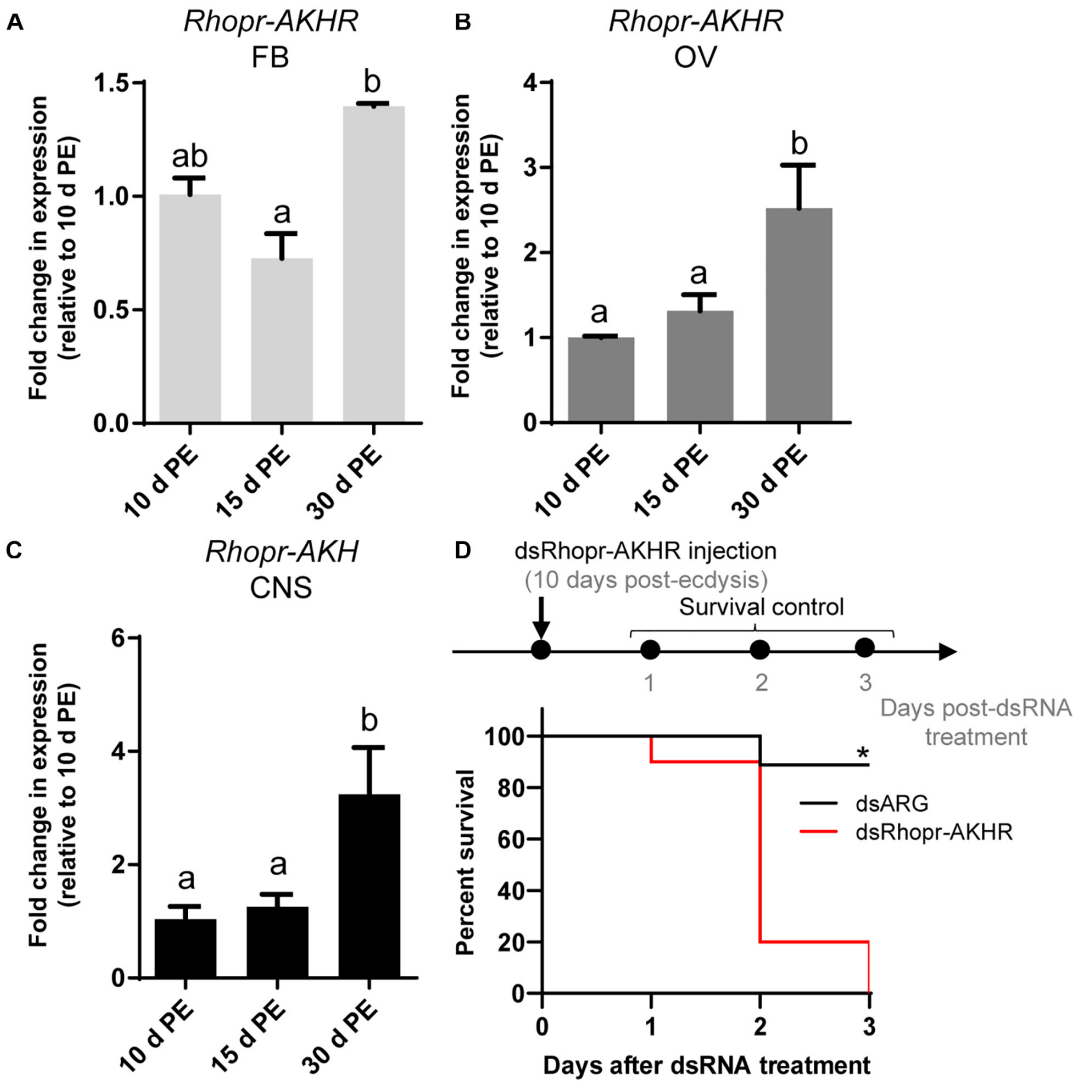

FIGURE 7 | Transcript expression of *Rhopr-AKHR* and *Rhopr-AKH* in fat body, ovaries and CNS following ecdysis into adults. *Rhopr-AKHR* transcript expression in the fat body **(A)** and ovaries **(B)**, and *Rhopr-AKH* transcript expression in the CNS **(C)** were assessed at various times post-ecdysis (PE) in adult females. The effects were measured by RT-qPCR. The *y*-axis represents the fold change in expression relative to 10 days PE (value ∼ 1). The results are shown as the mean ± SEM (n = 3–4, where each n represents a pool of tissues from 3 insects). The statistically significant differences were determined by a one-way ANOVA and a Tukey's test as the *post hoc* test. Significance of $P < 0.05$ is denoted using letters to indicate bars that are significantly different from others. **(D)** Percent survival of dsRhopr-AKHR injected insects with respect to control (dsARG) over 3 days in the unfed condition (n = 15). Differences in the survival curve were analyzed using the Log-Rank test (*$p < 0.001$).

break down nutrients stored in tissues and then release them into the hemolymph to sustain the female's lifespan until nutritional shortage is alleviated (Bell and Bohm, 1975; Leyria et al., 2014). In *R. prolixus*, the glycogen stored in the ovaries or fat body during the unfed condition (Leyria et al., 2020b) may progressively decline due to trehalose synthesis and release into the circulation for use by other tissues; indeed, trehalose is detected in the fat body of *R. prolixus* females under long periods of starvation. This may be the reason why there are measurable levels of circulating trehalose during the unfed condition. In a related triatomine species, *Dipetalogaster maxima*, ovarian nutritional resources, including carbohydrates, decrease when nutritional resources are scarce, reflecting adjustments in metabolism due to the physiological needs of the female (Leyria et al., 2014).

In *R. prolixus* females, a blood meal triggers an increase in trehalose concentration in the fat body, hemolymph and ovaries, reaching maximum at 4–5 days after feeding. In our experimental conditions, *R. prolixus* females begin laying eggs 5 days after a blood meal (Leyria et al., 2020a) and due to the asynchronous development of the ovarioles (Atella et al., 2005;

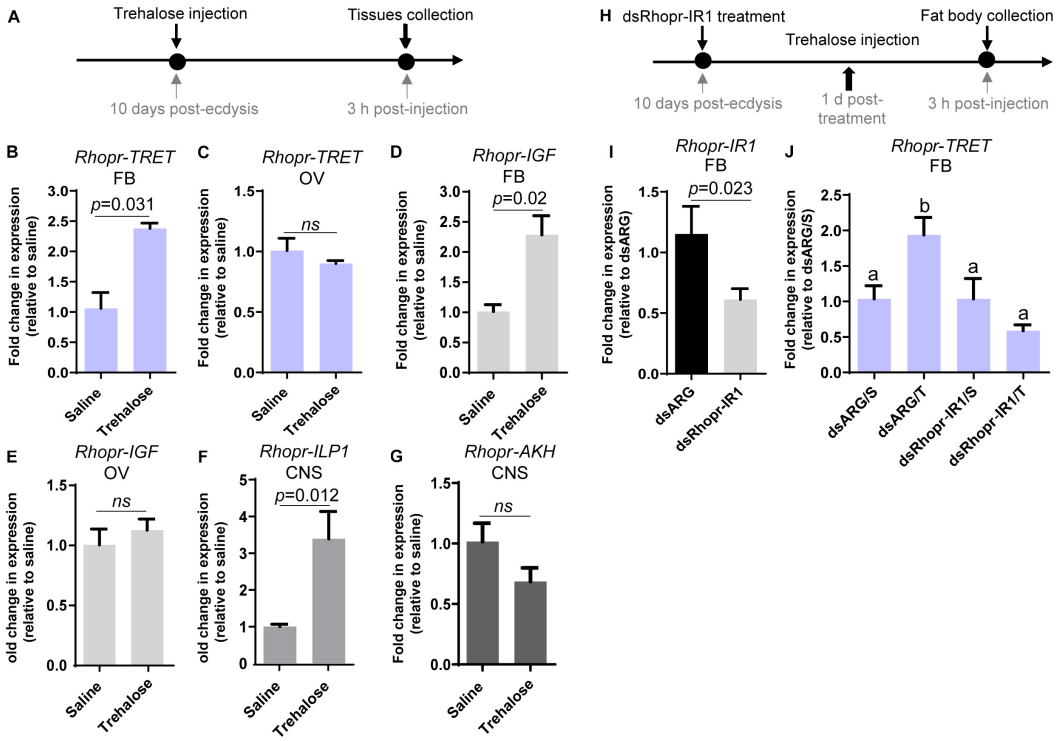

FIGURE 8 | Effects of trehalose injection on the expression of *Rhopr-TRET* and genes involved in insulin and AKH signaling. **(A)** Experimental scheme for **(B–G)**. Unfed adult females were injected with either trehalose or saline (control). The fat body, ovaries and CNS were dissected 3 h after trehalose injection. **(B)** *Rhopr-TRET* transcript expression in the fat body and **(C)** the ovaries; **(D)** *Rhopr-IGF* transcript expression in the fat body and **(E)** in ovaries; **(F)** *Rhopr-ILP1* and **(G)** *Rhopr-AKH* transcript expression in CNS. The effects were measured by RT-qPCR. The *y*-axis represents the fold change in expression relative to control (saline injection, value ∼ 1). **(H)** Experimental scheme for **(I,J)**. Panel **(I)** shows the knockdown efficiency of dsRhopr-IR1 treatments. Panel **(J)** shows the effects of down-regulation of *Rhopr-IR1* transcripts on *Rhopr-TRET* mRNA expression following trehalose stimulation. The *y*-axis represents the fold change in expression relative to dsARG injection after saline treatment (dsARG/S, value ∼ 1). In all the cases, the results are shown as the mean ± SEM (n = 4–5, where each n represents an individual tissue from 1 insect). Statistically significant differences were determined by Student's t-test in all graphs except for **(J)** in which a one-way ANOVA and Tukey's test as *post hoc* test was used (different letters indicate significant difference at $P < 0.05$). dsARG/S: dsARG insects with saline injection; dsARG/T: dsARG insects with trehalose injection; dsRhopr-IR1/S: dsRhopr/IR1 insects with saline injection; dsRhopr-IR1/T: dsRhopr-IR1 insects with trehalose injection.

Aguirre et al., 2011), triatomine females can lay eggs for at least 25–30 days. During this period, carbohydrates should be constantly produced, mainly by the key tissue involved in nutrient metabolism, the fat body, released and then stored by the oocytes. We evaluated the dynamics of the enzymes involved in trehalose homeostasis and found that in ovarian tissue, *TPS* remains almost constant during all time points evaluated in both nutritional states; however, in the fat body, *TPS* is up-regulated by ∼four–sixfold after a blood meal. Identifying that trehalose increases in the ovary after a blood meal is the first indication that its synthesis by the fat body may be necessary for the accumulation of carbohydrates by the ovaries during this rapid developmental phase of the oocytes, i.e., vitellogenesis (Valle, 1993; Roy et al., 2018). TPS has previously been detected and/or quantified in fat bodies of several species (Cui and Xia, 2009; Xu et al., 2009; Chen et al., 2010; Tang et al., 2010, 2018; Xiong et al., 2019; Liu et al., 2020) including *R. prolixus* females, where a transcriptome analysis reveals an up-regulation of this enzyme in the fat body of fed females (Leyria et al., 2020b). Interestingly, in *R. prolixus*, the concentration of trehalose in the fat body and hemolymph is lower than that found in other non-hematophagous species (Oda et al., 2000; Singtripop et al., 2002; Moriwaki et al., 2003; Michitsch and Steele, 2008; Huang et al., 2012; Kim and Hong, 2015; Kh and Keshan, 2019) and, more importantly, it is also lower compared to that found in *R. prolixus* males (Mariano et al., 2009). There is a peak of trehalose in the fat body of females around 5 days post-blood meal (∼600 pmol/fat body), while in males the maximum trehalose concentration is shown around 5–6 days post-feeding, but in the range of 30–40 nmol/tissue (Mariano et al., 2009). However, although trehalose titers in hemolymph of adult males is slightly higher at 3–4 days post-blood meal, the titers are similar to those found in females. The low amount of trehalose in *R. prolixus* compared to other insects may be due to its diet being carbohydrate poor. Overall, the results above indicate that in *R. prolixus*, carbohydrate metabolism is, in part, determined by sex, even at the same stage of development and nutritional state.

It is well known that mobilization of trehalose is critical for metabolic homeostasis (Steele, 1981; Arrese and Soulages, 2010). Trehalase enzymes and TRET are essential for this mobilization, with trehalase responsible for the breakdown of trehalose to glucose (Shukla et al., 2015), and TRET required

to transfer trehalose via the hemolymph from one tissue to another (Kanamori et al., 2010). As expected, trehalase mRNA levels, mainly the soluble form (s-Tre), are up-regulated during the unfed condition in both the fat body and ovaries of *R. prolixus* females. This finding further supports the hypothesis that nutritional shortage promotes not only the transfer of nutritional sources to other tissues, but also trehalose degradation (*in situ*) for energy generation. Although in some insects, such as the beet armyworm *Spodoptera exigua*, starvation induces an increase in circulating trehalose titers (Kim and Hong, 2015), in our experimental conditions the concentration of trehalose in the hemolymph of unfed *R. prolixus* females is the lowest of all the time points analyzed and this was also observed in unfed males by Mariano et al. (2009).

TRET was first described in the anhydrobiotic insect, *Polypedilum vanderplanki* and now known to be involved in the permeability of cells to trehalose in invertebrates and vertebrates (Kikawada et al., 2007). Rhopr-TRET is part of a mono-clade among the insect sugar transporters. The amino acid sequence of Rhopr-TRET is similar to transporters found to facilitative trehalose transport, particularly those found in other hemipterans, such as *C. lectularius* and *H. halys*. Interestingly, in *N. lugens*, a specific TRET, named Nlst8, is principally expressed in Malpighian tubules and is involved in trehalose reabsorption (Kikuta et al., 2012). Another disaccharide transporter, SCRT, was identified in *Drosophila melanogaster*, and is mainly involved in sucrose uptake in the intestinal tract, especially the hindgut (Meyer et al., 2011). In *R. prolixus* the highest expression of *Rhopr-TRET* is found in the fat body. Interestingly, we also show that *Rhopr-TRET* is up-regulated in the fat body after feeding, which is further supported by a recently published transcriptome analysis (Leyria et al., 2020b). This up-regulation remains throughout all the time points analyzed during the fed state, suggesting that the trehalose synthesized in the fat body is transported via Rhopr-TRET into the hemolymph. The circulating trehalose levels stay relatively stable until day 4 post-blood meal, but on day 5 increase three–fourfold. However, trehalose contained in the ovaries begins to be detected after day 1 post-blood meal. Despite this fact, *TPS* transcript levels in the ovaries do not show any obvious differences after feeding, indicating the importance of trehalose uptake by the ovaries rather than its synthesis. Santos et al. (2008, 2012) reported that follicles containing vitellogenic oocytes have higher trehalase activity, mainly due to a membrane-bound trehalase (m-Tre), which may provide glucose for carbohydrate accumulation, as demonstrated in *Bombyx mori* (Su et al., 1994). Interestingly, in *R. prolixus, Rhopr-TRET* is up-regulated after feeding (∼7–8 fold), coincident with the increase in trehalose in the ovaries, indicating that this carbohydrate could be transported from the hemolymph via Rhopr-TRET into the oocytes. These findings are not contradictory with those reported by Santos et al. (2008, 2012), but rather suggest that redundant pathways are synchronized for the same purpose in order to maximize the storage of carbohydrate by oocytes in a short period of time, as was demonstrate for lipid accumulation in other related species (Fruttero et al., 2011; Leyria et al., 2014). Thus, although Rhopr-TRET allows the release of trehalose from the fat body, it also seems to facilitate trehalose uptake by ovaries.

The responses of Rhopr-TRET may depend not only on the tissue in which it is expressed but also on specific hormonal control. As in mammals, circulating sugar levels in insects are mainly regulated by the action of two peptide hormone families, ILPs and AKHs (Toprak, 2020). The control of trehalose metabolism by ILPs, including circulating trehalose levels, as well as their participation in regulating the expression of trehalases and TPS, has been reported in several species (Bounias et al., 1993; Satake et al., 1997; Iwami, 2000; Wu and Brown, 2006; Broughton et al., 2008; Wang et al., 2020). However, until now, the link between insulin signaling and TRET has been scarcely studied, even though in vertebrates glucose transporter 4 (GLUT4) is translocated to the plasma membrane in response to insulin signals (Bryant and Gould, 2020). In this study, the down-regulation of *Rhopr-IR1* through RNA-mediated interference, and stimulation with exogenous insulins, show that insulin signaling is positively influencing *Rhopr-TRET* transcript expression in the ovaries of fed insects, a state where anabolic processes are required for egg formation and where it is known that the insulin signaling cascade is activated (Leyria et al., 2020a). Interestingly, this regulation is specific to *Rhopr-TRET* and not TPS, suggesting that insulin signaling is promoting trehalose mobilization more than its synthesis. When trehalose is injected into unfed females, mimicking a "fed condition," *Rhopr-ILP1* transcript expression increases in the CNS, and *Rhopr-IGF* and *Rhopr-TRET* transcripts increase in the fat body, demonstrating the importance of insulin cascade activation when the organism detects sources to promote anabolic processes. These effects following trehalose injection are not observed in the ovaries, showing the importance of the fat body as the main modulator of metabolic processes.

The down-regulation of *Rhopr-AKHR* through RNA-mediated interference, as well as the stimulation with exogenous Rhopr-AKH, reveals that the Rhopr-AKH signaling pathway is positively modulating the expression of *Rhopr-TRET* mRNA in ovaries of *R. prolixus* females but no significant differences were observed in the expression of *TPS*. A comparable result was recently reported in *Locusta migratoria*, where down-regulation of *AKHR* in the fat body decreases the expression of *TRET* but not of *TPS* (Zheng et al., 2020). We do not know how the nutritional state might be influencing this control. The first indication of the now named AKH/Red pigment-concentrating hormones (AKH/RPCH) family in insects was that of a hyperglycemic factor in the American cockroach *Periplaneta americana* (Steele, 1961). AKHs work by mobilizing energy reserves in the fat body and simultaneously inhibiting the storage of proteins, lipids or glycogen during periods of stressful situations, such as starvation (Lorenz and Gäde, 2009). However, studies using the cricket, *Gryllus bimaculatus*, have proposed that AKH could trigger the mobilization of energy substrates that are incorporated into growing oocytes (Lorenz and Anand, 2004; Lorenz and Gäde, 2009). In the nematode *Caenorhabditis elegans*, an AKH-like peptide was also reported as positively influencing reproductive processes (Lindemans et al., 2009) and in the tsetse

fly *Glossina morsitans* and the oriental fruit fly *Bactrocera dorsalis*, down-regulation of AKHR leads to a significant reduction of fecundity (Attardo et al., 2012; Hou et al., 2017). In addition, in *N. lugens,* AKH/AKHR signaling-mediated maintenance of trehalose levels in the hemolymph is closely associated with vitellogenin uptake and maturation of oocytes (Lu et al., 2019). Thus, understanding that AKH activates glycogen phosphorylase, an enzyme that leads to decreased glycogen stores and a subsequent increase in the production of trehalose (Gäde et al., 1997), we hypothesize that during vitellogenesis, *R. prolixus* females might require the mobilization of trehalose as well as other nutrients, via AKH signaling. Moreover, we cannot rule out that this signaling is also stimulating the expression of *Rhopr-TRET* in the ovaries thereby maximizing trehalose uptake during egg formation. Interestingly, it was recently reported that JH, a key hormone for triggering vitellogenesis in triatomines, induces transcript expression of TRET in the ovaries of the cabbage beetle *Colaphellus bowringi*, encouraging further studies on the interplay of different hormonal pathway in the regulation of TRET (Li et al., 2020).

Rhopr-AKHR transcript levels in the fat body and ovaries, along with the *Rhopr-AKH* transcript in the CNS, increase as the unfed condition progresses. Most importantly, the survival of dsRhopr-AKHR treated females decreases, indicating how vital AKH signaling is during a nutritional shortage. In *R. prolixus*, AKHR is regulated at the transcriptional level and is required for lipid mobilization under starvation (Alves-Bezerra et al., 2016). In starved insects of *S. exigua*, high titers of trehalose in the hemolymph arise from its release from tissues through TRET (Tang et al., 2012; Kim and Hong, 2015). Similarly, in the red flour beetle *Tribolium castaneum*, *TRET* transcript levels are higher in starved beetles and regulated by JH and not insulin signaling (Xu et al., 2013). These finding indicates that during the unfed condition Rhopr-TRET may be controlled by AKH signaling to mobilize carbohydrates. Hypertrehalosemic hormone (HrTH) belongs to the AKH/RPCH family (Keeley and Gäde, 2004). In a cockroach, *Blattella germanica*, HrTH is released during starvation to control the expression of genes related to catabolic processes via the FoxO (Forkhead box O) transcriptional factor (Süren-Castillo et al., 2014). Recently, we suggested that FoxO signaling is activated in ovaries and fat bodies of unfed females via down-regulation of insulin signaling (Leyria et al., 2020a). Considering this, the fine control of trehalose homeostasis via Rhopr-TRET during the unfed condition may be explained by the result of two antagonistic hormonal actions; the inhibition of insulin signaling and the up-regulation of AKH signaling.

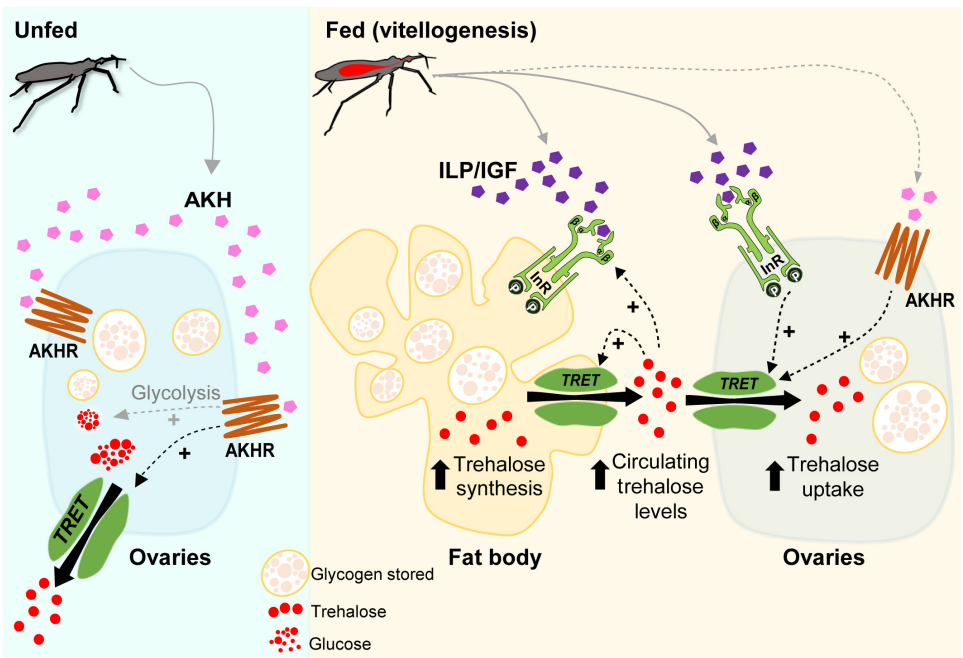

FIGURE 9 | Model of a potential regulatory pathway involved in Rhopr-TRET transcript expression in the fat body and ovaries of females of *Rhodnius prolixus* during unfed and fed stages. In *R. prolixus*, after a blood meal, we propose that insulin signaling is activated in ovaries and fat body and, along with other regulatory mechanisms, triggers vitellogenesis (Leyria et al., 2020a). Here, we demonstrate that trehalose content increases in the fat body and ovaries as days post-blood meal progress, as do the circulating levels in the hemolymph. We suggest that insulin-signaling activation, via Rhopr-IR1 (InR), is involved in *Rhopr-TRET* transcript expression that could then result in mediating a TRET facilitated bidirectional transfer of trehalose; the release of trehalose from the fat body and the uptake by the ovaries, satisfying the physiological needs required for egg formation. The potential up-regulation of *Rhopr-TRET* transcript via Rhopr-AKH signaling during vitellogenesis is also suggested, as well as a positive feedback of hemolymph trehalose levels on insulin signaling. In the unfed condition, Rhopr-AKH signaling might be involved in the release of trehalose from ovaries via Rhopr-TRET, thereby providing a source of energy for the insect during stressful situations such as starvation. The role of AKH signaling in promoting the glycolysis in unfed conditions to generate glucose as an energy source and/or trehalose to carbohydrate mobilization, as well as the release of Rhopr-ILP1/Rhopr-IGF and Rhopr-AKH after feeding, are assumed (gray dashed arrows). Rhopr-AKHR (AKHR).

We should point out that treatment with exogenous trehalose in unfed females promotes a decrease in the *Rhopr-AKH* transcript in the CNS, suggesting that AKH synthesis is down-regulated under nutrient stimulation. Coincidently, in *L. migratoria*, by *in vitro* assay, it was reported that exogenous trehalose inhibits the release of AKHs from the CC, at the level of the adipokinetic hormone-producing cells (Passier et al., 1997). Furthermore, when we evaluated the effects on *Rhopr-TRET* transcript expression in the ovaries by injection of hormones (*ex vivo* assays), Rhopr-AKH (3 h) appears to act faster than insulins (12 h), suggesting that the ovaries are more responsive to AKH than to insulin in an unfed state. Also, we evaluated the expression of the *TPS* transcript after manipulations to down- or up- regulate AKH and insulin signaling and the results show no significant differences compared to control insects. The same effect was observed in the beet armyworm *S. exigua* (Park and Kim, 2017).

Although the effects of insulin and AKH signaling on nutrient mobilization have been reported in *R. prolixus* (Marco et al., 2013; Patel et al., 2014; Zandawala et al., 2015; Alves-Bezerra et al., 2016; Defferrari et al., 2016a,b), the potential molecular mechanisms by which these hormones act on trehalose homeostasis have not previously been studied. Here, we demonstrate that trehalose content increases in the fat body and ovaries as days-post-blood meal progress, as do the circulating levels of trehalose in the hemolymph. We suggest that insulin-signaling activation, via Rhopr-IR1, is involved in *Rhopr-TRET* transcript expression that could then result in mediating a TRET facilitated bidirectional transfer of trehalose: the release of trehalose from the fat body and the uptake by the ovaries, satisfying the physiological needs required for egg formation. The potential up-regulation of *Rhopr-TRET* transcript via Rhopr-AKH signaling during vitellogenesis is also suggested, as well as a positive feedback of hemolymph trehalose levels on insulin signaling. In the unfed condition, Rhopr-AKH signaling might be involved in the release of trehalose from the ovaries via Rhopr-TRET, thereby providing a source of energy for the insect during stressful situations such as starvation (**Figure 9**) although the transcript expression of Rhopr-TRET is low in unfed insects relative to fed insects. The results indicate that in females of *R. prolixus*, trehalose homeostasis and its hormonal regulation by insulin and AKH signaling could play critical roles in adapting to different nutritional conditions. Further experiments using biochemical or functional assays could possibility reveal the entire regulatory mechanism of the trehalose metabolism in triatomines.

DATA AVAILABILITY STATEMENT

The original contributions generated for this study are included in the article/**Supplementary Material**, further inquiries can be directed to the corresponding author.

AUTHOR CONTRIBUTIONS

JL, AL, and IO designed the experiments and mapped out the manuscript. JL and HE-M performed the experiments. JL wrote the original draft of the manuscript and prepared all the figures. AL and IO edited, reviewed, and contributed to the writing of the manuscript. All authors contributed to the article and approved the submitted version.

FUNDING

This study was supported by the Natural Sciences and Engineering Research Council of Canada Discovery grants to AL (RGPIN-2019-05775) and IO (RGPIN-2017-06402).

SUPPLEMENTARY MATERIAL

The Supplementary Material for this article can be found online at: https://www.frontiersin.org/articles/10.3389/fphys.2021.624165/full#supplementary-material

REFERENCES

Aguirre, S. A., Fruttero, L. L., Leyria, J., Defferrari, M. S., Pinto, P. M., Settembrini, B. P., et al. (2011). Biochemical changes in the transition from vitellogenesis to follicular atresia in the hematophagous *Dipetalogaster maxima* (Hemiptera: Reduviidae). *Insect Biochem. Mol. Biol.* 41, 832–841. doi: 10.1016/j.ibmb.2011.06.005

Alves-Bezerra, M., De Paula, I. F., Medina, J. M., Silva-Oliveira, G., Medeiros, J. S., Gäde, G., et al. (2016). Adipokinetic hormone receptor gene identification and its role in triacylglycerol metabolism in the blood-sucking insect Rhodnius prolixus. *Insect Biochem. Mol. Biol.* 69, 51–60. doi: 10.1016/j.ibmb.2015.06.013

Arrese, E. L., and Soulages, J. L. (2010). Insect fat body: energy, metabolism, and regulation. *Annu. Rev. Entomol.* 55, 207–225. doi: 10.1146/annurev-ento-112408-085356

Artimo, P., Jonnalagedda, M., Arnold, K., Baratin, D., Csardi, G., de Castro, E., et al. (2012). ExPASy: SIB bioinformatics resource portal. *Nucleic Acids Res.* 40, W597–W603. doi: 10.1093/nar/gks400

Atella, G. C., Gondim, K. C., Machado, E. A., Medeiros, M. N., Silva-Neto, M. A., and Masuda, H. (2005). Oogenesis and egg development in triatomines: a biochemical approach. *An. Acad. Bras. Cienc.* 77, 405–430. doi: 10.1590/s0001-76520050003000005

Attardo, G. M., Benoit, J. B., Michalkova, V., Yang, G., Roller, L., Bohova, J., et al. (2012). Analysis of lipolysis underlying lactation in the tsetse fly, *Glossina morsitans*. *Insect Biochem. Mol. Biol.* 42, 360–370. doi: 10.1016/j.ibmb.2012.01.007

Badisco, L., Van Wielendaele, P., and Vanden Broeck, J. (2013). Eat to reproduce: a key role for the insulin signalling pathway in adult insects. *Front. Physiol.* 4:202. doi: 10.3389/fphys.2013.00202

Bednáøová, A., Kodrík, D., and Krishnan, N. (2013). Unique roles of glucagon and glucagon-like peptides: parallels in understanding the functions of adipokinetic hormones in stress responses in insects. *Comp. Biochem. Physiol. A Mol. Integr. Physiol.* 164, 91–100. doi: 10.1016/j.cbpa.2012.10.012

Bell, W. J., and Bohm, M. K. (1975). Oosorption in insects. *Biol. Rev. Camb. Philos. Soc.* 50, 373–396. doi: 10.1111/j.1469-185x.1975.tb01058.x

Blom, N., Gammeltoft, S., and Brunak, S. (1999). Sequence and structure-based prediction of eukaryotic protein phosphorylation sites. *J. Mol. Biol.* 294, 1351–1362. doi: 10.1006/jmbi.1999.3310

Bounias, M., Bahjou, A., Gourdoux, L., and Moreau, R. (1993). Molecular activation of a trehalase purified from the fat body of a coleopteran insect

(*Tenebrio molitor*), by an endogenous insulin-like peptide. *Biochem. Mol. Biol. Int.* 31, 249–266.

Brosnan, J. T. (1999). Comments on metabolic needs for glucose and the role of gluconeogenesis. *Eur. J. Clin. Nutr.* 53, S107–S111. doi: 10.1038/sj.ejcn.1600748

Broughton, S., Akic, N., Slack, C., Bass, T., Ikeya, T., Vinti, G., et al. (2008). Reduction of DILP2 in *Drosophila triages* a metabolic phenotype from lifespan revealing redundancy and compensation among DILPs. *PLoS One* 3:e3721. doi: 10.1371/journal.pone.0003721

Bryant, N. J., and Gould, G. W. (2020). Insulin stimulated GLUT4 translocation - Size is not everything! *Curr. Opin. Cell Biol.* 65, 28–34. doi: 10.1016/j.ceb.2020.02.006

Canavoso, L. E., Jouni, Z. E., Karnas, K. J., Pennington, J. E., and Wells, M. A. (2001). Fat metabolism in insects. *Annu. Rev. Nutr.* 21, 23–46. doi: 10.1146/annurev.nutr.21.1.23

Chen, J., Zhang, D., Yao, Q., Zhang, J., Dong, X., Tian, H., et al. (2010). Feeding-based RNA interference of a trehalose phosphate synthase gene in the brown planthopper, *Nilaparvata lugens*. *Insect Mol. Biol.* 19, 777–786. doi: 10.1111/j.1365-2583.2010.01038.x

Cruz, J., Mané-Padrós, D., Bellés, X., and Martín, D. (2006). Functions of the ecdysone receptor isoform-A in the hemimetabolous insect *Blattella germanica* revealed by systemic RNAi in vivo. *Dev. Biol.* 297, 158–171. doi: 10.1016/j.ydbio.2006.06.048

Cui, S. Y., and Xia, Y. X. (2009). Isolation and characterization of the trehalose-6-phosphate synthase gene from *Locusta migratoria* manilensis. *Insect Sci.* 16, 287–295. doi: 10.1111/j.1744-7917.2009.01268.x

de Azambuja, P., Garcia, E. S., and Ratcliffe, N. A. (1991). Aspects of classification of Hemiptera hemocytes from six triatomine species. *Mem. Inst. Oswaldo Cruz.* 86, 1–10. doi: 10.1590/s0074-02761991000100002

Defferrari, M. S., Da Silva, S. R., Orchard, I., and Lange, A. B. (2018). A Rhodnius prolixus insulin receptor and its conserved intracellular signalling pathway and regulation of metabolism. *Front. Endocrinol.* 9:745.

Defferrari, M. S., Orchard, I., and Lange, A. B. (2016a). An insulin-like growth factor in *Rhodnius prolixus* is involved in post-feeding nutrient balance and growth. *Front. Neurosci.* 10:566. doi: 10.3389/fendo.2018.00745

Defferrari, M. S., Orchard, I., and Lange, A. B. (2016b). Identification of the first insulin-like peptide in the disease vector *Rhodnius prolixus*: involvement in metabolic homeostasis of lipids and carbohydrates. *Insect. Biochem. Mol. Biol.* 70, 148–159. doi: 10.1016/j.ibmb.2015.12.009

Eberhard, F. E., Cunze, S., Kochmann, J., and Klimpel, S. (2020). Modelling the climatic suitability of Chagas disease vectors on a global scale. *eLife* 9:e52072. doi: 10.7554/eLife.52072

Elbein, A. D., Pan, Y. T., Pastuszak, I., and Carroll, D. (2003). New insights on trehalose: a multifunctional molecule. *Glycobiology* 13, 17R–27R. doi: 10.1093/glycob/cwg047

El-Gebali, S., Mistry, J., Bateman, A., Eddy, S. R., Luciani, A., Potter, S. C., et al. (2019). The Pfam protein families database in 2019. *Nucleic Acids Res.* 47, D427–D432. doi: 10.1093/nar/gky995

Felsenstein, J. (1985). Confidence limits on phylogenies: an approach using the bootstrap. *Evolution* 39, 783–791. doi: 10.1111/j.1558-5646.1985.tb00420.x

Foster, W. A. (1995). Mosquito sugar feeding and reproductive energetics. *Annu. Rev. Entomol.* 40, 443–474. doi: 10.1146/annurev.en.40.010195.002303

Fruttero, L. L., Frede, S., Rubiolo, E. R., and Canavoso, L. E. (2011). The storage of nutritional resources during vitellogenesis of *Panstrogylus megistus* (Hemiptera: Reduviidae): the pathways of lipophorin in lipid delivery to developing oocytes. *J. Insect Physiol.* 57, 475–486. doi: 10.1016/j.jinsphys.2011.01.009

Gäde, G., Hoffmann, K. H., and Spring, J. H. (1997). Hormonal regulation in insects: facts, gaps, and future directions. *Physiol. Rev.* 77, 963–1032. doi: 10.1152/physrev.1997.77.4.963

Hamoudi, Z., Lange, A. B., and Orchard, I. (2016). Identification and characterization of the corazonin receptor and possible physiological roles of the corazonin-signaling pathway in *Rhodnius prolixus*. *Front. Neurosci.* 10:357. doi: 10.3389/fnins.2016.00357

Hou, Q. L., Chen, E. H., Jiang, H. B., Wei, D. D., Gui, S. H., Wang, J. J., et al. (2017). Adipokinetic hormone receptor gene identification and its role in triacylglycerol mobilization and sexual behavior in the oriental fruit fly (*Bactrocera dorsalis*). *Insect Biochem. Mol. Biol.* 90, 1–13. doi: 10.1016/j.ibmb.2017.09.006

Huang, J. H., Bellés, X., and Lee, H. J. (2012). Functional characterization of hypertrehalosemic hormone receptor in relation to hemolymph trehalose and to oxidative stress in the cockroach *Blattella germanica*. *Front. Endocrinol.* 2:114. doi: 10.3389/fendo.2011.00114

Huang, J. H., and Lee, H. J. (2011). RNA interference unveils functions of the hypertrehalosemic hormone on cyclic fluctuation of hemolymph trehalose and oviposition in the virgin female *Blattella germanica*. *J. Insect Physiol.* 57, 858–864. doi: 10.1016/j.jinsphys.2011.03.012

Iwami, M. (2000). Bombyxin: an insect brain peptide that belongs to the insulin family. *Zool. Sci.* 17, 1035–1044. doi: 10.2108/zsj.17.1035

Jones, D. T., Taylor, W. R., and Thornton, J. M. (1992). The rapid generation of mutation data matrices from protein sequences. *Comput. Appl. Biosci.* 8, 275–282. doi: 10.1093/bioinformatics/8.3.275

Kanamori, Y., Saito, A., Hagiwara-Komoda, Y., Tanaka, D., Mitsumasu, K., Kikuta, S., et al. (2010). The trehalose transporter 1 gene sequence is conserved in insects and encodes proteins with different kinetic properties involved in trehalose import into peripheral tissues. *Insect Biochem. Mol. Biol.* 40, 30–37. doi: 10.1016/j.ibmb.2009.12.006

Keeley, L. L., and Gäde, G. (2004). *Adipokinetic and Hypertrehalosemic Neurohormones, in Encyclopedia of Entomology*. Dordrecht: Springer.

Kelley, L. A., Mezulis, S., Yates, C. M., Wass, M. N., and Sternberg, M. J. (2015). The Phyre2 web portal for protein modeling, prediction and analysis. *Nat. Protoc.* 10, 845–858. doi: 10.1038/nprot.2015.053

Kh, S. D., and Keshan, B. (2019). Mobilization of fat body glycogen and haemolymph trehalose under nutritional stress in *Bombyx mori* larvae in relation to their physiological age and the duration of food deprivation. *Biologia* 74, 649–660. doi: 10.2478/s11756-019-00196-0

Kikawada, T., Saito, A., Kanamori, Y., Nakahara, Y., Iwata, K., Tanaka, D., et al. (2007). Trehalose transporter 1, a facilitated and high-capacity trehalose transporter, allows exogenous trehalose uptake into cells. *Proc. Natl. Acad. Sci. U.S.A.* 104, 11585–11590. doi: 10.1073/pnas.0702538104

Kikuta, S., Hagiwara-Komoda, Y., Noda, H., and Kikawada, T. (2012). A novel member of the trehalose transporter family functions as an h(+)-dependent trehalose transporter in the reabsorption of trehalose in malpighian tubules. *Front. Physiol.* 3:290. doi: 10.3389/fphys.2012.00290

Kim, Y., and Hong, Y. (2015). Regulation of hemolymph trehalose level by an insulin-like peptide through diel feeding rhythm of the beet armyworm, *Spodoptera exigua*. *Peptides* 68, 91–98. doi: 10.1016/j.peptides.2015.02.003

Kumar, S., Stecher, G., Li, M., Knyaz, C., and Tamura, K. (2018). MEGA X: molecular evolutionary genetics analysis across computing platforms. *Mol. Biol. Evol.* 35, 1547–1549. doi: 10.1093/molbev/msy096

Lenaerts, C., Monjon, E., Van Lommel, J., Verbakel, L., and Vanden Broeck, J. (2019). Peptides in insect oogenesis. *Curr. Opin. Insect Sci.* 31, 58–64. doi: 10.1016/j.cois.2018.08.007

Leyria, J., Fruttero, L. L., Aguirre, S. A., and Canavoso, L. E. (2014). Ovarian nutritional resources during the reproductive cycle of the hematophagous *Dipetalogaster maxima* (Hemiptera: Reduviidae): focus on lipid metabolism. *Arch. Insect Biochem. Physiol.* 87, 148–163. doi: 10.1002/arch.21186

Leyria, J., Orchard, I., and Lange, A. B. (2020a). Transcriptomic analysis of regulatory pathways involved in female reproductive physiology of *Rhodnius prolixus* under different nutritional states. *Sci. Rep.* 10:11431. doi: 10.1038/s41598-020-67932-4

Leyria, J., Orchard, I., and Lange, A. B. (2020b). What happens after a blood meal? A transcriptome analysis of the main tissues involved in egg production in *Rhodnius prolixus*, an insect vector of Chagas disease. *PLoS Negl. Trop. Dis.* 14:e0008516. doi: 10.1371/journal.pntd.0008516

Li, J.-X., Cao, Z., Guo, Z., Tian, Z., Liu, W., Zhu, F., et al. (2020). Molecular characterization and functional analysis of two trehalose transporter genes in the cabbage beetle, *Colaphellus bowringi*. *J. Asia Pac. Entomol.* 23, 627–633. doi: 10.1016/j.aspen.2020.05.011

Li, L., Stoeckert, C. J. Jr., and Roos, D. S. (2003). OrthoMCL: identification of ortholog groups for eukaryotic genomes. *Genome Res.* 13, 2178–2189. doi: 10.1101/gr.1224503

Lindemans, M., Liu, F., Janssen, T., Husson, S. T., Mertens, I., Gäde, G., et al. (2009). Adipokinetic hormone signaling through the gonadotropin-releasing hormone receptor modulates egg-laying in Caenorhabditis elegans. *Proc. Natl. Acad. Sci. U.S.A.* 106, 1642–1647. doi: 10.1073/pnas.0809881106

Liu, X., Zou, Z., Zhang, C., Liu, X., Wang, J., Xin, T., et al. (2020). Knockdown of the trehalose-6-phosphate synthase gene using rna interference inhibits synthesis of trehalose and increases lethality rate in asian citrus psyllid, *Diaphorina citri* (Hemiptera: Psyllidae). *Insects* 11:E605. doi: 10.3390/insects11090605

Livak, K. J., and Schmittgen, T. D. (2011). Analysis of relative gene expression data using real-time quantitative PCR and the 2(-Delta Delta C(T)) method. *Methods* 25, 402–408. doi: 10.1006/meth.2001.1262

Lorenz, M. W., and Anand, A. N. (2004). Changes in the biochemical composition of fat body stores during adult development of female crickets, *Gryllus bimaculatus*. *Arch. Insect Biochem. Physiol.* 56, 110–119. doi: 10.1002/arch.20002

Lorenz, M. W., and Gäde, G. (2009). Hormonal regulation of energy metabolism in insects as a driving force for performance. *Integr. Comp. Biol.* 49, 380–392. doi: 10.1093/icb/icp019

Lu, K., Wang, Y., Chen, X., Zhang, X., Li, W., Cheng, Y., et al. (2019). Adipokinetic hormone receptor mediates trehalose homeostasis to promote vitellogenin uptake by oocytes in *Nilaparvata lugens*. *Front. Physiol.* 9:1904. doi: 10.3389/fphys.2018.01904

Majerowicz, D., Alves-Bezerra, M., Logullo, R., Fonseca-de-Souza, A. L., Meyer-Fernandes, J. R., Braz, G. R., et al. (2011). Looking for reference genes for real-time quantitative PCR experiments in *Rhodnius prolixus* (Hemiptera: Reduviidae). *Insect Mol. Biol.* 20, 713–722. doi: 10.1111/j.1365-2583.2011.01101.x

Marco, H. G., Simek, P., Clark, K. D., and Gäde, G. (2013). Novel adipokinetic hormones in the kissing bugs *Rhodnius prolixus*, *Triatoma infestans*, *Dipetalogaster maxima* and *Panstrongylus megistus*. *Peptides* 41, 21–30. doi: 10.1016/j.peptides.2012.09.032

Mariano, A. C., Santos, R., Gonzalez, M. S., Feder, D., Machado, E. A., Pascarelli, B., et al. (2009). Synthesis and mobilization of glycogen and trehalose in adult male *Rhodnius prolixus*. *Arch. Insect Biochem. Physiol.* 72, 1–15. doi: 10.1002/arch.20319

Mesquita, R. D., Vionette-Amaral, R. J., Lowenberger, C., Rivera-Pomar, R., Monteiro, F. A., Minx, P., et al. (2015). Genome of *Rhodnius prolixus*, an insect vector of Chagas disease, reveals unique adaptations to hematophagy and parasite infection. *Proc. Natl. Acad. Sci. U.S.A.* 112, 14936–14941. doi: 10.1073/pnas.1506226112

Meyer, H., Vitavska, O., and Wieczorek, H. (2011). Identification of an animal sucrose transporter. *J. Cell Sci.* 124, 1984–1991. doi: 10.1242/jcs.082024

Michitsch, J., and Steele, J. E. (2008). Carbohydrate and lipid metabolism in cockroach (*Periplaneta americana*) fat body are both activated by low and similar concentrations of Peram-AKH II. *Peptides* 29, 226–234. doi: 10.1016/j.peptides.2007.08.031

Millen, B. H., and Beckel, W. E. (1970). The effects of nutrient and non-nutrient diets on the fat body cell nuclei and nucleoli of starved nymphs of *Rhodnius prolixus* (Hemiptera). *Can. J. Zool.* 48, 489–493. doi: 10.1139/z70-083

Moriwaki, N., Matsushita, K., Nishina, M., and Kono, Y. (2003). High concentrations of trehalose in aphid hemolymph. *Appl. Entomol. Zool.* 38, 241–248. doi: 10.1303/aez.2003.241

Oda, Y., Uejima, M., Iwami, M., and Sakurai, S. (2000). Role of ecdysteroids in the dynamics of insect haemolymph sugar. *Zool. Sci.* 17, 785–789. doi: 10.2108/zsj.17.785

Park, Y., and Kim, Y. (2017). Identification of a hypertrehalosemic factor in *Spodoptera exigua*. *Arch. Insect Biochem. Physiol.* 95:e21386. doi: 10.1002/arch.21386

Parrou, J. L., and François, J. (1997). A simplified procedure for a rapid and reliable assay of both glycogen and trehalose in whole yeast cells. *Anal. Biochem.* 248, 186–188. doi: 10.1006/abio.1997.2138

Passier, P. C., Vullings, H. G., Diederenm, J. H., and Van der Horst, D. J. (1997). Trehalose inhibits the release of adipokinetic hormones from the corpus cardiacum in the African migratory locust, *Locusta migratoria*, at the level of the adipokinetic cells. *J. Endocrinol.* 153, 299–305. doi: 10.1677/joe.0.1530299

Patel, H., Orchard, I., Veenstra, J. A., and Lange, A. B. (2014). Reprint of "The distribution and physiological effects of three evolutionarily and sequence-related neuropeptides in *Rhodnius prolixus*: adipokinetic hormone, corazonin and adipokinetic hormone/corazonin-related peptide". *Gen. Comp. Endocrinol.* 203, 307–314. doi: 10.1016/j.ygcen.2014.07.001

Price, D. R., Tibbles, K., Shigenobu, S., Smertenko, A., Russell, C. W., Douglas, A. E., et al. (2010). Sugar transporters of the major facilitator superfamily in aphids; from gene prediction to functional characterization. *Insect Mol. Biol.* 2, 97–112. doi: 10.1111/j.1365-2583.2009.00918.x

Raikhel, A. S., and Dhadialla, T. S. (1992). Accumulation of yolk proteins in insect oocytes. *Annu. Rev. Entomol.* 37, 217–251. doi: 10.1146/annurev.en.37.010192.001245

Reynolds, C. R., Islam, S. A., and Sternberg, M. J. E. (2018). EzMol: a web server wizard for the rapid visualization and image production of protein and nucleic acid structures. *J. Mol. Biol.* 430, 2244–2248. doi: 10.1016/j.jmb.2018.01.013

Roy, S., Saha, T. T., Zou, Z., and Raikhel, A. S. (2018). Regulatory pathways controlling female insect reproduction. *Annu. Rev. Entomol.* 63, 489–511. doi: 10.1146/annurev-ento-020117-043258

Santos, R., Alves-Bezerra, M., Rosas-Oliveira, R., Majerowicz, D., Meyer-Fernandes, J. R., and Gondim, K. C. (2012). Gene identification and enzymatic properties of a membrane-bound trehalase from the ovary of *Rhodnius prolixus*. *Arch. Insect Biochem. Physiol.* 81, 199–213. doi: 10.1002/arch.21043

Santos, R., Mariano, A. C., Rosas-Oliveira, R., Pascarelli, B., Machado, E. A., Meyer-Fernandes, J. R., et al. (2008). Carbohydrate accumulation and utilization by oocytes of *Rhodnius prolixus*. *Arch. Insect Biochem. Physiol.* 67, 55–62. doi: 10.1002/arch.20217

Satake, S., Masumura, M., Ishizaki, H., Nagata, H., Suzuki, A., and Mizoguchi, A. (1997). An insulin-related peptide of insects reduces the major storage carbohydrates in the silkworm *Bombyx mori*. *Comp. Biochem. Physiol. B* 118, 349–357. doi: 10.1016/s0305-0491(97)00166-1

Shukla, E., Thorat, L. J., Nath, B. B., and Gaikwad, S. M. (2015). Insect trehalase: physiological signi?cance and potential applications. *Glycobiology* 25, 357–367. doi: 10.1093/glycob/cwu125

Sigrist, C. J. A., de Castro, E., Cerutti, L., Cuche, B. A., Hulo, N., Bridge, A., et al. (2013). New and continuing developments at PROSITE. *Nucleic. Acids Res.* 41, D344–D347. doi: 10.1093/nar/gks1067

Singtripop, T., Oda, Y., Wanichacheewa, S., and Sakurai, S. (2002). Sensitivities to juvenile hormone and ecdysteroid in the diapause larvae of *Omphisa fuscidentalis* based on the hemolymph trehalose dynamics index. *J. Insect Physiol.* 48, 817–824. doi: 10.1016/s0022-1910(02)00104-x

Steele, J. E. (1961). Occurence of a hyperglycaemic factor in the corpus cardiacum of an insect. *Nature* 18, 680–681. doi: 10.1038/192680a0

Steele, J. E. (1981). "The role of carbohydrate metabolism in physiological function," in *Energy Metabolism in Insects*, ed. R. G. H. Downer (Boston, MA: Springer), 101–133. doi: 10.1007/978-1-4615-9221-1_4

Su, Z. H., Ikedam, M., Sato, Y., Saito, H., Imai, K., Isobe, M., et al. (1994). Molecular characterization of ovary trehalase of the silkworm, *Bombyx mori* and its transcriptional activation by diapause hormone. *Biochim. Biophys. Acta.* 1218, 366–374. doi: 10.1016/0167-4781(94)90190-2

Süren-Castillo, S., Abrisqueta, M., and Maestro, J. L. (2014). FoxO is required for the activation of hypertrehalosemic hormone expression in cockroaches. *Biochim. Biophys. Acta.* 1840, 86–94. doi: 10.1016/j.bbagen.2013.08.015

Tang, B., Chen, J., Yao, Q., Pan, Z. Q., Xu, W. H., and Wang, S. G. (2010). Characterization of a trehalose-6-phosphate synthase gene from *Spodoptera exigua*, and its function identification through RNA interference. *J. Insect Physiol.* 56, 813–821. doi: 10.1016/j.jinsphys.2010.02.009

Tang, B., Wang, S., Wang, S. G., Wang, H. J., Zhang, J. Y., and Cui, S. Y. (2018). Invertebrate trehalose-6-phosphate synthase gene: genetic architecture, biochemistry, physiological function, and potential applications. *Front. Physiol.* 9:30. doi: 10.3389/fphys.2018.00030

Tang, B., Xu, Q., Zou, Q., Fang, Q., Wang, S., and Ye, G. (2012). Sequencing and characterization of glycogen synthase and glycogen phosphorylase genes from *Spodoptera exigua* and analysis of their function in starvation and excessive sugar intake. *Arch. Insect Biochem. Physiol.* 80, 42–62. doi: 10.1002/arch.21027

Thompson, S. N. (2003). Trehalose – the insect "Blood" sugar. *Adv. Insect Phys.* 31, 205–285. doi: 10.1016/S0065-2806(03)31004-5

Toprak, U. (2020). The role of peptide hormones in insect lipid metabolism. *Front. Physiol.* 11:434. doi: 10.3389/fphys.2020.00434

Valle, D. (1993). Vitellogenesis in insects and other groups–a review. *Mem. Inst. Oswaldo Cruz.* 88, 1–26. doi: 10.1590/s0074-02761993000100005

Wang, S. S., Li, G. Y., Liu, Y. K., Luo, Y. J., Xu, C. D., Li, C., et al. (2020). Regulation of carbohydrate metabolism by trehalose-6-phosphate synthase 3

in the brown Planthopper, *Nilaparvata lugens*. *Front. Physiol.* 11:575485. doi: 10.3389/fphys.2020.575485

Wigglesworth, V. B. (1936). The function of the corpus allatum in the growth and reproduction of *Rhodnius prolixus* (Hemiptera). *Q. J. Microsc. Sci.* 79, 91–121.

World Health Organization [WHO] (2020). *Chagas disease (American trypanosomiasis)*. Available online at: https://www.who.int/chagas/en/ (accessed March 30, 2020).

Wu, Q., and Brown, M. R. (2006). Signaling and function of insulin-like peptides in insects. *Annu. Rev. Entomol.* 51, 1–24. doi: 10.1146/annurev.ento.51.110104.151011

Xie, Y., Zheng, Y., Li, H., Luo, X., He, Z., Cao, S., et al. (2016). GPS-Lipid: a robust tool for the prediction of multiple lipid modification sites. *Sci. Rep.* 6:28249. doi: 10.1038/srep28249

Xiong, K. C., Wang, J., Li, J. H., Deng, Y. Q., Pu, P., Fan, H., et al. (2019). RNA interference of a trehalose-6-phosphate synthase gene reveals its roles during larval-pupal metamorphosis in *Bactrocera minax* (Diptera: Tephritidae). *J. Insect Physiol.* 92, 84–92. doi: 10.1016/j.jinsphys.2016.07.003

Xu, J., Bao, B., Zhang, Z. F., Yi, Y. Z., and Xu, W. H. (2009). Identification of a novel gene encoding the trehalose phosphate synthase in the cotton bollworm, *Helicoverpa armigera*. *Glycobiology* 19, 250–257. doi: 10.1093/glycob/cwn127

Xu, J., Sheng, Z., and Palli, S. R. (2013). Juvenile hormone and insulin regulate trehalose homeostasis in the red flour beetle, *Tribolium castaneum*. *PLoS Genet.* 9:e1003535. doi: 10.1371/journal.pgen.1003535

Zandawala, M., Hamoudi, Z., Lange, A. B., and Orchard, I. (2015). Adipokinetic hormone signalling system in the Chagas disease vector, *Rhodnius prolixus*. *Insect Mol. Biol.* 24, 264–276. doi: 10.1111/imb.12157

Zheng, H., Chen, C., Liu, C., Song, Q., and Zhou, S. (2020). Rhythmic change of adipokinetic hormones diurnally regulates locust vitellogenesis and egg development. *Insect Mol. Biol.* 29, 283–292. doi: 10.1111/imb.12633

Conflict of Interest: The authors declare that the research was conducted in the absence of any commercial or financial relationships that could be construed as a potential conflict of interest.

frontiers in Physiology

ORIGINAL RESEARCH
published: 24 February 2021
doi: 10.3389/fphys.2021.632506

*Hv*RNASET2 Regulate Connective Tissue and Collagen I Remodeling During Wound Healing Process

*Nicolò Baranzini†, Laura Pulze†, Gianluca Tettamanti, Francesco Acquati and Annalisa Grimaldi**

Department of Biotechnology and Life Science, University of Insubria, Varese, Italy

Several studies have recently demonstrated that the correct regeneration of damaged tissues and the maintaining of homeostasis after wounds or injuries are tightly connected to different biological events, involving immune response, fibroplasia, and angiogenetic processes, in both vertebrates and invertebrates. In this context, our previous data demonstrated that the *Hirudo verbana* recombinant protein r*Hv*RNASET2 not only plays a pivotal role in innate immune modulation, but is also able to activate resident fibroblasts leading to new collagen production, both *in vivo* and *in vitro*. Indeed, when injected in the leech body wall, which represents a consolidated invertebrate model for studying both immune response and tissue regeneration, *Hv*RNASET2 induces macrophages recruitment, fibroplasia, and synthesis of new collagen. Based on this evidence, we evaluate the role of *Hv*RNASET2 on muscle tissue regeneration and extracellular matrix (ECM) remodeling in r*Hv*RNASET2-injected wounded leeches, compared to PBS-injected wounded leeches used as control. The results presented here not only confirms our previous evidence, reporting that *Hv*RNASET2 leads to an increased collagen production, but also shows that an overexpression of this protein might influence the correct progress of muscle tissue regeneration. Moreover, due to its inhibitory effect on vasculogenesis and angiogenesis, *Hv*RNASET2 apparently interfere with the recruitment of the myoendothelial vessel-associated precursor cells that in turn are responsible for muscle regeneration during wound healing repair.

Keywords: innate immunity, invertebrates, medicinal leech, ribonucleases T2, collagen, regeneration

OPEN ACCESS

Edited by:
Fabio Gomes, Federal University of Rio de Janeiro, Brazil

Reviewed by:
Gabriela De Oliveira Paiva-Silva, Federal University of Rio de Janeiro, Brazil
Jacenir Mallet, Oswaldo Cruz Institute, Oswaldo Cruz Foundation (Fiocruz), Brazil
Eduardo José Lopes Torres, Rio de Janeiro State University, Brazil

***Correspondence:**
Annalisa Grimaldi
annalisa.grimaldi@uninsubria.it

† These authors have contributed equally to this work

Specialty section:
This article was submitted to Invertebrate Physiology, a section of the journal Frontiers in Physiology

Received: *23 November 2020*
Accepted: *25 January 2021*
Published: *24 February 2021*

Citation:
Baranzini N, Pulze L, Tettamanti G, Acquati F and Grimaldi A (2021) HvRNASET2 Regulate Connective Tissue and Collagen I Remodeling During Wound Healing Process. Front. Physiol. 12:632506. doi: 10.3389/fphys.2021.632506

INTRODUCTION

Correct tissue regeneration, following injuries or wounds, involves different biological processes, such as the scavenge of cellular debris and the activation of several processes such as vasculogenesis, angiogenesis, and stimulation/recruitment of immune cell progenitors. Both in vertebrates and in invertebrates, the accurate coordination of these events is essential to re-establish the original, healthy tissue architecture (Pieper et al., 2002; de Eguileor et al., 2005; Li et al., 2005; Grimaldi et al., 2010). Of note, after injuries, immunocompetent cells not only take part in the elimination of possible harmful invaders, but also preserve the homeostasis of tissues and organs and their functional integrity through the elimination of debris, thus avoiding the persistence of immunogenic residues that may induce toxicity and a prolonged inflammatory status within the tissue environment (Martin, 1997; Saltzman, 1999; Frantz et al., 2005). In addition, the

release of cytokines and growth factors, such as IL-6, TNF-alpha, and bFGF, by phagocytic cells promotes both fibroblasts proliferation and endothelial cells activation, which in turn leads to the development of new blood vessels (Tettamanti et al., 2003b; de Eguileor et al., 2005). Interestingly, the inflammation-mediated regeneration of tissues represents an evolutionarily conserved process, in which the interaction between regenerative events and the immune system has been observed in many vertebrate and invertebrate model systems (Grimaldi et al., 2009; Schorn et al., 2015; Godwin et al., 2017; Tasiemski and Salzet, 2017; Malagoli, 2018).

In order to investigate these processes, the medicinal leech *Hirudo verbana*, whose use in experimental biology entails minimal ethical concerns and is not regulated, is proposed here to achieve novel information about the mechanisms related to tissue regenerative processes (Grimaldi et al., 2011; Baranzini et al., 2017, 2020b; Girardello et al., 2017). Due to its relatively simple anatomy and small body size, the effects of a wide range of experimental stimuli are easily detected in this animal model in a very short period of time and throughout the entire muscular body wall. For instance, the whole wound healing process is easily detectable after surgical lesions, avoiding any equivocal evaluations, and the subsequent muscular regeneration involves well-established and evolutionary conserved cellular and molecular effectors (Grimaldi et al., 2010). Of note, as already reported in vertebrates, the processes of vasculogenesis, angiogenesis, fibroplasia, and the activation and migration of immunocompetent/muscle precursors cells represent the main steps implicated in restoring damaged tissues in leeches as well (de Eguileor et al., 1999a, 2001; Tettamanti et al., 2005; Grimaldi et al., 2009).

In leeches, wound healing first triggers an inflammatory phase characterized by a massive migration of both immune cells and fibroblasts toward the lesioned area, in which myofibroblast-like cells promote the formation of a pseudoblastema region (Huguet and Molinas, 1994, 1996; Grimaldi et al., 2011). At the same time, the botryoidal tissue, involved in myelo/erythroid and storage functions and promoting vasculogenesis, angiogenesis, and hematopoietic cells production (de Eguileor et al., 1999b, 2001), undergoes an abrupt transition from a cluster/cord-like structure to a hollow architecture typical of pre-vascular structures, in order to generate new capillary vessels, in whose lumen hematopoietic stem precursor cells (HSPCs) subsequently migrate. Most of these circulating immune precursors are recruited into the wounded area and, after leaving the bloodstream, extravasate into the connective tissue (Grimaldi et al., 2006). These cells are committed toward a myogenic or macrophage differentiation pathway by the expression of specific cytokines present in the extracellular matrix (ECM). As in vertebrates, we have previously identified a plethora of cytokines and growth factors in injured leech tissues, such as VEGF (vascular endothelial growth factor), and FGFb (fibroblast growth factor), which support neovessel formation, immune/fibroblast cells recruitment, and proliferation and tissue remodeling by establishing a crosstalk between the innate immune response and tissue regeneration (Grimaldi et al., 2004; Tettamanti et al., 2004, 2005; Baranzini et al., 2020b). In particular, FGFb induces fibroblast proliferation that in turn triggers new collagen synthesis, thus producing a fundamental scaffold for the immune cell migration, the correct orientation of new vessels, and the regeneration of damaged tissues (de Eguileor et al., 2004; Tettamanti et al., 2004). Indeed, collagen is not just a structural component of the ECM, but plays a crucial role in the modulation of different cell functions, including adhesion, growth, and differentiation (Birk and Zycband, 1994; Tettamanti et al., 2003b, 2005). VEGF signaling in leeches modulates vessels migration, proliferation, and survival of both endothelial and myogenic precursors cells within areas of regenerating tissues (Grimaldi et al., 2009, 2010). The different myogenic and endothelial fates of these precursor cells seem to be due to differential responses to VEGF concentrations. The exposure to a sustained and continuous source of VEGF maintains the proliferation and undifferentiated phenotype of hematopoietic $CD34^{+}$ precursor cells. The proliferation stimulus diminishes when the VEGF concentration decreases in the ECM surrounding the muscle fibers, permitting these hematopoietic/endothelial precursor cells to differentiate into muscle fibers.

Given the importance of angiogenesis, fibroplasia, and the innate immune response in the organization and homeostasis of tissues, further research is necessary to elucidate how these processes are interconnected and regulated by both cellular and molecular mechanisms. In this context, recent studies demonstrated that, in *H. verbana*, the T2 ribonuclease *Hv*RNASET2, besides modulating the inflammatory process by recruitment of immune cells in the injured/infected area, is also involved in ECM remodeling and stimulates the production of new collagen both *in vivo* and *in vitro* (Baranzini et al., 2019, 2020b). When injected in the leech body wall, *Hv*RNASET2 induces fibroplasia, connective tissue remodeling, and ECM reorganization, also promoting macrophages recruitment to the stimulated area (Baranzini et al., 2019). Interestingly, these results are supported by *in vitro* experiments conducted on human MRC5 fibroblast cells, in which *Hv*RNASET2 induces the synthesis of new collagen I (Baranzini et al., 2020b).

To better define the direct engagement of *Hv*RNASET2 in tissues reorganization and to obtain novel information about its biological role in a more physiological context, wounded leeches were treated with the recombinant r*Hv*RNASET2 enzyme at different timings, evaluating the ability to stimulate collagen I expression, ECM remodeling, and regeneration of injured tissues.

MATERIALS AND METHODS

Leeches (*H. verbana*, Annelida, and Hirudinea, from Ricarimpex, Eysines, France) measuring 10 cm were kept in lightly salted water (NaCl 1.5 g/l) in aerated tanks and kept in an incubator at 20°C. Uninjured and treated animals were anaesthetized by immersion in a 10% ethanol solution until they appeared completely asleep, before being dissected to remove the body wall region of interest.

Leeches were randomly divided into four separate experimental groups (three individuals for each time point) and submitted to various protocols and treatments.

Group 1 included uninjured leeches.

Group 2 included control leeches surgically injured with a razor, immediately injected once, in the same area, with 100 μl of sterilized PBS consisting of 138 mM of NaCl, 2.7 mM of KCl, 4.3 mM of Na2HPO4, and 1.5 mM of KH2PO4, (pH 7.4) to demonstrate that the injection of a vehicle solution alone did not exert a significant effect on wound healing. After 24, 48, 72 h, and 1 week, tissues were collected and fixed as described below. For each timing, experiments were performed in triplicate.

Group 3 included treated leeches surgically injured with a razor and immediately injected with 100 μl of sterilized PBS containing 100 ng of recombinant protein r*Hv*RNASET2, cloned and purified in the yeast *Pichia pastoris* as already described in other studies (Baranzini et al., 2020a,b), in order to verify the effects of the *H. verbana* T2 recombinant protein during the different phases of wound healing. After 24, 48, 72 h, and 1 week, tissues were collected and fixed. For each timing, experiments were performed in triplicate.

Embedding Tissue in Epoxy Resin for Morphological Analysis at Light and Transmission Electron Microscopy

Specimens of approximately 0.4 mm in thickness and 0.6 mm in length were dissected from the treated leech body wall area and immediately fixed for 2 h in 4% glutaraldehyde in 0.1 M cacodylate buffer at pH 7.4 (de Eguileor et al., 2001; Tettamanti et al., 2003a). After several washes in the same buffer, samples were postfixed for 1 h with 1% osmium tetroxide in cacodylate buffer 0.1 M at pH 7.4, dehydrated in a standard serial ethanol scale (70%, 90%, and absolute), and embedded in an Epon Araldite 812 mixture (Sigma-Aldrich, Milan, Italy). Sections for light microscopy (0.70 μm in thickness) were obtained with a Reichert Ultracut S ultratome (Leica, Wien, Austria), colored by the conventional methods with crystal violet and basic fuchsin [according to Moore et al. (1960)], and subsequently observed under the light microscope Nikon Eclipse (Ni, Nikon, Tokyo, Japan). Data were recorded with a DS-5 M-L1 digital camera system (Nikon). From the same samples, we obtained ultrathin sections (80 nm in thickness) with a Reichert Ultracut S ultratome (Leica) that were placed on copper grids (300 mesh, Sigma-Aldrich, Milan, Italy), counterstained by uranyl acetate and lead citrate, and observed with a Jeol 1010 EX transmission electron microscope (TEM) (Jeol, Tokyo, Japan). Data were recorded with a MORADA digital camera system (Olympus, Tokyo, Japan).

Embedding Tissue in Paraffin and Masson's Trichrome Staining

Tissues were fixed in 4% paraformaldehyde for 2 h and then washed three times in PBS solution. Subsequently, samples were dehydrated in an increasing scale of ethanol (30%, 50%, 70%, 90%, 96%, and absolute) and paraffin embedded. Sections (7 μm thick) obtained with a rotary microtome (Jung multicut 2045, Leica) were processed for Trichrome Masson staining (Trichromica kit, Bio Optica, Milan, Italy), as suggested by the datasheet. This coloring technique allows us to observe in blue the collagen and the reticular fibers, while in the red, cell cytoplasm. Images were recorded with a Nikon Digital Sight DS-SM optical Microscope (Nikon, Tokyo, Japan).

Immunofluorescence Assays

The same samples embedded in paraffin were analyzed by immunofluorescence assays. After paraffin removal, sections were rehydrated with a decreasing scale of ethanol (absolute, 96%, 90%, 70%, and 30%) and then pre-incubated for 30 min in BSA blocking solution (2% Bovine Serum Albumin and 0.1% Tween20 in PBS), which was also used to dilute both the primary and secondary antibodies. Samples were incubated with anti-COL1α1 (rabbit polyclonal, EMD Millipore, raised against peptide mapping at the C-terminal region of human collagen type I) and anti-RNASET2 (rabbit polyclonal, kindly donated by Professor Acquati) primary antibodies, diluted 1:200, for 1 h and after several washes in PBS buffer, they were incubated for 45 min with goat anti-rabbit FITC-conjugated (goat, Jackson ImmunoResearch Laboratories, Baltimore Pike, West Grove–PA, United States) and goat anti-rabbit Cy3-conjugated (goat, Jackson ImmunoResearch Laboratories, Baltimore Pike, West Grove, PA, United States), diluted 1:200, secondary antibodies. Nuclei were counterstained with 4,6-diamidino-2-Phenylinedole (DAPI, 0.1 mg/ml in PBS) for 3 min and slides were mounted with Cityfluor (Cityfluor Ltd., United Kingdom). Negative control experiments were performed omitting primary antibodies.

Double-labeling experiments were performed as previously described (Baranzini et al., 2017), in order to detect the co-localization between bFGFR, RNASET2, and CD34 with COL1α1. The primary antibodies anti-bFGFR (rabbit polyclonal, Santa Cruz Biotechnology, raised against peptide mapping at the C-terminal region of human Flg receptor), diluted 1:100, anti-RNASET2 (rabbit polyclonal), and anti-CD34 (rabbit polyclonal, abcam, raised against peptide mapping from the amino acid 350 to the C-terminal region of human CD34), diluted 1:200, were applied first. After several washes, sections were incubated with the goat anti-rabbit (Cy5)-conjugated (goat, Abcam England) secondary antibody, diluted 1:200. According to Würden and Homberg (1993), in order to block the binding of the second immunofluorescence cycle to the goat anti-rabbit IgGs previously utilized, sections were incubated with rabbit IgG (Jackson ImmunoResearch Laboratories, West Grove, PA, United States) at 1:50 for 2 h. After washing, every slide was treated with the anti-COL1α1 (rabbit, polyclonal, EMD Millipore) primary antibody, diluted 1:200. Procollagen1-α1 primary antibody was subsequently detected with a secondary (FITC)-conjugated goat anti-rabbit antibody (Abcam England), diluted 1:300. Samples were examined with the Nikon Eclipse Ni (Nikon, Tokyo, Japan) light and fluorescence microscope equipped with three different emission filters (360/420 nm for DAPI nuclear staining, 488/525 nm for FITC signals, and 550/580 nm for CY3 signals). Images were recorded with a Nikon digital sight DS-SM (Nikon, Tokyo, Japan) and mounted with Adobe Photoshop (Adobe Systems, San Jose, CA, United States).

RNA Extraction and qRT-PCR

Tissues extracted from uninjured or wounded and PBS- or *Hv*RNASET2-injected leeches were immediately frozen in liquid nitrogen and then homogenized with a mortar. The obtained homogenates were suspended in 1 mL of TRIzol reagent (Life Technologies) and incubated for 5 min at room temperature. Subsequently, 200 μl of chloroform was added and samples were centrifuged for 15 min at 13,000 rpm at 4°C. Once the different phases separated, 500 μl of the supernatant was recovered and gently mixed with 500 μl of isopropanol. After 10 min of centrifugation at 13,400 rpm, 1 mL of EtOH 75% in DEPC water was added to the precipitated RNA pellet, which was then centrifuged for 5 min at 10,000 rpm, resuspended in 40 μl of DEPC water, and incubated for 10 min at 55°C. The DNA contamination was eliminated by a TURBO DNA-free kit (Thermo Fisher Scientific) and samples were quantified, and purity was evaluated on 1% agarose gel.

In total, 2 μg of RNA were retro-transcribed into cDNA using M-MLV reverse transcriptase (Life Technologies) and qPCR was conducted in triplicate with the iTaq Universal SYBR Green Supermix (Bio-Rad, Hercules, CA) using a 96-well CFX Connect Real Time PCR Detection System (Bio-Rad). qPCR reaction mixtures had a final volume of 15 μl, with 2 μl of diluted cDNA and 10 μM of primers. The primers used for qPCR amplifications were as follows: COL1α1: Fw: 5′-AAGGGAGAGCAAGGAAGACA-3′, Rev: 5′-CCTG GTAAGCCATCAACACC-3′; *Hv*RNASET2: Fw: 5′-GGTCCCAA CTTCTGCACAAAGGAT-3′, Rev: 5′-GTTTGTCCCATTCATG CTTCCAGAA-3′; GAPDH: Fw: 5′-GAAGACTGTGGATGGA CCCT-3′, Rev: 5′-GTTGAGGACTGGGATGACCT-3′. To calculate the relative gene expression, the $2^{-\Delta\Delta Ct}$ method was performed, with GAPDH as the housekeeping gene. After the initial denaturation, qRT-PCR was performed at 95°C (10 s), 60°C (5 s), and 72°C (10 s) for 39 cycles. Graphs show the COL1α1 and *Hv*RNASET2 quantification (fold change) relative to the GAPDH gene expression.

Western Blot

Tissues obtained from wounded and PBS- or *Hv*RNASET2-injected leeches were immediately frozen in liquid nitrogen and then homogenized with a T10 basic ULTRA-TURRAX (IKA, Staufen, Germany) in 10 μl of RIPA buffer (50 mM of NaCl, 1% NP-40, 0.5% sodium deoxycholate, 0.1% SDS, 50 mM of Tris–HCl, pH 7.5, protease/phosphatase inhibitors cocktail) per mg of tissue. The lysates were clarified by centrifugation (13,000 rpm at 4°C for 20 min) and protein concentration was determined with the Biuret method. A total of 130 μg of protein extracts were subjected to 8% SDS-PAGE; separated proteins were transferred onto 0.45-μm pore size nitrocellulose membranes (Amersham Protran Premium, GE Healthcare, Chicago, IL, United States). The filters were blocked overnight at 4°C with 5% (w/v) non-fat dried milk in TBS (Tris-buffered saline) and then incubated for 2 h at room temperature with anti-COL1α1 antibody (rabbit, polyclonal) diluted 1:400 in TBS/5% milk; detection of glyceraldehydes 3-phosphate dehydrogenase (GAPDH) was used as loading control. After three washes of 10 min in TBST (Tris-buffered saline containing 0.1% Tween-20), the membranes were incubated for 1 h with horseradish-peroxidase conjugated anti-rabbit (dilution 1:7,500 in TBS/5% milk; Jackson ImmunoResearch Laboratories, West Grove, PA, United States) secondary antibody. The membranes were finally exposed to the enhanced chemiluminescence substrate (LiteAblot PLUS, EuroClone), followed by autoradiography on X-ray film (KODAK Medical X-Ray film, Z&Z Medical, IA, United States). Densitometric analysis was performed with the ImageJ software package[1]. The values are reported as the relative optical density of the bands, normalized to GAPDH.

Statistical Analyses

Western blot and qPCR experiments were performed in triplicate and data represent the mean values ± SEM. Statistical analyses were performed using GraphPad Prism 7 (GraphPad Software, La Jolla, CA, United States). Statistical differences were calculated by one-way ANOVA followed by Fisher's *post hoc* test, and $p < 0.05$ was considered statistically significant. In the qPCR assay, means with different asterisks represent a significant difference between wounded and PBS- or r*Hv*RNASET2-injected and untreated leeches at different times. In western blot analyses, means with different letters indicate significant difference between treatments at different times.

RESULTS

Morphological Analyses of the Body Wall in Injured and PBS/r*Hv*RNASET2-Injected Leeches

Morphological analyses were carried out on both undamaged and wounded PBS- or r*Hv*RNASET2-injected leeches by means of both light and TEM. Tissues were examined after 24, 48, 72 h, and 1 week from injuries, in order to evaluate the effect of *Hv*RNASET2 on wound healing and tissue regeneration.

The organization of the undamaged body wall (**Figures 1A,A'**) exhibited the typical structure of healthy leeches, in which, underneath the epithelium, few resident cells were present and muscle fibers were immersed in scant connective tissue (**Figure 1A'**). On the other side, in injured and PBS-injected leeches fixed after 24 h, wound healing was initiated with an inflammatory phase characterized by the migration of numerous macrophages, fibroblasts, and new vessels toward the lesioned area (**Figures 1B,B'**). After 24 h from injury and r*Hv*RNASET2 injection, a marked ECM deposition and a reduced number of vessels was visible in the lesioned area (**Figures 1C,C'**). Ultrastructural TEM analyses highlighted the presence of HSPCs in the neo-vessels only in injured PBS-injected leeches (**Figure 1D**), compared with lesioned and r*Hv*RNASET2-injected animals, in which a large collagen deposition occurred (**Figure 1E**).

In wounded and control PBS-injected leeches, fixed after 48 h (**Figure 1F**), the number of neo-vessels increased underneath

[1] http://rsbweb.nih.gov/ij/download.html

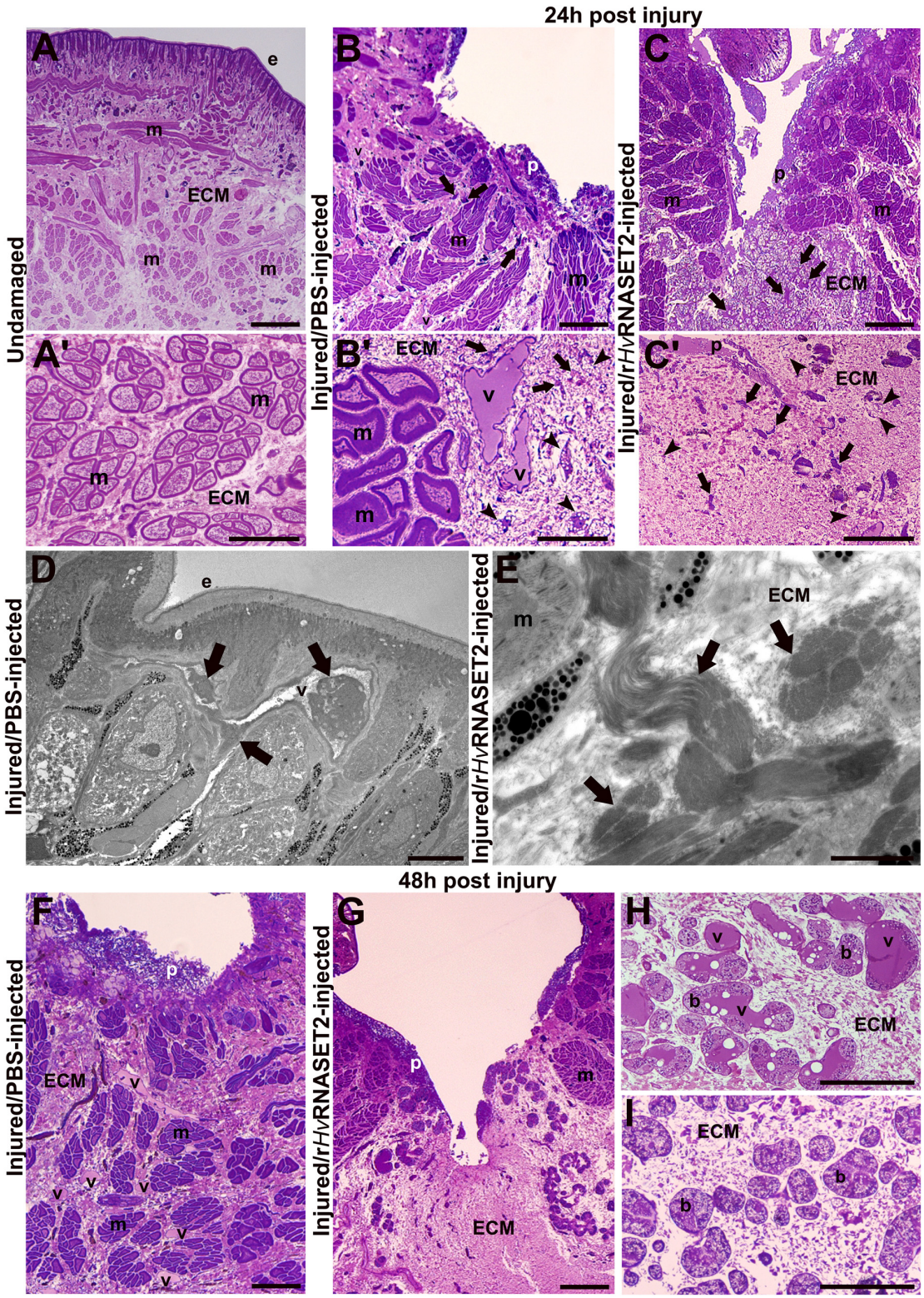

FIGURE 1 | Morphological analyses of the body wall in undamaged (group 1), control (group 2) injured, and PBS–or treated (group 3) *rHv*RNASET2-injected leeches fixed at 24 and 48 h post-treatment. In undamaged leeches **(A,A')**, tissue appears predominantly avascular and few resident cells are visible underneath the epithelium (e) and surrounding muscle fibers (m). In control leeches, fixed after 24 h **(B,B')**, an inflammatory phase arises, and neo-vessels (v), macrophages [arrows in panels **(B,B')**], and fibroblasts [arrowheads in panel **(B)**] are detectable in the lesioned area. In treated animals **(C,C')**, numerous immune cells (arrows) and

(Continued)

FIGURE 1 | Continued
fibroblasts (arrowheads) are visibly immersed in the abundant collagen (ECM). Details of TEM of control **(D)** and treated **(E)** leeches fixed after 24 h. HSPC (arrows) in the lumen of a vessel **(D)** and bundles of collagen fibrils (arrows) are visible **(E)**. In control tissues fixed after 48 h **(F,H)**, numerous blood vessels (v) are evident underneath the pseudoblastema (p) and among muscle fibers (m). Botryoidal tissue (b) appears activated in control animals and pre-vascular structures (v) are visible **(H)**. In treated animals fixed after 48 h **(G, I)**, a huge deposition of ECM in which no vessels are present is evident **(G)**. The botryoidal tissue (b) is in the inactivated form and appears arranged in cords or clusters **(I)**. Bars in panels **(A–C,F,G)** 100 μm; bars in panels **(A'–C',H,I)** 50 μm; bars in panels **(D,E)** 5 μm.

the pseudoblastema, compared to treated r*Hv*RNASET2-injected animals (**Figure 1G**). This evidence was supported by the analysis of the botryoidal tissue that in control samples changed its shape from a solid cord to a tubular and pre-vascular structure (**Figure 1H**), while in treated animals, it appeared inactivated and was arranged in cords or clusters (**Figure 1I**).

In control PBS-injected samples, fixed after 72 h (**Figure 2A**), a plug was visible under the epithelium. An organized muscle layer was present in the newly synthesized ECM, and HSPCs were clearly detectable in the lumen of neo-vessels (**Figures 2B,C**). By contrast, in leeches treated with the recombinant *Hv*RNASET2 enzyme a huge deposition of collagen was evident (**Figure 2D**). Numerous activated fibroblasts appeared elongated (**Figure 2E**) and star-shaped, characterized by the presence of multiple projections of cytoplasmic laminae stretching toward the extracellular space in which new collagen fibril deposition was identified (**Figure 2F**).

In addition, macrophages characterized by pseudopodia and blebs (Ma and Baumgartner, 2013; Eom, 2020) were observed in the healing region (**Figure 2G**).

One week after injury, the complete closure of the wound in control leeches was achieved, due to the formation of a thick pseudoblastema (**Figures 2H,I**). Furthermore, muscle tissue appeared to be largely repaired, as demonstrated by ultrastructural analysis using TEM showing differentiated muscle fibers surrounded by an abundant collagen matrix and in which contractile material was organized in sarcomeres (**Figure 2J**). In treated animals, although a thick pseudoblastema was visible, the lesioned area was filled by a massive amount of ECM, while muscle fibers were less represented (**Figures 2K–M**).

Masson's Trichrome Staining

Collagen-specific staining (**Figure 3**) was used to further investigate the effects of *Hv*RNASET2 on ECM remodeling in the healing region. In injured and PBS-injected leeches, the amount of ECM in the injured area and surrounding muscle fibers (**Figures 3A,C,E,G**) was less than that observed after treatment with r*Hv*RNASET2 (**Figures 3B,D,F,H**). Indeed, after r*Hv*RNASET2 injection, the amount of newly synthesized ECM increased 48 h after injury and treatment (**Figures 3D,F,H**). Furthermore, Masson's trichrome staining clearly showed that the muscle tissue underlying the scar region area was completely regenerated in control animals, whereas in injured r*Hv*RNASET2-treated leeches, only a few muscle fibers were recognizable in the newly synthesized compact collagenous scaffold (**Figures 3G,H**).

Immunofluorescence Analyses

The immunofluorescent assay performed on PBS (**Figures 4A,C,E,G**) and *Hv*RNASET2-injected (**Figures 4B,D,F,H**) leeches, showed an increase of *Hv*RNASET2 in the treated groups, as expected. Moreover, the identification of RNASET2^{+} cells, which was particularly evident in the wound healing area and in the underlying connective tissue, suggested that further expression of the endogenous enzyme was triggered on the resident cells by the injected *Hv*RNASET2 at the injured site.

To better characterize the composition of newly synthesized ECM during the wound healing phases and to evaluate the role of *Hv*RNASET2 in inducing collagen neo-synthesis, immunofluorescence assays were performed (**Figure 5**). In the body wall of wounded and PBS-injected leeches (**Figures 5A,C,E,G**), a lower detectable marker collagen I signal was displayed at different time points from injuries, whereas the production of collagen I progressively increased in r*Hv*RNASET2-treated animals (**Figures 5B,D,F,H**), as also demonstrated by the presence of numerous bFGFR-expressing fibroblasts in the same area (**Figures 6A,B**). Moreover, the immunolocalization of *Hv*RNASET2 definitively correlated the increased levels of collagen I with a higher expression of this enzyme. As expected, *Hv*RNASET2 signal was higher in the r*Hv*RNASET2-injected area after 48 h, due not only to recombinant protein injection, but also to r*Hv*RNASET2-induced recruitment of more fibroblasts (Baranzini et al., 2020b), which in turn produced new collagen I (**Figures 6C,D**). Furthermore, only a few CD34 positive cells were visible in the injured and r*Hv*RNASET2-treated leeches (**Figures 6E,H**) after 48 h, compared to those seen in control animals (**Figures 6E,G**). This finding suggested that the reduced recruitment of myeloid precursors was correlated with the absence of new blood vessel formation. No signals were detected in the negative control experiments in which the primary antibodies were omitted (**Supplementary Figures 1A–E**).

qPCR and Western Blot Analyses

The *Hv*RNASET2 expression levels and the rate of neosynthesized collagen I were also assessed by means of real-time qPCR and western blot assays at different timings (**Figure 7**). As shown in the qPCR graphs, in both PBS- and T2-injected leeches the expression levels of both *Hv*RNASET2 (**Figure 7A**) and collagen I (**Figure 7B**) was higher than the untreated leeches, used as control. However, the *Hv*RNASET2 gene appeared to be expressed at already significantly higher levels after 24 h, subsequently decreasing at 48 h, and then reaching a new peak after 1 week. By contrast, *Hv*RNASET2 expression levels in PBS-treated animals remained rather

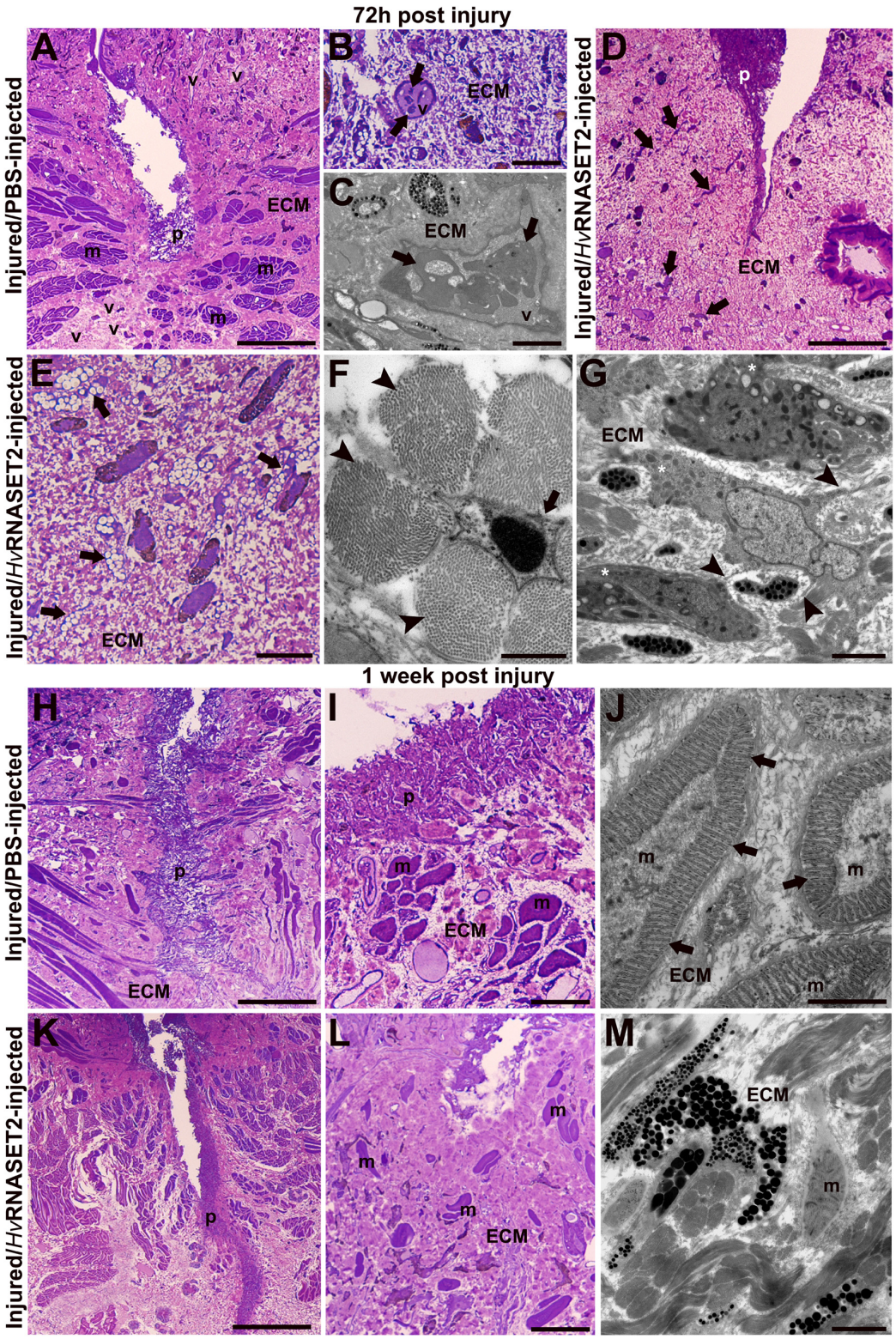

FIGURE 2 | Morphological analyses of the body wall in control (group 2) injured and PBS- or treated (group 3) *rHv*RNASET2-injected leeches fixed after 72 h and 1 week post-treatment. After 72 h **(A–C)**, in control leeches, numerous vessels (v) and an organized muscle layer are visible **(A)**. Details of light **(B)** and TEM **(C)** microscopes of HSPCs (arrows) in the vessel lumen. In treated leeches **(D–G),** numerous cells (arrows) are evident in the abundant collagen (ECM) underneath the pseudoblastema (p). Activated elongated **(E)** and star-shaped **(F)** fibroblasts (arrows) are involved in new collagen production [arrowhead in panel **(F)**]. Macrophages

(Continued)

FIGURE 2 | Continued
(G) characterized by pseudopodia (asterisks) and membrane blebs (arrowheads). After 1 week, in control animals, the wound is healed and underneath the thick pseudoblastema [p in panels **(H,I)**], a restored muscle layer (m) is evident **(I)**. TEM image showing muscle fibers, with organized sarcomeres (arrows), surrounded by newly synthesized extracellular matrix (ECM) **(J)**. In treated leeches fixed after 1 week, underneath the thick pseudoblastema [p in panels **(K,L)**], a few muscle fibers [m in panels **(L,M)**] are dispersed in the ECM. Bars in panels **(A,D,H,K)** 100 μm; bars in panels **(B,E,I,L)** 10 μm; bars in panels **(G,J,M)** 2 μm; bar in panel **(F)** 500 nm.

constant. A similar result in *Hv*RNASET2-treated leeches was observed for collagen I, whereby a high expression peak was observed after 24 h, subsequently decreased after 48 h, but then raised again, reaching maximum values at 1 week from treatment. It is worth noting that collagen I expression values were also constant in all timings in wounded and PBS-injected leeches. This evidence was also validated by western blot analyses (**Supplementary Figure 1F**) showing the presence of 140 kDa bands (corresponding to the molecular weight of collagen I). As visible in the graph (**Figure 7C**), a greater deposition of collagen I appeared more visible in r*Hv*RNASET2-injected animals, compared to PBS-injected samples.

DISCUSSION

After physical damages, inflammation represents the preliminary step necessary to restore both the precise original structure and the correct homeostasis of tissues. Injuries induce a sudden physiological change in the lesioned microenvironment, in which the release of different cytokines and growth factors promotes the activation of many enzymatic cascades and consequent cellular reactions (Mescher et al., 2017). The importance of a rapid immune response is essential to accurately coordinate the subsequent events and to prevent any incorrect outcomes, both in vertebrates and in invertebrates (Tettamanti et al., 2003b; de Eguileor et al., 2005). Moreover, besides the local immune reaction, the activated cells are involved in the production of new ECM components, which constitute the fundamental scaffold for the migration of inflammatory precursors, the formation of blood vessels, and the restoration of the original architecture (Grimaldi et al., 2006). Given the clinical importance in investigating the existing correlation between inflammation and wound healing events, the use of alternative animals models, such as the medicinal leech, piqued interest, improving not only the knowledge of many preserved biological processes, but also of the molecules that take part in them, which appear to be evolutionarily conserved (Mescher et al., 2017).

In this context, the leech *H. verbana*, showing several similarities with vertebrates, represents a suitable invertebrate model that allows us to add novel insights to tissue regeneration. Moreover, in leeches, it has been recently demonstrated that the *Hv*RNASET2 enzyme not only regulates the inflammatory response, recruiting macrophages toward challenge tissues, but also plays a pivotal role in connective tissue remodeling, triggering fibroblasts activation and ECM reorganization (Baranzini et al., 2020b). This evidence and the pleiotropic nature of T2 ribonucleic enzymes indicate that this protein acts as a key molecule that can coordinate both inflammation and regenerative events. To confirm this hypothesis, injured and PBS- or r*Hv*RNASET2-injected leeches were evaluated by means of morphological and molecular assays.

Compared to undamaged leeches (Baranzini et al., 2017, 2019), light and TEM analyses revealed that in PBS-injected control animals, after wounding several cells migrated to the lesioned area during the earlier healing phase, confirming that the inflammatory response also characterizes the regenerative process in leeches. Moreover, the reorganization of the connective tissue, due to an accentuate fibroplasia, allows for angiogenetic events and the appearance of new blood vessels. These mechanisms are regulated by both macrophages and fibroblasts, which increased around the pseudoblastema and were fundamental for the development of correct wound repair. Like in vertebrates (Wynn and Barron, 2010; Mescher et al., 2017), macrophages are considered to be the main effectors of inflammatory response and fibrosis participating in the elimination of apoptotic cells and cellular debris in leeches as well. These cells, characterized by filopodia and blebs, which are probably involved in driving the migration and cell-to-cell signaling of macrophages in the connective tissue (Ma and Baumgartner, 2013; Eom, 2020), are derived from hematopoietic myeloid precursors, which originate in the botryoidal tissue and migrate to the lesioned area toward the neo-vessels. The beginning of vasculogenesis, which involves the early formation of the vascular system, is characterized by a marked remodeling of the botryoidal tissue that in turn represents a mechanism for the fast recruitment of a large number of cells involved in immune defense, wound healing, and regeneration. These myeloid precursors possess the ability to activate diverse genetic programs in response to peculiar environmental stimulation and give rise to immune cells and/or to vessel-associated myoendothelial cells involved in muscle regeneration (Grimaldi et al., 2009; Grimaldi, 2016). In parallel, fibroblasts appear elongated and star-shaped, characterized by the presence of multiple cytoplasmic laminae projections stretching into the extracellular space, near which new collagen fibril deposition becomes evident. As in vertebrates, where fibroblasts act with other mesenchymal cells to release different molecular effectors (such as monocyte chemoattractant and prostaglandin E2) in order to recruit macrophages and regulate monocyte activation (Bernardo and Fibbe, 2013; Mescher et al., 2017), this also occurs in leeches where these $bFGF^{+}$ cells might promote both the inflammatory state and its subsequent resolution, directly producing new collagen I. Thus, in the medicinal leech, the continuous interaction between macrophages, fibroblasts, and other immune or mesenchymal cells avoids fibrotic events and promotes muscle regeneration and lesion repair after 1 week from injury, allowing the correct formation of the pseudoblastema and the complete closure of the wound.

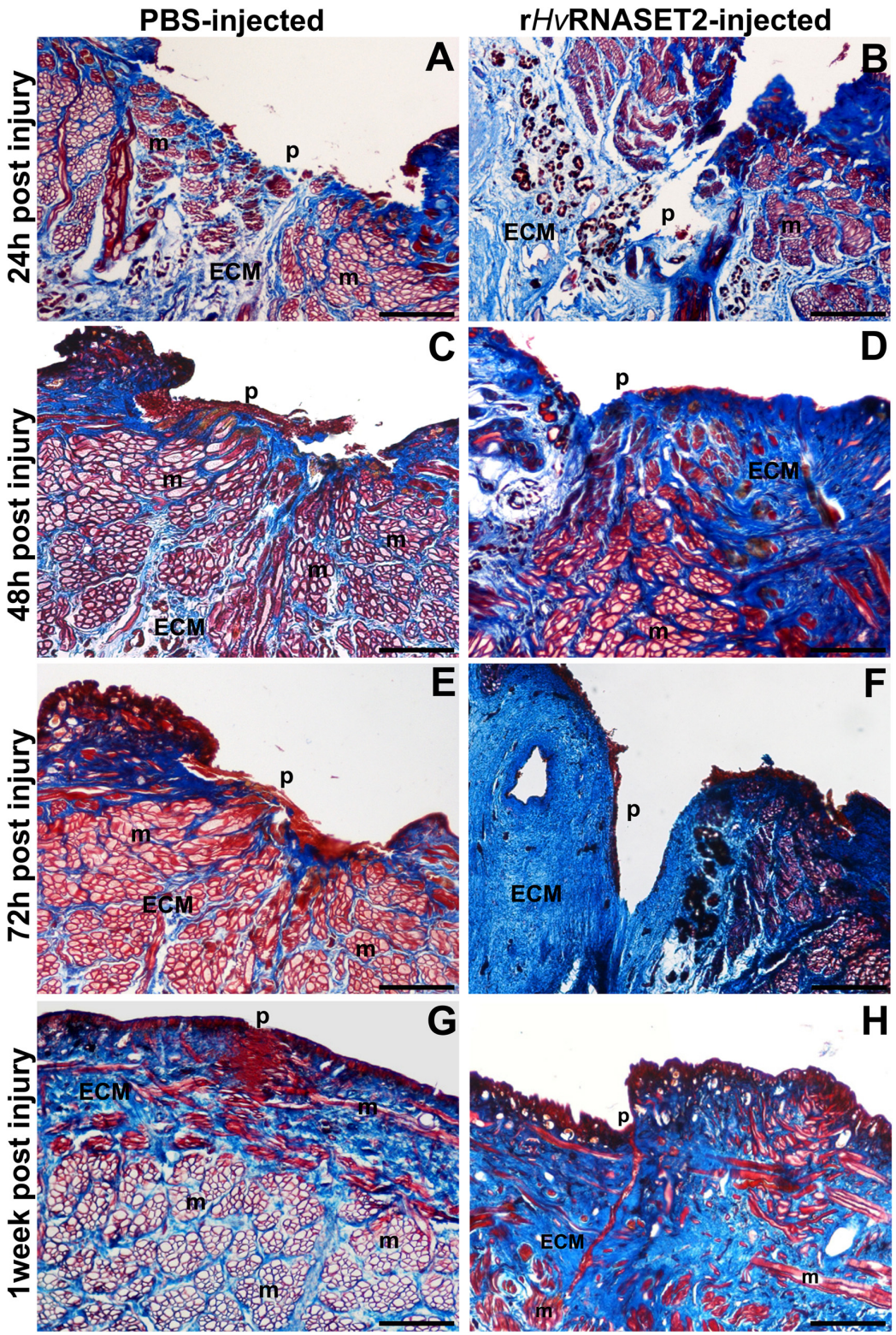

FIGURE 3 | Images of cross-sectioned leech body wall using a light microscope with Masson's trichrome collagen-specific staining. Collagen is colored in blue (ECM). In leeches treated with PBS **(A,C,E,G)**, collagen fibrils are visible among muscles (m) and underneath the pseudoblastema (p) and lesioned area, while the muscles fiber (m) reorganization is completely regenerated. In r*Hv*RNASET2-injected leeches, an increasing production of collagen is detectable, even after only 24 h **(B)**, which is also maintained after 48–72 h **(D,F)** and 1 week **(H)** from the lesion. Moreover, only a few muscle fibers (m) are recognizable in the newly synthesized compact collagenous scaffold **(G,H)**. p: pseudoblastema, ECM: extracellular matrix. Bars in panels **(A–H)** 100 μm.

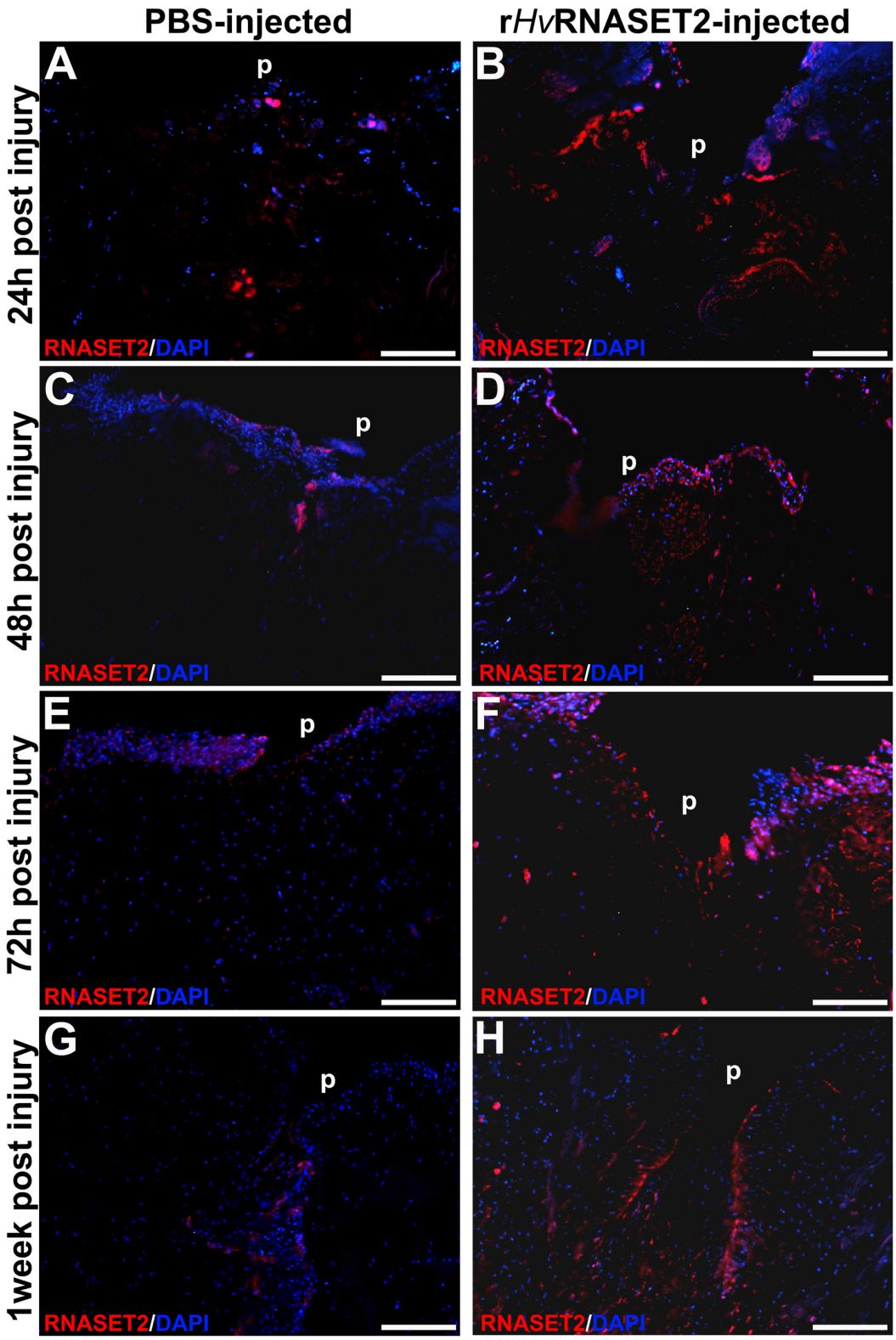

FIGURE 4 | Immunofluorescent analyses of injured and PBS or *rHv*RNASET2-injected leeches. In PBS-treated animals, an increasing signal for the anti-RNASET2 antibody is detected underneath the pseudoblastema (p) during different time points **(A,C,E,G)**. Instead, in *rHv*RNASET2-injected leeches, numerous *Hv*RNASET2^{+} cells are already visible after 24 h and the *Hv*RNASET2 signal is higher compared to that observed following PBS treatment in all timings **(B,D,F,H)**. Cell nuclei are stained in blue with DAPI. Bars in panels **(A–H)** 100 μm.

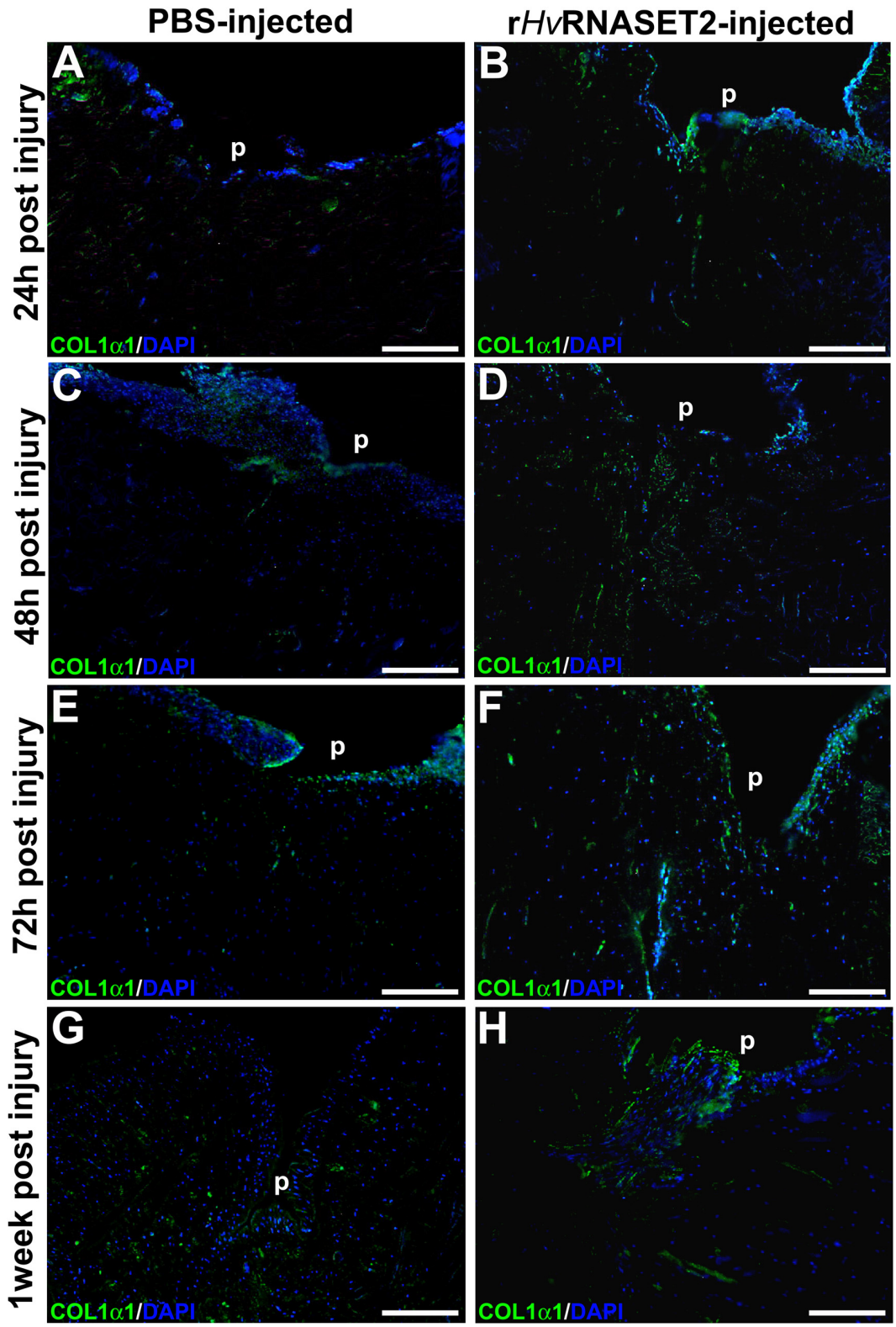

FIGURE 5 | Immunofluorescent analyses of injured and PBS or r*Hv*RNASET2-injected leeches. The primary anti-COL1α1 antibody highlights a different synthesis of collagen between the two different treatments. Injured and PBS-injected animals show a lower detectable signal **(A,C,E,G)**, while in injured and r*Hv*RNASET2-injected leeches, an abundant production of collagen is clearly detectable **(B,D,F,H)**. Cell nuclei are stained in blue with DAPI. p: pseudoblastema, ECM: extracellular matrix. Bars in panels **(A–H)** 100 μm.

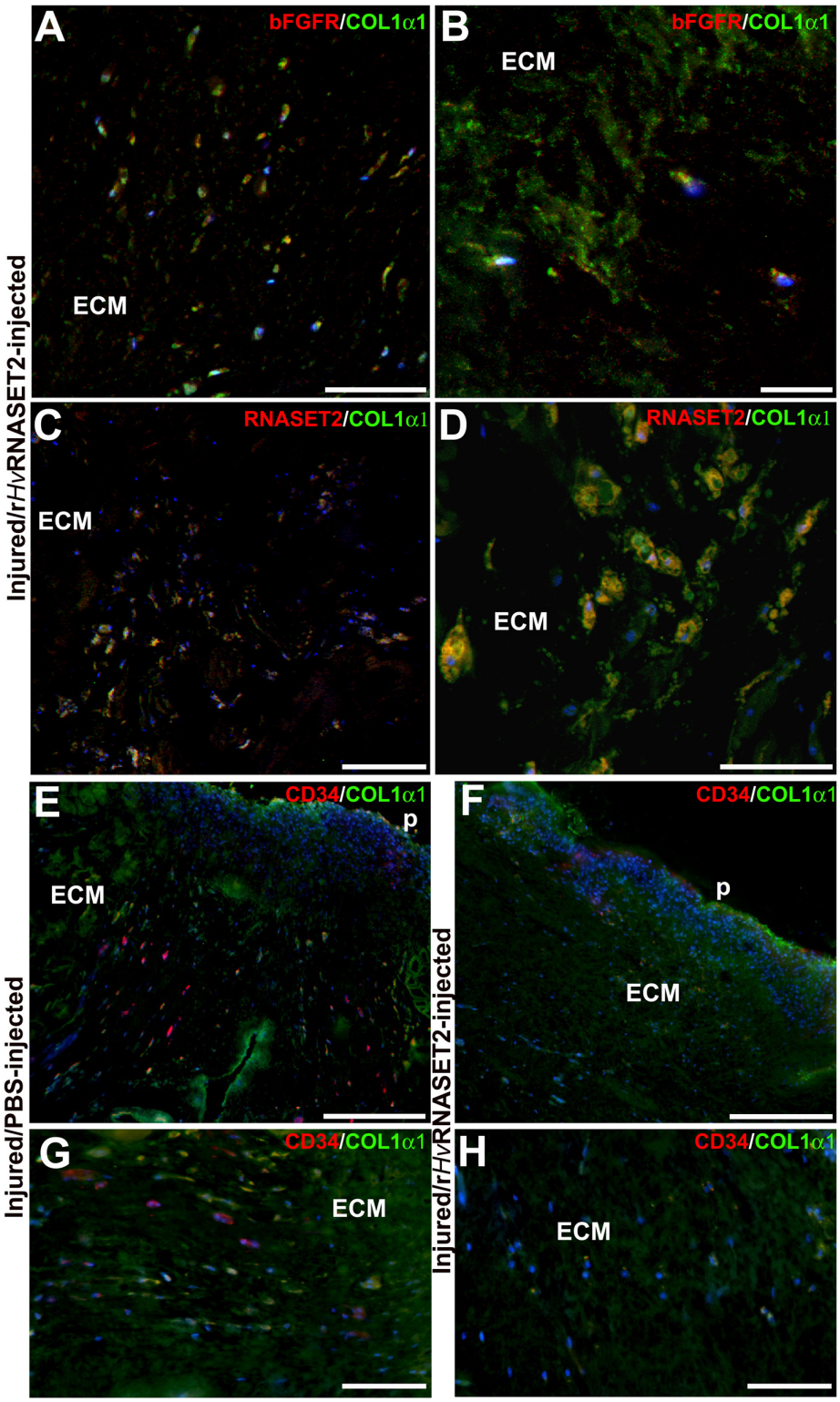

FIGURE 6 | Double immunolocalization of collagen1-α1 (in green) and bFGFR/RNASET2 (in red) of wounded and r*Hv*RNASET2-injected leeches **(A–D)**, and COL1α1 (in green) and CD34 (in red) of wounded and PBS- or r*Hv*RNASET2-injected animals **(E–H)** 48 h from injury. Numerous activated bFGFR^{+} fibroblasts are visible in the lesioned tissue, which are involved in new collagen I fibrils production **(A,B)**. Several cells appear positive for both RNASET2 and collagen1-α1 antibodies **(C,D)**, suggesting a direct correlation between *Hv*RNASET2 and collagen I. Moreover, numerous CD34^{+} HSPCs are found in PBS-injected leeches **(E,G)** compared to r*Hv*RNASET2-treated animals **(F,H)**. Nuclei are stained in blue with DAPI. p: pseudoblastema, ECM: extracellular matrix. Bars in panels **(A,C–E)** 100 μm; bars in panels **(B,F,G)** 50 μm; bar in panel **(D)** 20 μm.

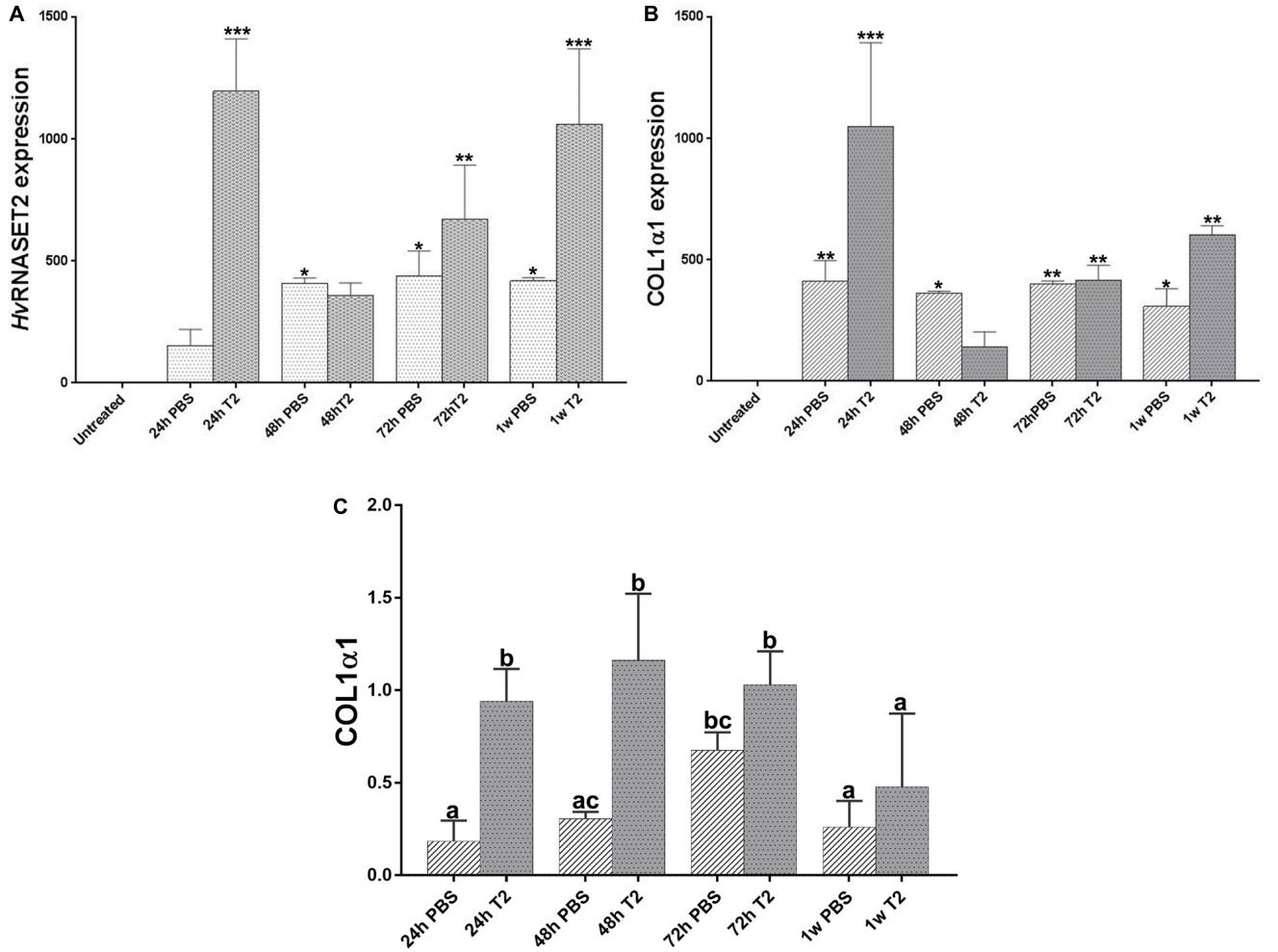

FIGURE 7 | Graphs showing qRT-PCR analyses related to *Hv*RNASET2 **(A)** and COL1α1 **(B)** mRNA expression in PBS or r*Hv*RNASET2-injected leeches. The graphs represent *Hv*RNASET2 and COL1α1 quantification relative to the expression of the endogenous gene GAPDH. The mRNA expression fold change of treated animals is compared with that of untreated leeches, used as control. Statistical differences were calculated by one-way ANOVA and $p < 0.05$ was considered statistically significant. Western blot analyses on wounded and PBS- or r*Hv*RNASET2-injected leeches **(C)**. The graph illustrates the expression levels of collagen1α1 at different time points, calculated by densitometric analysis. The values are reported as relative optical density of the bands normalized to glyceraldehyde 3-phosphate dehydrogenase (GAPDH). Means with different letters indicate significant difference between treatments at different times. $^{*}P < 0.5$, $^{**}P < 0.1$, $^{***}P < 0.01$.

Conversely, the overexpression of r*Hv*RNASET2 in the wounded area induces not only a significant increase in macrophages and type I granulocytes recruitment, confirming the ability of this enzyme to recruit various immunocompetent cells into the injured tissue (Baranzini et al., 2017, 2019), but also induces a massive deposition of ECM components, mainly evident 72 h post-injury. The deposition of new collagen I is due to the activation of numerous *Hv*RNASET2^{+}/bFGF^{+} fibroblasts, as also demonstrated by molecular analyses. Especially in wounded and RNASET2-injected leeches, both *Hv*RNASET2 and collagen I gene expression levels appeared to be already significantly increased 24 h from treatment, which then decreased and reached a new peak after 1 week.

Strikingly, unlike control PBS-injected leeches, in injured *Hv*RNASET2^{+}-injected animals a few vessels and muscle fibers were found in the newly formed connective tissue. These results lead us to hypothesize that although *Hv*RNASET2 promotes the formation of a solid collagen scaffold, its anti-angiogenic effect, already demonstrated in vertebrates (Acquati et al., 2011), might affect the number of CD34^{+} myoendothelial precursor cells recruited in the regenerating area. Thus, the incorrect regeneration of muscle tissue might be attributable to the failure to recruit these cells, which in physiological conditions are instead transported by the neo-vessels into the wound healing area and give rise to new muscle fibers (Grimaldi et al., 2009, 2010). Our hypothesis seems to be supported by the low number of vessels and by the considerably reduced angiogenesis process. Furthermore, in the wounded *Hv*RNASET2-injected leeches, the botryoidal tissue shows a typical inactivated form, arranged in cords or clusters.

CONCLUSION

Understanding the events combining innate immune response and regeneration have gained considerable importance in recent years as it is now clear that these two processes are closely related and are fundamental for tissue homeostasis. Indeed, it is well known that a reduced tissue regeneration capacity is linked to a reduced inflammation process. It is therefore becoming essential to understand how the immune system is able to regulate the correct restoration of tissues, in order also to develop new strategies in the therapeutic field.

Our study carried out in a medicinal leech alternative animal model, in addition to avoiding the use of vertebrates for research, could lay the foundation for the development of new clinical strategies by highlighting *Hv*RNASET2 as a possible regulator of ECM remodeling during wound healing. This enzyme, by inducing the activation of fibroblasts, promotes the synthesis of new collagen I and ECM remodeling. As a secondary effect, a reduction of the regeneration of muscle tissue occurs, due to the probable anti-angiogenic effect of this enzyme. We speculate that lower vascularization prevents the migration of muscle precursors normally vehiculated by the vessels in the regenerating area.

DATA AVAILABILITY STATEMENT

The original contributions presented in the study are included in the article/**Supplementary Material**, further inquiries can be directed to the corresponding author/s.

AUTHOR CONTRIBUTIONS

AG and FA conceived the experiments, and wrote and edited the manuscript. NB and LP equally contributed to this work performed the experiments, and statistical analyses. NB prepared the original draft of the manuscript and all the figures. GT edited the manuscript and provided expertise. All authors critically reviewed the manuscript.

FUNDING

This work was supported by the Associazione Amici dell'Insubria foundation and Consorzio Interuniversitario Biotecnologie (CIB) and by the Federico Ghidoni Memorial fund and Insubria Academic Research Funds (FAR) to AG, FA, and GT.

ACKNOWLEDGMENTS

LP is a Ph.D. student of life sciences and biotechnology, Biosciences and Surgical Technology course at the University of Insubria. We thank Laura Monti for her support in supplying recombinant *Hv*RNASET2, expressed in the *Pichia pastoris* heterologous expression system.

SUPPLEMENTARY MATERIAL

The Supplementary Material for this article can be found online at: https://www.frontiersin.org/articles/10.3389/fphys.2021.632506/full#supplementary-material

Supplementary Figure 1 | Immunolocalization (negative control) **(A–E)**. No signals are visible in anti-RNASET2 **(A)**, anti-COL1a1 **(B)**, CD34/COL1a1 **(C)**, bFGFR/COL1a1 **(D)**, and RNASET2/COL1a1 **(E)** negative control immunolocalizations, in which primary antibodies are omitted. Western blot immunoreactive bands of undamaged, injured, and PBS- or r*Hv*RNASET2-injected leeches, analyzed after 24, 48, 72 h, and 1 week post-treatment **(F)**. The anti-collagen I and anti-GAPDH antibodies detected in a leech tissue-specific immunoreactive band of about 140 and 37 kDa respectively, according to the molecular weight ladder (kDa).

REFERENCES

Acquati, F., Bertilaccio, S., Grimaldi, A., Monti, L., Cinquetti, R., Bonetti, P., et al. (2011). Microenvironmental control of malignancy exerted by RNASET2, a widely conserved extracellular RNase. *Proc. Natl. Acad. Sci. U.S.A.* 108, 1104–1109. doi: 10.1073/pnas.1013746108

Baranzini, N., De Vito, A., Orlandi, V. T., Reguzzoni, M., Monti, L., de Eguileor, M., et al. (2020a). Antimicrobial role of RNASET2 protein during innate immune response in the medicinal leech *Hirudo verbana*. *Front. Immunol.* 11:370. doi: 10.3389/fimmu.2020.00370

Baranzini, N., Monti, L., Vanotti, M., Orlandi, V. T., Bolognese, F., Scaldaferri, D., et al. (2019). AIF-1 and RNASET2 Play complementary roles in the innate immune response of medicinal leech. *J. Innate. Immun.* 11, 150–167. doi: 10.1159/000493804

Baranzini, N., Pedrini, E., Girardello, R., Tettamanti, G., de Eguileor, M., Taramelli, R., et al. (2017). Human recombinant RNASET2-induced inflammatory response and connective tissue remodeling in the medicinal leech. *Cell Tissue Res.* 368, 337–351. doi: 10.1007/s00441-016-2557-9

Baranzini, N., Weiss-Gayet, M., Chazaud, B., Monti, L., de Eguileor, M., Tettamanti, G., et al. (2020b). Recombinant HvRNASET2 protein induces marked connective tissue remodelling in the invertebrate model *Hirudo verbana*. *Cell Tissue Res.* 380, 565–579. doi:10.1007/s00441-020-03174-0

Bernardo, M. E., and Fibbe, W. E. (2013). Mesenchymal stromal cells: sensors and switchers of inflammation. *Cell Stem Cell* 13, 392–402. doi: 10.1016/j.stem.2013.09.006

Birk, D. E., and Zycband, E. (1994). Assembly of the tendon extracellular matrix during development. *J. Anat.* 184, 457–463.

de Eguileor, M., Grimaldi, A., Boselli, A., Tettamanti, G., Lurati, S., Valvassori, R., et al. (1999a). Possible roles of extracellular matrix and cytoskeleton in leech body wall muscles. *J. Microsc.* 196, 6–18. doi: 10.1046/j.1365-2818.1999.00600.x

de Eguileor, M., Grimaldi, A., Tettamanti, G., Ferrarese, R., Congiu, T., Protasoni, M., et al. (2001). Hirudo medicinalis: a new model for testing activators and inhibitors of angiogenesis. *Angiogenesis* 4, 299–312.

de Eguileor, M., Tettamanti, G., Grimaldi, A., Boselli, A., Scarì, G., Valvassori, R., et al. (1999b). Histopathological changes after induced injury in leeches1. *J. Invertebr. Pathol.* 74, 14–28. doi: 10.1006/jipa.1999.4850

de Eguileor, M., Tettamanti, G., Grimaldi, A., Congiu, T., Ferrarese, R., Perletti, G., et al. (2005). Leeches: immune response, angiogenesis and biomedical applications. *Curr. Pharm. Des.* 9, 133–147. doi: 10.2174/1381612033392198

de Eguileor, M., Tettamanti, G., Grimaldi, A., Perletti, G., Congiu, T., Rinaldi, L., et al. (2004). Hirudo medicinalis: avascular tissues for clear-cut angiogenesis studies? *Curr. Pharm. Des.* 10, 1979–1988. doi: 10.2174/1381612043384358

Eom, D. S. (2020). Airinemes: thin cellular protrusions mediate long-distance signalling guided by macrophages. *Open Biol.* 10:200039. doi: 10.1098/rsob.200039

Frantz, S., Vincent, K. A., Feron, O., and Kelly, R. A. (2005). Innate immunity and angiogenesis. *Circ. Res.* 96, 15–26. doi: 10.1161/01.RES.0000153188.68898.ac

Girardello, R., Baranzini, N., Tettamanti, G., de Eguileor, M., and Grimaldi, A. (2017). Cellular responses induced by multi-walled carbon nanotubes: *in vivo* and *in vitro* studies on the medicinal leech macrophages. *Sci. Rep.* 7:8871. doi: 10.1038/s41598-017-09011-9

Godwin, J. W., Debuque, R., Salimova, E., and Rosenthal, N. A. (2017). Heart regeneration in the salamander relies on macrophage-mediated control of fibroblast activation and the extracellular landscape. *NPJ Regen. Med.* 2:22. doi: 10.1038/s41536-017-0027-y

Grimaldi, A. (2016). Origin and fate of hematopoietic stem precursor cells in the leech *Hirudo medicinalis*. *Invertebr. Surviv. J.* 13, 257–268.

Grimaldi, A., Banfi, S., Bianchi, C., Greco, G., Tettamanti, G., Noonan, D., et al. (2010). The leech: a novel invertebrate model for studying muscle regeneration and diseases. *Curr. Pharm. Des.* 16, 968–977. doi: 10.2174/138161210790883417

Grimaldi, A., Banfi, S., Gerosa, L., Tettamanti, G., Noonan, D. M., Valvassori, R., et al. (2009). Identification, isolation and expansion of myoendothelial cells involved in leech muscle regeneration. *PLoS One* 4:e7652. doi: 10.1371/journal.pone.0007652

Grimaldi, A., Banfi, S., Vizioli, J., Tettamanti, G., Noonan, D. M., and de Eguileor, M. (2011). Cytokine loaded biopolymers as a novel strategy to study stem cells during wound-healing processes. *Macromol. Biosci.* 11, 1008–1019. doi: 10.1002/mabi.201000452

Grimaldi, A., Tettamanti, G., Perletti, G., Valvassori, R., and de Eguileor, M. (2006). Hematopoietic cell formation in leech wound healing. *Curr. Pharm. Des.* 12, 3033–3041. doi: 10.2174/138161206777947443

Grimaldi, A., Tettamanti, G., Rinaldi, L., Perletti, G., Valvassori, R., and de Eguileor, M. (2004). Role of cathepsin B in leech wound healing. *Invertebr. Surviv. J.* 1, 38–46.

Huguet, G., and Molinas, M. (1994). The pseudoblastema in the wound healing process of the leech *Hirudo medicinalis* L. (Hirudinea): changes in cell junctions. *J. Exp. Zool.* 269, 23–36. doi: 10.1002/jez.1402690104

Huguet, G., and Molinas, M. (1996). Myofibroblast-like cells and wound contraction in leech wound healing. *J. Exp. Zool.* 275, 308–316. doi:10.1002/(SICI)1097-010X(19960701)275:4<308::AID-JEZ9<3.0.CO;2-T

Li, W. W., Talcott, K. E., Zhai, A. W., Kruger, E. A., and Li, V. W. (2005). The role of therapeutic angiogenesis in tissue repair and regeneration. *Adv. Skin Wound Care* 18, 491–500. doi: 10.1097/00129334-200511000-00014

Ma, M., and Baumgartner, M. (2013). Filopodia and membrane blebs drive efficient matrix invasion of macrophages transformed by the intracellular parasite *Theileria annulata*. *PLoS One* 8:e75577. doi: 10.1371/journal.pone.0075577

Malagoli, D. (2018). Going beyond a static picture: the apple snail *Pomacea canaliculata* can tell us the life history of molluscan hemocytes. *Invertebr. Surviv. J.* 15, 61–65.

Martin, J. T. (1997). Development of an adjuvant to enhance the immune response to influenza vaccine in the elderly. *Biologicals* 25, 209–213. doi: 10.1006/biol.1997.0086

Mescher, A. L., Neff, A. W., and King, M. W. (2017). Inflammation and immunity in organ regeneration. *Dev. Comp. Immunol.* 66, 98–110. doi: 10.1016/j.dci.2016.02.015

Moore, R. D., Mumaw, V., and Schoenberg, M. D. (1960). Optical microscopy of ultrathin tissue sections. *J. Ultrastruct. Res.* 4, 113–116. doi: 10.1016/S0022-5320(60)90047-2

Pieper, J. S., Hafmans, T., Van Wachem, P. B., Van Luyn, M. J. A., Brouwer, L. A., Veerkamp, J. H., et al. (2002). Loading of collagen-heparan sulfate matrices with bFGF promotes angiogenesis and tissue generation in rats. *J. Biomed. Mater. Res.* 62, 185–194. doi: 10.1002/jbm.10267

Saltzman, C. L. (1999). Total ankle arthroplasty: state of the art. *Instr. Course Lect.* 48, 263–268.

Schorn, T., Drago, F., Tettamanti, G., Valvassori, R., de Eguileor, M., Vizioli, J., et al. (2015). Homolog of allograft inflammatory factor-1 induces macrophage migration during innate immune response in leech. *Cell Tissue Res,* 359, 853–864. doi: 10.1007/s00441-014-2058-7

Tasiemski, A., and Salzet, M. (2017). Neuro-immune lessons from an annelid: the medicinal leech. *Dev. Comp. Immunol.* 66, 33–42. doi: 10.1016/j.dci.2016.06.026

Tettamanti, G., Grimaldi, A., Congiu, T., Perletti, G., Raspanti, M., Valvassori, R., et al. (2005). Collagen reorganization in leech wound healing. *Biol. Cell* 97, 557–568. doi: 10.1042/BC20040085

Tettamanti, G., Grimaldi, A., Ferrarese, R., Palazzi, M., Perletti, G., Valvassori, R., et al. (2003a). Leech responses to tissue transplantation. *Tissue Cell* 35, 199–212. doi: 10.1016/S0040-8166(03)00027-2

Tettamanti, G., Grimaldi, A., Rinaldi, L., Arnaboldi, F., Congiu, T., Valvassori, R., et al. (2004). The multifunctional role of fibroblasts during wound healing in *Hirudo medicinalis* (Annelida, Hirudinea). *Biol. Cell* 96, 443–455. doi: 10.1016/j.biolcel.2004.04.008

Tettamanti, G., Grimaldi, A., Valvassori, R., Rinaldi, L., and de Eguileor, M. (2003b). Vascular endothelial growth factor is involved in neoangiogenesis in *Hirudo medicinalis* (Annelida, Hirudinea). *Cytokine* 22, 168–179. doi: 10.1016/s1043-4666(03)00176-5

Würden, S., and Homberg, U. (1993). A simple method for immunofluorescent double staining with primary antisera from the same species. *J. Histochem. Cytochem.* 41, 627–630. doi: 10.1177/41.4.8450202

Wynn, T., and Barron, L. (2010). Macrophages: master regulators of inflammation and fibrosis. *Semin. Liver Dis.* 30, 245–257. doi: 10.1055/s-0030-1255354

Conflict of Interest: The authors declare that the research was conducted in the absence of any commercial or financial relationships that could be construed as a potential conflict of interest.

frontiers in Physiology

ORIGINAL RESEARCH
published: 25 February 2021
doi: 10.3389/fphys.2021.642237

Comprehensive Quantitative Proteome Analysis of *Aedes aegypti* Identifies Proteins and Pathways Involved in *Wolbachia pipientis* and Zika Virus Interference Phenomenon

Michele Martins[1†], Luis Felipe Costa Ramos[1†], Jimmy Rodriguez Murillo[2], André Torres[3], Stephanie Serafim de Carvalho[1], Gilberto Barbosa Domont[1], Danielle Maria Perpétua de Oliveira[1], Rafael Dias Mesquita[1], Fábio César Sousa Nogueira[1], Rafael Maciel-de-Freitas[4] and Magno Junqueira[1]**

[1] Departamento de Bioquímica, Instituto de Química, Universidade Federal do Rio de Janeiro, Rio de Janeiro, Brazil, [2] Division of Chemistry I, Department of Medical Biochemistry and Biophysics, Karolinska Institute, Stockholm, Sweden, [3] Carlos Chagas Filho Biophysics Institute, Universidade Federal do Rio de Janeiro, Rio de Janeiro, Brazil, [4] Laboratório de Mosquitos Transmissores de Hematozoários, Instituto Oswaldo Cruz, Fiocruz, Rio de Janeiro, Brazil

Zika virus (ZIKV) is a global public health emergency due to its association with microcephaly, Guillain-Barré syndrome, neuropathy, and myelitis in children and adults. A total of 87 countries have had evidence of autochthonous mosquito-borne transmission of ZIKV, distributed across four continents, and no antivirus therapy or vaccines are available. Therefore, several strategies have been developed to target the main mosquito vector, *Aedes aegypti*, to reduce the burden of different arboviruses. Among such strategies, the use of the maternally-inherited endosymbiont *Wolbachia pipientis* has been applied successfully to reduce virus susceptibility and decrease transmission. However, the mechanisms by which *Wolbachia* orchestrate resistance to ZIKV infection remain to be elucidated. In this study, we apply isobaric labeling quantitative mass spectrometry (MS)-based proteomics to quantify proteins and identify pathways altered during ZIKV infection; *Wolbachia* infection; co-infection with *Wolbachia*/ZIKV in the *A. aegypti* heads and salivary glands. We show that *Wolbachia* regulates proteins involved in reactive oxygen species production, regulates humoral immune response, and antioxidant production. The reduction of ZIKV polyprotein in the presence of *Wolbachia* in mosquitoes was determined by MS and corroborates the idea that *Wolbachia* helps to block ZIKV infections in *A. aegypti.* The present study offers a rich resource of data that may help to elucidate mechanisms by which *Wolbachia* orchestrate resistance to ZIKV infection in *A. aegypti,* and represents a step further on the development of new targeted methods to detect and quantify ZIKV and *Wolbachia* directly in complex tissues.

Keywords: proteome, quantitative, *Aedes aegypti*, *Wolbachia*, Zika virus, immune response

OPEN ACCESS

Edited by:
Jose Luis Ramirez, United States Department of Agriculture (USDA), United States

Reviewed by:
Valérie Choumet, Institut Pasteur, France
José Henrique M. Oliveira, Federal University of Santa Catarina, Brazil

***Correspondence:**
Magno Junqueira
magnojunqueira@iq.ufrj.br
Rafael Maciel-de-Freitas
freitas@ioc.fiocruz.br

[†] These authors have contributed equally to this work

Specialty section:
This article was submitted to Invertebrate Physiology, a section of the journal Frontiers in Physiology

Received: *15 December 2020*
Accepted: *04 February 2021*
Published: *25 February 2021*

Citation:
Martins M, Ramos LFC, Murillo JR, Torres A, de Carvalho SS, Domont GB, de Oliveira DMP, Mesquita RD, Nogueira FCS, Maciel-de-Freitas R and Junqueira M (2021) Comprehensive Quantitative Proteome Analysis of Aedes aegypti Identifies Proteins and Pathways Involved in Wolbachia pipientis and Zika Virus Interference Phenomenon. Front. Physiol. 12:642237. doi: 10.3389/fphys.2021.642237

HIGHLIGHTS

- The abundance of ZIKV polyprotein is reduced in the presence of *Wolbachia*.
- Shotgun proteomics quantifies ZIKV and *Wolbachia* proteins directly in tissues.
- *Wolbachia* regulates proteins involved in ROS production.
- *Wolbachia* regulates humoral immune response and antioxidant production.
- Metabolism and detoxification processes were associated with mono infections.

INTRODUCTION

Zika virus (ZIKV) is a single-stranded RNA virus that belongs to the *Flavivirus* genus and Flaviviridae family. Originally discovered in a primate from the Zika forest in Uganda in 1947, remained unimportant for public health until the beginning of the 20th century (Dick et al., 1952). In 2014, ZIKV emerged in the Pacific islands and a few years later invaded the Americas, leading the World Health Organization to claim a global public health emergency due to its association with microcephaly in newborns and Guillain-Barré syndrome, neuropathy, and myelitis in children and adults (Campos et al., 2015; Barreto et al., 2016). As of May 2017, around 75% of inhabitants of the Yap Islands were infected with ZIKV, but no microcephaly was recorded. Whilst in Brazil more than 220,000 cases were recorded and more than 2,600 newborns had birth defects like microcephaly and other neuropathies (Baud et al., 2017).

The mosquito *Aedes aegypti* is the primary vector of ZIKV worldwide (Chouin-Carneiro et al., 2016; Ferreira-de-Brito et al., 2016). To date, no antivirus therapy or vaccines are available to mitigate ZIKV transmission, which increases the urgency for effective methods targeting the mosquito vector to reduce the burden of arboviruses as ZIKV. Among such strategies, the use of the maternally inherited endosymbiont *Wolbachia pipientis* has gained attention recently. The bacterium *Wolbachia* is naturally found in around 60% of arthropod species. Although *Wolbachia* does not naturally infect *A. aegypti*, some strains were transinfected by microinjection into this mosquito species with the further discovery of their pathogen-blocking properties (Moreira et al., 2009; Aliota et al., 2016; Dutra et al., 2016). The rationale underlying a mass release of *Wolbachia* infected mosquitoes is to replace the local *A. aegypti* population. Usually, it has high vector competence to arboviruses, like ZIKV, while the *Wolbachia* transinfected mosquitoes have reduced susceptibility and decreased transmission (Hoffmann et al., 2011). This approach is currently ongoing in at least 12 countries and the first communications showing its impact on disease transmission decrease are being revealed (Nazni et al., 2019; Indriani et al., 2020; Ryan et al., 2020).

The mechanisms which are orchestrated by *Wolbachia*, conferring resistance to arboviruses infection remain to be elucidated, however, it has been assigned to the activation of the mosquito immune system, down-regulation of genes that encode proteins or receptors necessary to the virus binding and depletion of host's resources essentials to the virus life cycle (Ford et al., 2020). When infected with *Wolbachia*, the mosquito Toll pathway is activated through the increase of reactive oxygen species (ROS), resulting in the production of antimicrobial peptides like cecropin (Pan et al., 2012). The gene expression modulation of tubulin, insulin receptors, and other genes seems to hinder the virus infection (Haqshenas et al., 2019; Paingankar et al., 2020). Also, it has been proposed that the lipids are relevant to *Wolbachia* infection. While one study implies it competes with the host's lipid resources (mainly cholesterol), others suggest it modulates the lipid production which can have a role blocking virus replication (Geoghegan et al., 2017; Koh et al., 2020; Manokaran et al., 2020).

Protein quantification on a genome-wide scale allows a systemic bird's-eye view of protein variation and pathway regulation under different conditions and samples (Choudhary and Mann, 2010). Therefore, it helps to highlight some features and emergent properties of complex systems, which could be obscured when the analysis is performed only from a reductionist point of view. In this way, mass spectrometry (MS)-based proteomics, together with robust bioinformatic tools, allows the formulation of more ambitious hypotheses due to the possibility of generating large and detailed datasets. Reliable large-scale protein quantification can be achieved using isobaric labeling and shotgun proteomics (Pappireddi et al., 2019). Several quantitative methods have already been successfully applied in insects to access differentially regulated proteins (De Mandal et al., 2020; García-Robles et al., 2020; Serteyn et al., 2020). The *A. aegypti* infection with Mayaro virus or microsporidian parasites have already been studied (Duncan et al., 2012; Vasconcellos et al., 2020) and a previous descriptive work was based on comparing the proteome of *A. aegypti* female heads during blood and sugar meals conditions (Nunes et al., 2016).

Here, we use an isobaric labeling-based quantitative proteomic strategy to interrogate the interaction between the *Wolbachia w*Mel strain and ZIKV infection in *A. aegypti* heads and salivary glands. *Wolbachia* is present in several tissues and organs in *A. aegypti* mosquitoes, with higher density in ovaries and tissues on the head and anterior part of the thorax, like the ommatidia cells, brain, salivary glands, and cardia (Moreira et al., 2009). To the best of our knowledge, this is the most complete proteome of *A. aegypti* reported so far, with a total of 3,790 proteins identified, corresponding to 25.75% of total protein-coding genes. This work includes the identification and quantification of several peptides from the ZIKV and 323 *Wolbachia* proteins in a complex sample tissue, paving the way to the development of sensitive approaches to detect and quantify the ZIKV and *Wolbachia* directly in the *A. aegypti* tissue via MS. Moreover, we describe and discuss proteins and pathways altered in *A. aegypti* during ZIKV infections, *Wolbachia* infections, co-infection *Wolbachia*/ZIKV, and compared with no infection.

MATERIALS AND METHODS

Mosquitoes

To access the effects of ZIKV and *Wolbachia* infection on *A. aegypti* proteome, we used mosquitoes from two different sites in Rio de Janeiro (Rio de Janeiro State, Brazil): Tubiacanga (22°47′06″S; 43°13′32″W) and Porto (22°53′43″S, 43°11′03″W), distant 13 km apart from each other. Tubiacanga was selected to represent an area in which mosquitoes have *Wolbachia* (*w*Mel strain) since it is the first site in Latin America with an established invasion (>90% frequency) (Garcia et al., 2019). Porto represents a *Wolbachia* free area. Eggs were collected through 80 ovitraps (Codeço et al., 2015) installed every 25–50 m each other in both sites. Ovitraps were placed over an extensive geographic area to ensure we captured the local *A. aegypti* genetic variability, collecting at least 500 eggs per site. The eggs were hatched and the mosquitoes were maintained at the insectary under a relative humidity of 80 ± 5% and a temperature of 25 ± 3°C, with *ad libitum* access to a 10% sucrose solution. The experimental infection was performed with mosquitoes from the F1 generation.

Viral Strain

Aedes aegypti females were orally infected with the ZIKV strain Asian genotype isolated from a patient in Rio de Janeiro (GenBank accession number KU926309). Previous reports have shown high infectivity of this ZIKV isolate to Rio de Janeiro *A. aegypti* populations, including Porto, which had 100% infected females after receive an infective blood meal (Fernandes et al., 2016; da Silveira et al., 2018; Petersen et al., 2018). Viral titers in supernatants were previously determined by serial dilutions in Vero cells, expressed in plaque-forming units per milliliters (PFU/ml). All the assays were performed with samples containing 3.55×10^6 PFU/ml. Viral stocks were maintained at −80°C until its use.

ZIKV Infection

Sugar supply was removed 36-h before mosquitoes were challenged with the infective blood meal to increase female's avidity. Six–seven days old inseminated *A. aegypti* females from each of the two populations (Tubiacanga and Porto) were separated in cylindrical plastic cages for blood-feeding. Oral infection procedures were performed through a membrane feeding system (Hemotek, Great Harwood, United Kingdom), adapted with a pig-gut covering, which gives access to human blood. The infective blood meals consisted of 1 ml of the supernatant of infected Vero cell culture, 2 ml of washed rabbit erythrocytes, and 0.5 mM of adenosine triphosphate (ATP) as phagostimulant. The same procedure and membrane feeding apparatus were used to feed control mosquitoes, i.e., control insects received a noninfectious blood meal, with 1 ml of Vero cell culture medium replacing the viral supernatant (therefore, with no ZIKV), 2 ml of washed rabbit erythrocytes, and 0.5 mM of ATP as phagostimulant. After the experimental infection, we had a total of 152 *A. aegypti* females.

Ethical Approval

The maintenance of *A. aegypti* colonies with *Wolbachia* in the lab were achieved by offering blood obtained from anonymous donors from the blood bank of the Rio de Janeiro State University, whose blood bags would be discarded due to small volume. We have no information on donors, including sex, age, and clinical condition, but the blood bank discards those bags positive for Hepatitis B, Hepatitis C, Chagas disease, syphilis, human immunodeficiency virus, and human T-cell lymphotropic virus. Before offering the blood for mosquitoes, it was screened for Dengue virus (DENV) using the Dengue NS1 Ag STRIP (Bio-Rad). The use of human blood was approved by the Fiocruz Ethical Committee (CAAE 53419815.9.0000.5248).

Protein Extraction for Proteomics

Proteins from a total of 152 *A. aegypti* females were processed, of which 39 were coinfected with *Wolbachia* and ZIKV (WZ); 36 non-infected (A); 35 infected with *Wolbachia* (W) only and 42 infected with ZIKV (Z). On 14 days post-infection, each mosquito head plus the salivary gland was separated from the body using needles and a scalpel blade which were sterilized after every single use (Schmid et al., 2017). Proteins were extracted by lysis with a buffer containing 7 M urea, 2 M thiourea, 50 mM HEPES pH 8, 75 mM NaCl, 1 mM EDTA, 1 mM PMSF, and protease/phosphatase inhibitor cocktails (Roche). Then, samples were vortexed, sonicated in a cold bath for 10 min and sonicated by the probe for 10 min. Lysates were centrifuged at 10,000 *g* for 10 min at 4°C and the supernatants were carefully transferred to new tubes for further steps.

Protein Digestion and iTRAQ Labeling

The protein concentration was determined by the Qubit Protein Assay Kit® fluorometric (Invitrogen), following the manufacturer's instructions. A total of 100 μg of proteins from each condition was processed. Protein samples were incubated with dithiothreitol (DTT; GE Healthcare) at 10 mM and 30°C for 1 h. Subsequently, iodoacetamide solution (GE Healthcare) was added, with a final concentration of 40 mM. The reaction was performed at room temperature, in the dark, for 30 min. The samples were diluted 10× with 50 mM HEPES buffer to reduce the concentration of urea/thiourea. The solution was incubated with trypsin (Promega) in a 1:50 (w/w, enzyme/protein) ratio at 37°C for 18 h. The resulting peptides were desalted with a C-18 macro spin column (Harvard Apparatus) and then vacuum dried. The dried peptides were labeled with isobaric tags for relative and absolute quantitation (iTRAQ) 4-plex (ABSciex). The labeling process was performed according to Murillo et al. (2017). Briefly, dried peptides were dissolved in 50 mM TEAB and iTRAQ tags were dissolved in dry ethanol, labeling was performed by mixing peptide and tag solutions for 1 h at room temperature. The four tag reactions were combined in a single tube (ratio 1:1:1:1) and dried in a speed vac prior to fractionation. Each condition was labeled as follows: (i) Tag 114 corresponds to sample W (*Wolbachia* infected); (ii) Tag 115 to sample A (none infection); (iii) Tag 116 to sample WZ (*Wolbachia* and ZIKV co-infection); and (iv) Tag 117 to sample Z (ZIKV infection).

Fractionation by Hydrophilic Interaction Chromatography and LC-MS/MS Analysis

The iTRAQ labeled peptide mixture was fractionated off-line by HILIC (hydrophilic interaction liquid chromatography) before LC-MS/MS analysis. The dried samples were resuspended in acetonitrile (ACN) 90% / trifluoroacetic acid (TFA) 0.1% and injected into Shimadzu UFLC chromatography using a TSKGel Amide-80 column (15 cm × 2 mm i.d. × 3 μm – Supelco), flow rate 0.2 ml/min; mobile phases A (ACN 85%/TFA 0.1%) and B (TFA 0.1%); gradient: 0% of phase B in 5 min; 0–10% of phase B from 5 to 10 min; 10–20% of phase B from 10 to 55 min; 20–100% of phase B from 55 to 60 min; and 100–0% of phase B from 60 to 65 min. For each pooled sample, eight fractions were collected and combined according to the separation and intensity of the peaks. The pools of fractions were dried in a speed vac and resuspend in 0.1% formic acid (FA). The samples were analyzed in Easy-nLC 1000 coupled to a Q-Exactive Plus mass spectrometer (Thermo Fisher Scientific). For each fraction (or pool of fractions), a linear gradient of 5–40% of B em 105 min, 40–95% in 8 min and 95% B in 5 min was performed in 120 min; phase A (0.1% FA), B (ACN 95%, 0.1% FA). Ionization was performed in an electrospray source with the acquisition of spectra in positive polarity by data-dependent acquisition (DDA) mode, spray voltage of 2.5 kV, and temperature of 200°C in the heated capillary. The acquisition was set as follows: full scan or MS1 in the range of 375–1,800 m/z, resolution of 70,000 (m/z 200), fragmentation of the 10 most intense ions in the HCD collision cell, with standardized collision energy (NCE) of 30, resolution of 17,000 in the acquisition of MS/MS spectra, the first mass of 110 m/z, isolation window of 2.0 m/z and dynamic exclusion of 45 s.

Data Analysis

The raw data were processed using Proteome Discoverer 2.4 Software (Thermo Fisher Scientific). Peptide identification was performed with the Sequest HT search engine against *A. aegypti* (genome version/assembly ID: INSDC: GCA_002204515.1), ZIKV, and *Wolbachia* databases provided by VectorBase (Giraldo-Calderón et al., 2015), ViPR (Pickett et al., 2012), and UniProt (The Uniprot Consortium, 2019), respectively. Searches were performed with peptide mass tolerance of 10 ppm, MS/MS tolerance of 0.1 Da, tryptic cleavage specificity, two maximum missed cleavage sites allowed, fixed modification of carbamidomethyl (Cys), variable modification of iTRAQ 4-plex (Tyr, Lys, and peptide N-terminus), phosphate (Ser, Thr, and Tyr), and oxidation (Met); peptides with high confidence were considered. False discovery rates (FDR) were obtained using Target Decoy PSM selecting identifications with a q-value equal or to less than 0.01. Data of all technical replicates were log2-transformed and normalized by subtracting the column median. Relative iTRAQ quantification analysis was carried out in the Perseus software, version 1.6.12.0 (Tyanova et al., 2016), based on the intensity of the fragmented reporter peaks in MS/MS.

Statistics and Gene Enrichment

For ZIKV peptides abundance comparison, statistical analysis was performed in experimental groups using T-test analysis (95% confidence values, $p < 0.05$), meanwhile for differential proteins was used one-way analysis of variance (ANOVA) and Tukey's multiple comparisons post-test (95% confidence values, $p < 0.05$) in Graphpad Prism 8.0.0 for Windows, GraphPad Software, San Diego, CA, United States, www.graphpad.com. Biological processes enrichment for differentially expressed proteins were performed using Fisher's Exact Test ($p < 0.05$) in VectorBase website (bit.ly/38OmEX0) (Ashburner et al., 2000; Giraldo-Calderón et al., 2015). The resulting Gene Ontology (GO) lists were summarized and represented in a network interaction format in REVIGO (Supek et al., 2011).

RESULTS AND DISCUSSION

Proteome Analysis

Proteomics has improved in recent years, especially considering its coverage and sensitivity, which offer more opportunities to study changes in the global proteome of complex tissues (Aebersold and Mann, 2016). Therefore, the use of isobaric-labeled quantitative proteomics measurements provides efficiency and increased depth coverage of proteomics analysis (Rauniyar and Yates, 2014). Peptides from the four experimental groups were labeled with iTRAQ 4-plex, enabling multiplexing of samples prior to off-line fractionation and LC-MS/MS analysis (**Figure 1**). We were able to identify 4,117 protein groups (**Table 1**), 26,898 peptides and 909,046 MS/MS spectra. The protein search was performed using *A. aegypti*, ZIKV, and *Wolbachia* databases simultaneously. Of all identified proteins, 3,790 belong to *A. aegypti*, 323 to *Wolbachia* and three unique peptides with a total of 10 PSMs to the ZIKV polyprotein (**Figure 2** and **Supplementary Figures 1**, **2**).

Quantitative Proteomics

The quantitative proteomics analysis was performed by comparing the four experimental groups using the normalized iTRAQ reporter ion intensity of identified peptides. Replicates were highly correlated (Pearson correlation mean of 0.97) and normalization methods were applied (**Supplementary Figure 3**). The 196 proteins with significant differences were statistically determined by the ANOVA test. Using the Tukey post-test ANOVA, we defined pairs of proteins with significant differences between the groups (**Supplementary Table 2**). The comparisons between the samples were: single-infected mosquitoes versus non-infected mosquitoes (W versus A and Z versus A); coinfected versus non-infected mosquitoes (WZ versus A); coinfected versus single-infected mosquitoes (WZ versus W and WZ versus Z).

Abundance of ZIKV Polyprotein Is Reduced in the Presence of *Wolbachia*

The quantitative analysis using the iTRAQ reporter ions from ZIKV peptides revealed that ZIKV proteins were more abundant in the absence of *Wolbachia* in contrast to mosquitoes coinfected

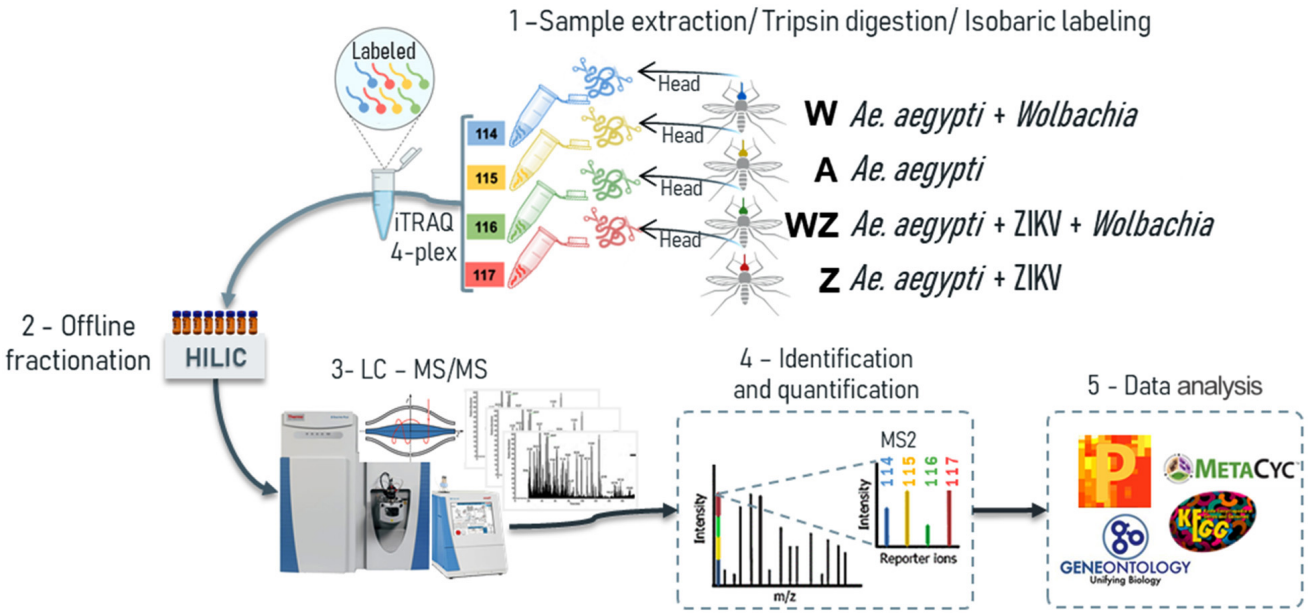

FIGURE 1 | The proteomics workflow carried out in the head + salivary gland of *A. aegypti* females used samples from four different conditions: A, non-infected mosquitoes; W, *Wolbachia* infected; Z, ZIKV infected; and WZ, *Wolbachia* and ZIKV infection. **1** – The samples were subjected to lysis and, subsequently, proteins were reduced, alkylated, and digested using trypsin. The resulting peptides were labeled with iTRAQ-4plex and combined in 1:1:1:1 ratio; **2** – labeled peptides were fractionated offline using HILIC chromatography; **3** – pool of fractions were analyzed by nLC–MS/MS in Q-Exactive Plus mass spectrometer; **4** – fragmentation of the attached tag release a low *m/z* reporter ions used for relative quantification of the peptides/proteins from which they originated; **5** – statistical analysis were performed in Perseus and bioinformatics analysis used Gene Ontology (GO) in the enrichment of proteins differentially regulated.

with ZIKV and *Wolbachia* (**Figure 2**). This latter condition showed reporter ions intensity compared to the background signal of uninfected mosquitoes (**Figure 2A**). This result indicates *Wolbachia* presence likely reduces virus replication in the female head and salivary gland (**Figure 2B**). Noteworthy, the presence of the *w*Mel strain in organs like salivary glands and ovaries of *A. aegypti* females induce the antiviral response that supports *Wolbachia* deployment to mitigate disease transmission.

The detection of ZIKV in the mosquito head + salivary gland was possible even considering that virus proteins were a minute fraction of all proteins identified. Peptides LITANPVITESTENS, SHTLWTDGIEESDLIIP, and LNQMSALEFYSYKK showed a robust increase in ZIKV infected tissue and this data represents a resource to further develop targeted proteomics methods to quantify ZIKV in infected mosquitoes (MS/MS spectra shown in **Supplementary Figure 1**).

Identification of Salivary Gland Proteins, Neuropeptides, and Hormones in Head Samples

During a blood meal, the female mosquitoes inject saliva into the host skin. The salivary glands produce a huge amount of molecules to avoid host responses against blood loss and to evade the host immune system (Ribeiro et al., 2016). For transmission of arboviroses, the virus must be secreted with the saliva during a blood meal in a vertebrate host (Linthicum et al., 1996). In this work, we took advantage of the sensitivity of protein detection by MS to detect and quantify proteins from the salivary gland, which are located on the anterior part of the thorax of *A. aegypti*. We compared the head proteome with two proteomes and one transcriptome (Wasinpiyamongkol et al., 2010; Ribeiro et al., 2016; Dhawan et al., 2017) from salivary glands of female mosquitoes to identify the salivary gland related proteins (**Figure 3**). We observed that among the 3,790 proteins identified in *A. aegypti* heads, 830 proteins were previously known to be expressed in the salivary glands. Moreover, we identified 77% of the proteins described by Wasinpiyamongkol et al. (2010) and 65% by Dhawan et al. (2017) in previous salivary gland proteome analysis. The 16 salivary proteins that were detected in all datasets probably are the most expressed and include inhibitors of platelet aggregation (salivary apyrase, AAEL006333-PA; apyrase precursor, AAEL006347PA), clotting inhibitors (SRPN23, AAEL002704-PB; SRPN26, AAEL003182-PA), aegyptins (AAEL010228-PA and AAEL010235-PA), angiopoietins (AAEL000749-PA and AAEL000726-PA), D7 family proteins (AAEL006417-PA and AAEL006424-PA), among others. We compared the 830 proteins previously known to be expressed in the salivary glands with the 196 differentially expressed proteins, to understand if these proteins could play a role during ZIKV and *Wolbachia* infections and/or co-infections. The modulation of saliva proteins is discussed below where the systemic changes in W, Z, and WZ will be addressed.

As a class of neuronal signal molecules, neuropeptides are produced by the neurosecretory cells, that are mainly located in the brain, suboesophageal ganglion, among others (Li et al., 2020). In insects, neuropeptides and their

TABLE 1 | Proteins with significative diferencial expression by ANOVA test ($p < 0.05$) and each respective pair analyzed by Tukey test.

Significant pairs (up-regulated_down-regulated)	Protein	(−Log ANOVA *P*-value)
A_Z;WZ_Z;A_W;WZ_W	AAEL026217-PA	4,271777813
WZ_Z;WZ_W;WZ_A	AAEL005656-PB myosin heavy chain, non-muscle or smooth muscle	2,514001451
WZ_W;WZ_A	AAEL009955-PB	2,195629072
A_W	AAEL001928-PA Act1: Actin-1	1,800850488
Z_WZ;W_WZ;A_WZ;W_Z;A_Z;A_W	AAEL012062-PX Na+/K+ ATPase alpha subunit	7,11879894
WZ_Z;A_Z	AAEL002565-PD titin	1,806231463
A_W	AAEL010975-PB paramyosin, long form	1,314499523
Z_W;A_W;WZ_W;WZ_Z;WZ_A	AAEL012897-PA aconitase, mitochondrial	4,240561485
WZ_A	AAEL009847-PB microtubule-associated protein	1,77714195
WZ_W	AAEL002851-PA tubulin beta chain	1,552090751
WZ_W	AAEL005422-PA pyrroline-5-carboxylate dehydrogenase	2,184255666
Z_W;WZ_W;Z_A;WZ_A	AAEL006138-PA	4,517435874
WZ_W;WZ_Z	AAEL002759-PD tropomyosin invertebrate	2,121497626
Z_W	AAEL011504-PA pupal cuticle protein, putative	1,607203142
WZ_W;A_W;WZ_Z;A_Z;A_WZ	AAEL006582-PH calcium-transporting ATPase sarcoplasmic/endoplasmic reticulum type	4,911628212
Z_W;A_W	AAEL002761-PAM tropomyosin invertebrate	1,677982154
A_W;WZ_W;Z_W;WZ_A;Z_A	AAEL006126-PA	4,511369267
WZ_Z;W_Z	AAEL001194-PA FAS1: fatty acid synthase	1,811428505
WZ_Z;A_Z;A_W	AAEL004297-PI ATP-citrate synthase	2,526180238
WZ_Z;WZ_W	AAEL012552-PA NADH-ubiquinone oxidoreductase	1,66727909
Z_W;WZ_W;Z_A;WZ_A	AAEL004988-PA Pgk: phosphoglycerate kinase	3,077106946
WZ_Z	AAEL006834-PA glutamate semialdehyde dehydrogenase	1,316789414
A_W	AAEL005798-PA ATP synthase subunit beta vacuolar	1,549407725
WZ_Z;WZ_A	AAEL013535-PA phosrestin ii (arrestin a) (arrestin 1)	2,17733154
Z_A;Z_W	AAEL015314-PM cAMP-dependent protein kinase type ii regulatory subunit	2,098280165
WZ_Z;A_Z;WZ_W;A_W	AAEL024235-PG	2,840685255
A_W	AAEL004423-PA mitochondrial F0 ATP synthase D chain, putative	1,402250531
A_Z;A_W	AAEL024583-PB	2,16614374
WZ_W;WZ_Z	AAEL017301-PA elongation factor 1-alpha	1,855121353
Z_W;WZ_W;A_W;WZ_Z;A_Z	AAEL012326-PA calmodulin	6,629410461
WZ_A;WZ_W;WZ_Z	AAEL010823-PA ATP synthase delta chain	2,406253156
WZ_Z;WZ_W;WZ_A	AAEL008542-PF kinesin heavy chain subunit	2,621489163
WZ_W;WZ_A	AAEL017096-PA elongation factor 1-alpha	1,635565462
WZ_W;WZ_A	AAEL017293-PA	2,296841727
Z_A;Z_W	AAEL008773-PA laminin A chain, putative	1,916965629
WZ_A;WZ_W	AAEL015458-PA Tf1: transferrin	2,50568231
WZ_Z;A_Z;A_W	AAEL000596-PB myosin	2,481800641
WZ_A;Z_A;Z_W;Z_WZ	AAEL013279-PB peptidyl-prolyl cis-trans isomerase (cyclophilin)	4,651840282
Z_W;WZ_W;WZ_A	AAEL011981-PA glutamate decarboxylase	3,261398284
Z_W;A_W;A_WZ	AAEL013952-PD prohibitin	2,15301324
WZ_W	AAEL010143-PA isocitrate dehydrogenase	1,974182672
WZ_W	AAEL005997-PA allergen, putative	1,313495456
WZ_W	AAEL012207-PF myosin light chain 1	1,319537308
WZ_A	AAEL001677-PA	1,609275972
WZ_W;WZ_Z	AAEL008844-PA calcium-binding protein, putative	2,040394666
W_A;WZ_A	AAEL004088-PH aldo-keto reductase	2,504453412
WZ_W;Z_W;A_W	AAEL011758-PA peptidyl-prolyl cis-trans isomerase f, ppif	2,772874519
W_A;WZ_A;W_Z;WZ_Z;WZ_W	AAEL014600-PA 4-hydroxyphenylpyruvate dioxygenase	5,467053042
Z_W;WZ_W	AAEL001082-PA	1,829540732
W_Z;W_WZ	AAEL004559-PJ synaptosomal associated protein	1,686140462
W_A;WZ_A	AAEL012827-PA endoplasmin	1,859306212
WZ_A;WZ_Z	AAEL001683-PA	2,403005778

(Continued)

TABLE 1 | Continued

Significant pairs (up-regulated_down-regulated)	Protein	(−Log ANOVA *P*-value)
WZ_W	AAEL001473-PC dynamin-associated protein	1,404560111
WZ_W;Z_W	AAEL007383-PE secreted ferritin G subunit precursor, putative	1,89879228
Z_W;A_W;WZ_W;WZ_Z;WZ_A	AAEL005407-PD annexin x	3,750898348
WZ_W;A_W;Z_W;A_WZ;Z_WZ;Z_A	AAEL008789-PA apolipophorin-III, putative	6,190366803
A_W	AAEL006946-PA chaperonin	1,282782467
WZ_A;Z_A;Z_W	AAEL011090-PA complement component	2,669480529
Z_A;WZ_A;WZ_W	AAEL009389-PA transaldolase	1,98264351
WZ_W;Z_W	AAEL023497-PA protein-L-isoaspartate O-methyltransferase	2,775892202
A_W;Z_W;WZ_W	AAEL004745-PA pupal cuticle protein, putative	2,586973455
Z_W;A_W;WZ_W;WZ_Z;WZ_A	AAEL019951-PG	4,789914023
WZ_A	AAEL000934-PI clathrin light chain	1,919802572
A_Z	AAEL004041-PD flotillin-2	1,321402995
Z_W;Z_WZ	AAEL013338-PA lethal(2)essential for life protein, l2efl	1,487090987
Z_A;WZ_A	AAEL010840-PB	2,229411597
Z_A;W_A;WZ_A;WZ_Z	AAEL001851-PB	4,012423993
WZ_A	AAEL004176-PB microtubule binding protein, putative	2,027657273
WZ_A	AAEL001794-PB macroglobulin/complement	1,757699803
A_W;Z_W;WZ_W	AAEL019778-PA	2,545595403
Z_WZ;Z_W	AAEL022352-PA	1,719161308
WZ_W	AAEL001946-PA four and a half lim domains	1,870893776
W_A;WZ_A;WZ_Z	AAEL017263-PA	2,835314331
WZ_W;Z_W	AAEL006271-PD CUSOD2: copper-zinc (Cu-Zn) superoxide dismutase	1,612285952
WZ_W	AAEL002185-PA cuticle protein, putative	2,210230165
Z_W;A_W;WZ_W	AAEL005946-PA NADH-ubiquinone oxidoreductase subunit B14.5b	3,524279291
A_Z	AAEL006948-PB tomosyn	1,630732328
WZ_W;A_W	AAEL006027-PB lipase	2,512978955
Z_WZ;W_WZ;Z_A;W_A	AAEL012206-PB microtubule-associated protein tau	3,461529529
W_A;WZ_A;Z_A	AAEL000762-PB LRIM19: leucine-rich immune protein (Coil-less)	2,533734366
Z_A;Z_W	AAEL013138-PA	2,190112627
WZ_Z;WZ_A	AAEL003888-PD ubiquitin	1,499108348
Z_WZ	AAEL014416-PC pupal cuticle protein 78E, putative	1,95874832
Z_A	AAEL025999-PA 40S ribosomal protein S17	1,533198334
WZ_W	AAEL009257-PA	1,735940859
W_A;Z_A;WZ_A;WZ_W;WZ_Z	AAEL017212-PA	4,19347108
WZ_A;WZ_Z;WZ_W	AAEL015424-PA adult cuticle protein, putative	2,324346555
A_W;WZ_W;A_Z;WZ_Z	AAEL009604-PG receptor expression-enhancing protein	2,983369006
A_WZ;W_WZ;Z_WZ;Z_A	AAEL018211-PB	4,186777407
WZ_W	AAEL010168-PA RpS2: 40S ribosomal protein S2	1,566481125
WZ_A	AAEL012865-PA	1,317062128
WZ_A	AAEL004148-PA heat shock protein 70 (hsp70)-interacting protein	1,394760066
W_WZ;Z_WZ	AAEL019767-PA	2,164853975
Z_W;A_W	AAEL019793-PB	1,761699228
Z_A	AAEL011982-PC cortactin	1,798033943
A_W	AAEL001864-PA eukaryotic translation initiation factor 4E binding protein (4EBP)	1,306963121
A_W	AAEL019718-PA	1,510324956
Z_A;Z_WZ	AAEL000028-PA CLIPB34: clip-domain serine protease family B.	1,708280762
W_WZ;A_WZ	AAEL007010-PA CYP6AG4: cytochrome P450	1,700443182
W_A	AAEL013808-PF fascin	1,388013685
WZ_A;WZ_Z	AAEL006406-PG Putative 14.5 kDa secreted protein	1,957996691
A_Z;A_W	AAEL009398-PA Pep12p, putative	1,979171968
A_W;A_Z	AAEL018664-PA COX2: cytochrome c oxidase subunit II	2,547584077
W_WZ;A_WZ	AAEL000090-PB secretory carrier-associated membrane protein (scamp)	2,674457264

(Continued)

TABLE 1 | Continued

Significant pairs (up-regulated_down-regulated)	Protein	(−Log ANOVA *P*-value)
W_WZ;W_Z	AAEL006719-PA AMY1: alpha-amylase I precursor (EC 3.2.1.1) (1,4-alpha-D-glucan glucanohydrolase)	1,919418688
WZ_W	AAEL006677-PA phospholipase a-2-activating protein	1,334478579
WZ_A;WZ_Z;WZ_W	AAEL003954-PA juvenile hormone-inducible protein, putative	2,79570589
WZ_A;Z_A;W_A	AAEL001402-PA LRIM10B: leucine-rich immune protein (Short)	2,43294121
WZ_A	AAEL003431-PA proteasome subunit beta type 7,10	1,308314374
W_WZ;Z_WZ;A_WZ;A_W;A_Z	AAEL005793-PA AMP dependent ligase	5,868868376
A_WZ;W_WZ;Z_WZ;Z_A;Z_W	AAEL009653-PA RpS30: 40S ribosomal protein S30	6,088741815
Z_A;W_A	AAEL008422-PD	1,806945766
A_Z;A_W;A_WZ	AAEL009314-PA adenylate cyclase	1,930417494
WZ_Z;W_Z;WZ_A;W_A	AAEL002245-PA	3,537852527
Z_A	AAEL001077-PA CLIPB45: clip-domain serine protease family B. Protease homologue.	1,565423585
A_WZ	AAEL004146-PA CRY1: cryptochrome 1	1,391490707
Z_WZ;A_WZ;A_W	AAEL003104-PC tripartite motif protein trim2,3	3,162779729
A_W;Z_W;A_WZ;Z_WZ	AAEL006124-PA mitochondrial import inner membrane translocase subunit TIM50	2,7915452
Z_W	AAEL006464-PA	1,348559818
Z_W;Z_WZ;Z_A	AAEL009642-PA cathepsin b	2,135923633
Z_WZ;Z_A	AAEL013119-PA charged multivesicular body protein	2,331529326
WZ_W;WZ_Z;WZ_A	AAEL014372-PA juvenile hormone-inducible protein, putative	2,942325794
Z_WZ;A_WZ;Z_W;A_W	AAEL008764-PA cuticle protein, putative	3,385118481
Z_A;WZ_A;W_A	AAEL010139-PA serine protease, putative	2,963764022
W_Z;W_WZ;W_A	AAEL014961-PA gdp mannose-4,6-dehydratase	2,125006815
A_W;A_Z;A_WZ	AAEL009863-PD sodium/dicarboxylate cotransporter, putative	3,502744434
Z_WZ;A_WZ;W_WZ	AAEL000556-PA CTL25: C-Type Lectin (CTL25)	2,692047592
W_A	AAEL010491-PB FKBP12: fk506-binding protein	1,445125001
Z_WZ;A_WZ;A_W;A_Z	AAEL003188-PA sphingosine phosphate lyase	3,331676114
W_A;W_WZ;W_Z	AAEL027103-PA	1,821833076
A_Z;A_WZ	AAEL006002-PA	2,106633723
W_WZ	AAEL005469-PB	2,324487859
WZ_W;A_W	AAEL006971-PA	1,967613183
A_WZ	AAEL020992-PE	1,369902298
W_Z;W_WZ	AAEL009974-PA ras-related protein Rab-8A, putative	1,757153294
W_A;WZ_A	AAEL009212-PG lola	1,512195091
WZ_W;Z_W	AAEL011070-PA CTLGA3: C-Type Lectin (CTL) – galactose binding.	2,201901256
A_W	AAEL018353-PB	1,570541993
Z_W;WZ_W;Z_A;WZ_A	AAEL008250-PC	2,137421729
W_WZ;W_A	AAEL008490-PC NADH dehydrogenase, putative	2,234786037
WZ_W;A_W;WZ_Z;A_Z;A_WZ	AAEL026670-PA	5,34600802
W_A	AAEL002135-PA tubulin-specific chaperone b (tubulin folding cofactor b)	1,71317976
A_W;A_Z	AAEL002350-PA	2,070802008
WZ_W;Z_W;A_W;A_WZ	AAEL011388-PA Vacuolar-sorting protein SNF8	6,982654776
W_WZ;A_WZ	AAEL002317-PE InR: Insulin-like receptor Precursor (MIR) (EC 2.7.10.1)	2,088114025
W_A;Z_A;WZ_A;WZ_W;WZ_Z	AAEL010059-PA bacterial-type ABC transport ATP-binding subunit? or RNAse l inhibitor	3,507872757
A_W;A_Z;A_WZ	AAEL022886-PA	2,240673165
W_A	AAEL015430-PB CLIPB19: clip-domain serine protease family B. Protease homologue.	2,153234226
Z_WZ	AAEL011433-PA small nuclear ribonucleoprotein sm d3	1,310683895
Z_W;WZ_W;A_W	AAEL019654-PB	2,186666781
Z_W;A_W;Z_WZ;A_WZ	AAEL015180-PB smooth muscle caldesmon, putative	2,511924586
A_WZ	AAEL003059-PB	1,594979945
W_Z	AAEL010408-PD GPRGBB2: GPCR GABA B Family	1,416228099

(Continued)

TABLE 1 | Continued

Significant pairs (up-regulated_down-regulated)	Protein	(−Log ANOVA *P*-value)
W_WZ;Z_WZ	AAEL006451-PB	1,791040044
W_WZ;Z_WZ;A_WZ;A_W	AAEL022232-PA	3,004180084
WZ_A;WZ_Z;WZ_W	AAEL014325-PA proteasome regulatory subunits	1,833896368
WZ_A	AAEL009833-PA mRpL46: mitochondrial ribosomal protein, L46, putative	1,348750399
Z_WZ;A_WZ;A_W	AAEL021103-PA	2,295144608
Z_WZ;W_WZ;A_WZ	AAEL011234-PC reticulon/nogo receptor	2,780134195
W_Z;W_A;W_WZ	AAEL010681-PA sodium/chloride dependent neurotransmitter transporter	2,743872823
Z_A;W_A;Z_WZ;W_WZ	AAEL008458-PA	3,128904889
WZ_A;Z_A;W_A;Z_WZ;W_WZ	AAEL007805-PA	3,307690677
W_A;Z_A;W_WZ;Z_WZ	AAEL002591-PA OBP13: odorant binding protein OBP13	3,101064427
WZ_W;A_W;Z_W;A_WZ;Z_WZ	AAEL019579-PA	3,390568158
W_WZ;Z_WZ	AAEL007821-PA signalosome, subunit 2, CSN8, putative	2,05489339
Z_WZ;A_WZ;W_WZ;W_Z;W_A	AAEL007420-PB SRPN25: serine protease inhibitor (serpin) homologue – unlikely to be inhibitory	3,948336385
WZ_W;A_W;WZ_Z;A_Z	AAEL019517-PA	2,852828682
WZ_Z;W_Z;WZ_A;W_A	AAEL002915-PA	1,982345339
W_Z;W_A;W_WZ	AAEL009589-PA	1,809032341
WZ_Z;WZ_A	AAEL009375-PK plekhh1	1,648776888
W_A	AAEL009951-PA dimeric dihydrodiol dehydrogenase	1,395167766
Z_WZ	AAEL014511-PE	1,422163284
Z_A;WZ_A;WZ_W;WZ_Z	AAEL029038-PA CECA: cecropin	4,563490639
Z_A;WZ_A;W_A;W_Z;W_WZ	AAEL002601-PA CLIPA1: clip-domain serine protease family A. Protease homologue.	2,487458073
Z_A;W_A;WZ_A	AAEL024070-PA putative small nuclear ribonucleoprotein snrnp smf	2,10243834
Z_WZ	AAEL000937-PA	1,954272132
A_WZ;Z_WZ;W_WZ	AAEL000330-PA	1,700894246
Z_WZ;A_WZ;W_WZ	AAEL005944-PA mRpS23: mitochondrial ribosomal protein, S23, putative	1,850199634
Z_A;W_A;W_WZ	AAEL018131-PB	2,234278377
WZ_Z;W_Z;A_Z	AAEL003991-PH alcohol dehydrogenase	2,241277965
Z_A;WZ_A;W_A	AAEL020192-PA	2,866821279
Z_WZ;Z_A;Z_W	AAEL021230-PA	2,059537005
Z_A;WZ_A;W_A;WZ_Z;W_Z	AAEL009026-PD ubiquitin-conjugating enzyme m	3,465385818
A_W	AAEL004300-PB	1,683474263
A_WZ	AAEL001950-PB	1,355021154
W_A;Z_A;Z_WZ	AAEL023091-PA	2,133515319
W_Z;W_WZ;W_A	AAEL013989-PA protein translocation complex beta subunit, putative	2,973482988
W_A	AAEL004406-PD	1,397828331
A_Z	AAEL012841-PA	1,589217982
A_W;Z_W;WZ_W;WZ_A;WZ_Z	AAEL011216-PG phosphatidylinositol-4,5-bisphosphate 4-phosphatase	3,386553816
Z_A;W_A;WZ_A	AAEL002102-PB	2,230950028
WZ_A;Z_A;W_A;Z_WZ;W_WZ;W_Z	AAEL018117-PB	3,946110261
Z_W;WZ_W;A_W	AAEL010791-PA Autophagy-specific protein, putative	3,986947222
W_Z;W_WZ;W_A	AAEL014516-PA metalloproteinase, putative	3,17627519
Z_W;A_W;A_WZ	AAEL011890-PC	2,288170865
W_Z;A_Z;W_WZ;A_WZ	AAEL008557-PA	2,838859624

receptors play important physiological processes such as development, reproduction, behavior, and feeding (Holt et al., 2002). A previous study that investigated the presence of neuropeptidomics in *A. aegypti* proteome carried out in the central nervous system (CNS) and midgut samples identified 43 neuropeptides and hormones (Predel et al., 2010). Of these, we were able to identify 13 in our head proteomics analysis (**Figure 4**): pyrokinin (PK) (AAEL012060), short

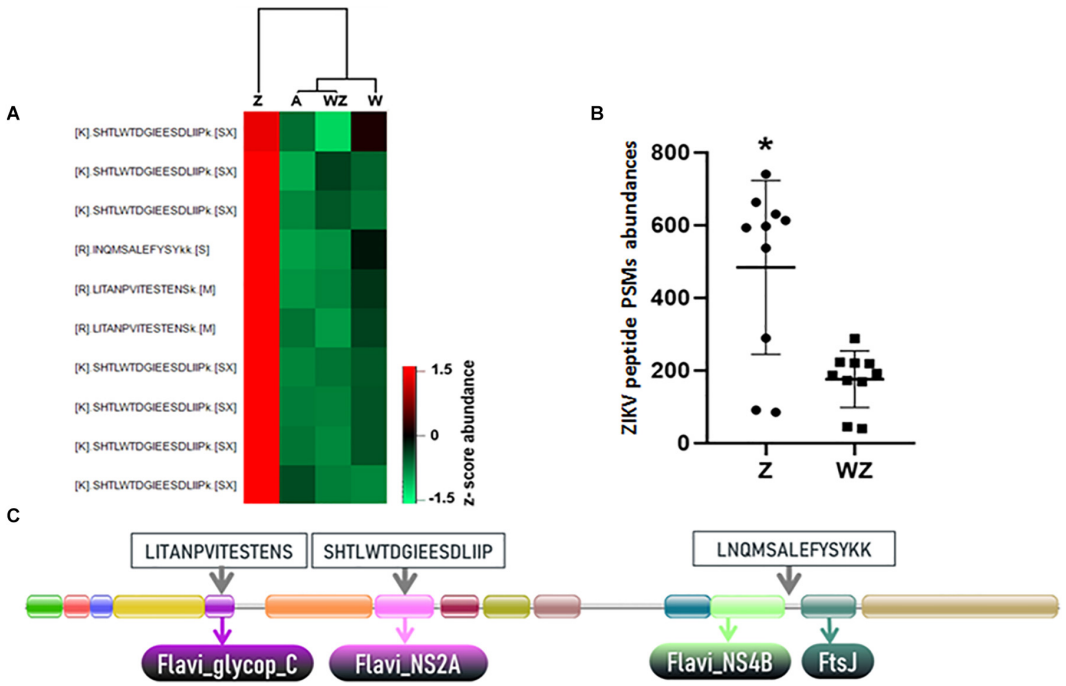

FIGURE 2 | Identification and quantification of ZIKV peptides. **(A)** Heatmap of ZIKV PSMs identified in the *A. aegypti* head + salivary gland generated in Perseus software using abundance values transformed by *z*-score. **(B)** Total abundance of peptides spectrum matches (PSMs) calculated from report ions intensities from the three ZIKV peptides identified in samples. "*" Means that in Statistical analysis (*T*-test; **P*-value 0.0011), developed by using the software GraphPad Prism 7.0, sample Z has a statistical difference to sample WZ. **(C)** Domain architecture of the complete ZIKV polyprotein obtained from the PFAM database (PF01570) (El-Gebali et al., 2018). The location within the conserved domains and amino acid sequence of the three unique ZIKV peptides identified in proteomics analysis are highlighted.

neuropeptide F (sNPF) (AAEL019691), neuropeptide-like precursor-1(NPLP) (AAEL012640), calcitonin-like diuretic hormone (DH-31) (AAEL008070), SIFamide (AAEL009858), crustacean cardioactive peptide (CCAP) (AAEL000630), allatotropin (AAEL009541), CAPA (AAEL005444), sulfakinin (SK) (AAEL006451), ovary ecdysteroidogenic hormone (OEH; neuroparsin A homolog) (AAEL004155), insulin-like peptide 1 and 7 (AAEL000937; AAEL024251), and adipokinetic hormone 1 (AKH) (AAEL011996). A few neuropeptides and hormones were modulated by co-infection and will be discussed afterward.

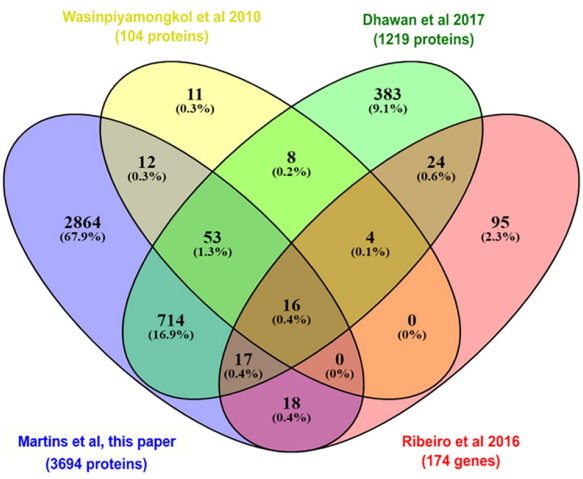

FIGURE 3 | Venn diagram comparing the set of proteins (isoforms were not considered) identified in this work (purple) with two previous proteomes of the salivary glands of *A. aegypti* (yellow; Wasinpiyamongkol et al., 2010 and green; Dhawan et al., 2017) and one transcriptome (red; Ribeiro et al., 2016) also carried out in salivary glands of *A. aegypti*, but in non-infected females.

ZIKV Infection Modulates Aerobic Metabolism, Lipids Pathways, and Immune System Response

By comparing mosquitoes infected and non-infected with ZIKV (**Figure 5** and **Supplementary Figure 4A**), we observe four main enriched processes: nicotinamide nucleotide metabolism, lipid transport, humoral innate response, and carbohydrate catabolism. Nicotinamide mononucleotide (NMN) is known for being an intermediator in NAD+ biosynthesis (Poddar et al., 2019; Hong et al., 2020), which participates actively in the aerobic metabolism process. This enrichment is mediated by the phosphoglycerate kinase (AAEL004988) and transaldolase (AAEL009389) upregulation, leading to carbohydrate catabolism elevation. The pentose phosphate pathway (PPP) was also up-regulated in our study as a response to transaldolase (AAEL009389) protein. The PPP is known to generate NADPH and pentoses (5-carbon sugars) as well as ribose 5-phosphate, a precursor for the synthesis of nucleotides, this led us

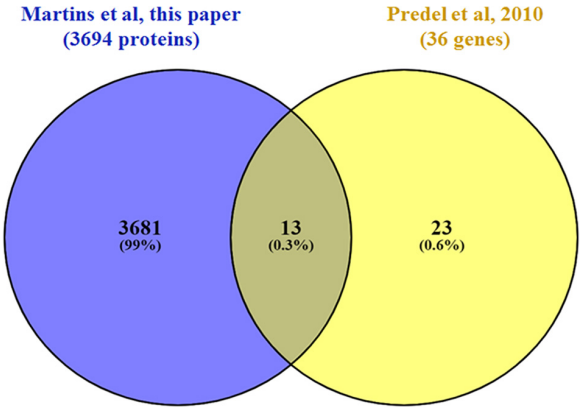

FIGURE 4 | Venn diagram comparing the set of neuropeptides and hormones (isoforms were not considered) identified in this work (purple) with those identified in Predel (yellow; Predel et al., 2010).

to relate the activation of PPP with the probation of nucleotide biosynthesis for virus replication (Guo et al., 2019). Both increased fluxes have been observed following Human Cytomegalovirus, Mayaro, and Kaposi-sarcoma viruses in human cells (El-Bacha and Da Poian, 2013).

Viruses are capable of modulating mitochondrial bioenergetics aiming to synthesize macromolecular precursors for self-replication, assembly and egress (El-Bacha and Da Poian, 2013). Thus, the enhancement of the lipid transport process should drive a redirection of these energetic resources to the viral capsids formation (Kuzmina et al., 2020), an event that was also described in *A. aegypti* coinfected with DENV and *Wolbachia* (Koh et al., 2020). Koh et al. (2020) compared lipid abundances between non-infected and DENV-3 infected mosquitoes and found that most modulated lipids are glycerophospholipids, as described earlier (Perera et al., 2012), with a higher level of unsaturated fatty acids and triacylglycerols. Glycerophospholipids modulation can be related to a virus attempt to build new virus capsids, as these lipids are a compound of this structure (Martín-Acebes et al., 2016). In our results, three genes related to lipid localization and transport were up-regulated: apolipophorin-III (AAEL008789) and two vitellogenin-A1 precursors (AAEL006126 and AAEL006138). Apolipophorins are protein components of lipoprotein particles that are essential for lipid transportation in the insect body, but apolipophorin-III can work as a pattern recognition receptor for insect immune system response (Wang et al., 2019), including in *A. aegypti* (Phillips and Clark, 2017). Lipid carrier protein lipophorin (Lp) and its lipophorin receptor (LpRfb) were significantly increased in *A. aegypti* after infections with Gram (+) bacteria and fungi, suggest that lipid metabolism is involved in the mosquito systemic immune responses to pathogens and parasites, as seen in studies before using fat body tissue (Cheon et al., 2006). The apolipophorin-III upregulation can be rolled to lipid transport and also to the immune response as ZIKV is expected to regulate them and the protein participates in both processes.

Another group of up-regulated biological processes includes an innate immune response in host cells due to virus infection (antimicrobial humoral response, humoral immune response, and response to biotic stimulus). Xi et al. (2008) found a significant role for the Toll pathway in DENV resistance regulation, and it was possible to identify differentially expressed antimicrobial peptide cecropin (AAEL029038) related to this pathway in our samples, confirming that Toll-pathway plays a major part in virus response (Xi et al., 2008; Pan et al., 2012; Kingsolver et al., 2013).

We observed down-regulation of tomosyn (AAEL006948), adenylate cyclase (AAEL009314), putative syntaxin-7 (AAEL009398), putative sodium/dicarboxylate cotransporter (AAEL009863), cytochrome c oxidase subunit II (AAEL018664), major facilitator superfamily domain-containing protein (AAEL006002), nuclear pore complex protein Nup188 (AAEL008557). and talin-1 (AAEL024235) related to cation transport processes. Also, three proteins were down-regulated: calcium-transporting ATPase sarcoplasmic/endoplasmic reticulum type (AAEL006582), Na+/K+ ATPase alpha subunit (AAEL012062), and calmodulin (AAEL012326-PA) related to cation transport processes as well. Similarly cytoskeleton, vesicle-mediated transport and ion transport-associated proteins down-regulation were described in CHIKV infection (Cui et al., 2020). Also, a recent study showed that Na+/K+ ATPase inhibition using two distinct drugs in mice helped to block ZIKV replication (Guo et al., 2020), suggesting that this down-regulation could be a mosquito cellular response to fight infection.

Adenosine triphosphate-citrate synthase (AAEL004297), sphingosine phosphate lyase (AAEL003188) and probable cysteine-tRNA synthetase (AAEL022886), proteins associated with amino acids insertion in the citric acid cycle, were also down-regulated and may lead to a decrease in citric acid cycle and oxidative phosphorylation processes. This phenomenon was also observed in *A. aegypti* salivary glands infected with DENV-2 (Chisenhall et al., 2014; Shrinet et al., 2018), suggesting the occurrence of cellular biomolecule and energy production control by virus infection to avoid mitochondrial exhaustion.

Wolbachia Endosymbiosis Interfere in Glycoconjugates Production Pathways, Aerobic Metabolism, Immune Response Induction, and Blood-Feeding Process

It is possible to notice in our data (**Figure 6** and **Supplementary Figures 3B, 4B**) an enrichment of GDP-mannose metabolism comparing mosquitoes non-infected with *Wolbachia*-mono infected. The enrichment was based on the upregulation of gdp mannose-4,6-dehydratase (AAEL014961), which converts GDP-mannose to GDP-4-dehydro-6-deoxy-D-mannose, the first of three steps for the conversion of GDP-mannose to GDP-fucose. This result suggests an induction caused by the presence of *Wolbachia* in insect cells to generate glycoconjugates, as GDP-mannose is a precursor for these molecules (Stick and Williams, 2009; Rexer et al., 2020), that may be used as elements to form new bacterial structures (García-del Portillo, 2020). An important

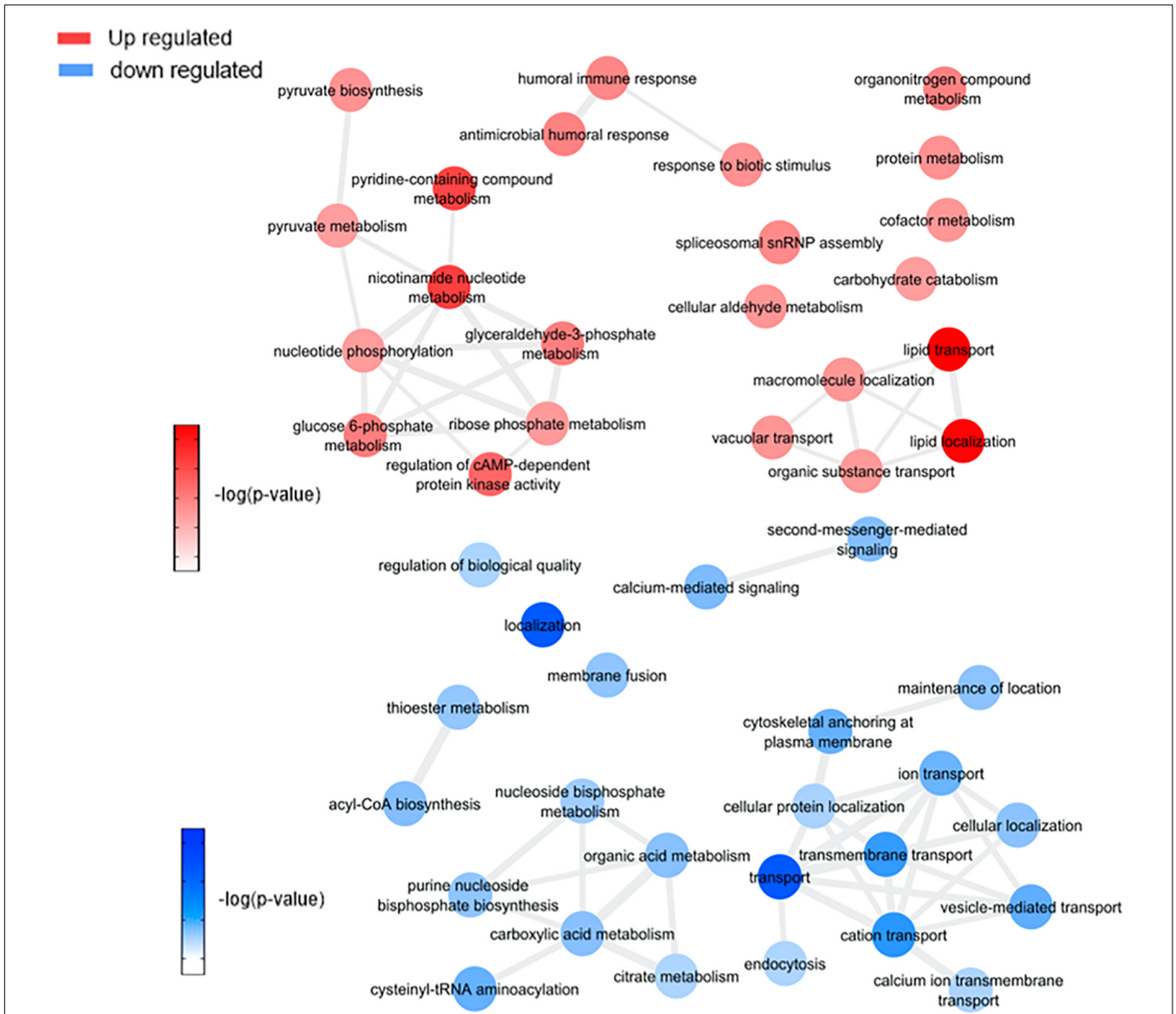

FIGURE 5 | Overview of significantly enriched GO [–log10 (*P*-value)] terms of ontological interaction network in biological processes of up-regulated (red) and down-regulated (blue) genes in ZIKV infected versus non-infected mosquitoes.

observation was the enrichment of processes downregulated related to the citric acid cycle in mosquito cells infected with *Wolbachia*. As shown by da Rocha Fernandes et al. (2014), *Wolbachia* modulated glycogen metabolism in *Aedes fluviatilis* embryos in favor of its aerobic metabolism (da Rocha Fernandes et al., 2014).

Up-regulation of 4-hydroxyphenylpyruvate dioxygenase (AAEL014600) can be related to plastoquinol and vitamin E (tocopherol) synthesis. Both molecules are described in the literature as participants of antioxidant response to different stimuli in organisms (MaitiDutta et al., 2020; Nowicka et al., 2020), including oxidative stress (Kumar et al., 2020; Minter et al., 2020). In this way, we consider that genes correlated to these pathways were regulated during *Wolbachia* infection because this microorganism can induce the expression of antioxidant proteins (Brennan et al., 2008). Moreover, 4-hydroxyphenylpyruvate dioxygenase is related to L-tyrosine degradation I and L-phenylalanine degradation IV, which are essential traits for blood-feeding arthropods, as they consume an amount of blood proteins and need to deal with a high quantity of free amino acids (Sterkel et al., 2016).

The *Wolbachia* infection up-regulated 10 salivary gland proteins, such as endoplasmin (AAEL012827-PA), which is required for proper folding of Toll-like receptors in mammals (Fitzgerald and Kagan, 2020), and FKBP12 (AAEL010491-PB) that has a prolyl isomerase activity and bidins to immunosuppressive molecules (Caminati and Procacci, 2020).

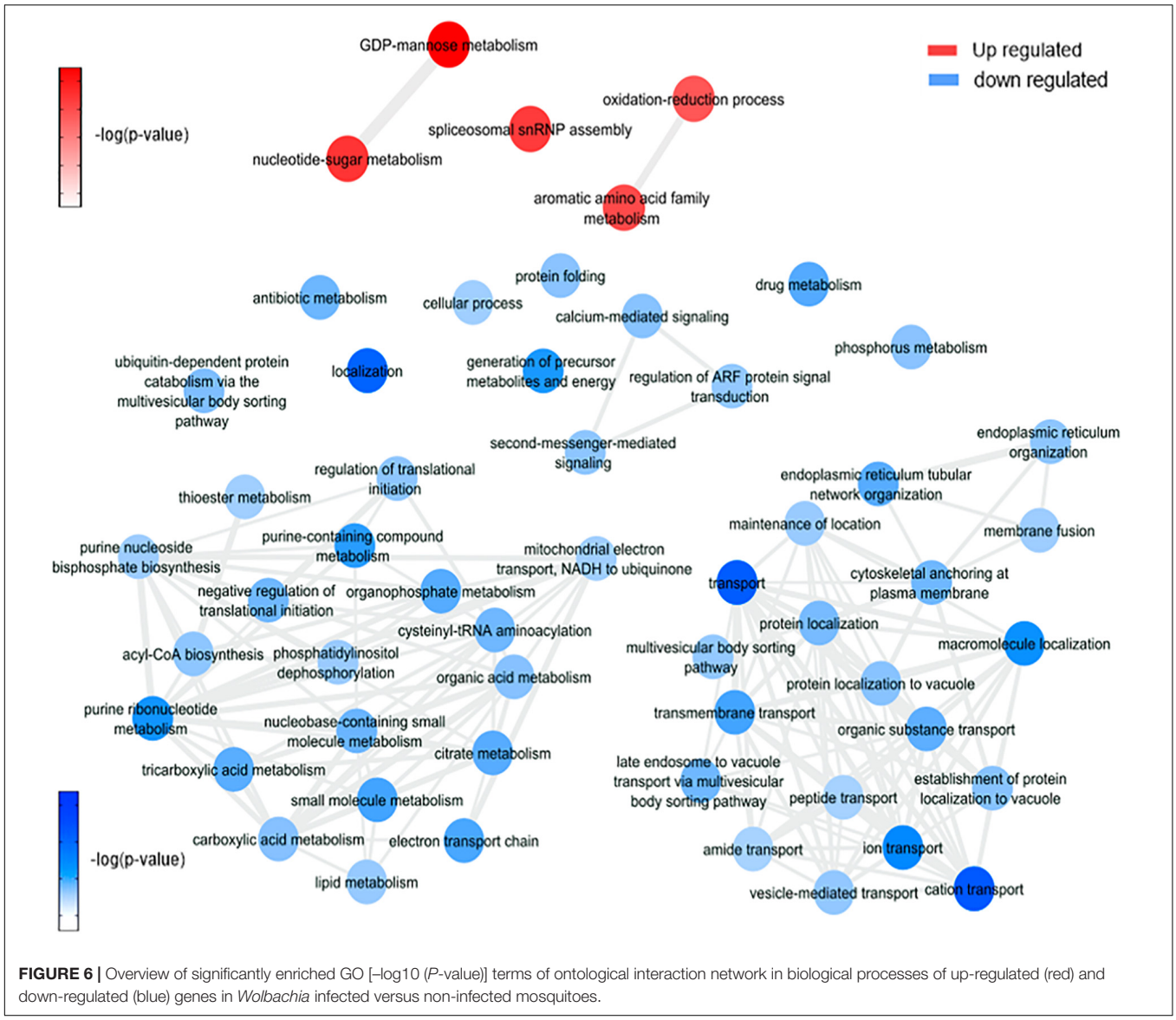

FIGURE 6 | Overview of significantly enriched GO [–log10 (*P*-value)] terms of ontological interaction network in biological processes of up-regulated (red) and down-regulated (blue) genes in *Wolbachia* infected versus non-infected mosquitoes.

Twenty salivary proteins were down-regulated by *Wolbachia* infection. Interestingly, the same ion related proteins down-regulated by ZIKV are also down-regulated by *Wolbachia*, moreover, proteins related with contraction such as paramyosin (AAEL010975-PA), tropomyosin (AAEL002761-PA), and Actin-1 (AAEL001928-PA) were also down-regulated. Also, a serine protease inhibitor 25 (SRPN25) (AAEL007420-PB) was also identified in our analysis. Its orthologue is Alboserpin, the major salivary gland anticoagulant in *Aedes albopictus*, which prevents coagulation in an atypical reversible interaction with factor Xa (coagulation activation factor), important for blood intake by female mosquitoes (Stark and James, 1998; Calvo et al., 2011). SRPN25 was up-regulated in W, which may infer that blood takes longer to coagulate, increasing mosquito enzymes access to digest blood. The consequence of these salivary proteins modulation suggests an impairment in salivary gland injection into the host and a possible reduction in the amount of blood ingestion during *Wolbachia* presence in the mosquito (Turley et al., 2009).

Co-infection Modulated Pathways and Processes Show an Induction in Reactive Oxygen Species Production That Can Lead to an Immune System Response to Virus Infection

This analysis was based on a comparison of the ZW with Z (**Figure 7** and **Supplementary Figure 4C**) and W (**Figure 8** and **Supplementary Figure 4D**) mosquito heads samples.

Zika virus and *Wolbachia* use mosquitoes cell machinery respectively to synthesize lipids and glycoconjugates molecules for their structural use, as mentioned before. According to WZ results, the enriched lipid synthesis biological processes remain up-regulated despite the *Wolbachia* presence, similarly

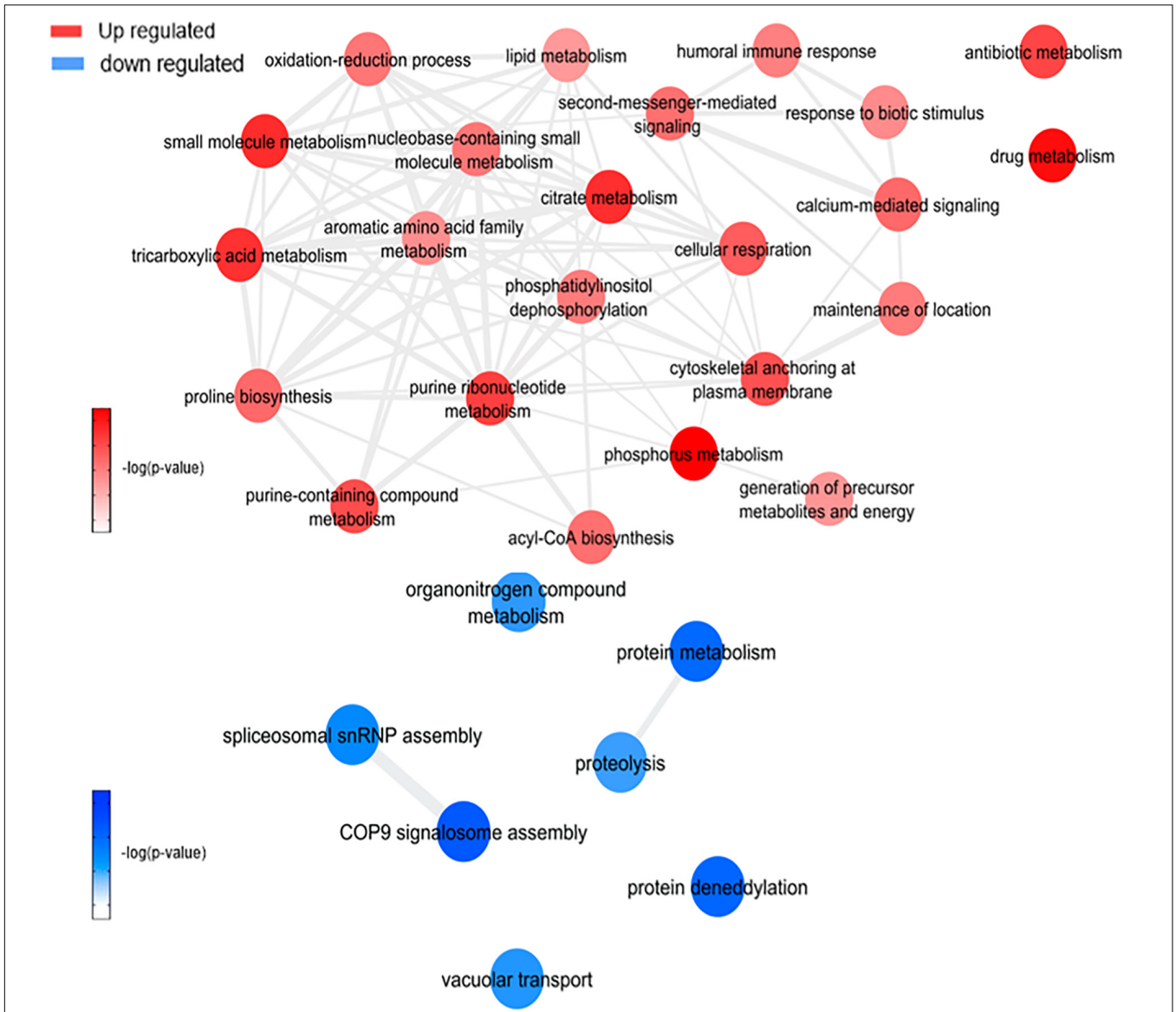

FIGURE 7 | Overview of significantly enriched GO [–log10 (*P*-value)] terms of ontological interaction network in biological processes of up-regulated (red) and down-regulated (blue) genes in coinfected mosquitoes versus ZIKV infected mosquitoes.

to ZIKV infection. Koh et al. (2020) confirmed such behavior during co-infection-induced intracellular events with DENV and *Wolbachia*, suggesting that they do not compete by lipids in host cell and virus-driven modulation dominates over that of *Wolbachia* (Koh et al., 2020), which may have occurred as well as in our experiment. In contrast, there is a down-regulation in GDP-mannose proteins genes synthesis, which may suggest that host cells no longer produce glycoconjugates for bacteria use.

Within the up-regulated genes in WZ compared to Z, ATP synthesis (ATPase subunit O; AAEL010823-PA), and cytoskeleton dynamics like microtubule binding and associated-proteins (AAEL009375-PK, AAEL004176-PB, and AAEL009847-PB) suggest activation of the ubiquitin-proteasome system. Indeed, it was previously reported in *Drosophila* and mosquito cell lines transfected, that *Wolbachia* relies on host proteolysis through ubiquitination to acquire essential amino acid for the infection (Fallon and Witthuhn, 2009; White et al., 2017). Flavivirus also need a functioning ubiquitin-proteasome system to complete their life cycle (Choy et al., 2015a,b), however, Ub3881 (AAEL003881), a ubiquitin-protein, is highly down-regulated in mosquitoes infected with DENV and its overexpression was able to control the virus infection (Troupin et al., 2016). In our analysis, we identified a paralog of the Ub3881 ubiquitin protein (AAEL003888), which was up-regulated in WZ versus Z and down-regulated in Z, suggesting that *Wolbachia* have a role in AAEL003888 expression enhancement which might target the

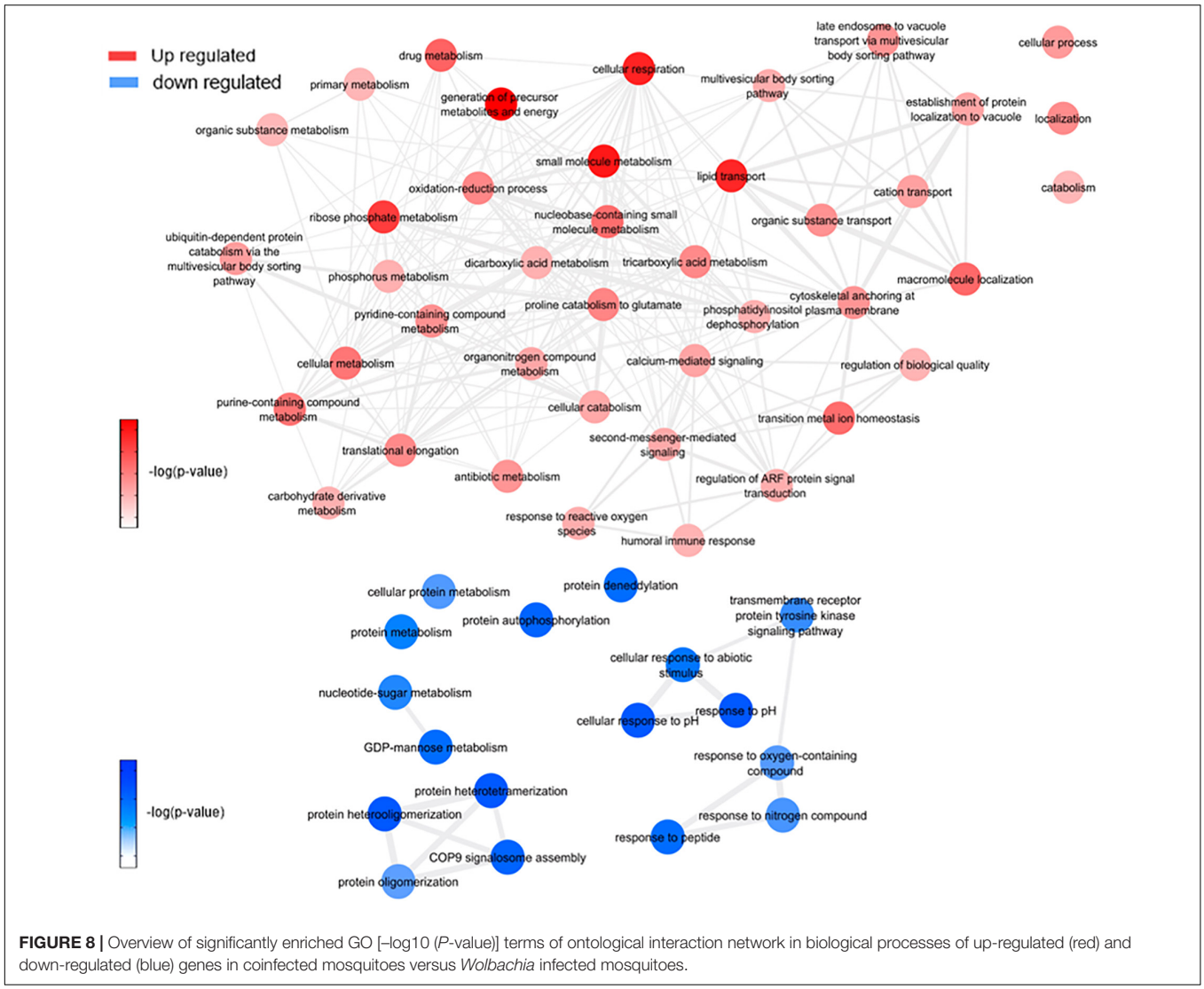

FIGURE 8 | Overview of significantly enriched GO [–log10 (*P*-value)] terms of ontological interaction network in biological processes of up-regulated (red) and down-regulated (blue) genes in coinfected mosquitoes versus *Wolbachia* infected mosquitoes.

envelope proteins of ZIKV for degradation, therefore hindering the virus assembly.

Exploring neuropeptides and hormones, neuropeptide sulfakinin (SK) (AAEL006451-PB) and insulin-like peptide (ILP) 1 (AAEL000937-PA) were down-regulated comparing WZ with Z. SK are a family of neuropeptides, homologous to mammalian gastrin/cholecystokinin (CCK), responsible for food uptake control in insects (Zels et al., 2015) while ILPs are known for signaling carbohydrates intake in cells (Nässel and Broeck, 2016). A recent study correlated SK influence in ILPs concentration, where a rise in SK concentration promotes ILPs production (Słocińska et al., 2020). SK down-regulation, observed in our data, may decrease in mosquito feeding satisfaction. This fact allied to ILP down-regulation, leading to a decrease in glycolysis cell assimilation, can be understood as a virus-infection influence to increase mosquito blood uptake, elevating ZIKV transmission success.

There are several processes up-regulated after enrichment comparison between WZ and Z. Cellular respiration, aerobic respiration, small molecule metabolic process, tricarboxylic acid cycle, oxidative phosphorylation, ATP synthesis coupled electron transport, respiratory electron transport chain, generation of precursor metabolites and energy, tricarboxylic acid metabolic process, nicotinamide nucleotide metabolic process, and cellular process were enriched up-regulated biological process by proteins genes ATP-citrate synthase (AAEL004297), glutamate semialdehyde dehydrogenase (AAEL006834), ATP synthase delta chain (AAEL010823), phosphatidylinositol-4,5-bisphosphate 4-phosphatase (AAEL011216), NADH-ubiquinone oxidoreductase (AAEL012552), mitochondrial aconitase (AAEL012897), 4-hydroxyphenylpyruvate dioxygenase (AAEL014600), titin (AAEL002565), and myosin (AAEL000596) up-regulation. The increase in aerobic respiration metabolism in *Wolbachia* infection proved to stimulate ROS production in insect cells as part of the host immune response, but it counterbalances with antioxidant pathways activation (Zug and Hammerstein, 2015). However, it was observed in WZ that the aerobic metabolism increases together with transition metal ions biological process

and pathways, mediated by putative secreted ferritin G subunit precursor (AAEL007383) and transferrin (AAEL015458), which can also generate ROS (Liu et al., 2016). ROS likely activates the Toll-immune pathway to confront ZIKV, similar to DENV infection (Selivanov et al., 2008). Also, two eukaryotic elongation factor 1-alpha (eEF1A) proteins (AAEL017096; AAEL017301) were up-regulated comparing WZ and Z. eEF1A increase was described as a response to endoplasmic reticulum stress caused by ROS in Chinese hamster ovary (Borradaile et al., 2005), which may have occurred in the mosquito. Another observed data was SRPN25 down-regulated in WZ, which was up-regulated in W. SRPN25 down-regulation in WZ highlights its function related to the insect immune system. Serpins can block the Toll signaling cascade and β-1,3-glucan-mediated melanin biosynthesis (Jiang et al., 2009), so its downregulation can infer that the insect immune system is activated.

This led us to understand insects defense mechanisms, induced by the presence of endosymbiotic bacteria, that may have been acting against virus infection: melanization activation mediated by SRPN25 down-regulation and Toll-pathway with the influence of SPRN25 down-regulation and the exacerbated production of ROS by aerobic metabolism increase. ROS occurs inside the mitochondria, after the oxidative phosphorylation stage, which has oxygen as the final electron acceptor, forming metabolic water. When oxygen is prematurely and incompletely reduced, it gives rise to superoxide anion, classified as ROS, together with hydrogen peroxide, hypochlorous acid, hydroxyl radical, singlet oxygen, and ozone (Lambert and Brand, 2009). Pan et al. described the relation between *Wolbachia* presence in *A. aegypti* and Toll-pathway activation by ROS to control DENV (Pan et al., 2012). This study not only confirms oxidative stress caused by Wolbachia, but also antioxidant genes expression as described earlier in this article. The role of symbiotic microorganisms in arbovirus infection of arthropods vectors is widely discussed, highlighting the importance of a ROS-mediated stimulation of the Toll-pathway and AMPs expression (Yin et al., 2020). As SPRN25 is down-regulated, serpins activity is up-regulated, which lead to serpins key response in the defense mechanism of insects, activating especially the Toll pathway, as well as ROS, and prophenoloxidase (PPO) cascade (Meekins et al., 2017). As for PPO cascade, it mediates melanization immune response in insects, including mosquito vectors (Christensen et al., 2005), It was already investigated that melanization suppression by SRPN activation can lead to a increase in viral infection (Toufeeq et al., 2019), calling attention to SRPN importance in mosquito immune response.

CONCLUSION

Proteomics analysis of female's head of *A. aegypti* during mono-infection with ZIKV or *Wolbachia* highlighted how those microorganisms use cell host for their benefits. Our data support that ZIKV may induces lipid synthesis and transport allied with glycolysis pathways while *Wolbachia* increases glycoconjugates production. During co-infection, *Wolbachia* probably helps *A. aegypti* to prevent virus infection by stimulating ROS production leading to Toll-pathway humoral immune response, together with antioxidant production to control cell homeostasis. This mechanism seems to be efficient since we have shown that peptides coming from the ZIKV polyprotein are reduced in female's heads of *A. aegypti* in the presence of *Wolbachia*. Our study has provided important insights into the differential manner in which *A. aegypti* proteome is systemically regulated during mono- and co-infections of ZIKV and *Wolbachia*. Ultimately, this work represents a rich resource for the insect research community to help elucidate the mechanisms by which *Wolbachia* orchestrate resistance to ZIKV infection in *A. aegypti* and it allows the generation of specific hypothesis-driven experiments in future studies.

DATA AVAILABILITY STATEMENT

The data presented in the study are deposited in the Proteome X Change repository, accession number PXD022665.

AUTHOR CONTRIBUTIONS

MM, LR, JM, AT, and SC performed the experiments and data analysis. MM and SC produced manuscript figures. MM, LR, JM, AT, SC, GD, DO, RM, FN, RM-D-F, and MJ wrote the manuscript. RM-D-F and MJ idealized and coordinated the study. All authors approved the manuscript.

FUNDING

The present work was supported by the Fundação Carlos Chagas Filho de Amparo à Pesquisa do Estado do Rio de Janeiro (FAPERJ) and Conselho Nacional de Desenvolvimento Científico e Tecnológico (CNPq).

ACKNOWLEDGMENTS

The authors thank Fabio Mendonça Gomes from Instituto de Biofísica Carlos Chagas Filho – UFRJ and Livia Goto-Silva from D'Or Institute for Research and Education (IDOR) for their critical reading of the manuscript.

SUPPLEMENTARY MATERIAL

The Supplementary Material for this article can be found online at: https://www.frontiersin.org/articles/10.3389/fphys.2021.642237/full#supplementary-material

REFERENCES

Aebersold, R., and Mann, M. (2016). Mass-spectrometric exploration of proteome structure and function. *Nature* 537, 347–355. doi: 10.1038/nature19949

Aliota, M. T., Walker, E. C., Yepes, A. U., Velez, I. D., Christensen, B. M., and Osorio, J. E. (2016). The wMel strain of Wolbachia reduces transmission of Chikungunya virus in *Aedes aegypti*. *PLoS Negl. Trop. Dis.* 10:e0004677. doi: 10.1371/journal.pntd.0004677

Ashburner, M., Ball, C. A., Blake, J. A., Botstein, D., Butler, H., Cherry, J. M., et al. (2000). Gene ontology: tool for the unification of biology. *Nat. Genet.* 25, 25–29. doi: 10.1038/75556

Barreto, M. L., Barral-Netto, M., Stabeli, R., Almeida-Filho, N., Vasconcelos, P. F. C., Teixeira, M., et al. (2016). Zika virus and microcephaly in Brazil: a scientific agenda. *Lancet* 387, 919–921. doi: 10.1016/S0140-6736(16)00545-6

Baud, D., Gubler, D. J., Schaub, B., Lanteri, M. C., and Musso, D. (2017). An update on Zika virus infection. *Lancet* 390, 2099–2109. doi: 10.1016/S0140-6736(17)31450-2

Borradaile, N. M., Buhman, K. K., Listenberger, L. L., Magee, C. J., Morimoto, E. T. A., Ory, D. S., et al. (2005). A critical role for eukaryotic elongation factor 1A-1 in lipotoxic cell death. *MBoC* 17, 770–778. doi: 10.1091/mbc.e05-08-0742

Brennan, L. J., Keddie, B. A., Braig, H. R., and Harris, H. L. (2008). The endosymbiont *Wolbachia pipientis* induces the expression of host antioxidant proteins in an *Aedes albopictus* cell line. *PLoS One* 3:e2083. doi: 10.1371/journal.pone.0002083

Calvo, E., Mizurini, D. M., Sá-Nunes, A., Ribeiro, J. M. C., Andersen, J. F., Mans, B. J., et al. (2011). Alboserpin, a factor Xa inhibitor from the mosquito vector of yellow fever, binds heparin and membrane phospholipids and exhibits antithrombotic activity. *J. Biol. Chem.* 286, 27998–28010. doi: 10.1074/jbc.M111.247924

Caminati, G., and Procacci, P. (2020). Mounting evidence of FKBP12 implication in neurodegeneration. *Neural Regen. Res.* 15, 2195–2202. doi: 10.4103/1673-5374.284980

Campos, G., Bandeira, A., and Sardi, S. (2015). Zika virus outbreak, Bahia, Brazil. *Emerg. Infect. Dis. J.* 21:1885. doi: 10.3201/eid2110.150847

Cheon, H.-M., Shin, S. W., Bian, G., Park, J.-H., and Raikhel, A. S. (2006). Regulation of lipid metabolism genes, lipid carrier protein lipophorin, and its receptor during immune challenge in the mosquito *Aedes aegypti*. *J. Biol. Chem.* 281, 8426–8435. doi: 10.1074/jbc.M510957200

Chisenhall, D. M., Londono, B. L., Christofferson, R. C., McCracken, M. K., and Mores, C. N. (2014). Effect of dengue-2 virus infection on protein expression in the salivary glands of *Aedes aegypti* mosquitoes. *Am. J. Trop. Med. Hyg.* 90, 431–437. doi: 10.4269/ajtmh.13-0412

Choudhary, C., and Mann, M. (2010). Decoding signalling networks by mass spectrometry-based proteomics. *Nat. Rev. Mol. Cell Biol.* 11, 427–439. doi: 10.1038/nrm2900

Chouin-Carneiro, T., Vega-Rua, A., Vazeille, M., Yebakima, A., Girod, R., Goindin, D., et al. (2016). Differential susceptibilities of *Aedes aegypti* and *Aedes albopictus* from the Americas to Zika Virus. *PLoS Negl. Trop. Dis.* 10:e0004543. doi: 10.1371/journal.pntd.0004543

Choy, M. M., Sessions, O. M., Gubler, D. J., and Ooi, E. E. (2015a). Production of infectious dengue virus in *Aedes aegypti* is dependent on the ubiquitin proteasome pathway. *PLoS Negl. Trop. Dis.* 9:e0004227. doi: 10.1371/journal.pntd.0004227

Choy, M. M., Zhang, S. L., Costa, V. V., Tan, H. C., Horrevorts, S., and Ooi, E. E. (2015b). Proteasome inhibition suppresses dengue virus egress in antibody dependent infection. *PLoS Negl. Trop. Dis.* 9:e0004058. doi: 10.1371/journal.pntd.0004058

Christensen, B. M., Li, J., Chen, C.-C., and Nappi, A. J. (2005). Melanization immune responses in mosquito vectors. *Trends Parasitol.* 21, 192–199. doi: 10.1016/j.pt.2005.02.007

Codeço, C. T., Lima, A. W. S., Araújo, S. C., Lima, J. B. P., Maciel-de-Freitas, R., Honório, N. A., et al. (2015). Surveillance of *Aedes aegypti*: comparison of house index with four alternative traps. *PLoS Negl. Trop. Dis.* 9:e0003475. doi: 10.1371/journal.pntd.0003475

Cui, Y., Liu, P., Mooney, B. P., and Franz, A. W. E. (2020). Quantitative proteomic analysis of Chikungunya virus-infected *Aedes aegypti* reveals proteome modulations indicative of persistent infection. *J. Proteome Res.* 19, 2443–2456. doi: 10.1021/acs.jproteome.0c00173

da Rocha Fernandes, M., Martins, R., Pessoa Costa, E., Pacidônio, E. C., Araujo, et al. (2014). The modulation of the symbiont/host interaction between *Wolbachia pipientis* and *Aedes fluviatilis* embryos by glycogen metabolism. *PLoS One* 9:e98966. doi: 10.1371/journal.pone.0098966

da Silveira, I. D., Petersen, M. T., Sylvestre, G., Garcia, G. A., David, M. R., Pavan, M. G., et al. (2018). Zika virus infection produces a reduction on *Aedes aegypti* lifespan but no effects on mosquito fecundity and oviposition success. *Front. Microbiol.* 9:3011. doi: 10.3389/fmicb.2018.03011

De Mandal, S., Lin, B., Shi, M., Li, Y., Xu, X., and Jin, F. (2020). iTRAQ-based comparative proteomic analysis of larval midgut from the beet armyworm, *Spodoptera exigua* (Hübner) (Lepidoptera: Noctuidae) challenged with the entomopathogenic bacteria *Serratia marcescens*. *Front. Physiol.* 11:442. doi: 10.3389/fphys.2020.00442

Dhawan, R., Mohanty, A. K., Kumar, M., Dey, G., Advani, J., Prasad, T. S. K., et al. (2017). Data from salivary gland proteome analysis of female *Aedes aegypti* Linn. *Data Brief.* 13, 274–277. doi: 10.1016/j.dib.2017.05.034

Dick, G. W. A., Kitchen, S. F., and Haddow, A. J. (1952). Zika Virus (I). Isolations and serological specificity. *Trans. R. Soc. Trop. Med. Hyg.* 46, 509–520. doi: 10.1016/0035-9203(52)90042-4

Duncan, A. B., Agnew, P., Noel, V., Demettre, E., Seveno, M., Brizard, J.-P., et al. (2012). Proteome of *Aedes aegypti* in response to infection and coinfection with microsporidian parasites. *Ecol. Evol.* 2, 681–694. doi: 10.1002/ece3.199

Dutra, H. L. C., Rocha, M. N., Dias, F. B. S., Mansur, S. B., Caragata, E. P., and Moreira, L. A. (2016). Wolbachia blocks currently circulating Zika virus isolates in Brazilian *Aedes aegypti* mosquitoes. *Cell Host Microbe* 19, 771–774. doi: 10.1016/j.chom.2016.04.021

El-Bacha, T., and Da Poian, A. T. (2013). Virus-induced changes in mitochondrial bioenergetics as potential targets for therapy. *Int. J. Biochem. Cell Biol.* 45, 41–46. doi: 10.1016/j.biocel.2012.09.021

El-Gebali, S., Mistry, J., Bateman, A., Eddy, S. R., Luciani, A., Potter, S. C., et al. (2018). The Pfam protein families database in 2019. *Nucleic Acids Res.* 47, 427–432. doi: 10.1093/nar/gky995

Fallon, A. M., and Witthuhn, B. A. (2009). Proteasome activity in a naïve mosquito cell line infected with *Wolbachia pipientis* wAlbB. *Vitro Cell. Dev. Biol. Anim.* 45, 460–466. doi: 10.1007/s11626-009-9193-6

Fernandes, R. S., Campos, S. S., Ferreira-de-Brito, A., Miranda, R. M., Barbosa, da Silva, K. A., et al. (2016). *Culex quinquefasciatus* from Rio de janeiro is not competent to transmit the local Zika Virus. *PLoS Negl. Trop. Dis.* 10:e0004993. doi: 10.1371/journal.pntd.0004993

Ferreira-de-Brito, A., Ribeiro, I. P., Miranda, R. M., Fernandes, R. S., Campos, S. S., Silva, K. A., et al. (2016). First detection of natural infection of *Aedes aegypti* with Zika virus in Brazil and throughout South America. *Memórias Instit. Oswaldo Cruz* 111, 655–658. doi: 10.1590/0074-02760160332

Fitzgerald, K. A., and Kagan, J. C. (2020). Toll-like receptors and the control of immunity. *Cell* 180, 1044–1066. doi: 10.1016/j.cell.2020.02.041

Ford, S. A., Albert, I., Allen, S. L., Chenoweth, S. F., Jones, M., Koh, C., et al. (2020). Artificial selection finds new hypotheses for the mechanism of Wolbachia-Mediated dengue blocking in mosquitoes. *Front. Microbiol.* 11:1456. doi: 10.3389/fmicb.2020.01456

Garcia, G. A., Sylvestre, G., Aguiar, R., da Costa, G. B., Martins, A. J., Lima, J. B. P., et al. (2019). Matching the genetics of released and local *Aedes aegypti* populations is critical to assure Wolbachia invasion. *PLoS Negl. Trop. Dis.* 13:e0007023. doi: 10.1371/journal.pntd.0007023

García-Robles, I., De Loma, J., Capilla, M., Roger, I., Boix-Montesinos, P., Carrión, P., et al. (2020). Proteomic insights into the immune response of the Colorado potato beetle larvae challenged with *Bacillus thuringiensis*. *Dev. Comp. Immunol.* 104:103525. doi: 10.1016/j.dci.2019.103525

García-del Portillo, F. (2020). Building peptidoglycan inside eukaryotic cells: a view from symbiotic and pathogenic bacteria. *Mol. Microbiol.* 113, 613–626. doi: 10.1111/mmi.14452

Geoghegan, V., Stainton, K., Rainey, S. M., Ant, T. H., Dowle, A. A., Larson, T., et al. (2017). Perturbed cholesterol and vesicular trafficking associated with dengue blocking in Wolbachia -infected *Aedes aegypti* cells. *Nat. Commun.* 8:526. doi: 10.1038/s41467-017-00610-8

Giraldo-Calderón, G. I., Emrich, S. J., MacCallum, R. M., Maslen, G., Dialynas, E., Topalis, P., et al. (2015). VectorBase: an updated bioinformatics resource for invertebrate vectors and other organisms related with human diseases. *Nucleic Acids Res.* 43, 707–713. doi: 10.1093/nar/gku1117

Guo, J., Jia, X., Liu, Y., Wang, S., Cao, J., Zhang, B., et al. (2020). Inhibition of Na + /K + ATPase blocks Zika virus infection in mice. *Commun. Biol.* 3, 380. doi: 10.1038/s42003-020-1109-8

Guo, X., Wu, S., Li, N., Lin, Q., Liu, L., Liang, H., et al. (2019). Accelerated metabolite levels of aerobic glycolysis and the pentose phosphate pathway are required for efficient replication of infectious spleen and kidney necrosis virus in chinese perch brain cells. *Biomolecules* 9:440. doi: 10.3390/biom9090440

Haqshenas, G., Terradas, G., Paradkar, P. N., Duchemin, J.-B., McGraw, E. A., and Doerig, C. (2019). A role for the insulin receptor in the suppression of dengue virus and Zika virus in wolbachia-infected mosquito cells. *Cell Rep.* 26, 529.e3–535.e3. doi: 10.1016/j.celrep.2018.12.068

Hoffmann, A. A., Montgomery, B. L., Popovici, J., Iturbe-Ormaetxe, I., Johnson, P. H., Muzzi, F., et al. (2011). Successful establishment of Wolbachia in Aedes populations to suppress dengue transmission. *Nature* 476, 454–457. doi: 10.1038/nature10356

Holt, R. A., Subramanian, G. M., Halpern, A., Sutton, G. G., Charlab, R., Nusskern, D. R., et al. (2002). The genome sequence of the malaria mosquito *Anopheles gambiae*. *Science* 298, 129–149. doi: 10.1126/science.1076181

Hong, W., Mo, F., Zhang, Z., Huang, M., and Wei, X. (2020). Nicotinamide mononucleotide: a promising molecule for therapy of diverse diseases by targeting NAD+ metabolism. *Front. Cell Dev. Biol.* 8:246. doi: 10.3389/fcell.2020.00246

Indriani, C., Tantowijoyo, W., Rancès, E., Andari, B., Prabowo, E., Yusdi, D., et al. (2020). Reduced dengue incidence following deployments of Wolbachia-infected *Aedes aegypti* in Yogyakarta, Indonesia: a quasi-experimental trial using controlled interrupted time series analysis. *Gates Open Res.* 4:50. doi: 10.12688/gatesopenres.13122.1

Jiang, R., Kim, E.-H., Gong, J.-H., Kwon, H.-M., Kim, C.-H., Ryu, K.-H., et al. (2009). Three pairs of protease-serpin complexes cooperatively regulate the insect innate immune responses. *J. Biol. Chem.* 284, 35652–35658. doi: 10.1074/jbc.M109.071001

Kingsolver, M. B., Huang, Z., and Hardy, R. W. (2013). Insect antiviral innate immunity: pathways, effectors, and connections. *J. Mol. Biol.* 425, 4921–4936. doi: 10.1016/j.jmb.2013.10.006

Koh, C., Islam, M. N., Ye, Y. H., Chotiwan, N., Graham, B., Belisle, J. T., et al. (2020). Dengue virus dominates lipid metabolism modulations in Wolbachia - coinfected *Aedes aegypti*. *Commun. Biol.* 3:e0007443. doi: 10.1038/s42003-020-01254-z

Kumar, A., Prasad, A., Sedlářová, M., Ksas, B., Havaux, M., and Pospíšil, P. (2020). Interplay between antioxidants in response to photooxidative stress in *Arabidopsis*. *Free Radic. Biol. Med.* 160, 894–907. doi: 10.1016/j.freeradbiomed.2020.08.027

Kuzmina, N. V., Loshkareva, A. S., Shilova, L. A., Shtykova, E. V., Knyazev, D. G., Zimmerberg, J., et al. (2020). Protein-lipid interactions in formation of viral envelopes. *Biophys. J.* 118:523a. doi: 10.1016/j.bpj.2019.11.2874

Lambert, A. J., and Brand, M. D. (2009). "Reactive oxygen species production by mitochondria," in *Mitochondrial DNA: Methods and Protocols Methods in Molecular Biology*^{TM}, ed. J. A. Stuart (Totowa, NJ: Humana Press), 165–181. doi: 10.1007/978-1-59745-521-3_11

Li, F., Zhao, X., Zhu, S., Wang, T., Li, T., Woolfley, T., et al. (2020). Identification and expression profiling of neuropeptides and neuropeptide receptor genes in *Atrijuglans hetaohei*. *Gene* 743:144605. doi: 10.1016/j.gene.2020.144605

Linthicum, K. J., Platt, K., Myint, K. S., Lerdthusnee, K., Inni, B. L., and Ghn, D. W. V. (1996). Dengue 3 virus distribution in the mosquito *Aedes aegypti*: an immunocytochemical study. *Medic. Vet. Entomol.* 10, 87–92. doi: 10.1111/j.1365-2915.1996.tb00086.x

Liu, K., Gao, Y., Liu, J., Wen, Y., Zhao, Y., Zhang, K., et al. (2016). Photoreactivity of metal–organic frameworks in aqueous solutions: metal dependence of reactive oxygen species production. *Environ. Sci. Technol.* 50, 3634–3640. doi: 10.1021/acs.est.5b06019

MaitiDutta, S., Chen, G., and Maiti, S. (2020). Tocopherol moderately induces the expressions of some human sulfotransferases, which are activated by oxidative stress. *Cell Biochem. Biophys.* 78, 439–446. doi: 10.1007/s12013-020-00938-x

Manokaran, G., Flores, H. A., Dickson, C. T., Narayana, V. K., Kanojia, K., Dayalan, S., et al. (2020). Modulation of acyl-carnitines, the broad mechanism behind Wolbachia-mediated inhibition of medically important flaviviruses in *Aedes aegypti*. *PNAS* 117, 24475–24483. doi: 10.1073/pnas.1914814117

Martín-Acebes, M. A., Vázquez-Calvo, Á, and Saiz, J.-C. (2016). Lipids and flaviviruses, present and future perspectives for the control of dengue, Zika, and West Nile viruses. *Prog. Lipid Res.* 64, 123–137. doi: 10.1016/j.plipres.2016.09.005

Meekins, D. A., Kanost, M. R., and Michel, K. (2017). Serpins in arthropod biology. *Semin. Cell Dev. Biol.* 62, 105–119. doi: 10.1016/j.semcdb.2016.09.001

Minter, B. E., Lowes, D. A., Webster, N. R., and Galley, H. F. (2020). Differential effects of MitoVitE, α-Tocopherol and Trolox on oxidative stress, mitochondrial function and inflammatory signalling pathways in endothelial cells cultured under conditions mimicking sepsis. *Antioxidants* 9:195. doi: 10.3390/antiox9030195

Moreira, L. A., Iturbe-Ormaetxe, I., Jeffery, J. A., Lu, G., Pyke, A. T., Hedges, L. M., et al. (2009). A Wolbachia symbiont in *Aedes aegypti* limits infection with dengue, chikungunya, and plasmodium. *Cell* 139, 1268–1278. doi: 10.1016/j.cell.2009.11.042

Murillo, J. R., Goto-Silva, L., Sánchez, A., Nogueira, F. C. S., Domont, G. B., and Junqueira, M. (2017). Quantitative proteomic analysis identifies proteins and pathways related to neuronal development in differentiated SH-SY5Y neuroblastoma cells. *EuPA Open Proteom.* 16, 1–11. doi: 10.1016/j.euprot.2017.06.001

Nässel, D. R., and Broeck, J. V. (2016). Insulin/IGF signaling in *Drosophila* and other insects: factors that regulate production, release and post-release action of the insulin-like peptides. *Cell. Mol. Life Sci.* 73, 271–290. doi: 10.1007/s00018-015-2063-3

Nazni, W. A., Hoffmann, A. A., NoorAfizah, A., Cheong, Y. L., Mancini, M. V., Golding, N., et al. (2019). Establishment of Wolbachia strain wAlbB in Malaysian populations of *Aedes aegypti* for dengue control. *Curr. Biol.* 29, 4241.e5–4248.e5. doi: 10.1016/j.cub.2019.11.007

Nowicka, B., Fesenko, T., Walczak, J., and Kruk, J. (2020). The inhibitor-evoked shortage of tocopherol and plastoquinol is compensated by other antioxidant mechanisms in *Chlamydomonas reinhardtii* exposed to toxic concentrations of cadmium and chromium ions. *Ecotoxicol. Environ. Saf.* 191:110241. doi: 10.1016/j.ecoenv.2020.110241

Nunes, A. T., Brito, N. F., Oliveira, D. S., Araujo, G. D. T., Nogueira, F. C. S., Domont, G. B., et al. (2016). Comparative proteome analysis reveals that blood and sugar meals induce differential protein expression in *Aedes aegypti* female heads. *Proteomics* 16, 2582–2586. doi: 10.1002/pmic.201600126

Paingankar, M. S., Gokhale, M. D., Deobagkar, D. D., and Deobagkar, D. N. (2020). *Drosophila melanogaster* as a model host to study arbovirus–vector interaction. *bioRxiv* doi: 10.1101/2020.09.03.282350

Pan, X., Zhou, G., Wu, J., Bian, G., Lu, P., Raikhel, A. S., et al. (2012). Wolbachia induces reactive oxygen species (ROS)-dependent activation of the Toll pathway to control dengue virus in the mosquito *Aedes aegypti*. *PNAS* 109, E23–E31. doi: 10.1073/pnas.1116932108

Pappireddi, N., Martin, L., and Wühr, M. (2019). A review on quantitative multiplexed proteomics. *ChemBioChem* 20, 1210–1224. doi: 10.1002/cbic.201800650

Perera, R., Riley, C., Isaac, G., Hopf-Jannasch, A. S., Moore, R. J., Weitz, K. W., et al. (2012). Dengue virus infection perturbs lipid homeostasis in infected mosquito cells. *PLoS Pathog.* 8:e1002584. doi: 10.1371/journal.ppat.1002584

Petersen, M. T., da Silveira, I. D., Tátila-Ferreira, A., David, M. R., Chouin-Carneiro, T., Van den Wouwer, L., et al. (2018). The impact of the age of first blood meal and Zika virus infection on *Aedes aegypti* egg production and longevity. *PLoS One* 13:e0200766. doi: 10.1371/journal.pone.0200766

Phillips, D. R., and Clark, K. D. (2017). *Bombyx mori* and *Aedes aegypti* form multi-functional immune complexes that integrate pattern recognition, melanization, coagulants, and hemocyte recruitment. *PLoS One* 12:e0171447. doi: 10.1371/journal.pone.0171447

Pickett, B. E., Sadat, E. L., Zhang, Y., Noronha, J. M., Squires, R. B., Hunt, V., et al. (2012). ViPR: an open bioinformatics database and analysis resource for virology research. *Nucleic Acids Res.* 40, D593–D598. doi: 10.1093/nar/gkr859

Poddar, S. K., Sifat, A. E., Haque, S., Nahid, N. A., Chowdhury, S., and Mehedi, I. (2019). Nicotinamide mononucleotide: exploration of diverse therapeutic applications of a potential molecule. *Biomolecules* 9:34. doi: 10.3390/biom9010034

Predel, R., Neupert, S., Garczynski, S. F., Crim, J. W., Brown, M. R., Russell, W. K., et al. (2010). Neuropeptidomics of the mosquito *Aedes aegypti*. *J. Proteome Res.* 9, 2006–2015. doi: 10.1021/pr901187p

Rauniyar, N., and Yates, J. R. (2014). Isobaric labeling-based relative quantification in shotgun proteomics. *Proteome Res.* 13, 5293–5309. doi: 10.1021/pr500880b

Rexer, T., Laaf, D., Gottschalk, J., Frohnmeyer, H., Rapp, E., and Elling, L. (2020). "Enzymatic synthesis of glycans and glycoconjugates," in *Advances in Biochemical Engineering/Biotechnology*, (Berlin: Springer), 1–50. doi: 10.1007/10_2020_148

Ribeiro, J. M. C., Martin-Martin, I., Arcà, B., and Calvo, E. (2016). A deep insight into the sialome of male and female *Aedes aegypti* mosquitoes. *PLoS One* 11:e0151400. doi: 10.1371/journal.pone.0151400

Ryan, P. A., Turley, A. P., Wilson, G., Hurst, T. P., Retzki, K., Brown-Kenyon, J., et al. (2020). Establishment of wMel Wolbachia in *Aedes aegypti* mosquitoes and reduction of local dengue transmission in cairns and surrounding locations in northern Queensland, Australia. *Gates Open Res.* 3:1547. doi: 10.12688/gatesopenres.13061.2

Schmid, M. A., Kauffman, E., Payne, A., Harris, E., and Kramer, L. D. (2017). Preparation of mosquito salivary gland extract and intradermal inoculation of mice. *Bio Protocol* 7:e2407.

Selivanov, V. A., Zeak, J. A., Roca, J., Cascante, M., Trucco, M., and Votyakova, T. V. (2008). The role of external and matrix pH in mitochondrial reactive oxygen species generation. *J. Biol. Chem.* 283, 29292–29300. doi: 10.1074/jbc.M801019200

Serteyn, L., Ponnet, L., Saive, M., Fauconnier, M.-L., and Francis, F. (2020). Changes of feeding behavior and salivary proteome of Brown Marmorated Stink Bug when exposed to insect-induced plant defenses. *Arthropod-Plant Interact.* 14, 101–112. doi: 10.1007/s11829-019-09718-8

Shrinet, J., Bhavesh, N. S., and Sunil, S. (2018). Understanding oxidative stress in aedes during chikungunya and dengue virus infections using integromics analysis. *Viruses* 10:314. doi: 10.3390/v10060314

Słocińska, M., Chowański, S., and Marciniak, P. (2020). Identification of sulfakinin receptors (SKR) in *Tenebrio molitor* beetle and the influence of sulfakinins on carbohydrates metabolism. *J. Comp. Physiol. B* 190, 669–679. doi: 10.1007/s00360-020-01300-6

Stark, K. R., and James, A. A. (1998). Isolation and characterization of the gene encoding a novel factor xa-directed anticoagulant from the yellow fever mosquito, *Aedes aegypti*. *J. Biol. Chem.* 273, 20802–20809. doi: 10.1074/jbc.273.33.20802

Sterkel, M., Perdomo, H. D., Guizzo, M. G., Barletta, A. B. F., Nunes, R. D., Dias, F. A., et al. (2016). Tyrosine detoxification is an essential trait in the life history of blood-feeding arthropods. *Curr. Biol.* 26, 2188–2193. doi: 10.1016/j.cub.2016.06.025

Stick, R. V., and Williams, S. J. (2009). "Chapter 11 - Glycoproteins and proteoglycans," in *Carbohydrates: The Essential Molecules of Life (Second Edition)*, eds R. V. Stick and S. J. Williams (Oxford: Elsevier), 369–412.

Supek, F., Bošnjak, M., Škunca, N., and Šmuc, T. (2011). REVIGO summarizes and visualizes long lists of gene ontology terms. *PLoS One* 6:e21800. doi: 10.1371/journal.pone.0021800

The Uniprot Consortium (2019). UniProt: a worldwide hub of protein knowledge. *Nucleic Acids Res.* 47, D506–D515. doi: 10.1093/nar/gky1049

Toufeeq, S., Wang, J., Zhang, S.-Z., Li, B., Hu, P., Zhu, L.-B., et al. (2019). Bmserpin2 is involved in BmNPV infection by suppressing melanization in *Bombyx mori*. *Insects* 10:399. doi: 10.3390/insects10110399

Troupin, A., Londono-Renteria, B., Conway, M. J., Cloherty, E., Jameson, S., Higgs, S., et al. (2016). A novel mosquito ubiquitin targets viral envelope protein for degradation and reduces virion production during dengue virus infection. *Biochim. Biophys. Acta Gen. Subj.* 1860, 1898–1909. doi: 10.1016/j.bbagen.2016.05.033

Turley, A. P., Moreira, L. A., O'Neill, S. L., and McGraw, E. A. (2009). Wolbachia infection reduces blood-feeding success in the dengue fever mosquito, *Aedes aegypti*. *PLoS Negl. Trop. Dis.* 3:e516. doi: 10.1371/journal.pntd.0000516

Tyanova, S., Temu, T., Sinitcyn, P., Carlson, A., Hein, M. Y., Geiger, T., et al. (2016). The Perseus computational platform for comprehensive analysis of (prote)omics data. *Nat. Methods* 13, 731–740. doi: 10.1038/nmeth.3901

Vasconcellos, A. F., Mandacaru, S. C., de Oliveira, A. S., Fontes, W., Melo, R. M., de Sousa, M. V., et al. (2020). Dynamic proteomic analysis of *Aedes aegypti* Aag-2 cells infected with Mayaro virus. *Parasit. Vect.* 13:297. doi: 10.1186/s13071-020-04167-2

Wang, X., Zhang, Y., Zhang, R., and Zhang, J. (2019). The diversity of pattern recognition receptors (PRRs) involved with insect defense against pathogens. *Curr. Opin. Insect Sci.* 33, 105–110. doi: 10.1016/j.cois.2019.05.004

Wasinpiyamongkol, L., Patramool, S., Luplertlop, N., Surasombatpattana, P., Doucoure, S., Mouchet, F., et al. (2010). Blood-feeding and immunogenic *Aedes aegypti* saliva proteins. *Proteomics* 10, 1906–1916. doi: 10.1002/pmic.200900626

White, P. M., Serbus, L. R., Debec, A., Codina, A., Bray, W., Guichet, A., et al. (2017). Reliance of Wolbachia on high rates of host proteolysis revealed by a genome-wide RNAi screen of Drosophila cells. *Genetics* 205, 1473–1488. doi: 10.1534/genetics.116.198903

Xi, Z., Ramirez, J. L., and Dimopoulos, G. (2008). The *Aedes aegypti* toll pathway controls dengue virus infection. *PLoS Pathog.* 4:e1000098. doi: 10.1371/journal.ppat.1000098

Yin, C., Sun, P., Yu, X., Wang, P., and Cheng, G. (2020). Roles of symbiotic microorganisms in arboviral infection of arthropod vectors. *Trends Parasitol.* 36, 607–615. doi: 10.1016/j.pt.2020.04.009

Zels, S., Dillen, S., Crabbé, K., Spit, J., Nachman, R. J., and Vanden Broeck, J. (2015). Sulfakinin is an important regulator of digestive processes in the migratory locust, *Locusta migratoria*. *Insect Biochem. Mol. Biol.* 61, 8–16. doi: 10.1016/j.ibmb.2015.03.008

Zug, R., and Hammerstein, P. (2015). Wolbachia and the insect immune system: what reactive oxygen species can tell us about the mechanisms of Wolbachia–host interactions. *Front. Microbiol.* 6:1201. doi: 10.3389/fmicb.2015.01201

Conflict of Interest: The authors declare that the research was conducted in the absence of any commercial or financial relationships that could be construed as a potential conflict of interest.

frontiers in Physiology

ORIGINAL RESEARCH
published: 25 February 2021
doi: 10.3389/fphys.2021.633093

"Urate and NOX5 Control Blood Digestion in the Hematophagous Insect *Rhodnius prolixus*"

Ana Caroline P. Gandara[1], Felipe A. Dias[1], Paula C. de Lemos[1], Renata Stiebler[1], Ana Cristina S. Bombaça[2], Rubem Menna-Barreto[2] and Pedro L. Oliveira[1,3]**

[1] Instituto de Bioquímica Médica Leopoldo de Meis, Universidade Federal do Rio de Janeiro, Rio de Janeiro, Brazil, [2] Instituto Oswaldo Cruz, Rio de Janeiro, Brazil, [3] Instituto Nacional de Ciência e Tecnologia em Entomologia Molecular, Rio de Janeiro, Brazil

Low levels of reactive oxygen species (ROS) are now recognized as essential players in cell signaling. Here, we studied the role of two conserved enzymes involved in redox regulation that play a critical role in the control of ROS in the digestive physiology of a blood-sucking insect, the kissing bug *Rhodnius prolixus*. RNAi-mediated silencing of *RpNOX5* and *RpXDH* induced early mortality in adult females after a blood meal. Recently, a role for *RpNOX5* in gut motility was reported, and here, we show that midgut peristalsis is also under the control of *RpXDH*. Together with impaired peristalsis, silencing either genes impaired egg production and hemoglobin digestion, and decreased hemolymph urate titers. Ultrastructurally, the silencing of *RpNOX5* or *RpXDH* affected midgut cells, changing the cells of blood-fed insects to a phenotype resembling the cells of unfed insects, suggesting that these genes work together in the control of blood digestion. Injection of either allopurinol (an XDH inhibitor) or uricase recapitulated the gene silencing effects, suggesting that urate itself is involved in the control of blood digestion. The silencing of each of these genes influenced the expression of the other gene in a complex way both in the unfed state and after a blood meal, revealing signaling crosstalk between them that influences redox metabolism and nitrogen excretion and plays a central role in the control of digestive physiology.

Keywords: urate, NADPH oxidase, ROS, blood digestion, *Rhodnius prolixus*

OPEN ACCESS

Edited by:
Jose Luis Ramirez, United States Department of Agriculture (USDA), United States

Reviewed by:
Marcela Barbosa Figueiredo, Swansea University, United Kingdom
Leonardo Luis Fruttero, National University of Córdoba, Argentina

****Correspondence:***
Ana Caroline P. Gandara
acpgandara@gmail.com
Pedro L. Oliveira
pedro@bioqmed.ufrj.br

Specialty section:
This article was submitted to Invertebrate Physiology, a section of the journal Frontiers in Physiology

Received: *24 November 2020*
Accepted: *27 January 2021*
Published: *25 February 2021*

Citation:
Gandara ACP, Dias FA, de Lemos PC, Stiebler R, Bombaça ACS, Menna-Barreto R and Oliveira PL (2021) "Urate and NOX5 Control Blood Digestion in the Hematophagous Insect Rhodnius prolixus". Front. Physiol. 12:633093. doi: 10.3389/fphys.2021.633093

INTRODUCTION

Reactive oxygen species (ROS) control many processes, from gene expression and protein translation to metabolism and cell signaling, and the NAD, NADP and thiol/disulfide systems are important for ROS signaling (Jones and Sies, 2015). ROS are produced in different parts of the cell and modulate key target functions *via* the oxidative modification of redox-sensitive essential proteins and alterations in redox homeostasis that are associated with many different disease conditions (Holmström and Finkel, 2014; Sies, 2017; Bardaweel et al., 2018).

NADPH oxidases (NOXes) are one of the major sources of cellular ROS, and they are still the focus of extensive research interest due to their exclusive function in producing ROS under normal physiological conditions. Arthropods have three NOX types (Gandara et al., 2017): NOX4-art, an arthropod-specific p22-*phox*-independent NOX4, and two calcium-dependent enzymes, DUOX,

which produces hydrogen peroxide (De Deken et al., 2002; Dias et al., 2013), and NOX5, which produces superoxide (Bánfi et al., 2001; Montezano et al., 2018). In the gut, DUOX-dependent ROS production from bacteria-stimulated *Drosophila melanogaster* mucosa is an important pathogen-killing mechanism (Ha et al., 2005) and can increase defecation as a defense response (Du et al., 2016). *Rhodnius prolixus* only has calcium-activated DUOX and NOX5, which are involved in eggshell hardening and gut motility, respectively, in this insect (Dias et al., 2013; Montezano et al., 2018).

Xanthine dehydrogenase (XDH) is widely distributed in metazoan organisms and catalyzes the reduction of NAD coupled to the successive oxidation of hypoxanthine to xanthine and xanthine to urate (Wang et al., 2016), in accordance with urate being the main nitrogen metabolism end-product of insects (Wigglesworth, 1931; Barrett and Friend, 1966, 1970; Briegel, 1986). In addition to this key role in nitrogen excretion, urate is an important regulator of redox balance (Hilliker et al., 1992). In *R. prolixus*, urate is the major antioxidant present in the hemolymph, where high concentrations (>5 mM) are attained after a blood meal (Souza et al., 1997).

The most canonical signaling pathway in the regulation of digestion in blood-feeding insects acts through the activation of neurons and endocrine cells in response to mechanical stimuli or nutrients (Thomsen and Muller, 1959; Maddrell, 1964; Persaud and Davey, 1971; Maddrell and Gardiner, 1975; Cole and Gillett, 1979; Houseman and Downe, 1983; Wu et al., 2020). The ingested blood induces proteinase production and nutrient uptake (Garcia and Garcia, 1977; Sanders et al., 2003; Henriques et al., 2017) to promote its own retention in the midgut (Caroci and Noriega, 2003) and to control ROS production in the gut (Oliveira et al., 2011; Gandara et al., 2016). The anterior midgut (AM) is involved in hemolysis, ion and water transport, carbohydrate digestion and glycogen and lipid storage (Billingsley, 1990; Vieira et al., 2015; Henriques et al., 2017). Once hemolysis starts in the AM (De Azambuja et al., 1983), hemoglobin and other proteins start being sent to the posterior midgut (PM), which stimulates proteinase activity (Garcia and Garcia, 1977). In the PM, high proteinase activity produces amino acids and heme (as byproducts of hemoglobin degradation), which are released to the hemolymph (Wigglesworth, 1943; Barrett, 1974) to be delivered to the ovaries for the production of yolk proteins during vitellogenesis (Atella et al., 2005). However, the cellular and molecular mechanisms underlying these sensory and physiological functions are poorly understood (LaJeunesse et al., 2010; Du et al., 2016).

In recent years, a significant research effort has focused on the function of intestinal ROS (Aviello and Knaus, 2018), in most cases, in gut immunity. Relatively little is known about the role of ROS in digestion and how host metabolic factors control the redox state and redox signaling. Blood-sucking insects ingest blood meals that are several-fold their weights before feeding. Vertebrate blood is comprised of 85% protein (dry weight), and the most abundant protein is hemoglobin. Therefore, these animals present a unique situation regarding nitrogen and redox metabolism, as large amounts of both amino acids and heme (a pro-oxidant molecule) are produced during the digestion of a blood meal (Graça-Souza et al., 2006; Sterkel et al., 2017). Here, while studying the roles of a ROS-producing enzyme (*RpNOX5*) and an antioxidant-producing enzyme (*RpXDH*), we identified blood ingestion-induced signaling mechanisms associated with changes in redox metabolism in a physiology insect model, the triatomine *R. prolixus*.

MATERIALS AND METHODS

Insects and Ethics Statement

All animal care and experimental protocols were conducted in accordance with the guidelines of the Committee for Evaluation of Animal Use for Research (Universidade Federal do Rio de Janeiro, CAUAP-UFRJ) and the NIH Guide for the Care and Use of Laboratory Animals (ISBN 0-309-05377-3). Protocols were approved by CAUAP-UFRJ under registry #IBQM 149-9. Dedicated technicians in the animal facility at the Instituto de Bioquímica Médica Leopoldo de Meis (UFRJ) carried out all protocols related to rabbit husbandry under strict guidelines, with supervision of veterinarians to ensure appropriate animal handling. *R. prolixus* colony was maintained at 28°C and 70–80% relative humidity, and the insects used were adult mated females fed rabbit blood at 3-week intervals.

Identification of the *RpNOX5* and *RpXDH* Genes

A local BLAST search using the cDNA sequences of NOX5 and XDH as queries was used to identify NOX5 and XDH sequences in the *R. prolixus* transcriptome (Ribeiro et al., 2014). These partial cDNAs were used to identify the full-length transcripts of NOX5 (RPRC008329) and XDH (RPRC011533) in the *R. prolixus* genome database available at VectorBase (Version RproC3) (Mesquita et al., 2015).

RpNOX5 and *RpXDH* Structures

Transmembrane α-helices were predicted using the TMHMM server v.2.0, available from the Center for Biological Sequence Analysis, and the amino acid residue hydrophobicity profile was analyzed (Kyte and Doolittle, 1982). The alignments were performed with ClustalW software (Larkin et al., 2007), using the following sequences: *Acyrthosiphon pisum* (NOX5, Gene ID 328705704 and XDH, Gene ID 328699235), *Anopheles gambiae* (NOX5, Gene ID 158297105 and XDH, Gene ID 118789655), *Drosophila melanogaster* (NOX5, Gene ID 161077140 and XDH, Gene ID 17737937) and *Homo sapiens* (NOX5, Gene ID 74717091 and XDH, Gene ID 91823271). The positions of conserved domains and residues were identified at Pfam[1] and edited in GeneDoc (Nicholas and Nicholas, 1997).

RNA Extraction, Conventional PCR, and qPCR

Total RNA was extracted from tissues using TRIzol (Invitrogen) according to the manufacturer's protocol. RNA was treated with

[1]http://pfam.sanger.ac.uk/

RNase-free DNase I (Fermentas International Inc., Canada), and cDNA was synthesized using the High-Capacity cDNA Reverse Transcription kit (Applied Biosystems, United States). cDNA from the salivary glands, heart, Malpighian tubules, anterior midgut, posterior midgut, hindgut, fat body, cerebrum, flight muscle and ovary was PCR-amplified using PCR master mix (Fermentas International Inc., Canada), and the same primers were used for qPCR (described below). The fragments were separated by agarose gel electrophoresis (2% w/v), and their sizes were compared with GeneRulerTM 100 bp Plus DNA ladder fragments (Fermentas International Inc., Canada). qPCR was performed on a StepOnePlus real-time PCR system (Applied Biosystems, United States) using Power SYBR Green PCR master mix (Applied Biosystems, United States). The comparative Ct method (Livak and Schmittgen, 2001) was used to compare gene expression levels. The *R. prolixus EF-1 S* rRNA gene (RPRC015041) was used as an endogenous control (Majerowicz et al., 2011). The primer pairs used for the amplification of the NOX5, XDH and EF-1 cDNA fragments for both conventional and real-time PCR, named NOX5Rt, XDHRt and EF1Rt, respectively, are described in **Supplementary Table 1**.

RNAi Experiments

To investigate the function of *RpXDH* and *RpNOX5*, gene silencing was performed by injecting dsRNA into the insect hemocoel. A 457-bp fragment from the *RpNOX5* gene and a 461-bp fragment from the *RpXDH* gene were amplified from reverse-transcribed RNAs extracted from *R. prolixus* tissues using the primer pairs NOX5Ds1 and XDHDs1, respectively. The amplification products were subjected to nested PCR with an additional pair of primers (NOX5Ds2 and XDHDs2) that included the T7 promoter sequence in each fragment. The primers mentioned above are described in **Supplementary Table 1**. The nested PCRs generated 497-bp and 444-bp fragments of *RpNOX5* and *RpXDH*, respectively. These fragments were used as a template to synthesize double-stranded RNA (dsRNA) specific for *RpNOX5* (dsNOX5) and *RpXDH* (dsXDH) using the MEGAscript RNAi kit (Ambion, United States) according to the manufacturer's protocol. An unrelated dsRNA (dsMal) specific for the *Escherichia coli* MalE gene (Gene ID 948538) was used as a control for the off-target effects of dsRNA. The Mal fragment was amplified from the Litmus 28i-mal plasmid (New England Biolabs, United States) with a single primer (T7, 5-TAATACGACTCACTATAGGG-3) specific for the T7 promoter sequence that is on both sides of the MalE sequence. 21–22 days after the first blood feeding as adults, females were injected in the hemocoel with 1 μL of sterile distilled water containing 1 mg/mL dsRNA using a 5 μL Hamilton syringe. Six days after dsRNA injection, the insects were fed rabbit blood (blood-fed condition) or just dissected (unfed condition).

Images and Video Acquisition of Gut Contractions

Insects were dissected 7 days after a blood meal (ABM), and the midguts were photographed. After removing the wings and legs, water drops were placed on the dorsal surface of the abdominal cuticle to improve the visualization of the movements of internal organs in the live insects, and 2-minute videos were acquired, as previously published (Montezano et al., 2018). Squares containing areas with partial visualization of the AM close to an ovary were selected. Using the Multimeasure option in ImageJ, the ratio of the dark areas (AM) to the white areas (ovary) was extracted and plotted against time to evaluate peristaltic movement (referred to as peristaltic contraction amplitude).

Hemoglobin Quantification

AMs were dissected just after the blood meal (between 0.5–2 h), 4 days and 7 days ABM and homogenized in 250 μL of PBS (10 mM Na–phosphate, 0.15 M NaCl, pH 7.4). Hemoglobin content was assayed with a colorimetric kit (K023 kit, Bioclin, Brazil) based on the Drabkin method (Drabkin and Austin, 1935), according to the manufacturer's protocol. The absorbance of the supernatants was read at 540 nm with a plate spectrophotometer (Spectramax M3, Molecular Devices, United States).

Heme Quantitation

Quantitation of total heme was performed by the alkaline pyridine method (Falk, 1964) using the extinction values of the subtraction spectra (reduced-oxidized heme spectra). The posterior midguts and hindguts were collected individually and homogenized in 1 mL of 0.1 M NaOH. The tubes were centrifuged for 10 min at 15,000 × *g*, and the supernatants were collected. An aliquot of 10 μL of supernatant was added to 190 μL of 0.1 M NaOH, 200 μL of distilled water and 500 μL of alkaline pyridine solution [20% (v/v) 1 M NaOH, 48% (v/v) pyridine, 32% (v/v) water]. Visible light spectra were collected (500–600 nm) using a Shimadzu UV-2550 spectrophotometer (Japan) before and after the samples were reduced with sodium dithionite.

Urate Quantification

Hemolymph (3 μL) was collected 4 days ABM, in the presence of phenylthiourea, diluted with 12 μL of ultrapure water and used immediately for assays in 96-well plates, according to the guidelines of the colorimetric kit (Doles, Brazil), based on the uricase reaction coupled to H_2O_2 4-aminoantipyrine oxidation by peroxidase (Barham and Trinder, 1972). Samples were incubated at 37°C for 30 min and read at 520 nm with a plate spectrophotometer (Spectra Max M3, Molecular Devices, United States).

Ex vivo ROS Microscopy Assays

As previously described (Gandara et al., 2016), the wings, legs and dorsal plaques were removed. Initially, to assess ROS levels, the hemolymph was replaced with a 50 μM solution of the oxidant-sensitive fluorophore dihydroethidium (hydroethidine, DHE) (Invitrogen, United States) in L15 medium culture (Gibco, United States) containing 5% (v/v) fetal bovine serum. The samples were incubated in the dark at 28°C for 20 min. Then, the midguts were washed with 0.15 M NaCl and immediately transferred to a glass slide for fluorescence microscopy analysis. Quantitative evaluation of fluorescence was performed using a 20 X objective and 100-ms exposure with a Zeiss Observer Z1

(Germany) with a Zeiss Axio Cam MrM Zeiss. The data were analyzed using AxioVision version 4.8 software. The #15 filter set (excitation BP, 546/12 nm; beam splitter FT, 580 nm; emission LP, 590 nm) was used for DHE labeling.

Transmission Electron Microscopy

Rhodnius prolixus AMs and PMs were dissected without feeding or 4 days ABM and fixed with 2.5% glutaraldehyde in 0.1 M Na-cacodylate buffer (pH 7.2) at room temperature for 1 h at 25°C and postfixed with a solution of 1% OsO_4, 0.8% potassium ferricyanide and 2.5 mM $CaCl_2$ in the same buffer for 1 h at 25°C. The samples were dehydrated in an ascending acetone series and embedded in five steps in PolyBed 812 resin (1:3, 1:1, 1:2, 2:3, and pure resin). Ultrathin sections were stained with uranyl acetate and lead citrate and examined with a Jeol JEM1011 transmission electron microscope (Japan) at Plataforma de Microscopia Eletrônica in Fundação Oswaldo Cruz.

Allopurinol and Uricase Injections

Allopurinol (Sigma, United States) or uricase (Sigma, United States) was dissolved in *R. prolixus* physiological saline containing 130 mM NaCl, 8.6 mM KCl, 8.3 mM $MgCl_2$, 10.2 mM $NaHCO_3$, 4.3 mM Na_2HPO_4, 34 mM glucose, and 2 mM $CaCl_2$ (Maddrell, 1969). The allopurinol solution needed to be heated at 50°C in a dry bath for several minutes to ensure complete dissolution. Three days before the blood meal, unfed insects were injected with 40 μg of allopurinol or 1 U of uricase using a Hamilton syringe, and the insects were dissected 4 days ABM. Control insects received *R. prolixus* saline only.

Intestinal Microbiota Evaluation

Whole homogenates of individual AM or PM were serially diluted, plated on BHI agar and kept at 28°C for 7 days, after which the number of colonies was evaluated. In insects from our colony, *Rhodococcus rhodnii* is the only cultivable bacterium that grows on culture plates.

Statistical Analysis

All experiments were repeated at least twice, and statistical analyses were performed using GraphPad Prism.

RESULTS

Structural Features and Domains of *RpXDH* and *RpNOX5*

R. prolixus NOX5 and XDH, hereafter called *RpNOX5* and *RpXDH*, respectively, were initially found in a digestive apparatus transcriptome analysis (Ribeiro et al., 2014), and full-length predicted CDSs were identified in the genome (Mesquita et al., 2015) (**Supplementary Figures 1**, **2**). **Supplementary Figure 3** shows the characteristic domains (EF-hand, transmembrane and NOX domains) of *RpNOX5*, which are conserved among all NOX5 orthologs (Kawahara et al., 2007) and *RpXDH* also has all canonical XDH domains.

RpNOX5 or *RpXDH* Silencing Induces Early Mortality

RpXDH and *RpNOX5* mRNA were expressed in all tissues tested (**Supplementary Figure 4**). Efficient *RpNOX5* silencing was achieved before blood meal (by six days after *RpNOX5* dsRNA injection) but this effect was transient, and *RpNOX5* expression level recovered to control values at 4 days ABM). *RpXDH* silencing was achieved only by 4 days after a blood meal (**Supplementary Figure 5**). However, both *RpNOX5* or *RpXDH* silencing by RNAi induced early mortality in blood-fed adult females (**Figure 1**), revealing essential roles of both enzymes.

RpNOX5 or *RpXDH* Silencing Impairs Blood Digestion

RpXDH or RpNOX5 silencing impaired egg development (almost no eggs were laid by silenced insects – data not shown) (**Figure 2A**) and AM peristalsis (**Figure 2C**). We also observed reduced PM content and very commonly the hindgut was enlarged and with a yellowish content in silenced animals (**Figure 2B**), but diuresis was not evaluated. In triatomine insects, no blood digestion occurs in the AM; blood proteins are kept undigested in the AM and are gradually transferred to the PM, where protein degradation is accomplished by means of cysteinic and aspartic proteinases, resulting in the release of heme from hemoglobin (Houseman and Downe, 1982). The silencing of *RpXDH or RpNOX5* produced a marked decrease in blood meal digestion, as revealed both by using the progressive reduction in hemoglobin content of the AM as a proxy for the pace of blood meal digestion (**Figure 3A**) or accumulation of heme in the PM and hindgut (**Figure 3B**). Overall, virtually identical phenotypes were obtained by the individual silencing of *RpXDH*

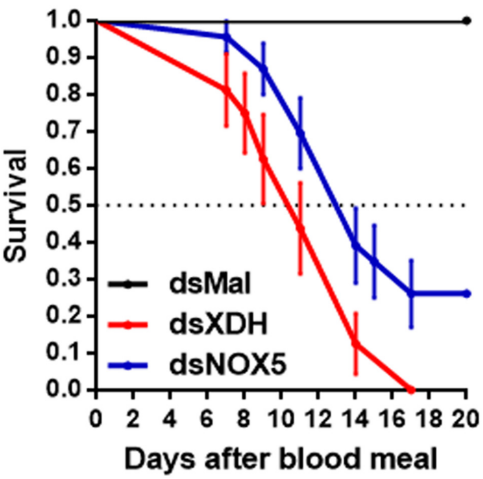

FIGURE 1 | *RpNOX5* or *RpXDH* silencing induces early mortality in adult *R. prolixus* after a blood meal. Insects were fed rabbit blood, and dead individuals were counted daily. The horizontal dotted line represents 50% survival (n = 16–23 insects). $P < 0.0001$ for dsXDH- and dsNOX5-injected animals compared with dsMal-injected animals. Mantel-Cox and Gehan-Breslow-Wilcoxon test. The data represent the mean ± SEM.

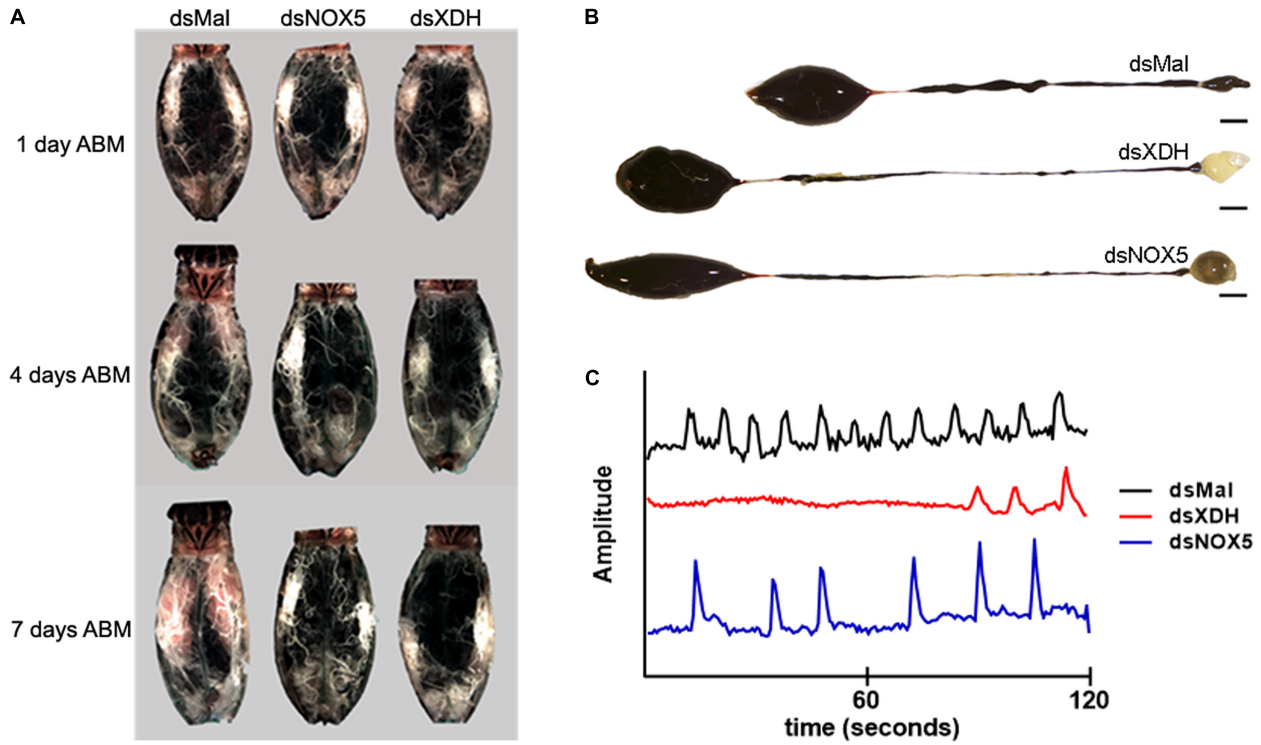

FIGURE 2 | *RpNOX5* and *RpXDH* gene products affect midgut peristalsis. Insects were dissected 1, 4-, or 7-days ABM, and the organs were imaged. **(A)** The ovaries of silenced insects did not develop eggs. **(B)** Blood digestion inhibition is evidenced by reduced PM content in silenced insects compared to the control (dsMal). Scale bar: 30 mm. **(C)** The AM peristalsis pattern is altered, and the frequency of contraction is reduced in silenced insects. Representative traces of the relative amplitude of midgut contraction in a time interval of 2 min are shown. The mean frequency of contraction peaks (peaks/2 min, mean ± SEM) were 11.57 ± 1.21 (dsMal), 4.0 ± 1.45 (dsXDH) and 5.32 ± 1.21 (dsNOX5) (14–27 insects).

or *RpNOX5*, suggesting that these genes are involved in the control of blood digestion.

RpNOX5 or *RpXDH* Silencing Causes Cell Damage in Gut

Transmission electron microscopy (TEM) analysis showed that unfed guts are stalled in an apparent autophagy-related structures that are reversed by a blood meal, as shown in the control animals (dsMal) in **Figure 3C**. However, silencing of *RpXDH* or *RpNOX5* led to a similar autophagic phenotype, characterized by loss of cytosolic density, increases in the size and number of autophagosomes, and a recurrent mitochondrial damage, with washed out matrix aspect, loss of cristae, and the presence of concentric membranar structures inside the organelle.

RpNOX5 or *RpXDH* Silencing Results in Altered ROS Levels Without Affecting the Gut Microbiota

As both enzymes are involved in the regulation of redox metabolism, ROS levels were evaluated by means of DHE fluorescence, an oxidant-sensitive probe. Unexpectedly, oxidant levels were higher in both the AM and PM of insects silenced for *RpNOX5*, a ROS-producing enzyme (**Figure 4A**). In contrast, insects silenced for *RpXDH* (an antioxidant-producing enzyme) showed only a trend (without statistical difference) of upregulation in ROS levels in the PM, compared with control insects (**Figure 4A**). As ROS production has been implicated in the control of both pathogens and indigenous microbiota (Ha et al., 2005; Oliveira et al., 2011), we evaluated the effect of *RpNOX5* or *RpXDH* silencing on the *R. prolixus* microbiota, which is known to be dominated by a mutualist symbiont, *R. rhodnii* (Baines, 1956). Despite the increase in ROS levels with *RpNOX5* silencing (**Figure 4A**), the results showed no statistically significant change in the bacterial population in *RpNOX5*-silenced insects compared to the control insects, although we did observe a trend toward an increase in the bacterial population, especially in the AM (**Figure 4B**).

Urate-Mediated Regulation of Blood Digestion

To test whether urate itself could be one of the signals involved in the control of blood digestion, insects were treated with allopurinol, an XDH inhibitor (Elion et al., 1963), or were injected with uricase to enzymatically reduce circulating urate levels. Urate titers in hemolymph decreased in insects with *RpXDH* silencing, as expected but were also markedly reduced after *RpNOX5* silencing (**Figure 5A**). Injection of allopurinol or uricase in the hemocoel 3 days before a

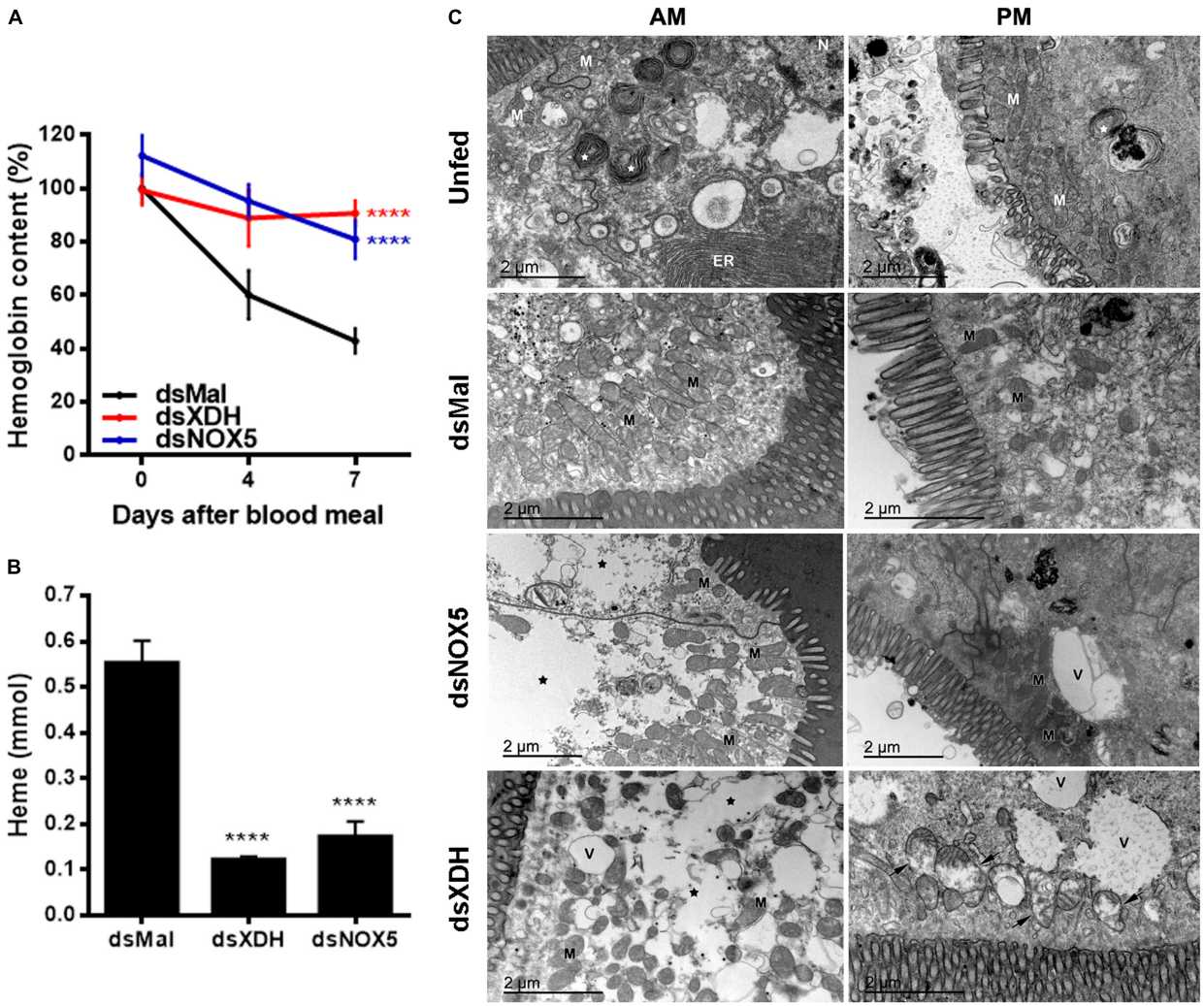

FIGURE 3 | Silencing of *RpNOX 5* or *RpXDH* impairs blood digestion. **(A)** Data show the hemoglobin content of the AM (100% is the hemoglobin content of the AM of control insects (dsMal) 2 h ABM). Insects with gene silencing have more hemoglobin than controls at 7 days ABM (11–24 insects). **(B)** Data show the heme content of the PM (a product of blood digestion) 4 days ABM. dsXDH- and dsNOX5-injected animals presented less heme in the PM than did control insects (9–11 insects per condition). **(C)** AM and PM were dissected before receiving a blood meal (unfed) or 4 days ABM and processed for TEM. *RpNOX5* or *RpXDH* silencing causes cell damage in the gut, with decreased cell density in the AM and mitochondrial injury in the PM. ER, endoplasmic reticulum; V, vacuoles; M, mitochondria; white star, autophagy; black star, loss of cytosolic density; black arrow,: mitochondrial collapse with washed out aspect and loss of cristae as well as the formation of concentric membranar structures inside the organelle (9–24 insects). ****$P < 0.0001$, compared with dsMal-injected animals. One-way ANOVA and Dunnett's or Dunn's multiple comparisons posttest were used. The data represent the mean ± SEM.

blood meal closely recapitulated the gene silencing phenotype (**Figure 2A**), inhibiting blood digestion (**Figure 5B**) and egg production (**Figure 5C**).

RpNOX5 and *RpXDH* Reciprocal Transcriptional Control

In the AM, *RpNOX5* showed reduced levels in the unfed insects and approached control levels at 4 days ABM (**Supplementary Figure 5A**). This transient silencing observed suggests that the signaling action of *RpNOX5* occurs before the 4th day ABM. The interruption of the signaling pathway by RNAi before the canonical signaling provoked by the arrival of blood in the midgut, was sufficient to prevent the triggering of the peristalsis/digestion process and generate a resilient effect. Effective *RpXDH* silencing in the AM was observed only at the later time point (**Supplementary Figure 5B**). The abovementioned similar phenotypes obtained with *RpNOX5* or *RpXDH* silencing led us to hypothesize that these gene products could influence each other's function at the transcriptional level. However, a complex pattern appeared when the effect of *RpXDH* or *RpNOX5* silencing on the expression of the other gene was evaluated; in unfed insects, the silencing of *RpXDH* 6 days beforehand markedly reduced *RpNOX5* expression, and *RpNOX5* silencing also resulted in a slight (non-significant) trend toward an increase in *RpXDH* mRNA levels (**Figure 6**). On the other

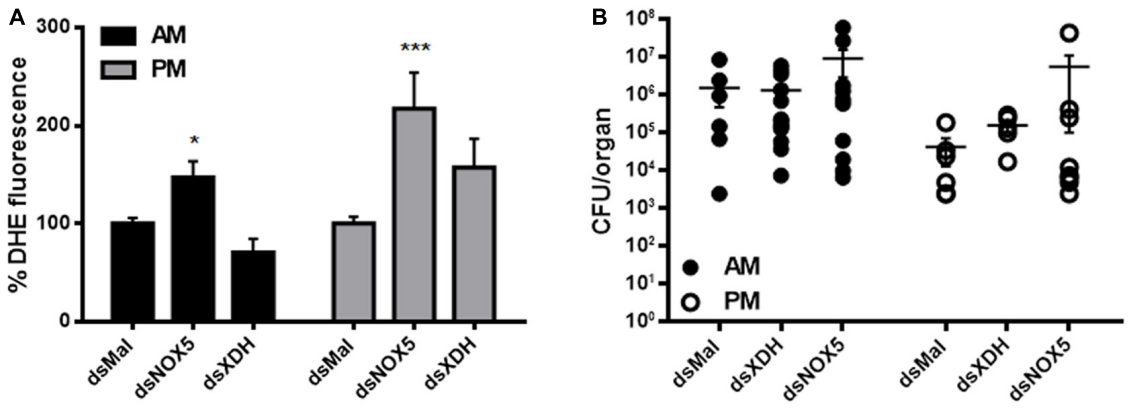

FIGURE 4 | ROS levels were increased in *RpNOX5*-silenced animals without changes in the gut microbiota. **(A)** Midguts of insects dissected 4 days ABM were incubated with 50 μM DHE, and the fluorescence images were analyzed (8–20 insects). $^{*}P < 0.05$, $^{***}P < 0.0001$ compared with dsMal-injected animals. ANOVA and Dunnett's test were used to compare dsMal-injected animals. The data represent the mean ± SEM. **(B)** Evaluation of the cultivable population of *Rhodococcus rhodnii* from blood-fed midguts dissected 4 days ABM (5–13 insects). No significant differences were found. Kruskal-Wallis test, Dunn's multiple comparisons posttest, compared with dsMal-injected animals. AM, anterior midgut; PM, posterior midgut.

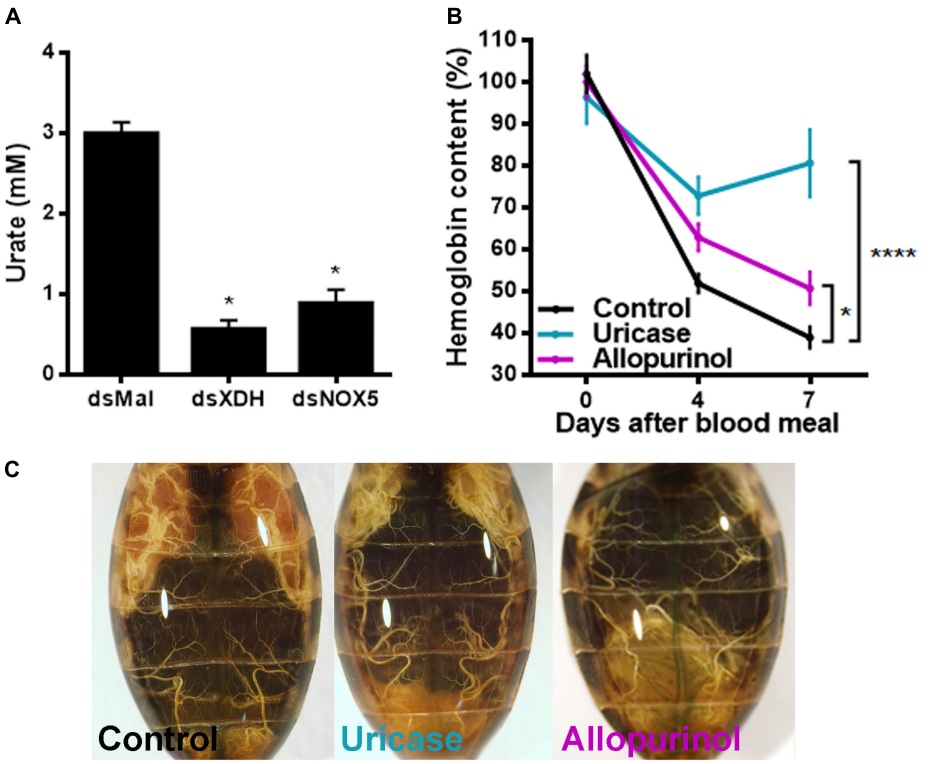

FIGURE 5 | Allopurinol and uricase injection reproduces the phenotype induced by *RpXDH* RNAi. **(A)** Urate concentration in the hemolymph (16 insects per condition). **(B)** Hemoglobin content in anterior midguts. Three days before a blood meal, unfed insects were injected with 40 μg of allopurinol or 1 U of uricase into the hemocoel. Control insects received 10 μL of *R. prolixus* saline (8–49 insects). **(C)** Representatives images of injected animals. $^{*}P < 0.05$; $^{****}P < 0.0001$ compared with dsMal-injected animals **(A)** or saline-injected animals **(B)**. One-way ANOVA and Dunnett's multiple comparisons posttest were used. The data represent the mean ± SEM.

hand, at the later time point (4 days ABM), *RpNOX5*-silenced insects showed reduced *RpXDH* levels, while in the *RpXDH*-silenced insects, the *RpNOX5* levels seemed to have returned to control levels (**Figure 6**).

DISCUSSION

In several animal models, including insects that are important vectors of human disease, both reactive oxygen and nitrogen

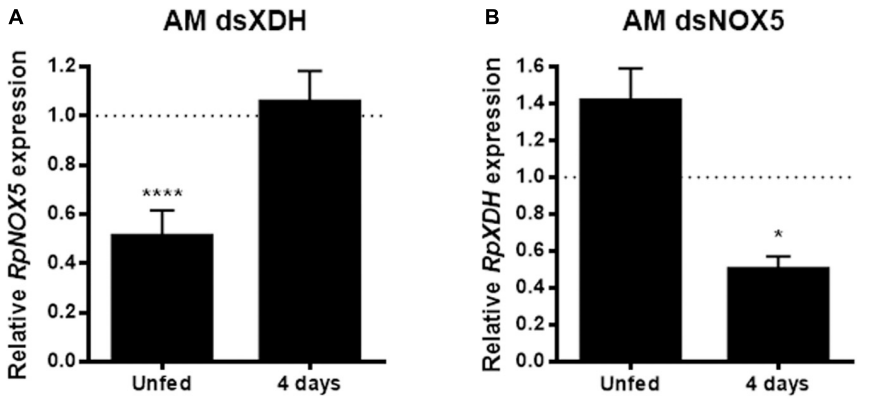

FIGURE 6 | *RpNOX5* and *RpXDH* gene products interfere with each other's expression levels. **(A)** *RpNOX5* and **(B)** *RpXDH* expression levels in the anterior midgut (AM). qPCR assays were performed with individual AMs dissected 6 days after dsRNA injection (unfed) or 4 days ABM. Expression levels were normalized to the level detected in the dsMal-injected animals (9–23 insects). $^*P < 0.0001$ compared with dsMal-injected animals. Unpaired *t*-test. The data represent the mean ± SEM.

species have been implicated as major players in gut immunity. These molecules are known to control both pathogenic and indigenous microbiota and are often described as killing microbes directly or together with other immune mechanisms, such as the insect complement-like protein thioester containing protein (TEP-1) (Oliveira et al., 2012). Here, we studied two enzymes involved in redox balance, the ROS-producing NOX5 enzyme (Bánfi et al., 2001) and an antioxidant enzyme, XDH, which produces the main endogenous ROS-scavenging low-molecular-weight antioxidant in insects (Hilliker et al., 1992; Souza et al., 1997). Our results indicate that urate is an essential signal in the regulation of blood digestion in *R. prolixus* through a mode of action that involves crosstalk between NOX5 and XDH.

Peristaltic contractions move the food along functionally distinct segments of the digestive apparatus and therefore are an essential component of digestive physiology, controlling in this way the pace of digestion. Peristalsis is regulated by neuropeptides in insects (Barrett et al., 1993; Onken et al., 2004; Brugge et al., 2008; Nozawa et al., 2009; LaJeunesse et al., 2010; Villalobos-Sambucaro et al., 2015). In the *D. melanogaster* ovary, NOX5-derived ROS, together with signaling through the proctolin receptor, elevate intracellular calcium, triggering ovarian muscle contraction (Ritsick et al., 2007). A recent report showed a role for NOX5 in the motility of both mammalian smooth muscle and the *R. prolixus* gut, mediated by calcium-calmodulin and endoplasmic reticulum–regulated mechanisms (Montezano et al., 2018).

Here, we show that, in addition to inhibiting peristalsis, *RpNOX5* silencing results in overall digestion impairment and lethality. Efficient silencing of *RpNOX5* was transient, being observed just before the insects were fed, and recovery to normal expression levels was attained by 4 days ABM. This result suggests that the action of *RpNOX5* in the control of digestion is an early event, occurring just after the blood meal and generating a resilient effect that cannot be corrected by reestablishing gene expression levels. Regarding the physiological mechanism behind the severity of the phenotype, one possibility is that these global effects may be a consequence of gut peristalsis inhibition, which delays hemoglobin delivery to the PM, eventually impairing oogenesis. However, our results showed that silencing either *RpNOX5* or *RpXDH* similarly affected cell integrity, including the AM, which is the first segment that receives the incoming blood meal. The arrival of the blood meal in the triatomine midgut is accompanied by large characteristic changes in epithelial cells, which are not seen in the tissues from the *RpNOX5*/*RpXDH*-silenced insects, which display a large number of autophagosomes and damaged mitochondria, despite the presence of blood in their midguts. These changes are reminiscent of those observed in the midgut of *R. prolixus* (Billingsley, 1988) and other triatomine hemipterans that were starved for extended periods of time (Azevedo et al., 2009; Rocha et al., 2010). The appearance of the tissues (as well as other aspects of blood digestion evaluated here) suggests that the insects with either *RpNOX5* or *RpXDH* silencing were not able to trigger a signal for blood digestion, despite the presence of a large blood meal, thus being trapped in a "physiologically unfed status." A fasting state has deleterious effects on mitochondrial health and quality control, which results in the removal of damaged components by autophagy (Liesa and Shirihai, 2013). One limitation of the present study was that autophagy was identified exclusively based on ultrastructural data, and further research using molecular markers for autophagy is needed to clarify this point. This would cause the accumulation of dysfunctional units and an increase in ROS generation, where counterintuitively, *RpNOX5* silencing increased ROS levels in both the anterior and posterior midguts. In line with this scenario, it was shown in this insect that starvation markedly increased mitochondrial ROS production in the gut and that this effect was reversed by blood feeding (Gandara et al., 2016). Therefore, it is possible to speculate that the redox signaling impairment caused by *RpNOX5* or *RpXDH* silencing could lead to increased mitochondrial ROS, decreased urate levels in the hemolymph and nutrient shortage due to inhibition of digestion, which, together, would induce crucial morphological changes that could explain their anticipated deaths.

As ROS production in the gut is involved in the control of indigenous microbiota, alterations in the microbiota might be

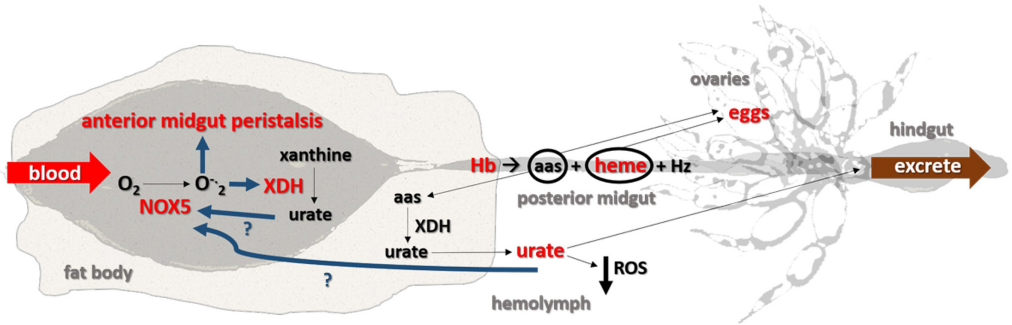

FIGURE 7 | Proposed model. Once blood reaches the anterior midgut, NOX5 is activated, which converts molecular oxygen (O_2) into superoxide (O^{-}_2), stimulates midgut peristalsis and increases XDH expression. Urate in the midgut may stimulate NOX5 activation. Hemoglobin (Hb) in the anterior midgut is then directed to the posterior midgut, where it is digested into amino acids (aas) and heme and later converted to hemozoin (Hz) to be excreted. Amino acids and heme reach the hemolymph and are then delivered to the ovaries to produce eggs. Some of the amino acids derived from a blood meal are converted into urate in the fat body and act as antioxidant in the hemolymph before eventually being excreted as the final byproduct of nitrogen metabolism. Removing urate from the system (by RNAi silencing or pharmacology) impairs redox homeostasis involving XDH and NOX5. The molecules/functions/pathways in red were assessed in this study and increased after a blood meal; the signaling pathways in dark blue are hypothesized and, the components shown in black were obtained from the literature. The organs are not shown into scale.

an alternative explanation for this severe phenotype. However, *RpNOX5* silencing resulted in modest (if any) alterations in the population of the probiotic symbiont. As no other bacterial species were found in the gut (not shown), as in normal symbionts, it seems unlikely that dysbiosis was the cause of the deleterious phenotype.

The role of XDH has already been studied in *Aedes aegypti*, in which XDH silencing resulted in adult mosquito death after a blood meal (Isoe et al., 2017). These researchers interpreted their data as representing the dual role of urate, both as an antioxidant and as the main end-product of nitrogen metabolism. This essential role of XDH in a blood-feeding insect, further highlighted here by the impact of XDH silencing on digestion, has a major physiological implication, as it suggests that nitrogen excretion exerts feedback control over digestive physiology. This is of utmost relevance because proteins account for 85% of the dry-weight composition of vertebrate blood, and therefore, the production of ammonia (and its excretion as urate) is mandatory to allow the use of the carbon skeleton of amino acids for the production of other basic biomolecules (e.g., carbohydrates and lipids) as energy sources and raw material for structural components.

One of the effects of silencing *RpNOX5* that was not obvious was the reduction in urate concentration in the hemolymph. This might be at least in part attributed to the reduction in digestive activity, which could decrease the production of amino acids and then reduce urate formation. However, we also showed that uricase injection can mimic *RpXDH* or *RpNOX5* silencing, which suggests that urate is a necessary signal for maintaining tissue integrity and regulating digestion and proper handling of a blood meal. Considering the findings described above and that the evaluation of the mRNA levels of both enzymes shown here that revealed a complex reciprocal mutual effect between these enzymes, we hypothesize the existence of crosstalk at the transcriptional and posttranscriptional levels between *RpXDH* and *RpNOX5* and their products urate and superoxide.

Taken together, the data obtained here led us to propose that both superoxide produced by NOX5 and urate produced by XDH are signaling molecules with critical roles in the redox regulation of blood digestion in *R. prolixus*. These results are summarized in the scheme presented in **Figure 7**, which highlights the cellular and molecular mechanisms that are involved in the control of blood digestion and contribute to adapt these insects to hematophagy.

DATA AVAILABILITY STATEMENT

The original contributions presented in the study are included in the article/**Supplementary Material**, further inquiries can be directed to the corresponding author/s.

ETHICS STATEMENT

The animal study was reviewed and approved by CAUAP-UFRJ under registry #IBQM 149-9.

AUTHOR CONTRIBUTIONS

PO conceived and coordinated the study. AG and PO designed the experiments and wrote the manuscript. AG performed the experiments shown in **Figures 1**, **2**, **3A**, **4**, **6**, and **Supplementary Figures 1**, **2**, **4**, **5**. FD performed and analyzed the experiment shown in **Figure 5A**, **Supplementary Figure 3**, and **Supplementary Table 1**, and provided technical assistance. PL performed the experiments shown in **Figures 5B,C**, and provided technical assistance. RS performed and analyzed the experiment shown in **Figure 3B**. AG, AB, and RM-B performed and analyzed the experiment shown in **Figure 3C**. All authors analyzed the results and approved the final version of the manuscript.

FUNDING

This work was supported by grants from Conselho Nacional de Desenvolvimento Científico e Tecnológico (CNPq), Coordenação de Aperfeiçoamento de Pessoal de Nível Superior (CAPES), and Fundação de Amparo à Pesquisa do Estado do Rio de Janeiro (FAPERJ).

ACKNOWLEDGMENTS

We would like to thank all members of the Laboratory of Biochemistry of Hematophagous Arthropods, Patricia I.S. Cavalcante, José de S. Lima Junior, Gustavo Ali, Lauriene Severiano, S. R. Cássia, SRD Hob, and F Nur for their technical assistance. We would also like to thank Hatisaburo Masuda and Marcos Horácio Pereira, for helping with the video acquisition protocol. AG would like to dedicate this manuscript to her grandparents Julieta Paiva Ferreira and Alberto Gandara for their full support since she has decided to be a scientist. You will be forever in her heart.

SUPPLEMENTARY MATERIAL

The Supplementary Material for this article can be found online at: https://www.frontiersin.org/articles/10.3389/fphys.2021.633093/full#supplementary-material

REFERENCES

Atella, G. C., Gondim, K. C., Machado, E. A., Medeiros, M. N., and Masuda, H. (2005). Oogenesis and egg development in triatomines. *An. Acad. Bras. Cienc.* 77, 405–430. doi: 10.1590/s0001-37652005000300005

Aviello, G., and Knaus, U. G. (2018). NADPH oxidases and ROS signaling in the gastrointestinal tract. *Mucosal Immunol.* 11, 1011–1023. doi: 10.1038/s41385-018-0021-8

Azevedo, D. O., Neves, C. A., Mallet, J. R., Gonçalves, T. C., Zanuncio, J. C., and Serrão, J. E. (2009). "Notes on midgut ultrastructure of *Cimex hemipterus* (*Hemiptera*: *Cimicidae*). *J. Med. Entomol.* 46, 435–441. doi: 10.1603/033.046.0304

Baines, B. Y. S. (1956). The role of the symbiotic bacteria in the nutrition of *Rhodnius prolixus*. *J. Exp. Biol.* 33, 533–541.

Bánfi, B., Molnár, G., Maturana, A., Steger, K., Hegedûs, B., Demaurex, N., et al. (2001). A Ca2+-activated NADPH oxidase in testis, spleen, and lymph nodes. *J. Biol. Chem.* 276, 37594–37601. doi: 10.1074/jbc.M103034200

Bardaweel, S. K., Gul, M., Alzweiri, M., Ishaqat, A., Alsalamat, H. A., and Bashatwah, R. M. (2018). "Reactive oxygen species: the dual role in physiological and pathological conditions of the human body. *Eurasian J. Med.* 50, 193–201. doi: 10.5152/eurasianjmed.2018.17397

Barham, D., and Trinder, P. (1972). An improved colour reagent for the determination of blood glucose by the oxidase system. *Analyst* 97, 142–145. doi: 10.1039/an9729700142

Barrett, F. M. (1974). Changes in the concentration of free amino acids in the haemolymph of *Rhodnius prolixus* during the fifth instar. *Comp. Biochem. Physiol. B* 48, 241–250. doi: 10.1016/0305-0491(74)90200-4

Barrett, F. M., and Friend, W. G. (1966). Studies on the uric acid concentration the haemolymph of fifth instar larvae of *R prolixus*. *J. Insect Physiol.* 12, 1–7.

Barrett, F. M., and Friend, W. G. (1970). Uric acid synthesis in *Rhodnius prolixus*. *J. Insect Physiol.* 16, 121–129. doi: 10.1016/0022-1910(70)90119-8

Barrett, F. M., Orchard, I., and Tebrugge, V. (1993). Characteristics of serotonin-induced cyclic AMP elevation in the integument and anterior midgut of the blood-feeding bug, *Rhodnius prolixus*. *J. Insect Physiol.* 39, 581–587. doi: 10.1016/0022-1910(93)90040-X

Billingsley, P. F. (1988). Morphometric analysis of *Rhodnius prolixus* Stal (*Hemiptera*: *Reduviidae*). *Tissue Cell* 20, 291–301. doi: 10.1016/0040-8166(88)90050-x

Billingsley, P. F. (1990). The ultrastructure of the midgut of hematophagous insects. *Annu. Rev. Entomol.* 35, 219–248. doi: 10.1146/annurev.en.35.010190.001251

Briegel, H. (1986). Protein catabolism and nitrogen partitioning during oogenesis in the mosquito. *J. Insect Physiol.* 32, 455–462. doi: 10.1016/0022-1910(86)90006-5

Brugge, V. A., Schooley, D. A., and Orchard, I. (2008). Amino acid sequence and biological activity of a calcitonin-like diuretic hormone (DH 31) from *Rhodnius prolixus*. *J. Insect Physiol.* 211, 382–390. doi: 10.1242/jeb.013771

Caroci, A. S., and Noriega, F. G. (2003). Free amino acids are important for the retention of protein and non-protein meals by the midgut of *Aedes aegypti* females. *J. Insect Physiol.* 49, 839–844. doi: 10.1016/S0022-1910(03)00134-3

Cole, S. J., and Gillett, J. D. (1979). The influence of the brain hormone on retention of blood in the mid-gut of the mosquito *Aedes aegypti* (L.). III. The involvement of the ovaries and ecdysone. *Proc. R. Soc. Lond. Biol. Sci.* 205, 411–422. doi: 10.1098/rspb.1979.0074

De Azambuja, P., Guimarães, J. A., and Garcia, E. S. (1983). Haemolytic factor from the crop of *Rhodnius prolixus*: evidence and partial characterization. *J. Insect Physiol.* 29, 833–837. doi: 10.1016/0022-1910(83)90149-X

De Deken, X., Wang, D., Dumont, J. E., and Miot, F. (2002). Characterization of ThOX proteins as components of the thyroid H2O2-generating system. *Exp. Cell Res.* 273, 187–196. doi: 10.1006/excr.2001.5444

Dias, F. A., Gandara, A. C., Queiroz-Barros, F. G., Oliveira, R. L., Sorgine, M. H., Braz, G. R., et al. (2013). Ovarian dual oxidase (Duox) activity is essential for insect eggshell hardening and waterproofing. *J. Biol. Chem.* 288, 35058–35067. doi: 10.1074/jbc.M113.522201

Drabkin, D. L., and Austin, J. H. (1935). Spectrophotometry of HbNO and SHb. *J. Biol. Chem.* 112, 51–65.

Du, E. J., Ahn, T. J., Kwon, I., Lee, J. H., Park, J. H., Park, S. H., et al. (2016). TrpA1 regulates defecation of food-borne pathogens under the control of the duox pathway. *PLoS Genet.* 12:e1005773. doi: 10.1371/journal.pgen.1005773

Elion, B., Callahan, S., Nathan, H., Biebek, S., Rundles, R. W., and Hikhings, G. H. (1963). Potentiation by inhibition of drug degradation. *Biochem. Pharmacol.* 12, 85–93. doi: 10.1016/0006-2952(63)90012-1

Falk, J. E. (1964). *Porphyrins and Metalloporphyrins. Their General, Physical and Coordination Chemistry, and Laboratory Methods*. London: Elsevier Publishing Company.

Gandara, A. C. P., Oliveira, J. H. M., Nunes, R. D., Goncalves, R. L. S., Dias, F. A., Hecht, F., et al. (2016). Amino acids trigger down-regulation of superoxide via TORC pathway in the midgut of *Rhodnius prolixus*. *Biosci. Rep.* 36:e00321. doi: 10.1042/BSR20160061

Gandara, A. C. P., Torres, A., Bahia, A. C., Oliveira, P. L., and Schama, R. (2017). Evolutionary origin and function of NOX4-art, an arthropod specific NADPH oxidase. *BMC Evol. Biol.* 17:92. doi: 10.1186/s12862-017-0940-0

Garcia, E. D., and Garcia, M. L. (1977). Control of protease secretion in the intestine of fifth instar larvae of *Rhodnius prolixus*. *J. Insect Physiol.* 23, 247–251. doi: 10.1016/0022-1910(77)90038-5

Graça-Souza, A. V., Maya-Monteiro, C., Paiva-Silva, G. O., Braz, G. R. C., Paes, M. C., Sorgine, M. H. F., et al. (2006). Adaptations against heme toxicity in blood-feeding arthropods. *Insect Biochem. Mol. Biol.* 36, 322–335. doi: 10.1016/j.ibmb.2006.01.009

Ha, E. M., Oh, C. T., Bae, Y. S., and Lee, W. J. (2005). Immunity a direct role for dual oxidase in drosophila gut immunity. *Science* 310, 847–850. doi: 10.1126/science.1117311

Henriques, B. S., Gomes, B., da Costa, S. G., Moraes, C. D. S., Mesquita, R. D., Dillon, V. M., et al. (2017). Genome wide mapping of peptidases in *Rhodnius prolixus*: identification of protease gene duplications, horizontally transferred proteases and analysis of peptidase A1 structures, with considerations on their role in the evolution of hematophagy in triatomi. *Front. Physiol.* 8:1051. doi: 10.3389/fphys.2017.01051

Hilliker, A. J., Duyf, B., Evans, D., and Phillips, J. P. (1992). Urate-null rosy mutants of *Drosophila melanogaster* are hypersensitive to oxygen stress. *PNAS* 89, 4343–4347. doi: 10.1073/pnas.89.10.4343

Holmström, K. M., and Finkel, T. (2014). Cellular mechanisms and physiological consequences of redox-dependent signalling. *Nat. Rev. Mol. Cell Biol.* 15, 411–421. doi: 10.1038/nrm3801

Houseman, J. G., and Downe, A. E. R. (1982). Characterization of an acidic proteinase from the posterior midgut of *Rhodnius prolixus* Stal (*Hemiptera*: *Reduviidae*). *Insect Biochem.* 12, 651–655. doi: 10.1016/0020-1790(82)90052-X

Houseman, J. G., and Downe, A. E. R. (1983). Activity cycles and the control of four digestive proteinases in the posterior midgut of *Rhodnius prolixus* Stål (*Hemiptera*: *Reduviidae*). *J. Insect Physiol.* 29, 141–148. doi: 10.1016/0022-1910(83)90137-3

Isoe, J., Petchampai, N., Isoe, Y. E., Co, K., Mazzalupo, S., and Scaraffia, P. Y. (2017). Xanthine dehydrogenase-1 silencing in *Aedes aegypti* mosquitoes promotes a blood feeding – induced adulticidal activity. *FASEB* 31, 2276–2286. doi: 10.1096/fj.201601185R

Jones, D. P., and Sies, H. (2015). The redox code. *Antioxid. Redox Signal.* 23, 734–746. doi: 10.1089/ars.2015.6247

Kawahara, T., Quinn, M. T., and Lambeth, J. D. (2007). Molecular evolution of the reactive oxygen-generating NADPH oxidase (Nox/Duox) family of enzymes. *BMC Evol. Biol.* 7:109. doi: 10.1186/1471-2148-7-109

Kyte, J., and Doolittle, R. F. (1982). A simple method for displaying the hydropathic character of a protein. *J. Mol. Biol.* 157, 105–132. doi: 10.1016/0022-2836(82)90515-0

LaJeunesse, D. R., Johnson, B., Presnell, J. S., Catignas, K. K., and Zapotoczny, G. (2010). Peristalsis in the junction region of the *Drosophila* larval midgut is modulated by DH31 expressing enteroendocrine cells. *BMC Physiol.* 10:14. doi: 10.1186/1472-6793-10-14

Larkin, M. A., Blackshields, G., Brown, N. P., Chenna, R., Mcgettigan, P. A., McWilliam, H., et al. (2007). Clustal W and clustal X version 2.0. *Bioinformatics* 23, 2947–2948. doi: 10.1093/bioinformatics/btm404

Liesa, M., and Shirihai, O. S. (2013). Mitochondrial dynamics in the regulation of nutrient utilization and energy expenditure. *Cell Metab.* 17, 491–506. doi: 10.1016/j.cmet.2013.03.002

Livak, K. J., and Schmittgen, T. D. (2001). Analysis of relative gene expression data using real-time quantitative PCR and the 2-ΔΔCT method. *Methods* 25, 402–408. doi: 10.1006/meth.2001.1262

Maddrell, S. H., and Gardiner, B. O. (1975). Induction of transport of organic anions in malpighian tubules of *Rhodnius*. *J. Exp. Biol.* 63, 755–761.

Maddrell, S. H. P. (1964). Excretion in the blood-sucking bug *R prolixus*. *J. Exp. Biol.* 41, 163–176.

Maddrell, S. H. P. (1969). Secretion by the malpighian tubules of *Rhodnius*. The movements of ions and water. *J. Exp. Biol.* 51, 71–97.

Majerowicz, D., Alves-Bezerra, M., Logullo, R., Fonseca-De-Souza, A. L., Meyer-Fernandes, J. R., Braz, G. R. C., et al. (2011). Looking for reference genes for real-time quantitative PCR experiments in *Rhodnius prolixus* (*Hemiptera*: *Reduviidae*). *Insect Mol. Biol.* 20, 713–722. doi: 10.1111/j.1365-2583.2011.01101.x

Mesquita, R. D., Vionette-Amaral, R. J., Lowenberger, C., Rivera-Pomar, R., Monteiro, F. A., Minx, P., et al. (2015). Genome of *Rhodnius prolixus*, an insect vector of chagas disease, reveals unique adaptations to hematophagy and parasite infection. *Proc. Natl. Acad. Sci. U.S.A.* 112, 14936–14941. doi: 10.1073/pnas.1506226112

Montezano, A. C., Camargo, L. L., Persson, P., Rios, F. J., Harvey, A. P., Anagnostopoulou, A., et al. (2018). NADPH oxidase 5 is a pro-contractile nox isoform and a point of cross-talk for calcium and redox signaling-implications in vascular function. *J. Am. Heart Assoc.* 7:e009388. doi: 10.1161/JAHA.118.009388

Nicholas, K. B., and Nicholas, H. B. (1997). *GeneDoc: A Tool for Editing and Annotating Multiple Sequence Alignments*. Available online at: http://www.psc.edu/biomed/genedoc (accessed November 23, 2020).

Nozawa, K., Kawabata-Shoda, E., Doihara, H., Kojima, R., Okada, H., Mochizuki, S., et al. (2009). TRPA1 regulates gastrointestinal motility through serotonin release from enterochromaffin cells. *Proc. Natl. Acad. Sci. U.S.A.* 106, 3408–3413. doi: 10.1073/pnas.0805323106

Oliveira, G. A., Lieberman, J., and Barrillas-Mury, C. (2012). Epithelial nitration by a peroxidase/NOX5 system mediates mosquito antiplasmodial immunity. *Science* 335, 856–859. doi: 10.1126/science.1209678

Oliveira, J. H. M., Gonçalves, R. L. S., Lara, F. A., Dias, F. A., Gandara, A. C. P., Menna-Barreto, R. F. S., et al. (2011). Blood meal-derived heme decreases ROS levels in the midgut of *Aedes aegypti* and allows proliferation of intestinal microbiota. *PLoS Pathog.* 7:e1001320. doi: 10.1371/journal.ppat.1001320

Onken, H., Moffett, S. B., and Moffett, D. F. (2004). The anterior stomach of larval mosquitoes (*Aedes aegypti*): effects of neuropeptides on transepithelial ion transport and muscular motility. *J. Exp. Biol.* 207, 3731–3739. doi: 10.1242/jeb.01208

Persaud, C. E., and Davey, K. G. (1971). The control of proteases synthesis in the intestine of adults of *Rhodnius prolixus*. *J. Insect Physiol.* 17, 1429–1440. doi: 10.1016/0022-1910(71)90152-1

Ribeiro, J. M. C., Genta, F. A., Sorgine, M. H. F., Logullo, R., Mesquita, R. D., Paiva-Silva, G. O., et al. (2014). An Insight into the transcriptome of the digestive tract of the bloodsucking bug, *Rhodnius prolixus*. *PLoS Negl. Trop. Dis.* 8:e2594. doi: 10.1371/journal.pntd.0002594

Ritsick, D. R., Edens, W. A., Finnerty, V., and Lambeth, J. D. (2007). "Nox regulation of smooth muscle contraction. *Free Radic. Biol. Med.* 43, 31–38. doi: 10.1016/j.freeradbiomed.2007.03.006

Rocha, L. L., Neves, C. A., Zanuncio, J. C., and Serrão, J. E. (2010). Digestive cells in the midgut of *Triatoma vitticeps* (Stal, 1859) in different starvation periods. *C. R. Biol.* 333, 405–415. doi: 10.1016/j.crvi.2010.02.001

Sanders, H. R., Evans, A. M., Ross, L. S., and Gill, S. S. (2003). Blood meal induces global changes in midgut gene expression in the disease vector, *Aedes aegypti*. *Insect Biochem. Mol. Biol.* 33, 1105–1122. doi: 10.1016/s0965-1748(03)00124-3

Sies, H. (2017). Hydrogen peroxide as a central redox signaling molecule in physiological oxidative stress: oxidative eustress. *Redox Biol.* 11, 613–619. doi: 10.1016/j.redox.2016.12.035

Souza, A. V., Petretski, J. H., Marilene, D., Bechara, E. J. H., and Oliveira, P. L. (1997). "Urate protects a blood-sucking insect against hemin-induced oxidative stress. *Free Radic. Biol. Med.* 22, 209–214. doi: 10.1016/s0891-5849(96)00293-6

Sterkel, M., Oliveira, J. H. M., Bottino-Rojas, V., Paiva-Silva, G. O., and Oliveira, P. L. (2017). The dose makes the poison?: nutritional overload determines the life traits of blood-feeding arthropods. *Trends Parasitol.* 33, 633–644. doi: 10.1016/j.pt.2017.04.008

Thomsen, E., and Muller, I. B. (1959). Neurosecretion and intestinal proteinase activity in an insect, *Calliphora erythrocepha*/a meig. *Nature* 183, 1401–1402. doi: 10.1038/1831401a0

Vieira, L. R., Polomé, A., Mesquita, R. D., Salmon, D., Braz, G. R., and Bousbata, S. (2015). Protein 2DE reference map of the anterior midgut of the blood-sucking bug *Rhodnius prolixus*. *Proteomics* 15, 3901–3904. doi: 10.1002/pmic.201400472

Villalobos-Sambucaro, M. J., Lorenzo-Figueiras, A. N., Riccillo, F. L., Diambra, L. A., Noriega, F. G., and Ronderos, J. R. (2015). Allatotropin modulates myostimulatory and cardioacceleratory activities in *Rhodnius prolixus* (Stal). *PLoS One* 10:e0124131. doi: 10.1371/journal.pone.0124131

Wang, C. H., Zhang, C., and Xing, X. H. (2016). Xanthine dehydrogenase: an old enzyme with new knowledge and prospects. *Bioengineered* 7, 395–405. doi: 10.1080/21655979.2016.1206168

Wigglesworth, B. Y. V. B. (1931). The physiology of excretion in a blood sucking insect *R prolixus*. *J. Exp. Biol.* 8, 428–441.

Wigglesworth, V. B. (1943). The fate of haemoglobin in *Rhodnius prolixus* (*Hemiptera*) and other blood-sucking arthropods. *Proc. R. Soc. Lond. Biol. Sci.* 131, 313–339. doi: 10.1098/rspb.1943.0010

Wu, K., Li, S., Wang, J., Ni, Y., Huang, W., Liu, Q., et al. (2020). Peptide hormones in the insect midgut. *Front. Physiol.* 11:191. doi: 10.3389/fphys.2020.00191

Conflict of Interest: The authors declare that the research was conducted in the absence of any commercial or financial relationships that could be construed as a potential conflict of interest.

frontiers in Physiology

REVIEW
published: 02 March 2021
doi: 10.3389/fphys.2021.638033

Non-immune Traits Triggered by Blood Intake Impact Vectorial Competence

Octavio A. C. Talyuli[1†], Vanessa Bottino-Rojas[1†‡], Carla R. Polycarpo[1,2], Pedro L. Oliveira[1,2] and Gabriela O. Paiva-Silva[1,2]*

[1] *Instituto de Bioquímica Médica Leopoldo de Meis, Universidade Federal do Rio de Janeiro, Rio de Janeiro, Brazil,* [2] *Instituto Nacional de Ciência e Tecnologia em Entomologia Molecular, Rio de Janeiro, Brazil*

OPEN ACCESS

Edited by:
Aram Megighian, University of Padua, Italy

Reviewed by:
Nazzy Pakpour, California State University, East Bay, United States
Daniele Pereira Castro, Oswaldo Cruz Foundation (Fiocruz), Brazil

***Correspondence:**
Gabriela O. Paiva-Silva
gosilva@bioqmed.ufrj.br

[†] These authors have contributed equally to this work

[‡] Present address:
Vanessa Bottino-Rojas, Department of Microbiology and Molecular Genetics, University of California, Irvine, Irvine, CA, United States

Specialty section:
This article was submitted to Invertebrate Physiology, a section of the journal Frontiers in Physiology

Received: *04 December 2020*
Accepted: *08 February 2021*
Published: *02 March 2021*

Citation:
Talyuli OAC, Bottino-Rojas V, Polycarpo CR, Oliveira PL and Paiva-Silva GO (2021) Non-immune Traits Triggered by Blood Intake Impact Vectorial Competence. Front. Physiol. 12:638033. doi: 10.3389/fphys.2021.638033

Blood-feeding arthropods are considered an enormous public health threat. They are vectors of a plethora of infectious agents that cause potentially fatal diseases like Malaria, Dengue fever, Leishmaniasis, and Lyme disease. These vectors shine due to their own physiological idiosyncrasies, but one biological aspect brings them all together: the requirement of blood intake for development and reproduction. It is through blood-feeding that they acquire pathogens and during blood digestion that they summon a collection of multisystemic events critical for vector competence. The literature is focused on how classical immune pathways (Toll, IMD, and JAK/Stat) are elicited throughout the course of vector infection. Still, they are not the sole determinants of host permissiveness. The dramatic changes that are the hallmark of the insect physiology after a blood meal intake are the landscape where a successful infection takes place. Dominant processes that occur in response to a blood meal are not canonical immunological traits yet are critical in establishing vector competence. These include hormonal circuitries and reproductive physiology, midgut permeability barriers, midgut homeostasis, energy metabolism, and proteolytic activity. On the other hand, the parasites themselves have a role in the outcome of these blood triggered physiological events, consistently using them in their favor. Here, to enlighten the knowledge on vector–pathogen interaction beyond the immune pathways, we will explore different aspects of the vector physiology, discussing how they give support to these long-dated host–parasite relationships.

Keywords: tolerance, vector competence, blood-feeding, immunity, pathogens, parasite–vector interaction, insect physiology, midgut homeostasis

INTRODUCTION

For a long time, the traditional thinking on the insect vector–pathogen interaction described this relationship as impinging a low or even no fitness cost to the insect host (Sisterson, 2009; Powell, 2019). However, the discovery of the insect immune system brought to the scene a plethora of immune genes that were frequently modulated by the infection and, in several cases, the upregulation of these genes promptly reduced pathogen burden (Saraiva et al., 2016; Shaw et al., 2018; Telleria et al., 2018; Matetovici et al., 2019; Salcedo-Porras and Lowenberger, 2019). These findings led to a large number of studies on the immune signaling pathways and immune effector

genes capable of decreasing or blocking pathogen burden and vector competence, which could lead to the possibility of limiting the disease prevalence under field conditions.

The immunology conceptual framework that has dominated the last century is the idea that the capacity to eliminate the infectious agent is the hallmark of the organism's reaction against the infection. This so-called pathogen resistance and the path that eventually leads to health are considered synonymous with the elimination of the infectious agent. However, in the last decade, several studies have directed attention to the ability of organisms to reduce deleterious effects of infections without relying on the elimination of the parasite, but rather acting by alternative mechanisms that could restore tissue homeostasis, reducing self-inflicted damage caused by the host immune reaction or by the pathogen directly (Chovatiya and Medzhitov, 2014). Some early studies have termed this disease endurance (Casadevall and Pirofski, 1999; Graham et al., 2005; Ayres et al., 2008). Later these processes directed to reduce fitness loss due to infection were grouped under the concept of disease tolerance (Medzhitov et al., 2012). The tolerance to disease is highlighted here as a way to fight infection. Mechanistic studies show that a wide variety of processes are implicated in disease tolerance, such as stress response, tissue homeostasis, wound repair, and energy metabolism (Shaw et al., 2018). Essentially, this fresh outlook in immunology changes the microbe-killing focus of the immune response to the promotion of host health and survival through a global regulation of physiological responses (Lissner and Schneider, 2018). In insects, these studies were mainly performed with model insects, especially *Drosophila* (Lissner and Schneider, 2018) and the concept of disease tolerance has not yet been explored in the context of the interaction between insect vectors and the pathogens they transmit, as recently pointed (Oliveira et al., 2020).

Blood-feeding is a central event in the life cycle of both the insect vector and the pathogens they transmit. Typically, few parasites or viruses are taken up by the insect along with a blood meal. The number of pathogens in the blood meal is known as the critical bottleneck that will define the success of the infection. After a meal, the midgut becomes an aggressive environment, quickly populated by digestive enzymes that can potentially attack the pathogen. Moreover, it is colonized by an exuberant indigenous microbiota that may be a competitor for the incoming invader, at a clear numerical disadvantage. In addition, like all epithelial tissues, one of the main functions of the gut epithelium is to be a barrier of protection from the external world and to select what should enter into the organism. For most hematophagous insects, blood is the essential source of amino acids used to make yolk proteins. Therefore, hormonal control of reproduction is usually triggered by blood intake, which is tightly linked to the pace of blood digestion (Hagedorn, 2004). Several reports have shown hormonal effects on parasite infectivity, which, in some cases, have been attributed to a crosstalk between hormone signaling cascades and immune pathways (Nunes et al., 2020). Finally, for most blood-sucking insects, vertebrate hosts might be available more than once in a lifetime, and the effect of multiple blood meals have been shown to affect the life of pathogens by mechanisms that are not fully understood (Serafim et al., 2018). To summarize, the physiology of blood digestion of the hematophagous insect is the actual landscape where pathogens transmitted by them will thrive or not, a concept that was also revised by Nouzova et al. (2019). More importantly, the functioning of these processes ultimately defines the fitness cost of the infection to the insect vector, a major variable that affects vectorial capacity. Here we have addressed just some topics of vector physiology to illustrate the general concept that the performance of host organism integrated basic functions is critical to the success of the vector/pathogen association. As these are multiple and comprehensive topics, our intention is not to exhaust the analysis of the literature related to them. More than that, our goal is to highlight the need of examining the role of these and other non-immune basic aspects of insect physiology, not reviewed here, in determining the vector competence.

BLOOD DIGESTION AND METABOLIC SIGNALING

Some hematophagous arthropods feed on blood for their whole life cycle such as ticks and triatomine bugs, while in others, like mosquitoes and sandflies, only female adults feed on blood. In the adult stages, blood meals are strictly essential for oogenesis for most species. However, even for those few autogenous insects that use their teneral reserves to make the first batch of eggs, the following cycles of ovarian growth rely on vertebrate blood, and therefore, reproductive success depends on blood-feeding. The ingestion of a blood meal elicits a response in the gut-brain axis known to involve the central nervous system, the enteric nervous system, and the gastrointestinal tract (Hagedorn, 2004). The gut-brain crosstalk not only ensures the proper maintenance of gastrointestinal homeostasis but has multiple effects on insect physiology through neural, endocrine, immune, and humoral links (Gonzalez et al., 1999; Brown et al., 2008; Castillo et al., 2011; Gulia-Nuss et al., 2011). The nutritional intake connects intermediary metabolism to sexual maturation, oogenesis, microbiota colonization, and immune response, the latter being triggered by the encounter of the vector with pathogens.

Strictly speaking, digestion starts with hydrolysis of food by a vast array of digestive enzymes secreted after a meal (proteinases, carbohydrases, and lipases) that, together with nutrient transporting proteins, are needed to process nutrients in the gut (Santiago et al., 2017). However, in the context of hematophagous insects, proteases have received far more attention because blood is composed mainly of proteins (90% of dry weight), leading those insects to translate an arsenal of proteases to support protein digestion (Lehane, 2005; Brackney et al., 2010; Henriques et al., 2017; Sterkel et al., 2017). In most insects, proteolysis is based on trypsin and other serine

Abbreviations: TG, triacylglycerol; TGFβ, transforming growth factor-beta; ILP, insulin-like peptides; PI3K, phosphoinositide 3-kinase; PKC, protein kinase C; ERK, extracellular signal-regulated kinase; MEK, MAPK/ERK kinase; NFκB, nuclear factor kappa-light-chain-enhancer of activated B cells; NRF-2, nuclear factor erythroid 2–related factor 2; OXR1, oxidation resistance protein 1; cGMP, cyclic guanosine monophosphate.

proteases, in contrast to triatomines and ticks, where aspartic and cysteine proteases drive protein digestion (Sojka et al., 2008; Santiago et al., 2017; Henriques et al., 2021). Initially, protein degradation was described as accomplished by a few enzymes of each type, but genome sequencing in mosquitoes, triatomines, sandflies and ticks showed the existence of multiple copies of enzymes in all classes, revealing extensive gene duplications that probably occurred after the acquisition of the blood-feeding habit, suggesting the need for redundancy or some type of functional differentiation among enzymes of the same family (Sojka et al., 2008; Henriques et al., 2017; Santiago et al., 2017).

The possibility of pathogens being targeted by digestive enzymes and/or the manipulation of the host's digestion process by the pathogens has been addressed in several studies, but most of them were performed before the genomic expansion of digestive proteases was acknowledged. Insect digestive tracts vary extensively in morphology and physicochemical properties, factors that greatly influence the potential interaction between their also diverse set of transmissible pathogens and digestive milieu. The activity of proteolytic enzymes in the gut of *Anopheles* mosquitoes does not appear to be affected by *Plasmodium* infection. In addition, differences in the activity of digestive proteases in general are not observed among mosquitoes with different levels of susceptibility to infection (Feldman et al., 1990; Chege et al., 1996; Jahan et al., 1999). However, proteolytic activities present in the midgut lumen are required to activate a chitinase secreted by these parasites that is essential in the initial event of midgut infection (Shahabuddin et al., 1993). In the *Leishmania mexicana-Lutzomyia*'s pair, the pathogen promotes a decrease of trypsin activity in the vector's gut, increasing parasite burden. Trypsin knockdown exerts the same effect (Sant'Anna et al., 2009), probably making the parasite more resistant to the highly degradative habitat of midgut lumen. In contrast, in the triatomine bug *Rhodnius prolixus*, the activity of cathepsin D-like enzymes increases upon infection by *Trypanosoma cruzi* (Borges et al., 2006). Still, its inhibition did not affect parasite development in the conditions tested (Garcia and Gilliam, 1980). As we can see, the existing examples concerning proteases in the vector-parasite interaction were based on the analysis of total enzymatic activities, which resulted from the action of multiple enzymes belonging to the same class. These facts might be the answer to the diversity of responses observed among the different groups of insects. It would be interesting to know what are the specific proteases involved in the different events and if they can have the same role in the different vector-parasite pairs.

For enveloped viruses, it is known that the establishment of a successful infection is highly dependent on the fusion of the viral envelope with host cell membranes, where the envelope proteins need to be activated by proteolytic processing by host cell proteases (Klenk and Garten, 1994). As for *Aedes aegypti* infection by dengue virus, treating the mosquito with a trypsin inhibitor before exposure to the virus decreases the midgut infection, which can be partially rescued when the virus is previously incubated with bovine trypsin (Molina-Cruz et al., 2005). In this case, the authors discuss the possibility of the virus be pre-processed by trypsin before gut epithelia invasion, enhancing its virulence. In contrast, another work published in 2008 showed that silencing the late trypsin 5G1 or the addition of soybean trypsin inhibitor to the infectious blood meals increased midgut infection rates by DENV-2 (Brackney et al., 2008). The latter work was confirmed by a study showing that prior colonization of *Ae. aegypti* with the fungus *Talaromyces* sp. induced the downregulation of many digestive enzymes, including several trypsins, resulting in higher susceptibility to dengue infection. Moreover, knockdown of these trypsin genes was able to recapitulate the fungus-induced decrease in viral infection (Angleró-Rodríguez et al., 2017b). Although controversial, the studies made with dengue and *Ae. aegypti* suggest that blood digestion mediated by trypsins may influence the rate of DENV-2 infection. Although the literature on the subject is scarce, proteases may influence vector infection by viruses. The determination of the precise time course of viral invasion and protease expression together with the repertoire of proteases in the mosquito midgut would allow for a more comprehensive approach of the contribution of each digestive enzyme for mosquito vectorial competence.

There is now a general agreement that the successful infection of an insect vector involves a tripartite interaction between the insect, the pathogens and the intestinal microbiota (Cirimotich et al., 2011; Ramirez et al., 2012), a concept that has been verified for different host/pathogens associations (Castro et al., 2012; Narasimhan and Fikrig, 2015; Romoli and Gendrin, 2018; Telleria et al., 2018). Interestingly, studies performed with mammalian models revealed that proteases both from the host or from the microbiota are important modulators of intestinal homeostasis and are involved in the interaction with pathogens (Buzza et al., 2010; Motta et al., 2019; Edogawa et al., 2020; Kriaa et al., 2020). Therefore, it is tempting to speculate if the influence of proteases on vector infection by pathogens is not at least partially mediated by a role of these enzymes on intestinal microbiota.

In addition to proteins, vertebrate blood is also enriched with lipids. Host lipid usage by pathogens and regulatory changes of lipid metabolism triggered by infection appear as key players in several host-pathogen relationships, being essential determinants for vector competence, as recently revised by O'neal et al. (2020). Digestive lipases, such as TG lipases, are flux generating enzymes for lipid metabolism pathways. The essential process of absorption of digested lipids from the blood meal by midgut cells is followed by an increased lipid transport from the midgut to other tissues, to support development and oogenesis. This lipid transfer is promoted by lipophorin, the main hemolymph lipoprotein, and results in lipid accumulation in the fat body (revised by Gondim et al., 2018). Interestingly, *Plasmodium* oocysts in the *Aedes* gut basal lamina hijack mosquito lipophorin to support the parasite development (Atella et al., 2009) and knockdown of lipophorin by RNA interference (RNAi) strongly restricted development of *Plasmodium* oocysts, reducing their number by 90% (Cheon et al., 2006; Rono et al., 2010). Similarly, induction of lipophorin synthesis is observed in *C. quinquefasciatus* with the filaria *Wuchereria bancrofti* (Kumar and Paily, 2011).

Host lipid remodeling is also observed in vertebrate infection by arboviruses to support their replication (Ng et al., 2008; Fernández de Castro et al., 2016; Leier et al., 2020). Similar

reprogramming events have already been shown in vector cells (Perera et al., 2012; O'neal et al., 2020). An increase in the number of lipid droplets has been observed in *Aedes albopictus* C6/36 cells infected with dengue virus (Samsa et al., 2009). Furthermore, lipidomic analyses of the same DENV-infected cells revealed a large number of differentially expressed genes of diverse classes of lipids such as phospholipids and sphingolipids (Perera et al., 2012). On the same way, *Ae. aegypti* Aag2 cell line showed a regulation in the expression of lipid-related genes upon dengue 2 infection (Barletta et al., 2016). Besides, *in vivo* lipidomics showed that dengue infection in *Ae. aegypti* mosquitoes changed the lipid profile, mainly based on the inhibition of acylglycerolphosphate acyltransferase (AGAPT1), leading to an accumulation of phospholipids that support the viral replication (Chotiwan et al., 2018; Vial et al., 2019).

The blood-fed *Ae. aegypti* gut seems to increase the expression of many lipid-related genes, such as fatty acid synthase and perilipin-like proteins, which boost lipid droplet formation after blood meal (Barletta et al., 2016). Lipid droplets were shown in mammals to serve as a signaling platform involved with the synthesis of bioactive lipids (eicosanoids) (Vallochi et al., 2018). In *Aedes* mosquitoes, it has been shown that the midgut epithelia synthesize prostaglandins in response to the microbiota expansion in a phospholipase A-dependent manner that tunes the innate immune system against viral infection (Barletta et al., 2020). Similarly, *Anopheles gambiae* midgut produces prostaglandins in response to microbiota elicitors upon *Plasmodium* invasion, which triggers a cellular immune response (Barletta et al., 2019). The bug *R. prolixus* humoral and cellular responses seem to be modulated by eicosanoids as well (Azambuja et al., 2017). Using *T. rangeli* infection model, it was demonstrated that the insect reduces the arachidonic acid (the eicosanoid precursor) circulating in the hemolymph, leading to an inhibition of hemocytes phagocytic activity in the hemolymph (Garcia et al., 2004b; Figueiredo et al., 2008). Although eicosanoids/prostaglandins are part of the immune molecular arsenal in insects, these arthropods lack the canonical cyclooxygenase (COX), a key enzyme to convert the arachidonic acid into eicosanoids (Varvas et al., 2009). This is intriguing because those insects respond to the treatment with pharmacological COX inhibitors, such as indomethacin and acetylsalicylic acid, impairing the eicosanoid synthesis and modulating the immune response (Garcia et al., 2004a; Barletta et al., 2020). A question that remains open is what are the enzymes that play the role of canonical vertebrate COX in insects. In this sense, a specific peroxinectin named Pxt, that catalyzes the formation of the prostaglandin H2 (PGH_2), was identified in the follicle cells of *Drosophila* (Tootle et al., 2011). Later the same COX-Like activity was identified in the moth *Spodoptera exigua* (Park et al., 2014). Additionally, Barletta et al. (2019) showed that *An. gambiae* heme peroxidases 7 and 8 are important enzymes to synthesize the prostaglandin by the mosquito gut epithelia, suggesting possible candidates for alternative enzymes with COX-like activities.

The interplay between the lipid metabolism pathways and the autophagy-related molecular machinery, named as lipophagy, and its role in physiological and pathological processes in mammals has received increased attention in the last few years (Schulze et al., 2017; Kounakis et al., 2019). Recently, it was demonstrated that the Chagas' disease vector *R. prolixus* can use lipophagy during starvation to increase life span and locomotor activity (Santos-Araujo et al., 2020). It would be interesting to verify how this lipophagic machinery works under infection by either *T. cruzi*, a parasite limited to the intestinal environment, or *T. rangeli*, which is capable to invade the hemocoel and colonize salivary glands. Moreover, in enteric-infected *Drosophila*, an immune response is assembled by a lipophagy-dependent activation of DUOX (Lee et al., 2018). Thus, the contribution of lipophagy to the success of vectors' infection by their respective pathogens, remains obscure and deserve to be investigated.

Insects do not synthesize cholesterol *de novo*, meaning that this lipid has to be absorbed from the diet over their lifetime (Clark and Block, 1959; Zande, 1967). It has been shown in mammalian models that different immune challenges entail cholesterol mobilization (Tall and Yvan-Charvet, 2015). In the case of viruses, the infection interferes in several aspects of cholesterol metabolism, needed for the formation of cell membranes and intimately related to both the entry of viral particles in the cell and their exportation (Osuna-Ramos et al., 2018). Unfortunately, literature on vector biology only tangentially looked at this particular aspect, pointing out some genes involved in cholesterol metabolism and cellular traffic, such as the Niemann Pick 1 protein and the Sterol Carrier Protein 2, as host factors that allow the viral multiplication in the mosquito (Junjhon et al., 2014; Jupatanakul et al., 2014, 2017; Fu et al., 2015; Chotiwan et al., 2018). Dengue infection blocking by *Wolbachia* in mosquitoes also correlates with changes in cholesterol metabolism, trafficking, and accumulation (Geoghegan et al., 2017). Moreover, even though cholesterol is known as a precursor for the hormone ecdysone (Canavoso et al., 2001), the association between viral infection and hormonal signaling is largely unknown. Nevertheless, definitive evidence showing the contribution of dietary cholesterol to the viral replication in mosquito is still lacking. Additionally, it is also unexplored how serum cholesterol fluctuation in populations from endemic areas could correlate to the viral transmission by mosquitoes.

Some medical relevant parasites such as Apicomplexan and Trypanosomatids, similarly to insects, lack the capacity of *de novo* cholesterol synthesis (Coppens, 2013; Pereira et al., 2015). In order to differentiate and proliferate in the insect gut, they obtain cholesterol from the vertebrate's plasma low-density lipoprotein (LDL) (Labaied et al., 2011; De Cicco et al., 2012; Petersen et al., 2017). Lipophorin, mentioned previously to be hijacked from mosquitoes by parasites, might be the lipoprotein responsible for cholesterol import during the parasite insect stage. However, this hypothesis remains to be tested.

Most articles that compare carbohydrate metabolism of vectors-fed in sugar-rich diets with those fed on blood have focused on the fat body and physiological homeostasis. Sugar metabolism in these animals is controlled at the hormonal level by ILP and juvenile hormone (JH) (Clifton and Noriega, 2011; Hansen et al., 2014; Hou et al., 2015; Roy et al., 2015). It is increasingly clear that parasites can dramatically change the cellular energy metabolism of their arthropod vectors, as recently

revised by Samaddar et al. (2020). Still, for mosquito-arbovirus interactions, the knowledge on such metabolic alterations is limited. An *in vitro* study showed that Zika virus infection in *Ae. albopictus* drives the glucose metabolism toward the pentose phosphate pathway, differently from human cells that increase flux to the tricarboxylic acid cycle (Thaker et al., 2019). Activation of the pentose pathway provides NADPH for antioxidant pathways, which control the intracellular redox state. Maintaining the redox balance would be beneficial for viruses as it would protect them from oxidative damage. However, the relevance of these changes to the course of viral infection has not been experimentally addressed in the literature yet, despite alterations in expression of metabolic enzymes being regularly observed in transcriptomic analyses of infected vector digestive apparatus (Padrón et al., 2014; Angleró-Rodríguez et al., 2017a; Etebari et al., 2017; Narasimhan et al., 2017; Coutinho-Abreu et al., 2020). A large amount of gene expression data on vector infection has now accumulated, and it could be used to direct studies focusing on the crosstalk between canonical immunity pathways and carbohydrate/energy metabolism, the so-called immunometabolism, and the relevance of them to vector biology (Samaddar et al., 2020).

As in other organisms, in addition to its digestive role, the digestive tract functions as a nutrient sensor. Intestinal signaling is involved in integrative processes that link nutritional availability with behavior and metabolism and the microbial intestinal world, including eventual pathogens that come along with the food. One of the few reports on this subject showed that in *Ae. aegypti* blood intake triggers nutrient-sensing signaling, such as the Target of Rapamycin (TOR), responsible for translation of early trypsin (Brandon et al., 2008). This is extremely important for the course of digestion, as this initial event coordinates the late digestive phase (Barillas-Mury et al., 1995; Brackney et al., 2010). A broad spectrum of cellular mechanisms depends on a signaling pathway. The routes taken will rest on the pairs of signaling molecules and receptors that trigger the process. In addition to nutrients such as amino acids and heme, which act also as signaling molecules (Hansen et al., 2004; Oliveira et al., 2011a; Bottino-Rojas et al., 2015; Short et al., 2017), a blood meal brings also regulatory peptides that act as neurochemicals and hormones, like vertebrate insulin, insulin like growth factor (IGF1), TGF-β and other cytokines. Furthermore, the presence of parasites in the blood meal can antagonize or potentiate the effects of these vertebrate-borne signaling molecules in the vector organism (Pakpour et al., 2013a). The resulting cellular responses can be beneficial or detrimental to pathogen development. Most of the studies on signaling pathways and vector susceptibility/resistance to infection have focused on their role in the activation of immune pathways. These studies have been extensively discussed previously by others (Pakpour et al., 2013a, 2014; Urbanski and Rosinski, 2018; Sharma et al., 2019; Nunes et al., 2020). Among the best-known signaling pathways in insect vector species is the insulin/insulin-like growth factor signaling pathway (IIS), which is involved in the regulation of growth, longevity, reproduction and immunity. *An. stephensi* stimulated with human ILPs induces ROS-mediated signaling, without oxidative damage that culminates with NFκB inhibition, allowing the *Plasmodium falciparum* oocyst development (Surachetpong et al., 2011; Pakpour et al., 2012). On the other hand, dietary insulin showed a negative impact on flavivirus replication in *Ae. aegypti* and *Ae. albopictus* cells, and *Culex quinquefasciatus* adult mosquitoes, in a mechanism dependent on JAK/Stat activation (Ahlers et al., 2019). Furthermore, it was shown that insulin receptor knockdown in *C. quinquefasciatus* blocks filarial parasite development (Nuss et al., 2018).

The IIS pathway comprehends two branches: the mitogen-activated protein kinase (MAPK) and the phosphatidylinositol 3-kinase (PI3K)/Akt. A series of studies have shown that both branches are modulated by host blood components. Host growth factors/cytokines affect the mosquito-malaria parasite interaction by modulating the MAPK signaling pathway. Ingested human IGF1 reduces phosphorylation of the MAPK ERK signaling protein in *An. stephensi* midgut and decrease the intensity and prevalence of *P. falciparum* infection (Drexler et al., 2013). Accordingly, the mammalian host TGF-β-1 induces the expression of nitric oxide synthase and reduces the prevalence of *Plasmodium* infection in *An. stephensi*. This effect is inhibited by the activation of ERK (Surachetpong et al., 2009). Interestingly, TGF-β also appears to be critical for the survival of parasites such as *T. cruzi* and *Leishmania amazonensis* in mammalian hosts (Barral-Netto et al., 1992; Ming et al., 1995; Omer et al., 2000). However, the impact of host TGF-β on the interaction of these parasites with their vectors has not yet been investigated.

Regarding the PI3K/AKT, Corby-Harris et al. (2010) showed that the overexpression of an activated form of Akt in *An. stephensi*, a regulator of IIS, shortened the mosquito lifespan and increased resistance to *P. falciparum*. Lately, the same group showed that the sustained Akt activation in the mosquito midgut resulted in mitochondrial dysfunction coupled to Akt-mediated repression of autophagy and compromised midgut epithelial structure. The perturbation of midgut homeostasis enhanced parasite resistance and decreased mosquito lifespan (Luckhart et al., 2013).

Insulin-like peptides induced by blood-feeding trigger vitellogenesis in the fat body of *Ae. aegypti* and act as regulators of the blood digestion in the gut (Gulia-Nuss et al., 2011; Roy and Raikhel, 2012). In *An. stephensi,* ILPs interfere in the mosquitoes intermediary metabolism and nutrient intake (Pietri et al., 2016). Interestingly, *P. falciparum* soluble products induce the expression of ILPs in *An. stephensi*, through both the MEK/ERK and PI3K/Akt branches of IIS and inhibiting *P. falciparum* development *in vivo* by affecting mosquito immune effector genes (Pietri et al., 2015). This ILP-mediated inhibition of parasite development is somehow contradictory with the previous findings that human insulin could favor the parasite growth, raising the possibility that even being structurally similar, vector and host insulins can elicit distinct gut responses to *Plasmodium* infection. Moreover, Castillo et al. (2011) showed that the insulin signaling pathway can directly regulate hemocyte proliferation in *Ae. aegypti*. The same study also highlights an interesting observation regarding blood-feeding: resistance and tolerance to the same bacterial pathogen dramatically change

due to blood meal digestion and/or mobilization of resources for reproduction (Castillo et al., 2011).

The PKC pathway is part of this complex signaling network that responds to infection in different vectors. Inhibition of PKC blocks West Nile virus entry in C6/36 cells by inhibiting endosomal sorting (Chu et al., 2006). In *Ae. aegypti*, activation of PKC by the heme released during the digestion of blood decreases ROS production and allows an increased proliferation of indigenous microbiota (Oliveira et al., 2011a). However, the effect of PKC pathway on viral infection has not been investigated until now. PKCs have also been shown to be expressed in the midgut epithelia of *An. gambiae* and *An. stephensi* after a blood meal. As in *Ae. aegypti*, the *An. stephensi* PKC activation was also linked to the decrease of midgut epithelial barrier, resulting in the greater development of *P. falciparum* oocysts (Pakpour et al., 2013b), without modulation of NF-κB-dependent immune factors, thus indicating that the regeneration of the midgut epithelium is essential for infection control, as also suggested by Taracena et al. (2018).

So far, in spite of the advances discussed here, it remains widely unclear how this network of nutritional signaling pathways reflects on the parasite/host interaction. This reinforces the need to build a more holistic view of the interplay between metabolic changes and the canonical immune responses to vector transmitted pathogens that occur after a blood meal, using the integrative conceptual framework of immunometabolism.

PERITROPHIC MATRIX

The mammalian gastrointestinal epithelium is protected by the secretion of a mucus layer, mostly composed of highly glycosylated proteins (mucins) (Johansson et al., 2013; Sicard et al., 2017). The hydrophilic O-linked oligosaccharides that coat these proteins give them the physical and chemical properties that support the mucus protective role. Mucins are secreted by specialized cells, such as goblet cells in the intestine, and have a short half-life, which ensures the constant renewal of the mucus barrier (Deplancke and Gaskins, 2001). This barrier is essential to the digestive tract as it protects the tissue from mechanical damage by food particles, chemical aggression (pH and action of digestive enzymes) and limits direct contact with the microbiota. Although frequently neglected or ignored, insect gut also presents a bonafide mucous layer, with transcriptomic data revealing abundant expression of mucins in the midgut (Terra et al., 2018). The peritrophic matrix (PM) is an extracellular structure found in the intestinal lumen of insects that is ascribed a major role as a protective layer in the midgut, usually described as analogous to the vertebrate mucus. The PM was first described by Lyonet in 1762 and is composed of glycosylated proteins embedded in chitin fibers (for reviews see Lehane, 1997; Terra, 2001, Terra et al., 2018). PMs can be classified into two different types: Type 1 is secreted by all epithelial cells as a continuous gel-like structure that completely packages the food bolus and is formed in response to feeding. The type 2 PM is a membranous structure characterized by its constitutive secretion by a midgut region called cardia and delimits an area between the epithelium and the PM, the ectoperitrophic space. It has a tubular morphology and lines the whole gut epithelium (Shao et al., 2001). Adult mosquitoes such as *Ae. aegypti* and *Anopheles* sp. secrete type 1 PM after a blood meal but present the type 2 PM at larval stages. The same is observed in the sandfly *L. longipalpis* (Secundino et al., 2005). *Glossina* spp. and *Drosophila* present the type 2 PM also in the adult stage. Hemipteran insects like the Chagas' disease vectors are an exception in that they lack the classical PM and the lipidic perimicrovillar membranes are responsible for the PM functions (Terra, 2001; Hegedus et al., 2019). In the case of ticks, the PM is a chitin-containing extracellular layer that covers the digestive cells, displaying a very distinct morphology to that of a typical insect PM (Matsuo et al., 2003; Grigoryeva, 2010; Kotsyfakis et al., 2015), probably reflecting their peculiar tick digestive physiology, based on intracellular digestion of host blood proteins (Lara et al., 2005).

In most insects, the PM functions as a molecular sieve, controlling the traffic of molecules between the intestinal epithelium to the lumen, compartmentalizing the digestion and protecting the epithelium from potentially cytotoxic molecules (Billingsley and Rudin, 1992). However, several of these roles have been scarcely investigated in blood-feeding insects such as mosquitoes. For example, it has been shown that disruption of PM by the action of exogenous chitinases increases the blood digestion rate, an unexpected effect that was attributed to augmented access of intestinal proteases to the blood bolus (Villalon et al., 2003). Also, the *Ae. aegypti* PM binds heme released during the digestion of hemoglobin, which was hypothesized to reduce its oxidative potential (Pascoa et al., 2002).

In contrast, the PM acting as a barrier that limits exposure to the microbial world has been more thoroughly investigated. In mammals, the relative lack of an exuberant immune response against the intestinal microbiota has been attributed to the mucus acting as a barrier that avoids direct contact between the microbiota and the epithelium and not to the microbiota subverting the host immune response, a phenomenon named as "immunological ignorance" by Hooper (2009). Thus, immune homeostasis is attained largely by the mucus layer limiting the exposure of enterocytes to the microbiota (Li et al., 2018). Similarly, in insects, the secretion of the PM approaches this pivotal immune barrier function, as it compartmentalizes the microbiota and its immune elicitors, avoiding the overexposure of the gut epithelium (Buchon et al., 2009; Kuraishi et al., 2011, 2013; Weiss et al., 2014). In this way, it was demonstrated that *An. gambiae* mosquitoes express a heme peroxidase, which is essential to crosslink the PM proteins/mucins, supporting the correct assembly of this barrier. Once this peroxidase is knocked down, the PM barrier is compromised and the gut epithelia is exposed to microbial elicitors that over activate the intestinal immune system (Kumar et al., 2010).

When the microbiota and the PM layer barrier function become unbalanced, the intestinal cell homeostasis is rapidly affected. Both in mosquito and *Drosophila* the gut stem cell populations respond to biotic and abiotic injury and their activation is prevented by the PM presence (Micchelli and Perrimon, 2006; Buchon et al., 2013; Janeh et al., 2017;

Taracena et al., 2018). In *Ae. aegypti*, when the PM structure is compromised by inhibition of chitin synthesis, the epithelial midgut is exposed to the microbiota, which in turn activates the generation of ROS, causing tissue damage and leading to a regenerative response based on mitotic proliferation of progenitor cells (Taracena et al., 2018). Complementary to this mechanism, it was shown in *Anopheles* mosquitoes that genes related to the synthesis of chitin and peritrophins – that together form the structural backbone of the PM – have their expression stimulated by proliferation of the intestinal microbiota (Rodgers et al., 2017). This effect closely recapitulates the mammalian response of goblet cells that prompt the secretion of stored mucus after exposition to native and pathogenic bacteria (Coconnier et al., 1998; Deplancke and Gaskins, 2001).

In mosquitoes, the intestinal microbiota experiences an explosive expansion after a blood meal. Of course, this microbial blooming is fueled by the sudden increase in the availability of nutrients, jumping from a few thousand bacterial cells in sugar-fed *Ae. aegypti* to a plateau of a few million cells in a single midgut by 12 h after blood-feeding (Oliveira et al., 2011a). However, this is probably well below the microbial population that could be supported by an unrestrained growth of bacteria in about 2 ml of blood, posing a question that has not yet been properly addressed: how fine-tuning regulation of the microbial growth is attained? At least one of such mechanisms is the production of ROS by the gut epithelium, as already mentioned above (Ha et al., 2005a; Oliveira et al., 2011a). Consistently, it was shown that gut ROS production is also attenuated by the barrier function of the PM (Taracena et al., 2018), highlighting the existence of mechanisms that balance the microbe-killing mucosal response in a way that is neither too detrimental to the host nor to the microbiota. Of interest, this mode of operation can also be relevant during infection by pathogenic microorganisms.

The first encounter between the insect host and a vectored parasite coincides with the blood digestion in the midgut, exactly when the PM is formed, making it plausible that this immune barrier can regulate the infection's success. Anopheline mosquitoes ingest *Plasmodium* gametocytes that will fertilize and generate the ookinetes, which will invade the intestinal epithelium by secreting chitinases activated by mosquito digestive enzymes, allowing the parasite to traverse the PM. The invasion will happen around 24 h after feeding, concomitantly with PM formation peak (Huber et al., 1991; Shahabuddin et al., 1993). Moreover, it has been shown that proteins present in the matrix can function as anchors for the parasite, promoting its penetration process (Zhang et al., 2015). Although one would expect the PM might impose a barrier to the parasite infection in the gut, several reports showed instead that the absence of this structure decreases the gut parasitemia (Billingsley and Rudin, 1992; Shahabuddin et al., 1995; Baia-da-Silva et al., 2018). The PM regulation is also essential for Leishmanial infection of sandflies (Coutinho-Abreu et al., 2010). *Leishmania* parasites do not invade the epithelium but hide in the ectoperitrophic space (between the epithelium and the PM) anchored to epithelial cells, which likely protect them from the action of digestive proteases (Pimenta et al., 1997; Ramalho-Ortigao, 2010). For the *Glossina* – *T. brucei* pair, for a long time it was not understood how the parasites crossed the flies' PM. However, recent evidence was provided that the expression of genes related to the PM formation was influenced by infection. In these studies, the authors show that *T. brucei* targets the cardia, causing the discontinuation of PM type I secretion and allowing them to invade the ectoperitrophic space (Aksoy, 2019; Rose et al., 2020).

In the Chagas disease parasite replicative stage, the *T. cruzi* epimastigotes, adhesion to the kissing bug perimicrovillar membranes seems important for their division (Gonzalez et al., 1999). Treatment of the intestinal tissue with antiserum against the perimicrovillar membrane reduces the trypanosomatid development in the vector (Gonzalez et al., 2006). As mentioned above, kissing bugs don't have a PM but perimicrovillar membranes, which are phospholipid membranes secreted by the gut and that, analogous to the PM, define a perimicrovillar space (Terra, 1988). The *T. cruzi* epimastigotes are attached to these perimicrovillar membranes through their flagella and membrane glycoinositolphospholipids. Hydrophobic proteins located in their surface and sugar residues present in perimicrovillar membrane glycoproteins appear to be necessary for this interaction (Zingales et al., 1982; Golgher et al., 1993; Pereira-Chioccola et al., 2000; Alves et al., 2007; Nogueira et al., 2007). In *R. prolixus*, it has been shown that another function of the perimicrovillar membranes is the promotion of the aggregation of heme molecules, forming nucleation sites that convert heme into hemozoin crystals and hence preventing heme toxicity toward both the host and the parasite, that consequently creates a favorable environment for pathogen growth (Oliveira et al., 2000; Stiebler et al., 2014; Ferreira et al., 2018).

The role of the *Ae. aegypti* matrix in controlling viral infections has not been investigated so far. It is not clear whether the viral particle can get through the pores of the matrix or if the invasion of the epithelium occurs in the first hours after the meal, when the matrix has not yet been completely modeled. The latter hypothesis is the most accepted by the community, although there is a knowledge gap behind this topic (Franz et al., 2015).

In non-hematophagous insects, it is suggested that the peritrophic matrix secretion integrates the hormonal signaling, mediated by ecdysone, to the pathways downstream to nutritional sensors (Merzendorfer and Zimoch, 2003). Feeding mosquitoes with an artificial diet of low nutritional value that promotes distension of the epithelium stimulates the synthesis of a fragile and short-lived matrix, different from the robust structure observed upon blood-feeding (Dinglasan et al., 2009; Whiten et al., 2018). Thus, it is worth assessing whether the matrix synthesis is controlled by nutritional/metabolic sensors (such as the target of rapamycin, TOR and AMP-activated protein kinase, AMPK) regulated upon blood arrival, in addition to the molecules released during digestion, such as heme, hormonal signaling induced by digestion (e.g., ecdysone and ILP) or microbial community expansion.

The understanding of the PM as a barrier that coordinates the insect intestinal immune activation beyond its digestive aspect, leads to new perceptions and insights. For example, maintenance of cellular homeostasis in addition to tissue damage repair may be central to disease tolerance (Oliveira et al., 2020), while current state of literature focuses on infection resistance. Future studies

are needed that address how the microbe-associated patterns are presented to the gut epithelia, and consequently how the classical immune system will be tuned and shape the parasite life history.

INTESTINAL REDOX HOMEOSTASIS

Historically, research on reactive oxygen species (ROS) was pushed to a central position in biology after the discovery of superoxide dismutase (McCord and Fridovich, 1969). The scene was dominated for about 30 years by the study of the role of ROS in pathologic conditions (Lambeth, 2007; Liu et al., 2018), where oxidative stress was defined as an imbalance between antioxidant mechanisms and production of ROS by several sources, including microbe-killing NADPH oxidases of immune cells. However, the discovery of the signaling role of nitric oxide (NO) in the regulation of diverse aspects of cell physiology, followed by several reports on hydrogen peroxide acting as a second messenger of several hormones and growth factors, led to a change in paradigm, with the introduction of redox signaling and redox homeostasis as novel steering concepts (Reth, 2002; Jones, 2006; Veal et al., 2007; Jones and Sies, 2015).

As already mentioned above, the digestive apparatus of most animals is also home to an abundant and specific microbial community that is now recognized as having a major and pleiotropic impact on the physiology of the metazoan host (Douglas, 2019). However, the mechanisms that control the growth rate of the intestinal microbiota are still not fully understood. Seminal studies in *Drosophila* revealed that an intestinal Dual oxidase (DUOX) produced H_2O_2 in response to the presence of microorganisms in the gut lumen (Ha et al., 2005a,b). Importantly, they also showed that the gut epithelium was protected from H_2O_2 by its dismutation to H_2O by a heme-peroxidase that at the time was mistakenly called "Immune regulated catalase." A DUOX enzyme found in *Ae. aegypti* mosquitoes has its activities decreased upon ingestion of a blood meal, leading to a marked reduction of ROS levels in the midgut (Oliveira et al., 2011a). Inhibition of the mosquito DUOX caused an increase in the size of the indigenous intestinal microbiota (Oliveira et al., 2011a), revealing a role of ROS metabolism in fine-tuning the symbiotic relationship between the commensal microbial community and the mosquito, in addition to its canonical immune action in the defense against pathogens.

Several other reports addressed the relation between ROS and pathogens in insect vectors. In an elegant work, Liu et al. (2016) showed that RNAi silencing of mosquito DUOX increased dengue virus replication in the midgut. Viral NS1 protein present in the host plasma enhanced susceptibility of the mosquito to DENV infection by reducing expression of DUOX, as well as of NoxM/Nox4-art (a NOX-4 homolog specific of the arthropod lineage, Gandara et al., 2017). Moreover, the iron concentration in the host's blood was inversely correlated to the prevalence and viral load of mosquito infection by dengue virus (Zhu et al., 2019). The catalase knockdown in *Ae. aegypti* changed the mosquito's susceptibility to DENV but had no impact on the Zika virus (ZKV) establishment. On the other hand, the ZKV viral load in the mosquito midgut was decreased by the redox imbalance promoted by down-regulation of NRF2 antioxidant transcription factor, suggesting that other components of the redox homeostasis downstream of NRF2 are involved in the control of ZKV infection (Bottino-Rojas et al., 2018). Among those, there are canonical NRF2 targets, such glutathione S-transferase and cytochrome P450, suggested to be active in maintaining tissue homeostasis during blood digestion in the mosquito (Bottino-Rojas et al., 2018, 2019). The reduction of viral load by ROS has been explained in most cases by assuming it is inflicting direct damage to the viral particle. However, experimental proof for this hypothesis is still lacking. Interestingly, an alternative mechanism emerged from the demonstration that redox imbalance and its associated cellular damage in *Ae. aegypti* and *Ae. albopictus* midgut led to increased programmed cell death, triggering a homeostatic response based on tissue-repairing mitotic activity of intestinal stem cells (Janeh et al., 2017; Taracena et al., 2018). The same report showed that this increased cellular turnover in the gut epithelia negatively impacted vector susceptibility to arbovirus infection (Taracena et al., 2018). Notwithstanding, in mosquito strains naturally refractory to viral infection, resistance was dependent on the proper recruitment of stem cells via Delta/Notch signaling pathway (Taracena et al., 2018).

In a way similar to what happens with the mosquito down-regulation of ROS production after a blood meal (Oliveira et al., 2011a), the kissing bug *R. prolixus* also decreases the intestinal ROS generation after blood-feeding (Gandara et al., 2016). However, this is not triggered by the dietary heme, as it was shown for *Ae. aegypti* (Oliveira et al., 2011a), but by the nutritional intake, which increases amino acid levels and activates the TOR pathway, impacting negatively the production of mitochondrial ROS by an yet uncharacterized mechanism (Gandara et al., 2016). Nogueira et al. (2015) showed that while high levels of H_2O_2 reduced growth of the *T. cruzi* epimastigote stages, low levels increased proliferation. In contrast, antioxidant molecules reduced the proliferation of epimastigotes but increased conversion to the infective trypomastigote form, revealing that ROS levels in the bug digestive apparatus have a complex regulatory role on the life cycle of the parasite.

The phlebotomine *L. longipalpis* presents an interesting illustration of how redox homeostasis in the normal gut physiology is relevant for the parasite. In the sandfly, there is a decrease in the intestinal ROS generation upon feeding (Diaz-Albiter et al., 2012), similar to *Ae. aegypti* (Oliveira et al., 2011a) and *R. prolixus* (Gandara et al., 2016). ROS levels are increased by infection with a *Serratia marcescens* strain pathogenic for the sandfly, and uric acid (an antioxidant) administration to the sugar meal increased virulence of this bacteria, revealing that the ROS-producing pathways in the gut can be controlled by immune signaling (Diaz-Albiter et al., 2012). In contrast, *Leishmania mexicana* infection does not increase ROS levels after a blood meal (Diaz-Albiter et al., 2012), but silencing the sandfly catalase or maintaining them fed in sugar meal supplemented with H_2O_2 decreased the intestinal parasite load. This result revealed that not only is the parasite capable of evading immune activation of ROS, but it is additionally benefited by the down-regulation

of ROS levels that is part of the normal physiology of the host. However, this goes beyond simple immune evasion by the parasite, as another report, also from Dillon's group, showed that *Leishmania* infection indeed protected flies from death by *Serratia* co-infection, but without reducing *Serratia* levels (Sant'Anna et al., 2014), strongly suggesting that the *Leishmania* is acting by triggering tolerance to disease mechanisms, thereby reducing damage and preventing fitness loss, without killing of the pathogen (in this case, the *Serratia* bacterium).

A *Plasmodium* refractory *An. gambiae* strain was appointed to have intrinsic higher levels of H_2O_2, which increases even more after an infectious blood meal as part of its antiparasitic defense mediated mainly by hemocytes (Kumar et al., 2003; Molina-Cruz et al., 2008) and this could be attributed to higher mitochondrial ROS production in the refractory mosquitoes (Oliveira et al., 2011b; Gonçalves et al., 2012). The antioxidant defenses induced by blood-feeding in this model seem to be in part under the control of a redox sensor, called OXR1, that regulates both the expression of antioxidant enzymes and the success of parasite infection (Jaramillo-Gutierrez et al., 2010).

Anopheles mosquitoes have a unique redox metabolism upon feeding and infection, described as part of the so-called "time bomb model" where the midgut invasion by the parasites triggers an epithelial response based on protein nitration, activation of peroxidases, and, consequently, apoptosis of those invaded cells (Han et al., 2001; Kumar et al., 2004). This complex intestinal response to the ookinete invasion was molecularly dissected, revealing the role of NOX5, a NADPH oxidase member, as the source of ROS. It works with a heme peroxidase to mediate the parasite nitration (Oliveira et al., 2012). While these studies point to a conventional "immune" function for NOX5, recently, the NOX5 enzymes were shown to regulate muscular function, both in mammalian blood vessel smooth muscle contraction and in the intestinal peristalsis in *R. prolixus* (Montezano et al., 2018), adding some more complexity to this scenario and bringing about the possibility of the existence of a crosstalk between physiological mechanisms and the microbiota.

The role of reactive nitrogen species (RNS) in the metabolism of hematophagous vectors was initially revealed by the demonstration that increases in NO levels limited the development of *P. falciparum* in *An. stephensi* (Luckhart et al., 1998). Subsequent works performed by the same group led to the molecular characterization of nitric oxide synthase (NOS) (Luckhart and Rosenberg, 1999) and the modulation of NOS expression during infection by factors such as the parasite's hemozoin pigment (Akman-Anderson et al., 2007) and glycosylphosphatidylinositols (Lim et al., 2005). It was also shown that the *An. gambiae* NOS gene is controlled by Jak/Stat pathway upon infection with *P. berghei* (Gupta et al., 2009). Nitrogen reactive species have a complex chemistry, acting not only through the canonical effect of NO on cGMP formation, but also via its reaction with superoxide forming peroxynitrite. This highly reactive intermediate modifies amino acid side chains and generates derivatives such as nitrotyrosine or nitrosothiols, which are formed in the mosquito gut and are modulated by infection, having profound effects on cell signaling (Kumar et al., 2004; Gupta et al., 2005; Peterson and Luckhart, 2006; Peterson et al., 2007; Oliveira et al., 2012). While protein nitration was shown to be relevant in triggering an anti-plasmodium response (Oliveira et al., 2012), global and mechanistic analyses of nitrosative signaling on insect physiology are still scarce. More recently, it has been reported that the kissing bug *R. prolixus* produces NO in response to *T. rangeli* (Whitten et al., 2007), and NOS inhibition allowed the proliferation of *T. cruzi* parasites in the insect gut (Batista et al., 2020). Nonetheless, the role of RNS-involved pathways and their oxidative implications to parasites/virus infection of mosquitoes or other vectors is still largely unknown and exposes an important avenue for future investigation.

Another way to positively modulate intestinal ROS in mosquitoes is through native microbiota elicitors (Oliveira et al., 2011a; Xiao et al., 2017), and this can have consequences for pathogens. An *Enterobacter* strain isolated from the midgut of wild-caught mosquito was shown to decrease *P. falciparum* infection by inducing ROS generation in the gut. The infection load was restored in the presence of vitamin C (Cirimotich et al., 2011). Accordingly, in *An. gambiae*, blood digestion increases catalase expression and activity in the midgut epithelium and catalase knockdown turns the mosquito more resistant to *P. falciparum* infection (Molina-Cruz et al., 2008). In contrast, in *An. aquasalis*, infection with *Plasmodium vivax* is increased upon catalase silencing (Bahia et al., 2013). Along with the positive effect of ROS on *T. cruzi* development in triatomine bugs discussed above (Nogueira et al., 2015), this report on *P. vivax* and *An. aquasalis* highlight the complexity of the links between redox homeostasis and parasite/host relationship, which is not explained by a simplistic microbe-killing role of ROS. Even in the several reports mentioned above where ROS levels are inversely correlated with pathogen infection (such as in the *Aedes*/arbovirus), it is not completely clear how much these ROS are produced under the control of canonical immune signaling pathways and how much is derived from the "regular" physiology, such as handling of heme and iron intake, control of microbiota, muscular activity or reticulum stress.

REPRODUCTIVE PHYSIOLOGY AND HORMONAL REGULATION

Vertebrate blood-feeding is a decisive evolutionary trait needed to obtain nutrients for egg development. Different species vary dramatically in their reproductive output. Some insects, like mosquitoes, are able to lay hundreds of eggs each time they take a blood meal and this feature impacts deeply their density in endemic areas (Shaw and Catteruccia, 2019). The reproductive fitness of vectors represents a promising target to prevent disease transmission because it interferes directly with the burden caused by large populations. Nonetheless, there is evidence that these organisms balance their energy investment into different life processes, often leading to fitness trade-offs between survival, immunity, and reproduction (Schwenke et al., 2016). Therefore, biological pathways essential for reproductive fitness directly or indirectly influence elements that govern vectorial capacity.

In general, it is considered that activation of immune responses decreases reproductive output in a diverse array

of insects. Amongst blood-feeding vectors, parasite-induced fecundity reduction is a strategy that is evident in many vector/parasite associations (Hurd, 2003). In malaria-mosquito systems, a challenge with bacterial components or *Plasmodium* infection promotes apoptosis of follicle cells and reduces the accumulation of protein in the ovaries, as well as the number of eggs laid (Hogg and Hurd, 1995; Ahmed et al., 2002; Ahmed and Hurd, 2006; Pigeault and Villa, 2018). An immune-mediated arrest of oogenesis was also reported in other disease vectors such as the triatomine bug *R. prolixus* and tsetse flies (Hu et al., 2008; de Medeiros et al., 2009), suggesting resource allocation toward immunity to achieve recovery from infection. Besides, it is also true that reproductively active insects have reduced resistance to infection (Schwenke et al., 2016). In mosquitoes, it was shown that the same molecular processes involved in delivering blood-acquired nutrients to maturing eggs also favor the development of *Plasmodium* oocysts in the midgut and diminish the efficiency of parasite killing by the mosquito immune system (Rono et al., 2010). Recently, it was shown that transgenic *An. gambiae* mosquitoes with reduced reproductive capacity have a significantly higher malaria transmission potential, due to an increase in parasite growth rates (Shaw et al., 2020). Due to the direct implications in currently proposed control strategies (e.g., eggless mosquitoes for population suppression) and the vacancy of descriptions of resource reallocation mechanisms in other insect vector species, this subject deserves a greater deal of attention in the field.

Hormonal control is a critical mechanism for the physiological trade-off between reproduction and immunity. JH and 20-Hydroxyecdysone (20E) are key regulators of metamorphosis and reproduction in all holometabolous insects (as reviewed by Roy et al., 2018). Specifically, the balance between JH and 20E is essential for egg maturation. In most insects, increased JH levels promote egg production and provisioning and, in contrast, high 20E titers result in the resorption of immature vitellogenic eggs (Gruntenko and Rauschenbach, 2008). However, in female mosquitoes, digestion and ovarian development are physiologically integrated through a cascade of ecdysteroid signaling initiated after a blood meal (Hansen et al., 2014). Beyond the induction of synthesis and secretion of yolk protein precursors in the fat body, 20E is shown to regulate a number of additional genes that could impact parasite development in different species. In *D. melanogaster*, ecdysone triggers a precise signaling pathway shown to modulate expression levels of antimicrobial peptides and interfere with resistance mechanisms in the context of bacterial infections (Flatt et al., 2008; Rus et al., 2013). The chemical inhibition of ecdysone signaling in the blood-feeding triatomine *R. prolixus* is able to suppress cellular and humoral immune responses, disrupting gut microbial homeostasis (de Azambuja et al., 1991; Vieira et al., 2021).

Anopheline mosquitoes are a unique model for ecdysone studies due to their strict anautogeny and male transfer of 20E to females during a monandrous copulation. The mating-induced increase in oogenesis is mediated by vitellogenic lipid transporters that also facilitate *Plasmodium* development by reducing the parasite-killing ability (Rono et al., 2010). Additionally, mating affects longevity and induces changes in the midgut that can increase susceptibility to the parasite (Dao et al., 2010; Dahalan et al., 2019). In contrast, the topical application of a 20E agonist shortens lifespan, prevents mating and egg production, and significantly blocks *P. falciparum* development (Childs et al., 2016). Therefore, 20E exerts a long-range regulation of multiple physiological processes that are highly relevant to the mosquito's competence to transmit malaria: reproductive success, parasite development, and longevity. Recently, a direct influence of 20E on cellular immune function and antipathogen immunity in mosquitoes was demonstrated. Blood-feeding of *An. gambiae* females or direct 20E injections increase phagocytic activity and this ecdysone-mediated immune priming reduces bacteria and *Plasmodium berghei* survival (Reynolds et al., 2020). However, some argue that in natural settings, the coevolution of parasite and vector has led to a less conflicting relationship, in which the immune response is toned down, and the potential cost of infection for invertebrate hosts is minimized (Mitchell and Catteruccia, 2017). Werling et al. (2019) provided evidence of a positive correlation between mosquito and parasite fitness dependent on 20E signaling. By genetic ablation of ovary development and impairment of 20E endogenous production, it was determined that ecdysone signaling is required for *P. falciparum* development via the production of mosquito host-derived lipids (Werling et al., 2019). This supports a model where the provision of lipid molecules during vitellogenesis is used by the parasite to increase survival and optimize its transmission (Costa et al., 2018). Therefore, the intricate interplay mediated by 20E between insect reproductive physiology and parasite development remains partially unresolved. It is possible that ecdysone signaling has tissue and/or threshold-specific actions, enabling the establishment of infection while boosting anti-parasite responses through distinct mechanisms. To warrant a proper impact in pathogen transmission of future discoveries, further research should ideally consider field/natural conditions and be focused on parasite-vector based combinations that occur in the wild.

Juvenile hormones control almost every aspect of insect's life. The seminal studies of Wigglesworth, started in the early 1930s, established the existence and major roles of JH in insects, regulating tissue morphogenesis, vitellogenesis and immune response, acting primarily as an 'inhibitory hormone' (Wigglesworth, 1965). Additionally, strong evidence across a range of insect taxa endorse the model in which mating increases JH titers and suppresses 20E, promoting egg development and inhibiting immune capability (Schwenke et al., 2016). Much of what we know of the molecular regulation of JH in blood-feeding species comes from studies in *Ae. aegypti*. Here, the rate of JH synthesis in young stages of mosquitoes is in close correlation with their nutritional status (Noriega, 2004). JH also has essential functions in adult females where it controls post-eclosion maturation, leads to reproductive competency and ability to feed on blood, and regulates gene expression after blood-feeding (Clifton and Noriega, 2011; Roy et al., 2015). Aside from morphological alterations in the ovary, transcriptional JH-induced changes in the fat body render this tissue competent to respond to ecdysone produced by the ovary after blood-feeding

(Zou et al., 2013). Moreover, JH is delivered by *Ae. aegypti* males during mating, which increases egg development by directing nutritional resources toward reproduction (Klowden and Chambers, 1991; Clifton et al., 2014). In *Drosophila*, a similar mating-induced expression of JH results in a remodeling of the female midgut, leading to cell division, increased organ size and ultimately a higher food intake (Reiff et al., 2015). However, in mosquitoes, a midgut-remodeling process in mated females has not been addressed yet. This event is relevant in disease vectors because it could be aimed to favor nutrient absorption toward egg provisioning, but also benefit pathogen development by deviating resources from immunity and supporting a higher parasite count due to an expanded gut area. JH is transported to target tissues by the hemolymph carrier juvenile hormone-binding protein (JHBP) where it binds to the methoprene-tolerant (Met) receptor and exerts its pleiotropic effects. One of the overall processes affected by Met depletion in mosquitoes is lipid metabolism (Wang et al., 2017), which could have a deep impact on the mounting of immune responses to pathogens and parasite maturation (Cheon et al., 2006). Recently, Kim et al. (2020) described a specific role for JH, through JHBP mutation, in regulating innate immune responses and the development of hemocytes in *Ae. aegypti*. JHBP-deficient mosquitoes are immunosuppressed at the humoral and cellular levels, and present a severe susceptibility to bacterial infection (Kim et al., 2020). These results call for more detailed studies exploring the role of JH signaling on vector infection by disease pathogens.

Blood-feeding initiates a complex series of physiological events in the gut, fat body and ovary that are integrated by the actions of JH, 20E and peptide hormones. Among the topics that could earn further exploration, the modulating role of sex hormones and their effects on non-reproductive organs are poorly understood in blood-feeding insects. Recently, in *Drosophila*, it was proven that an ecdysone-dependent signaling from the ovaries to the gut promotes growth of the intestine (Ahmed et al., 2020). In addition, the insect midgut produces certain hormones when it recognizes harmful components or pathogenic bacteria in an ingested meal; concurrently, these hormones regulate other tissues and organs (as reviewed in Wu et al., 2020). Given that blood digestion, parasite development and vitellogenesis require the coordination of molecular events in three different abdominal tissues, these inter-organ relationships have relevance in the context of vector–parasite interactions and deserve further attention. Furthermore, between insects of the different taxa, the diversity in life history traits may lead to distinctive adaptations of these systems (Schwenke et al., 2016) and the study of reproductive processes with respect to species-specific features can help the identification of novel targets for vector control.

MULTIPLE BLOOD-FEEDINGS

The competence to support pathogen development varies between vectors due to many biological aspects, which include not only immunity but also feeding behavior and nutritional status (Lefèvre et al., 2013). Frequency of feeding is undisputedly an important factor in relation to human infections with insect-transmitted diseases (Kramer and Ebel, 2003; Das et al., 2017). Multiple blood meals can increase vectorial capacity by promoting the contact of the disease-carrying insect with susceptible hosts. In the study of vector biology, it is widely accepted for blood-feeding dipterans that host seeking is halted by a full blood meal (Klowden, 1990). However, a number of observations where gravid females still display host-seeking behavior motivated a reconsideration of this assumption (Scott et al., 1993; Guzman et al., 1994; Beier, 1996; Matthews et al., 2016). As most vectors of diseases need to take additional blood meals after becoming infected to complete the transmission cycle, pathogens may have evolved mechanisms to promote their success, redefining the role of uninfected blood-feedings in the epidemiology of these diseases.

One of the classic entomological parameters used in malaria transmission models rely on the proportion of bites experienced per person and the number of total bites taken by a mosquito per gonotrophic cycle (Tedrow et al., 2019). Due to their low reserves, anophelines frequently seek more than one blood meal at each oviposition cycle (Beier, 1996). This behavioral aspect of *Anopheles* females appears to increase not only fecundity, but also longevity and resistance to insecticides (Oliver and Brooke, 2017). Interestingly, the development of the malaria parasite seems to equally affect and be affected by frequent blood meals, which accelerate oocyst maturation and sporozoite development (Beier et al., 1989; Ponnudurai et al., 1989), and are induced by pathogen–vector manipulation to further enhance transmission (Cator et al., 2012). Shaw et al. (2020) proved that previously infected *An. gambiae* females, when provided a second uninfected blood meal, present an increase in oocyst growth rates and faster accumulation of sporozoites in the salivary glands, which can indeed amplify local malaria transmission potential (Shaw et al., 2020). Therefore, this previously overlooked multiple feeding behavior is a justifiable current trend of investigation in vector-borne pathogen transmission.

In the phlebotomine sand fly species *Lutzomyia*, a higher proportion of insects heavily infected can be found after the second blood meal (Moraes et al., 2018). Also, the subsequential feeding induces a faster proliferation of *Leishmania* parasite infective forms and its rapid migration to the vector proboscis, increasing vectorial competence during the second gonotrophic cycle (Elnaiem et al., 1994; Vivenes et al., 2001). Furthermore, it has been recently proven that the taking of a second uninfected blood meal by *Leishmania*-infected sand flies triggers a specialized developmental stage of the parasites, the retroleptomonad promastigotes, which is a replicative form and amplifies both the host infection and the infectiveness of the bite (Serafim et al., 2018).

As previously mentioned, blood-feeding triggers intense physiological changes to the gut tissue – including mechanical distention of the midgut, altered cell homeostasis, and changed permeability of the basal lamina – that could aid pathogen dissemination out of the midgut (Okuda et al., 2007; Dong et al., 2017; Taracena et al., 2018). Indeed, in the mosquito *Ae. aegypti*, stretching of the gut tissue over consecutive blood-feedings seems to be a critical factor causing the midgut basal lamina to become

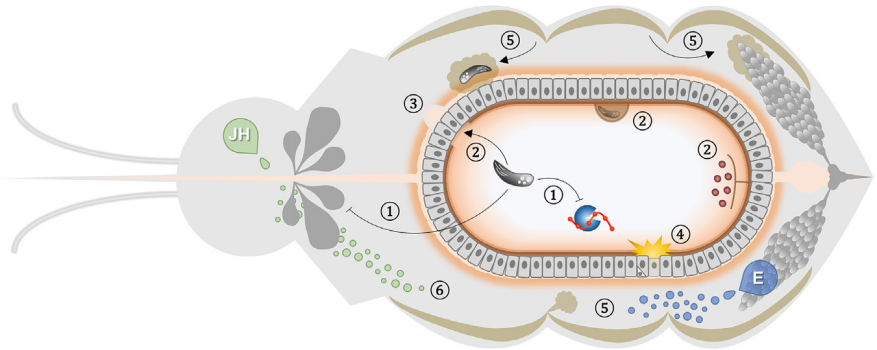

FIGURE 1 | Generic representation of non-immune elements that affect vector-pathogen interaction. The scheme depicts a frontal plane of a blood-feeding insect showing the relative position and interactions of the different non-immune players involved in diverse parasite-vector associations. Organ and cell sizes are not up to scale. **(1)** Parasites can manipulate feeding rate and digestion activity of the host (Stierhof et al., 1999; Sant'Anna et al., 2009). **(2)** Peritrophic matrix regulates intestinal infection, requiring parasite escape to establish invasion (Huber et al., 1991; Rose et al., 2020); allowing parasite anchoring to ectoperitrophic space (Pimenta et al., 1997; Zhang et al., 2015); and compartmentalizing microbiota to ensure immune ignorance of the epithelium (Weiss et al., 2014). **(3)** Blood-feeding-induced microperforations in the basal lamina support pathogen dissemination (Kantor et al., 2018; Armstrong et al., 2020). **(4)** Rupture of the peritrophic matrix barrier activates ROS generation that triggers an epithelial response to infection (Oliveira et al., 2011a; Taracena et al., 2018). Juvenile Hormone (JH) and Ecdysone (E) are key regulators of the physiological trade-off between reproduction and immunity. **(5)** Ovary ecdysone production exerts paramount effects such as fat body-induced provision of lipid molecules during vitellogenesis that can reduce the parasite-killing ability and support its development (Rono et al., 2010; Werling et al., 2019). **(6)** Juvenile hormone influence diverse physiological processes in the insect that can impact pathogen success such as ability to feed on blood, midgut remodeling, reproductive competency, gene expression regulation, lipid metabolism and immune response mounting (Clifton and Noriega, 2011; Zou et al., 2013; Roy et al., 2015; Kim et al., 2020).

permissive for viral escape (Kantor et al., 2018; Cui et al., 2019). Due to blood-feeding-induced microperforations in the basal lamina, virus-infected individuals fed an additional non-infectious blood meal disseminate and transmit viruses more efficiently than single-fed mosquitoes (Armstrong et al., 2020). It is interesting to note that the previous discussed transfer of male reproductive gland substances during mating in *Ae. aegypti* can increase blood-feeding frequency, potentially affecting pathogen transmission by female mosquitoes (Villarreal et al., 2018). One could simply postulate that the enhanced or accelerated parasite/pathogen development upon a sequential feeding is due to the higher availability of nutrients. However, other hypotheses can explain this phenomenon, like the aforementioned diversion of energy from the immune response to support oogenesis, and further evolutionary adaptations exploited by the parasite that favor their own development and transmission.

One of the most intriguing propositions in this field is that vector-borne parasites directly manipulate phenotypic traits of their vectors and hosts in ways that increase the contact between them, hence favoring transmission. Major observational examples include *Plasmodium*, *Leishmania,* and *Trypanosoma* spp. manipulating the behavior of mosquitoes, sand flies and kissing bugs, respectively (Hurd, 2003). Frequently studied changes include alterations of biting rates in vectors and increased attractiveness of vertebrate hosts (Lefèvre and Thomas, 2008). Moreover, interesting direct evidence suggests that parasite infection reduces the insect feeding efficiency, prolonging probing time, thus enhancing the likelihood of infecting multiple hosts during a single feeding cycle (Stierhof et al., 1999; van den Abbeele et al., 2010). According to this hypothesis, in malaria-mosquito systems, vector manipulation by the parasites decreases vertebrate host seeking during the pre-infectious phase, lowering the risk of mosquito death during early parasite development. Once the vectors have become infectious, these proceedings are again increased (Schwartz and Koella, 2001). Hence, mosquitoes harboring transmissible sporozoites would be more likely to bite several people per night (Koella et al., 1998). However, most of the evidence of manipulation comes from avian or rodent model systems and is focused on isolated components of mosquito host-feeding process (e.g., host detection, probing, piercing, blood ingestion and terminating the feed) (Friend and Smith, 1977). Therefore, the complexity of human malaria models makes it difficult to characterize how infection affects this multiple set of behaviors (Cator et al., 2012). Furthermore, when long evolutionary association between specific *Plasmodium* and *Anopheles* species combinations are tested, distinct or null alterations are shown (Nguyen et al., 2017; Stanczyk et al., 2019). Overall, behavioral manipulations stand as a complex phenomenon that continues to require careful observations with the use of different methods and multidisciplinary approaches (Lefèvre et al., 2006).

Regardless of the mechanism, vector-borne disease transmission depends on the frequency at which the insect vector bites humans. Therefore, fundamental investigations on the impact of complex vector behaviors, and of the ecology and evolution of vector–pathogen interactions, remain key aspects needed to generate better predictions of disease transmission and of the efficacy of control interventions. The varied transmission strategies evolved by pathogens and the vectors' behavioral changes induced by them can affect how current control tools work. Moreover, biting frequency and how bites are distributed among different people also can have significant epidemiologic effects (Woolhouse et al., 1997; Cooper et al., 2019).

High multiple-feeding rates can explain why reducing vector populations alone is difficult for prevention and support the argument for additional studies on feeding behavior (Harrington et al., 2014). Given that multiple blood-feedings directly increase the number of potentially infective encounters, this impact should be considered on model predictions and, accordingly, shape specific vector control strategies. This could mitigate the possibility of underestimating transmission intensity, which could lead to a misunderstanding of the impact of vector control (Tedrow et al., 2019).

CONCLUDING REMARKS

The growing impact of vector-borne diseases urgently calls for the development of new entomological interventions. Increasing knowledge on insect biology and insect–pathogen interactions that help unravel the processes that determine vectorial capacity will fuel innovative approaches to stop transmission (Shaw and Catteruccia, 2019). Insect hosts can resist infection or limit/tolerate the deleterious effects caused by the pathogen. Tolerance refers to all host defense mechanisms that limit 'damage to functions and structures' during infection, without interfering with pathogen load, as defined more than 60 years ago by plant pathologists (Caldwell et al., 1958). Therefore, resistance has a negative effect on pathogen fitness, whereas tolerance does not. The genetic trade-off between resistance and tolerance can shape the successful evolutionary interactions in a vector-pathogen system (Lambrechts and Saleh, 2019; Oliveira et al., 2020).

Here, we strengthen the argument that the insect vector response to infection does not merely activate immune pathways as a mechanism of resistance. It also encompasses a broad range of adaptive consequences, including metabolic alterations, stress responses, and tissue repair. Many of these are related to blood-feeding and reproduction (**Figure 1**). These events can lead to improved survival of the insect despite active pathogen replication. The impact of infection on the vector can thus be tuned by the parasite to favor both physiological host homeostasis and completion of the transmission cycle. Moreover, the target for natural selection is seldom one isolated organ or a discrete event, but rather are the multisystemic processes that involve pathogen acquisition and development within the vector. Despite recent advances in the knowledge of physiological mechanisms that can work as non-canonical immunological traits, several elements have yet to be unfolded. Future novel vector control strategies may arise rooted in integrated system biology research to target physiological aspects that act as protective mechanisms and contribute to tolerance to infection. In this way, innovative and effective tools can be used, in an evolutionary considerate manner, to mitigate the great burden imposed on societies by vector-borne diseases.

AUTHOR CONTRIBUTIONS

All authors listed have made a substantial, direct and intellectual contribution to the work, and approved it for publication.

FUNDING

This work was supported by the Conselho Nacional de Desenvolvimento Científico e Tecnológico (CNPq), Coordenação de Aperfeiçoamento de Pessoal de Nível Superior (CAPES), and Fundação de Amparo à Pesquisa do Estado do Rio de Janeiro (FAPERJ).

ACKNOWLEDGMENTS

The authors would like to thank S. R. Cássia for careful reading of this manuscript.

REFERENCES

Ahlers, L. R. H., Trammell, C. E., Carrell, G. F., Mackinnon, S., Torrevillas, B. K., Chow, C. Y., et al. (2019). Insulin potentiates JAK/STAT signaling to broadly inhibit flavivirus replication in insect vectors. *Cell Rep.* 29, 1946.e5–1960.e5. doi: 10.1016/j.celrep.2019.10.029

Ahmed, A. M., Baggott, S. L., Maingon, R., and Hurd, H. (2002). The costs of mounting an immune response are reflected in the reproductive fitness of the mosquito *Anopheles gambiae*. *Oikos* 97, 371–377. doi: 10.1034/j.1600-0706.2002.970307.x

Ahmed, A. M., and Hurd, H. (2006). Immune stimulation and malaria infection impose reproductive costs in *Anopheles gambiae* via follicular apoptosis. *Microbes Infect.* 8, 308–315. doi: 10.1016/j.micinf.2005.06.026

Ahmed, S. M. H., Maldera, J. A., Krunic, D., Paiva-Silva, G. O., Pénalva, C., Teleman, A. A., et al. (2020). Fitness trade-offs incurred by ovary-to-gut steroid signalling in *Drosophila*. *Nature* 584, 415–419. doi: 10.1038/s41586-020-2462-y

Akman-Anderson, L., Olivier, M., and Luckhart, S. (2007). Induction of nitric oxide synthase and activation of signaling proteins in *Anopheles mosquitoes* by the malaria pigment, hemozoin. *Infect. Immun.* 75, 4012–4019. doi: 10.1128/IAI.00645-07

Aksoy, S. (2019). Tsetse peritrophic matrix influences for trypanosome transmission. *J. Insect Physiol.* 118:103919. doi: 10.1016/j.jinsphys.2019.103919

Alves, C. R., Albuquerque-Cunha, J. M., Mello, C. B., Garcia, E. S., Nogueira, N. F., Bourguingnon, S. C., et al. (2007). *Trypanosoma cruzi*: Attachment to perimicrovillar membrane glycoproteins of *Rhodnius prolixus*. *Exp. Parasitol.* 116, 44–52. doi: 10.1016/j.exppara.2006.11.012

Angleró-Rodríguez, Y. I., MacLeod, H. J., Kang, S., Carlson, J. S., Jupatanakul, N., and Dimopoulos, G. (2017a). *Aedes aegypti* molecular responses to zika virus: modulation of infection by the toll and Jak/Stat immune pathways and virus host factors. *Front. Microbiol.* 8:2050. doi: 10.3389/fmicb.2017.02050

Angleró-Rodríguez, Y. I., Talyuli, O. A. C., Blumberg, B. J., Kang, S., Demby, C., Shields, A., et al. (2017b). An *Aedes aegypti*-associated fungus increases susceptibility to dengue virus by modulating gut trypsin activity. *eLife* 6, 1–20. doi: 10.7554/eLife.28844

Armstrong, P. M., Ehrlich, H. Y., Magalhaes, T., Miller, M. R., Conway, P. J., Bransfield, A., et al. (2020). Successive blood meals enhance virus dissemination within mosquitoes and increase transmission potential. *Nat. Microbiol.* 5, 239–247. doi: 10.1038/s41564-019-0619-y

Atella, G. C., Bittencourt-Cunha, P. R., Nunes, R. D., Shahabuddin, M., and Silva-Neto, M. A. C. (2009). The major insect lipoprotein is a lipid source to mosquito stages of malaria parasite. *Acta Trop.* 109, 159–162. doi: 10.1016/j.actatropica.2008.10.004

Ayres, J. S., Freitag, N., and Schneider, D. S. (2008). Identification of *Drosophila* mutants altering defense of and endurance to listeria monocytogenes infection. *Genetics* 178, 1807–1815. doi: 10.1534/genetics.107.083782

Azambuja, P., Garcia, E. S., Waniek, P. J., Vieira, C. S., Figueiredo, M. B., Gonzalez, M. S., et al. (2017). *Rhodnius prolixus*: from physiology by Wigglesworth to recent studies of immune system modulation by *Trypanosoma cruzi* and *Trypanosoma rangeli*. *J. Insect Physiol.* 97, 45–65. doi: 10.1016/j.jinsphys.2016.11.006

Bahia, A. C., Oliveira, J. H. M., Kubota, M. S., Araújo, H. R. C., Lima, J. B. P., Ríos-Velásquez, C. M., et al. (2013). The role of reactive oxygen species in *Anopheles aquasalis* response to *Plasmodium vivax* infection. *PLoS One* 8:e57014. doi: 10.1371/journal.pone.0057014

Baia-da-Silva, D. C., Alvarez, L. C. S., Lizcano, O. V., Costa, F. T. M., Lopes, S. C. P., Orfanó, A. S., et al. (2018). The role of the peritrophic matrix and red blood cell concentration in *Plasmodium vivax* infection of *Anopheles aquasalis*. *Parasit. Vectors* 11:148. doi: 10.1186/s13071-018-2752-5

Barillas-Mury, C. V., Noriega, F. G., and Wells, M. A. (1995). Early trypsin activity is part of the signal transduction system that activates transcription of the late trypsin gene in the midgut of the mosquito, *Aedes aegypti*. *Insect Biochem. Mol. Biol.* 25, 241–246. doi: 10.1016/0965-1748(94)00061-L

Barletta, A. B. F., Alves, L. R., Nascimento Silva, M. C. L., Sim, S., Dimopoulos, G., Liechocki, S., et al. (2016). Emerging role of lipid droplets in *Aedes aegypti* immune response against bacteria and *Dengue virus*. *Sci. Rep.* 6:19928. doi: 10.1038/srep19928

Barletta, A. B. F., Alves e Silva, T. L., Talyuli, O. A. C., Luna-Gomes, T., Sim, S., Angleró-Rodríguez, Y., et al. (2020). Prostaglandins regulate humoral immune responses in *Aedes aegypti*. *PLoS Negl. Trop. Dis.* 14:e0008706. doi: 10.1371/journal.pntd.0008706

Barletta, A. B. F., Trisnadi, N., Ramirez, J. L., and Barillas-Mury, C. (2019). Mosquito midgut prostaglandin release establishes systemic immune priming. *iScience* 19, 54–62. doi: 10.1016/j.isci.2019.07.012

Barral-Netto, M., Barral, A., Brownell, C., Skeiky, Y., Ellingsworth, L., Twardzik, D., et al. (1992). Transforming growth factor-beta in leishmanial infection: a parasite escape mechanism. *Science* 257, 545–548. doi: 10.1126/science.1636092

Batista, K. K., da, S., Vieira, C. S., Florentino, E. B., Caruso, K. F. B., Teixeira, P. T. P., et al. (2020). Nitric oxide effects on *Rhodnius prolixus's* immune responses, gut microbiota and *Trypanosoma cruzi* development. *J. Insect Physiol.* 126:104100. doi: 10.1016/j.jinsphys.2020.104100

Beier, J. C. (1996). Frequent blood-feeding and restrictive sugar-feeding behavior enhance the malaria vector potential of *Anopheles gambiae* s.l. and An. funestus (Diptera: Culicidae) in Western Kenya. *J. Med. Entomol.* 33, 613–618. doi: 10.1093/jmedent/33.4.613

Beier, J. C., Oster, C. N., Koros, J. K., Onyango, F. K., Githeko, A. K., Rowton, E., et al. (1989). Effect of human circumsporozoite antibodies in *Plasmodium*-infected *Anopheles* (Diptera: Culicidae). *J. Med. Entomol.* 26, 547–553. doi: 10.1093/jmedent/26.6.547

Billingsley, P. F., and Rudin, W. (1992). The role of the mosquito peritrophic membrane in bloodmeal digestion and infectivity of *Plasmodium* species. *J. Parasitol.* 78, 430–440. doi: 10.2307/3283640

Borges, E. C., Machado, E. M. M., Garcia, E. S., and Azambuja, P. (2006). *Trypanosoma cruzi*: effects of infection on cathepsin D activity in the midgut of *Rhodnius prolixus*. *Exp. Parasitol.* 112, 130–133. doi: 10.1016/j.exppara.2005.09.008

Bottino-Rojas, V., Pereira, L. O. R., Silva, G., Talyuli, O. A. C., Dunkov, B. C., Oliveira, P. L., et al. (2019). Non-canonical transcriptional regulation of heme oxygenase in *Aedes aegypti*. *Sci. Rep.* 9, 1–12. doi: 10.1038/s41598-019-49396-3

Bottino-Rojas, V., Talyuli, O. A. C., Carrara, L., Martins, A. J., James, A. A., Oliveira, P. L., et al. (2018). The redox-sensing gene Nrf2 affects intestinal homeostasis, insecticide resistance, and Zika virus susceptibility in the mosquito *Aedes aegypti*. *J. Biol. Chem.* 293, 9053–9063. doi: 10.1074/jbc.RA117.001589

Bottino-Rojas, V., Talyuli, O. A. C., Jupatanakul, N., Sim, S., Dimopoulos, G., Venancio, T. M., et al. (2015). Heme signaling impacts global gene expression, immunity and dengue virus infectivity in *Aedes aegypti*. *PLoS One* 10:e0135985. doi: 10.1371/journal.pone.0135985

Brackney, D. E., Isoe, J., Black, W. C., Zamora, J., Foy, B. D., Miesfeld, R. L., et al. (2010). Expression profiling and comparative analyses of seven midgut serine proteases from the yellow fever mosquito, *Aedes aegypti*. *J. Insect Physiol.* 56, 736–744. doi: 10.1016/j.jinsphys.2010.01.003

Brackney, D. E., Olson, K. E., and Foy, B. D. (2008). The effects of midgut serine proteases on dengue virus type 2 infectivity of *Aedes aegypti*. *Am. J. Trop. Med. Hyg.* 79, 267–274. doi: 10.4269/ajtmh.2008.79.267

Brandon, M. C., Pennington, J. E., Isoe, J., Zamora, J., Schillinger, A.-S., and Miesfeld, R. L. (2008). TOR signaling is required for amino acid stimulation of early trypsin protein synthesis in the midgut of *Aedes aegypti* mosquitoes. *Insect Biochem. Mol. Biol.* 38, 916–922. doi: 10.1016/j.ibmb.2008.07.003

Brown, M. R., Clark, K. D., Gulia, M., Zhao, Z., Garczynski, S. F., Crim, J. W., et al. (2008). An insulin-like peptide regulates egg maturation and metabolism in the mosquito *Aedes aegypti*. *Proc. Natl. Acad. Sci. U.S.A.* 105, 5716–5721. doi: 10.1073/pnas.0800478105

Buchon, N., Broderick, N. A., and Lemaitre, B. (2013). Gut homeostasis in a microbial world: insights from *Drosophila melanogaster*. *Nat. Rev. Microbiol.* 11, 615–626. doi: 10.1038/nrmicro3074

Buchon, N., Broderick, N. A., Poidevin, M., Pradervand, S., and Lemaitre, B. (2009). *Drosophila* intestinal response to bacterial infection: activation of host defense and stem cell proliferation. *Cell Host Microbe* 5, 200–211. doi: 10.1016/j.chom.2009.01.003

Buzza, M. S., Netzel-Arnett, S., Shea-Donohue, T., Zhao, A., Lin, C. Y., List, K., et al. (2010). Membrane-anchored serine protease matriptase regulates epithelial barrier formation and permeability in the intestine. *Proc. Natl. Acad. Sci. U.S.A.* 107, 4200–4205. doi: 10.1073/pnas.0903923107

Caldwell, R. M., Schafer, J. F., Compton, L. E., and Patterson, F. L. (1958). Tolerance to cereal leaf rusts. *Science* 128, 714–715. doi: 10.1126/science.128.3326.714

Canavoso, L. E., Jouni, Z. E., Karnas, K. J., Pennington, J. E., and Wells, M. A. (2001). Fat metabolism in insects. *Annu. Rev. Nutr.* 21, 23–46. doi: 10.1146/annurev.nutr.21.1.23

Casadevall, A., and Pirofski, L. (1999). Host-pathogen interactions: redefining the basic concepts of virulence and pathogenicity. *Infect. Immun.* 67, 3703–3713. doi: 10.1128/IAI.67.8.3703-3713.1999

Castillo, J., Brown, M. R., and Strand, M. R. (2011). Blood feeding and insulin-like peptide 3 stimulate proliferation of hemocytes in the mosquito *Aedes aegypti*. *PLoS Pathog.* 7:e1002274. doi: 10.1371/journal.ppat.1002274

Castro, D. P., Moraes, C. S., Gonzalez, M. S., Ratcliffe, N. A., Azambuja, P., and Garcia, E. S. (2012). *Trypanosoma cruzi* immune response modulation decreases microbiota in *Rhodnius prolixus* gut and is crucial for parasite survival and development. *PLoS One* 7:e36591. doi: 10.1371/journal.pone.0036591

Cator, L. J., Lynch, P. A., Read, A. F., and Thomas, M. B. (2012). Do malaria parasites manipulate mosquitoes? *Trends Parasitol.* 28, 466–470. doi: 10.1016/j.pt.2012.08.004

Chege, G. M. M., Pumpuni, C. B., and Beier, J. C. (1996). Proteolytic enzyme activity and *Plasmodium falciparum* sporogonic development in three species of *Anopheles mosquitoes*. *J. Parasitol.* 82:11. doi: 10.2307/3284108

Cheon, H. M., Sang, W. S., Bian, G., Park, J. H., and Raikhel, A. S. (2006). Regulation of lipid metabolism genes, lipid carrier protein lipophorin, and its receptor during immune challenge in the mosquito *Aedes aegypti*. *J. Biol. Chem.* 281, 8426–8435. doi: 10.1074/jbc.M510957200

Childs, L. M., Cai, F. Y., Kakani, E. G., Mitchell, S. N., Paton, D., Gabrieli, P., et al. (2016). Disrupting mosquito reproduction and parasite development for malaria control. *PLoS Pathog.* 12:e1006060. doi: 10.1371/journal.ppat.1006060

Chotiwan, N., Andre, B. G., Sanchez-Vargas, I., Islam, M. N., Grabowski, J. M., Hopf-Jannasch, A., et al. (2018). Dynamic remodeling of lipids coincides with dengue virus replication in the midgut of *Aedes aegypti* mosquitoes. *PLoS Pathog.* 14:e1006853. doi: 10.1371/journal.ppat.1006853

Chovatiya, R., and Medzhitov, R. (2014). Stress, inflammation, and defense of homeostasis. *Mol. Cell* 54, 281–288. doi: 10.1016/j.molcel.2014.03.030

Chu, J. J. H., Leong, P. W. H., and Ng, M. L. (2006). Analysis of the endocytic pathway mediating the infectious entry of mosquito-borne flavivirus West Nile into *Aedes albopictus* mosquito (C6/36) cells. *Virology* 349, 463–475. doi: 10.1016/j.virol.2006.01.022

Cirimotich, C. M., Dong, Y., Clayton, A. M., Sandiford, S. L., Souza-Neto, J. A., Mulenga, M., et al. (2011). Natural microbe-mediated refractoriness to *Plasmodium* infection in *Anopheles gambiae*. *Science* 332, 855–858. doi: 10.1126/science.1201618

Clark, A. J., and Block, K. (1959). The absence of sterol synthesis in insects. *J. Biol. Chem.* 234, 2578–2582.

Clifton, M. E., Correa, S., Rivera-Perez, C., Nouzova, M., and Noriega, F. G. (2014). Male *Aedes aegypti* mosquitoes use JH III transferred during copulation to

influence previtellogenic ovary physiology and affect the reproductive output of female mosquitoes. *J. Insect Physiol.* 64, 40–47. doi: 10.1016/j.jinsphys.2014.03.006

Clifton, M. E., and Noriega, F. G. (2011). Nutrient limitation results in juvenile hormone-mediated resorption of previtellogenic ovarian follicles in mosquitoes. *J. Insect Physiol.* 57, 1274–1281. doi: 10.1016/j.jinsphys.2011.06.002

Coconnier, M. H., Dlissi, E., Robard, M., Laboisse, C. L., Gaillard, J. L., and Servin, A. L. (1998). Listeria monocytogenes stimulates mucus exocytosis in cultured human polarized mucosecreting intestinal cells through action of listeriolysin O. *Infect. Immun.* 66, 3673–3681.

Cooper, L., Kang, S. Y., Bisanzio, D., Maxwell, K., Rodriguez-Barraquer, I., Greenhouse, B., et al. (2019). Pareto rules for malaria super-spreaders and super-spreading. *Nat. Commun.* 10, 1–9. doi: 10.1038/s41467-019-11861-y

Coppens, I. (2013). Targeting lipid biosynthesis and salvage in apicomplexan parasites for improved chemotherapies. *Nat. Rev. Microbiol.* 11, 823–835. doi: 10.1038/nrmicro3139

Corby-Harris, V., Drexler, A., Watkins de Jong, L., Antonova, Y., Pakpour, N., Ziegler, R., et al. (2010). Activation of *Akt* signaling reduces the prevalence and intensity of Malaria Parasite infection and lifespan in *Anopheles stephensi* Mosquitoes. *PLoS Pathog* 6:e1001003. doi: 10.1371/journal.ppat.1001003

Costa, G., Gildenhard, M., Eldering, M., Lindquist, R. L., Hauser, A. E., Sauerwein, R., et al. (2018). Non-competitive resource exploitation within mosquito shapes within-host malaria infectivity and virulence. *Nat. Commun.* 9, 1–11. doi: 10.1038/s41467-018-05893-z

Coutinho-Abreu, I. V., Serafim, T. D., Meneses, C., Kamhawi, S., Oliveira, F., and Valenzuela, J. G. (2020). Leishmania infection induces a limited differential gene expression in the sand fly midgut. *BMC Genomics* 21:608. doi: 10.1186/s12864-020-07025-8

Coutinho-Abreu, I. V., Sharma, N. K., Robles-Murguia, M., and Ramalho-Ortigao, M. (2010). Targeting the midgut secreted PpChit1 reduces leishmania major development in its natural vector, the sand fly *Phlebotomus papatasi*. *PLoS Negl. Trop. Dis.* 4:e901. doi: 10.1371/journal.pntd.0000901

Cui, Y., Grant, D. G., Lin, J., Yu, X., and Franz, A. W. E. (2019). Zika virus dissemination from the midgut of *Aedes aegypti* is facilitated by bloodmeal-mediated structural modification of the midgut basal lamina. *Viruses* 11:1056. doi: 10.3390/v11111056

Dahalan, F. A., Churcher, T. S., Windbichler, N., and Lawniczak, M. K. N. (2019). The male mosquito contribution towards malaria transmission: Mating influences the *Anopheles* female midgut transcriptome and increases female susceptibility to human malaria parasites. *PLoS Pathog.* 15:e1008063. doi: 10.1371/journal.ppat.1008063

Dao, A., Kassogue, Y., Adamou, A., Diallo, M., Yaro, A. S., Traore, S. F., et al. (2010). Reproduction-longevity trade-off in *Anopheles gambiae* (Diptera: Culicidae). *J. Med. Entomol.* 47, 769–777. doi: 10.1603/ME10052

Das, S., Muleba, M., Stevenson, J. C., Pringle, J. C., and Norris, D. E. (2017). Beyond the entomological inoculation rate: characterizing multiple blood-feeding behavior and *Plasmodium falciparum* multiplicity of infection in *Anopheles* mosquitoes in northern Zambia. *Parasit. Vectors* 10, 1–13. doi: 10.1186/s13071-017-1993-z

de Azambuja, P., Garcia, E. S., Ratcliffe, N. A., and David Warthen, J. (1991). Immune-depression in *Rhodnius prolixus* induced by the growth inhibitor, azadirachtin. *J. Insect Physiol.* 37, 771–777. doi: 10.1016/0022-1910(91)90112-D

De Cicco, N. N. T., Pereira, M. G., Corrêa, J. R., Andrade-Neto, V. V., Saraiva, F. B., Chagas-Lima, A. C., et al. (2012). LDL uptake by *Leishmania amazonensis*: involvement of membrane lipid microdomains. *Exp. Parasitol.* 130, 330–340. doi: 10.1016/j.exppara.2012.02.014

de Medeiros, M. N., Belmonte, R., Soares, B. C. C., de Medeiros, L. N., Canetti, C., Freire-de-Lima, C. G., et al. (2009). Arrest of oogenesis in the bug *Rhodnius prolixus* challenged with the fungus *Aspergillus niger* is mediated by immune response-derived PGE2. *J. Insect Physiol.* 55, 151–158. doi: 10.1016/j.jinsphys.2008.10.019

Deplancke, B., and Gaskins, H. R. (2001). Microbial modulation of innate defense: Goblet cells and the intestinal mucus layer. *Am. J. Clin. Nutr.* 73, 1131S–1141S.

Diaz-Albiter, H., Sant'Anna, M. R. V., Genta, F. A., and Dillon, R. J. (2012). Reactive oxygen species-mediated immunity against *Leishmania mexicana* and *Serratia marcescens* in the phlebotomine sand fly *Lutzomyia longipalpis*. *J. Biol. Chem.* 287, 23995–24003. doi: 10.1074/jbc.M112.376095

Dinglasan, R. R., Devenport, M., Florens, L., Johnson, J. R., McHugh, C. A., Donnelly-Doman, M., et al. (2009). The *Anopheles gambiae* adult midgut peritrophic matrix proteome. *Insect Biochem. Mol. Biol.* 39, 125–134. doi: 10.1016/j.ibmb.2008.10.010

Dong, S., Balaraman, V., Kantor, A. M., Lin, J., Grant, D. A. G., Held, N. L., et al. (2017). Chikungunya virus dissemination from the midgut of *Aedes aegypti* is associated with temporal basal lamina degradation during bloodmeal digestion. *PLoS Negl. Trop. Dis.* 11:e0005976. doi: 10.1371/journal.pntd.0005976

Douglas, A. E. (2019). Simple animal models for microbiome research. *Nat. Rev. Microbiol.* 17, 764–775. doi: 10.1038/s41579-019-0242-1

Drexler, A., Nuss, A., Hauck, E., Glennon, E., Cheung, K., Brown, M., et al. (2013). Human IGF1 extends lifespan and enhances resistance to *Plasmodium falciparum* infection in the malaria vector *Anopheles stephensi*. *J. Exp. Biol.* 216, 208–217. doi: 10.1242/jeb.078873

Edogawa, S., Edwinson, A. L., Peters, S. A., Chikkamenahalli, L. L., Sundt, W., Graves, S., et al. (2020). Serine proteases as luminal mediators of intestinal barrier dysfunction and symptom severity in IBS. *Gut* 69, 62–73. doi: 10.1136/gutjnl-2018-317416

Elnaiem, D. A., Ward, R. D., and Young, P. E. (1994). Development of *Leishmania chagasi* (Kinetoplastida: Trypanosomatidae) in the second blood-meal of its vector *Lutzomyia longipalpis* (Diptera: Psychodidae). *Parasitol. Res.* 80, 414–419. doi: 10.1007/BF00932379

Etebari, K., Hegde, S., Saldaña, M. A., Widen, S. G., Wood, T. G., Asgari, S., et al. (2017). Global transcriptome analysis of *Aedes aegypti* mosquitoes in response to Zika virus infection. *mSphere* 2, 1648–1659. doi: 10.1128/mSphere.00456-17

Feldman, A. M., Billingsley, P. F., and Savelkoul, E. (1990). Bloodmeal digestion by strains of *Anopheles stephensi* Liston (Diptera: Culicidae) of differing susceptibility to *Plasmodium falciparum*. *Parasitology* 101, 193–200. doi: 10.1017/S003118200006323X

Fernández de Castro, I., Tenorio, R., and Risco, C. (2016). Virus assembly factories in a lipid world. *Curr. Opin. Virol.* 18, 20–26. doi: 10.1016/j.coviro.2016.02.009

Ferreira, C. M., Stiebler, R., Saraiva, F. M., Lechuga, G. C., Walter-Nuno, A. B., Bourguignon, S. C., et al. (2018). Heme crystallization in a Chagas disease vector acts as a redox-protective mechanism to allow insect reproduction and parasite infection. *PLoS Negl. Trop. Dis.* 12:e0006661. doi: 10.1371/journal.pntd.0006661

Figueiredo, M. B., Genta, F. A., Garcia, E. S., and Azambuja, P. (2008). Lipid mediators and vector infection: *Trypanosoma rangeli* inhibits *Rhodnius prolixus* hemocyte phagocytosis by modulation of phospholipase A2 and PAF-acetylhydrolase activities. *J. Insect Physiol.* 54, 1528–1537. doi: 10.1016/j.jinsphys.2008.08.013

Flatt, T., Heyland, A., Rus, F., Porpiglia, E., Sherlock, C., Yamamoto, R., et al. (2008). Hormonal regulation of the humoral innate immune response in *Drosophila melanogaster*. *J. Exp. Biol.* 211, 2712–2724. doi: 10.1242/jeb.014878

Franz, A., Kantor, A., Passarelli, A., and Clem, R. (2015). Tissue barriers to arbovirus infection in mosquitoes. *Viruses* 7, 3741–3767. doi: 10.3390/v7072795

Friend, W. G., and Smith, J. J. B. (1977). Factors affecting feeding by bloodsucking insects. *Annu. Rev. Entomol.* 22, 309–331. doi: 10.1146/annurev.en.22.010177.001521

Fu, Q., Inankur, B., Yin, J., Striker, R., and Lan, Q. (2015). Sterol carrier protein 2, a critical host factor for dengue virus infection, alters the cholesterol distribution in mosquito Aag2 cells. *J. Med. Entomol.* 52, 1124–1134. doi: 10.1093/jme/tjv101

Gandara, A. C. P., Oliveira, J. H. M., Nunes, R. D., Goncalves, R. L. S., Dias, F. A., Hecht, F., et al. (2016). Amino acids trigger down-regulation of superoxide via TORC pathway in the midgut of *Rhodnius prolixus*. *Biosci. Rep.* 36, 916–922. doi: 10.1042/BSR20160061

Gandara, A. C. P., Torres, A., Bahia, A. C., Oliveira, P. L., and Schama, R. (2017). Evolutionary origin and function of NOX4-art, an arthropod specific NADPH oxidase. *BMC Evol. Biol.* 17:92. doi: 10.1186/s12862-017-0940-0

Garcia, E. S., and Gilliam, F. C. (1980). *Trypanosoma cruzi* development is independent of protein digestion in the gut of *Rhodnius prolixus*. *J. Parasitol.* 66, 1052–1053.

Garcia, E. S., Machado, E. M. M., and Azambuja, P. (2004a). Effects of eicosanoid biosynthesis inhibitors on the prophenoloxidase-activating system and microaggregation reactions in the hemolymph of *Rhodnius prolixus*

infected with *Trypanosoma rangeli*. *J. Insect Physiol.* 50, 157–165. doi: 10.1016/j.jinsphys.2003.11.002

Garcia, E. S., Machado, E. M. M., and Azambuja, P. (2004b). Inhibition of hemocyte microaggregation reactions in *Rhodnius prolixus* larvae orally infected with *Trypanosoma rangeli*. *Exp. Parasitol.* 107, 31–38. doi: 10.1016/j.exppara.2004.03.015

Geoghegan, V., Stainton, K., Rainey, S. M., Ant, T. H., Dowle, A. A., Larson, T., et al. (2017). Perturbed cholesterol and vesicular trafficking associated with dengue blocking in Wolbachia-infected *Aedes aegypti* cells. *Nat. Commun.* 8:526. doi: 10.1038/s41467-017-00610-8

Golgher, D. B., Colli, W., Souto-Padrón, T., and Zingales, B. (1993). Galactofuranose-containing glycoconjugates of epimastigote and trypomastigote forms of *Trypanosoma cruzi*. *Mol. Biochem. Parasitol.* 60, 249–264. doi: 10.1016/0166-6851(93)90136-L

Gonçalves, R. L. S., Oliveira, J. H. M., Oliveira, G. A., Andersen, J. F., Oliveira, M. F., Oliveira, P. L., et al. (2012). Mitochondrial reactive oxygen species modulate mosquito susceptibility to *Plasmodium* infection. *PLoS One* 7:e41083. doi: 10.1371/journal.pone.0041083

Gondim, K. C., Atella, G. C., Pontes, E. G., and Majerowicz, D. (2018). Lipid metabolism in insect disease vectors. *Insect Biochem. Mol. Biol.* 101, 108–123. doi: 10.1016/j.ibmb.2018.08.005

Gonzalez, M. S., Hamedi, A., Albuquerque-Cunha, J. M., Nogueira, N. F. S., De Souza, W., Ratcliffe, N. A., et al. (2006). Antiserum against perimicrovillar membranes and midgut tissue reduces the development of *Trypanosoma cruzi* in the insect vector, *Rhodnius prolixus*. *Exp. Parasitol.* 114, 297–304. doi: 10.1016/j.exppara.2006.04.009

Gonzalez, M. S., Nogueira, N. F. S., Mello, C. B., De Souza, W., Schaub, G. A., Azambuja, P., et al. (1999). Influence of brain and azadirachtin on *Trypanosoma cruzi* development in the vector, *Rhodnius prolixus*. *Exp. Parasitol.* 92, 100–108. doi: 10.1006/expr.1998.4387

Graham, A. L., Allen, J. E., and Read, A. F. (2005). Evolutionary causes and consequences of immunopathology. *Annu. Rev. Ecol. Evol. Syst.* 36, 373–397. doi: 10.1146/annurev.ecolsys.36.102003.152622

Grigoryeva, L. A. (2010). Morpho-functional changes in the midgut of ixodid ticks (Acari: Ixodidae) during the life cycle. *Entomol. Rev.* 90, 405–409. doi: 10.1134/S0013873810030073

Gruntenko, N. E., and Rauschenbach, I. Y. (2008). Interplay of JH, 20E and biogenic amines under normal and stress conditions and its effect on reproduction. *J. Insect Physiol.* 54, 902–908. doi: 10.1016/j.jinsphys.2008.04.004

Gulia-Nuss, M., Robertson, A. E., Brown, M. R., and Strand, M. R. (2011). Insulin-like peptides and the target of rapamycin pathway coordinately regulate blood digestion and egg maturation in the mosquito *Aedes aegypti*. *PLoS One* 6:e0020401. doi: 10.1371/journal.pone.0020401

Gupta, L., Kumar, S., Yeon, S. H., Pimenta, P. F. P., and Barillas-Mury, C. (2005). Midgut epithelial responses of different mosquito-*Plasmodium* combinations: The actin cone zipper repair mechanism in *Aedes aegypti*. *Proc. Natl. Acad. Sci. U.S.A.* 102, 4010–4015. doi: 10.1073/pnas.0409642102

Gupta, L., Molina-Cruz, A., Kumar, S., Rodrigues, J., Dixit, R., Zamora, R. E., et al. (2009). The STAT pathway mediates late-phase immunity against *Plasmodium* in the mosquito *Anopheles gambiae*. *Cell Host Microbe* 5, 498–507. doi: 10.1016/j.chom.2009.04.003

Guzman, H., Walters, L. L., and Tesh, R. B. (1994). Histologic detection of multiple blood meals in *Phlebotomus duboscqi* (Diptera: Psychodidae). *J. Med. Entomol.* 31, 890–897. doi: 10.1093/jmedent/31.6.890

Ha, E.-M., Oh, C.-T., Bae, Y. S., and Lee, W.-J. (2005a). A direct role for dual oxidase in *Drosophila* gut immunity. *Science* 310, 847–850. doi: 10.1126/science.1117311

Ha, E.-M., Oh, C.-T., Ryu, J.-H., Bae, Y.-S., Kang, S.-W., Jang, I.-H., et al. (2005b). An antioxidant system required for host protection against gut infection in *Drosophila*. *Dev. Cell* 8, 125–132. doi: 10.1016/j.devcel.2004.11.007

Hagedorn, H. (2004). "Mosquito endocrinology," in *Biology of Disease Vectors*, 2nd Edn, ed. W. Marquardt (Amsterdam: Elsevier).

Han, Y. S., Thompson, J., Kafatos, F. C., and Barillas-Mury, C. (2001). Molecular interactions between *Anopheles stephensi* midgut cells and *Plasmodium berghei*: the time bomb theory of ookinete invasion of mosquitoes. *EMBO J.* 20, 1483–1483. doi: 10.1038/sj.emboj.7593651b

Hansen, I. A., Attardo, G. M., Park, J.-H., Peng, Q., and Raikhel, A. S. (2004). Target of rapamycin-mediated amino acid signaling in mosquito anautogeny. *Proc. Natl. Acad. Sci. U.S.A.* 101, 10626–10631. doi: 10.1073/pnas.0403460101

Hansen, I. A., Attardo, G. M., Rodriguez, S. D., and Drake, L. L. (2014). Four-way regulation of mosquito yolk protein precursor genes by juvenile hormone-, ecdysone-, nutrient-, and insulin-like peptide signaling pathways. *Front. Physiol.* 5:103. doi: 10.3389/fphys.2014.00103

Harrington, L. C., Fleisher, A., Ruiz-Moreno, D., Vermeylen, F., Wa, C. V., Poulson, R. L., et al. (2014). Heterogeneous feeding patterns of the dengue vector, *Aedes aegypti*, on individual human hosts in Rural Thailand. *PLoS Negl. Trop. Dis.* 8:e0003048. doi: 10.1371/journal.pntd.0003048

Hegedus, D. D., Toprak, U., and Erlandson, M. (2019). Peritrophic matrix formation. *J. Insect Physiol.* 117:103898. doi: 10.1016/j.jinsphys.2019.103898

Henriques, B. S., Gomes, B., da Costa, S. G., da Moraes, C. S., Mesquita, R. D., Dillon, V. M., et al. (2017). Genome wide mapping of peptidases in *Rhodnius prolixus*: identification of protease gene duplications, horizontally transferred proteases and analysis of peptidase A1 structures, with considerations on their role in the evolution of hematophagy in Triatomi. *Front. Physiol.* 8:1051. doi: 10.3389/fphys.2017.01051

Henriques, B. S., Gomes, B., Oliveira, P. L., Garcia, E., de, S., Azambuja, P., et al. (2021). Characterization of the temporal pattern of blood protein digestion in *Rhodnius prolixus*: first description of early and late gut cathepsins. *Front. Physiol.* 11:509310. doi: 10.3389/fphys.2020.509310

Hogg, J. C., and Hurd, H. (1995). *Plasmodium yoelii* nigeriensis : the effect of high and low intensity of infection upon the egg production and bloodmeal size of *Anopheles stephensi* during three gonotrophic cycles. *Parasitology* 111, 555–562. doi: 10.1017/S0031182000077027

Hooper, L. V. (2009). Do symbiotic bacteria subvert host immunity? *Nat. Rev. Microbiol.* 7, 367–374. doi: 10.1038/nrmicro2114

Hou, Y., Wang, X. L., Saha, T. T., Roy, S., Zhao, B., Raikhel, A. S., et al. (2015). Temporal coordination of carbohydrate metabolism during mosquito reproduction. *PLoS Genet.* 11:e1005309. doi: 10.1371/journal.pgen.1005309

Hu, C., Rio, R. V. M., Medlock, J., Haines, L. R., Nayduch, D., Savage, A. F., et al. (2008). Infections with immunogenic trypanosomes reduce tsetse reproductive fitness: potential impact of different parasite strains on vector population structure. *PLoS Negl. Trop. Dis.* 2:e0000192. doi: 10.1371/journal.pntd.0000192

Huber, M., Cabib, E., and Miller, L. H. (1991). Malaria parasite chitinase and penetration of the mosquito peritrophic membrane. *Proc. Natl. Acad. Sci. U.S.A.* 88, 2807–2810. doi: 10.1073/pnas.88.7.2807

Hurd, H. (2003). Manipulation of medically important insect vectors by their parasites. *Annu. Rev. Entomol.* 48, 141–161. doi: 10.1146/annurev.ento.48.091801.112722

Jahan, N., Docherty, P. T., Billingsley, P. F., and Hurd, H. (1999). Blood digestion in the mosquito, *Anopheles stephensi*: the effects of *Plasmodium yoelii* nigeriensis on midgut enzyme activities. *Parasitology* 119, 535–541. doi: 10.1017/S0031182099005090

Janeh, M., Osman, D., and Kambris, Z. (2017). Damage-induced cell regeneration in the midgut of *Aedes albopictus* mosquitoes. *Sci. Rep.* 7:44594. doi: 10.1038/srep44594

Jaramillo-Gutierrez, G., Molina-Cruz, A., Kumar, S., and Barillas-Mury, C. (2010). The *Anopheles gambiae* oxidation resistance 1 (OXR1) gene regulates expression of enzymes that detoxify reactive oxygen species. *PLoS One* 5:e11168. doi: 10.1371/journal.pone.0011168

Johansson, M. E. V., Sjövall, H., and Hansson, G. C. (2013). The gastrointestinal mucus system in health and disease. *Nat. Rev. Gastroenterol. Hepatol.* 10, 352–361. doi: 10.1038/nrgastro.2013.35

Jones, D. P. (2006). Redefining oxidative stress. *Antioxid. Redox Signal.* 8, 1865–1879. doi: 10.1089/ars.2006.8.1865

Jones, D. P., and Sies, H. (2015). The redox code. *Antioxid. Redox Signal.* 23, 734–746. doi: 10.1089/ars.2015.6247

Junjhon, J., Pennington, J. G., Edwards, T. J., Perera, R., Lanman, J., and Kuhn, R. J. (2014). Ultrastructural characterization and three-dimensional architecture of replication sites in dengue virus-infected mosquito cells. *J. Virol.* 88, 4687–4697. doi: 10.1128/jvi.00118-14

Jupatanakul, N., Sim, S., Angleró-Rodríguez, Y. I., Souza-Neto, J., Das, S., Poti, K. E., et al. (2017). Engineered *Aedes aegypti* JAK/STAT pathway-mediated immunity to dengue virus. *PLoS Negl. Trop. Dis.* 11:e0005187. doi: 10.1371/journal.pntd.0005187

Jupatanakul, N., Sim, S., and Dimopoulos, G. (2014). *Aedes aegypti* ML and Niemann-Pick type C family members are agonists of dengue virus infection. *Dev. Comp. Immunol.* 43, 1–9. doi: 10.1016/j.dci.2013.10.002

Kantor, A. M., Grant, D. G., Balaraman, V., White, T. A., and Franz, A. W. E. (2018). Ultrastructural analysis of chikungunya virus dissemination from the midgut of the yellow fever mosquito, *Aedes aegypti*. *Viruses* 10:571. doi: 10.3390/v10100571

Kim, I. H., Castillo, J. C., Aryan, A., Martin-Martin, I., Nouzova, M., Noriega, F. G., et al. (2020). A mosquito juvenile hormone binding protein (mJHBP) regulates the activation of innate immune defenses and hemocyte development. *PLoS Pathog.* 16:e1008288. doi: 10.1371/journal.ppat.1008288

Klenk, H. D., and Garten, W. (1994). Host cell proteases controlling virus pathogenicity. *Trends Microbiol.* 2, 39–43. doi: 10.1016/0966-842X(94)90123-6

Klowden, M. J. (1990). The endogenous regulation of mosquito reproductive behavior. *Experientia* 46, 660–670. doi: 10.1007/BF01939928

Klowden, M. J., and Chambers, G. M. (1991). Male accessory gland substances activate egg development in nutritionally stressed *Aedes aegypti* mosquitoes. *J. Insect Physiol.* 37, 721–726. doi: 10.1016/0022-1910(91)90105-9

Koella, J. C., Sorensen, F. L., and Anderson, R. A. (1998). The malaria parasite, *Plasmodium falciparum*, increases the frequency of multiple feeding of its mosquito vector, *Anopheles gambiae*. *Proc. R. Soc. B Biol. Sci.* 265, 763–768. doi: 10.1098/rspb.1998.0358

Kotsyfakis, M., Schwarz, A., Erhart, J., and Ribeiro, J. M. C. (2015). Tissue- and time-dependent transcription in Ixodes ricinus salivary glands and midguts when blood-feeding on the vertebrate host. *Sci. Rep.* 5, 1–10. doi: 10.1038/srep09103

Kounakis, K., Chaniotakis, M., Markaki, M., and Tavernarakis, N. (2019). Emerging roles of lipophagy in health and disease. *Front. Cell Dev. Biol.* 7:185. doi: 10.3389/fcell.2019.00185

Kramer, L. D., and Ebel, G. D. (2003). Dynamics of flavivirus infection in mosquitoes. *Adv. Virus Res.* 60, 187–232. doi: 10.1016/S0065-3527(03)60006-0

Kriaa, A., Jablaoui, A., Mkaouar, H., Akermi, N., Maguin, E., and Rhimi, M. (2020). Serine proteases at the cutting edge of IBD: Focus on gastrointestinal inflammation. *FASEB J.* 34, 7270–7282. doi: 10.1096/fj.202000031RR

Kumar, B. A., and Paily, K. P. (2011). Up-regulation of lipophorin (Lp) and lipophorin receptor (LpR) gene in the mosquito, *Culex quinquefasciatus* (Diptera: Culicidae), infected with the filarial parasite, *Wuchereria bancrofti* (Spirurida: Onchocercidae). *Parasitol. Res.* 108, 377–381. doi: 10.1007/s00436-010-2075-8

Kumar, S., Christophides, G. K., Cantera, R., Charles, B., Han, Y. S., Meister, S., et al. (2003). The role of reactive oxygen species on *Plasmodium melanotic* encapsulation in *Anopheles gambiae*. *Proc. Natl. Acad. Sci. U.S.A.* 100, 14139–14144. doi: 10.1073/pnas.2036262100

Kumar, S., Gupta, L., Yeon, S. H., and Barillas-Mury, C. (2004). Inducible peroxidases mediate nitration of *Anopheles* midgut cells undergoing apoptosis in response to *Plasmodium* invasion. *J. Biol. Chem.* 279, 53475–53482. doi: 10.1074/jbc.M409905200

Kumar, S., Molina-Cruz, A., Gupta, L., Rodrigues, J., and Barillas-Mury, C. (2010). A peroxidase/dual oxidase system modulates midgut epithelial immunity in *Anopheles gambiae*. *Science* 327, 1644–1648. doi: 10.1126/science.1184008

Kuraishi, T., Binggeli, O., Opota, O., Buchon, N., and Lemaitre, B. (2011). Genetic evidence for a protective role of the peritrophic matrix against intestinal bacterial infection in *Drosophila melanogaster*. *Proc. Natl. Acad. Sci. U.S.A.* 108, 15966–15971. doi: 10.1073/pnas.1105994108

Kuraishi, T., Hori, A., and Kurata, S. (2013). Host-microbe interactions in the gut of *Drosophila melanogaster*. *Front. Physiol.* 4:375. doi: 10.3389/fphys.2013.00375

Labaied, M., Jayabalasingham, B., Bano, N., Cha, S. J., Sandoval, J., Guan, G., et al. (2011). *Plasmodium salvages* cholesterol internalized by LDL and synthesized de novo in the liver. *Cell. Microbiol.* 13, 569–586. doi: 10.1111/j.1462-5822.2010.01555.x

Lambeth, J. D. (2007). Nox enzymes, ROS, and chronic disease: an example of antagonistic pleiotropy. *Free Radic. Biol. Med.* 43, 332–347. doi: 10.1016/j.freeradbiomed.2007.03.027

Lambrechts, L., and Saleh, M. C. (2019). Manipulating mosquito tolerance for arbovirus control. *Cell Host Microbe* 26, 309–313. doi: 10.1016/j.chom.2019.08.005

Lara, F. A., Lins, U., Bechara, G. H., and Oliveira, P. L. (2005). Tracing heme in a living cell: hemoglobin degradation and heme traffic in digest cells of the cattle tick *Boophilus microplus*. *J. Exp. Biol.* 208, 3093–3101. doi: 10.1242/jeb.01749.

Lee, K.-A., Cho, K.-C., Kim, B., Jang, I.-H., Nam, K., Kwon, Y. E., et al. (2018). Inflammation-modulated metabolic reprogramming is required for DUOX-dependent gut immunity in *Drosophila*. *Cell Host Microbe* 23, 338.e5–352.e5. doi: 10.1016/j.chom.2018.01.011

Lefèvre, T., Koella, J. C., Renaud, F., Hurd, H., Biron, D. G., and Thomas, F. (2006). New prospects for research on manipulation of insect vectors by pathogens. *PLoS Pathog.* 2:e0020072. doi: 10.1371/journal.ppat.0020072

Lefèvre, T., and Thomas, F. (2008). Behind the scene, something else is pulling the strings: Emphasizing parasitic manipulation in vector-borne diseases. *Infect. Genet. Evol.* 8, 504–519. doi: 10.1016/j.meegid.2007.05.008

Lefèvre, T., Vantaux, A., Dabiré, K. R., Mouline, K., and Cohuet, A. (2013). Non-genetic determinants of mosquito competence for malaria parasites. *PLoS Pathog.* 9:e1003365. doi: 10.1371/journal.ppat.1003365

Lehane, M. (2005). *The Biology of Blood-Sucking in Insects*, 2nd Edn. Cambridge, MA: Cambridge University Press.

Lehane, M. J. (1997). Peritrophic matrix structure and function. *Annu. Rev. Entomol.* 42, 525–550. doi: 10.1146/annurev.ento.42.1.525

Leier, H. C., Weinstein, J. B., Kyle, J. E., Lee, J.-Y., Bramer, L. M., Stratton, K. G., et al. (2020). A global lipid map defines a network essential for Zika virus replication. *Nat. Commun.* 11:3652. doi: 10.1038/s41467-020-17433-9

Li, Z., Quan, G., Jiang, X., Yang, Y., Ding, X., Zhang, D., et al. (2018). Effects of metabolites derived from gut microbiota and hosts on pathogens. *Front. Cell. Infect. Microbiol.* 8:314. doi: 10.3389/fcimb.2018.00314

Lim, J., Gowda, D. C., Krishnegowda, G., and Luckhart, S. (2005). Induction of nitric oxide synthase in *Anopheles stephensi* by *Plasmodium falciparum*: mechanism of signaling and the role of parasite glycosylphosphatidylinositols. *Infect. Immun.* 73, 2778–2789. doi: 10.1128/IAI.73.5.2778-2789.2005

Lissner, M. M., and Schneider, D. S. (2018). The physiological basis of disease tolerance in insects. *Curr. Opin. Insect Sci.* 29, 133–136. doi: 10.1016/j.cois.2018.09.004

Liu, J., Liu, Y., Nie, K., Du, S., Qiu, J., Pang, X., et al. (2016). Flavivirus NS1 protein in infected host sera enhances viral acquisition by mosquitoes. *Nat. Microbiol.* 1:16087. doi: 10.1038/nmicrobiol.2016.87

Liu, Z., Ren, Z., Zhang, J., Chuang, C. C., Kandaswamy, E., Zhou, T., et al. (2018). Role of ROS and nutritional antioxidants in human diseases. *Front. Physiol.* 9:477. doi: 10.3389/fphys.2018.00477

Luckhart, S., Giulivi, C., Drexler, A. L., Antonova-Koch, Y., Sakaguchi, D., Napoli, E., et al. (2013). Sustained activation of akt elicits mitochondrial dysfunction to block *Plasmodium falciparum* infection in the mosquito host. *PLoS Pathog.* 9:e1003180. doi: 10.1371/journal.ppat.1003180

Luckhart, S., and Rosenberg, R. (1999). Gene structure and polymorphism of an invertebrate nitric oxide synthase gene. *Gene* 232, 25–34. doi: 10.1016/S0378-1119(99)00121-3

Luckhart, S., Vodovotz, Y., Ciu, L., and Rosenberg, R. (1998). The mosquito *Anopheles stephensi* limits malaria parasite development with inducible synthesis of nitric oxide. *Proc. Natl. Acad. Sci. U.S.A.* 95, 5700–5705. doi: 10.1073/pnas.95.10.5700

Matetovici, I., De Vooght, L., and Van Den Abbeele, J. (2019). Innate immunity in the tsetse fly (Glossina), vector of African trypanosomes. *Dev. Comp. Immunol.* 98, 181–188. doi: 10.1016/j.dci.2019.05.003

Matsuo, T., Sato, M., Inoue, N., Yokoyama, N., Taylor, D., and Fujisaki, K. (2003). Morphological studies on the extracellular structure of the midgut of a tick, *Haemaphysalis longicornis* (Acari: Ixodidae). *Parasitol. Res.* 90, 243–248. doi: 10.1007/s00436-003-0833-6

Matthews, B. J., McBride, C. S., DeGennaro, M., Despo, O., and Vosshall, L. B. (2016). The neurotranscriptome of the *Aedes aegypti* mosquito. *BMC Genomics* 17:32. doi: 10.1186/s12864-015-2239-0

McCord, J. M., and Fridovich, I. (1969). Superoxide dismutase. An enzymic function for erythrocuprein (hemocuprein). *J. Biol. Chem.* 244, 6049–6055.

Medzhitov, R., Schneider, D. S., and Soares, M. P. (2012). Disease tolerance as a defense strategy. *Science* 335, 936–941. doi: 10.1126/science.1214935

Merzendorfer, H., and Zimoch, L. (2003). Chitin metabolism in insects: structure, function and regulation of chitin synthases and chitinases. *J. Exp. Biol.* 206, 4393–4412. doi: 10.1242/jeb.00709

Micchelli, C. A., and Perrimon, N. (2006). Evidence that stem cells reside in the adult *Drosophila* midgut epithelium. *Nature* 439, 475–479. doi: 10.1038/nature04371

Ming, M., Ewen, M. E., and Pereira, M. E. A. (1995). Trypanosome invasion of mammalian cells requires activation of the TGFβ signaling pathway. *Cell* 82, 287–296. doi: 10.1016/0092-8674(95)90316-X

Mitchell, S. N., and Catteruccia, F. (2017). Anopheline reproductive biology: Impacts on vectorial capacity and potential avenues for malaria control. *Cold Spring Harb. Perspect. Med.* 7:14. doi: 10.1101/cshperspect.a025593

Molina-Cruz, A., DeJong, R. J., Charles, B., Gupta, L., Kumar, S., Jaramillo-Gutierrez, G., et al. (2008). Reactive oxygen species modulate *Anopheles gambiae* immunity against bacteria and *Plasmodium*. *J. Biol. Chem.* 283, 3217–3223. doi: 10.1074/jbc.M705873200

Molina-Cruz, A., Gupta, L., Richardson, J., Bennett, K., Black, W., and Barillas-Mury, C. (2005). Effect of mosquito midgut trypsin activity on dengue-2 virus infection and dissemination in *Aedes aegypti*. *Am. J. Trop. Med. Hyg.* 72, 631–637. doi: 10.4269/ajtmh.2005.72.631

Montezano, A. C., Camargo, L. D. L., Persson, P., Rios, F. J., Harvey, A. P., Anagnostopoulou, A., et al. (2018). NADPH Oxidase 5 Is a pro-contractile nox isoform and a point of cross-talk for calcium and redox signaling-implications in vascular function. *J. Am. Heart Assoc.* 7, 1–15. doi: 10.1161/JAHA.118.009388

Moraes, C. S., Aguiar-Martins, K., Costa, S. G., Bates, P. A., Dillon, R. J., and Genta, F. A. (2018). Second blood meal by female *Lutzomyia longipalpis*?: enhancement by oviposition and its effects on digestion, longevity, and leishmania infection. *Biomed. Res. Int.* 2018, 1–10. doi: 10.1155/2018/2472508

Motta, J. P., Denadai-Souza, A., Sagnat, D., Guiraud, L., Edir, A., Bonnart, C., et al. (2019). Active thrombin produced by the intestinal epithelium controls mucosal biofilms. *Nat. Commun.* 10, 1–12. doi: 10.1038/s41467-019-11140-w

Narasimhan, S., and Fikrig, E. (2015). Tick microbiome: the force within. *Trends Parasitol.* 31, 315–323. doi: 10.1016/j.pt.2015.03.010

Narasimhan, S., Schuijt, T. J., Abraham, N. M., Rajeevan, N., Coumou, J., Graham, M., et al. (2017). Modulation of the tick gut milieu by a secreted tick protein favors Borrelia burgdorferi colonization. *Nat. Commun.* 8, 1–16. doi: 10.1038/s41467-017-00208-0

Ng, C. G., Coppens, I., Govindarajan, D., Pisciotta, J., Shulaev, V., and Griffin, D. E. (2008). Effect of host cell lipid metabolism on alphavirus replication, virion morphogenesis, and infectivity. *Proc. Natl. Acad. Sci. U.S.A.* 105, 16326–16331. doi: 10.1073/pnas.0808720105

Nguyen, P. L., Vantaux, A., Hien, D. F. S., Dabiré, K. R., Yameogo, B. K., Gouagna, L. C., et al. (2017). No evidence for manipulation of *Anopheles gambiae*, *An. coluzzii* and *An. arabiensis* host preference by *Plasmodium falciparum*. *Sci. Rep.* 7, 1–11. doi: 10.1038/s41598-017-09821-x

Nogueira, N. F. S., Gonzalez, M. S., Gomes, J. E., de Souza, W., Garcia, E. S., Azambuja, P., et al. (2007). *Trypanosoma cruzi*: Involvement of glycoinositolphospholipids in the attachment to the luminal midgut surface of *Rhodnius prolixus*. *Exp. Parasitol.* 116, 120–128. doi: 10.1016/j.exppara.2006.12.014

Nogueira, N. P., Saraiva, F. M. S., Sultano, P. E., Cunha, P. R. B. B., Laranja, G. A. T., Justo, G. A., et al. (2015). Proliferation and differentiation of *Trypanosoma cruzi* inside its vector have a new trigger: Redox status. *PLoS One* 10:e0116712. doi: 10.1371/journal.pone.0116712

Noriega, F. G. (2004). Nutritional regulation of JH synthesis: A mechanism to control reproductive maturation in mosquitoes? *Insect Biochem. Mol. Biol.* 34, 687–693. doi: 10.1016/j.ibmb.2004.03.021

Nouzova, M., Clifton, M. E., and Noriega, F. G. (2019). Mosquito adaptations to hematophagia impact pathogen transmission. *Curr. Opin. Insect Sci.* 34, 21–26. doi: 10.1016/j.cois.2019.02.002

Nunes, C., Sucena, É, and Koyama, T. (2020). Endocrine regulation of immunity in insects. *FEBS J.* 2020:15581. doi: 10.1111/febs.15581

Nuss, A. B., Brown, M. R., Murty, U. S., and Gulia-Nuss, M. (2018). Insulin receptor knockdown blocks filarial parasite development and alters egg production in the southern house mosquito, *Culex quinquefasciatus*. *PLoS Negl. Trop. Dis.* 12:e0006413. doi: 10.1371/journal.pntd.0006413

Okuda, K., de Almeida, F., Mortara, R. A., Krieger, H., Marinotti, O., and Tania Bijovsky, A. (2007). Cell death and regeneration in the midgut of the mosquito, *Culex quinquefasciatus*. *J. Insect Physiol.* 53, 1307–1315. doi: 10.1016/j.jinsphys.2007.07.005

Oliveira, G. D. A., Lieberman, J., and Barillas-Mury, C. (2012). Epithelial nitration by a peroxidase/NOX5 system mediates mosquito antiplasmodial immunity. *Science* 335, 856–859. doi: 10.1126/science.1209678

Oliveira, J. H., Bahia, A. C., and Vale, P. F. (2020). How are arbovirus vectors able to tolerate infection? *Dev. Comp. Immunol.* 103:103514. doi: 10.1016/j.dci.2019.103514

Oliveira, J. H. M., Gonçalves, R. L. S., Lara, F. A., Dias, F. A., Gandara, A. C. P., Menna-Barreto, R. F. S., et al. (2011a). Blood meal-derived heme decreases ROS levels in the midgut of *Aedes aegypti* and allows proliferation of intestinal microbiota. *PLoS Pathog.* 7:e1001320. doi: 10.1371/journal.ppat.1001320

Oliveira, J. H. M., Gonçalves, R. L. S., Oliveira, G. A., Oliveira, P. L., Oliveira, M. F., and Barillas-Mury, C. (2011b). Energy metabolism affects susceptibility of *Anopheles gambiae* mosquitoes to *Plasmodium* infection. *Insect Biochem. Mol. Biol.* 41, 349–355. doi: 10.1016/j.ibmb.2011.02.001

Oliveira, M. F., Silva, J. R., Dansa-Petretski, M., De Souza, W., Braga, C. M. S., Masuda, H., et al. (2000). Haemozoin formation in the midgut of the blood-sucking insect *Rhodnius prolixus*. *FEBS Lett.* 477, 95–98. doi: 10.1016/S0014-5793(00)01786-5

Oliver, S. V., and Brooke, B. D. (2017). The effects of ingestion of hormonal host factors on the longevity and insecticide resistance phenotype of the major malaria vector *Anopheles arabiensis* (Diptera: Culicidae). *PLoS One* 12:e0180909. doi: 10.1371/journal.pone.0180909

Omer, F. M., Kurtzhals, J. A., and Riley, E. M. (2000). Maintaining the immunological balance in parasitic infections: a role for TGF-β? *Parasitol. Today* 16, 18–23. doi: 10.1016/S0169-4758(99)01562-8

O'neal, A. J., Butler, L. R., Rolandelli, A., Gilk, S. D., and Pedra, J. H. F. (2020). Lipid hijacking: A unifying theme in vector-borne diseases. *eLife* 9:e61675. doi: 10.7554/eLife.61675

Osuna-Ramos, J. F., Reyes-Ruiz, J. M., and Del Ángel, R. M. (2018). The role of host cholesterol during flavivirus infection. *Front. Cell. Infect. Microbiol.* 8:388. doi: 10.3389/fcimb.2018.00388

Padrón, A., Molina-Cruz, A., Quinones, M., Ribeiro, J. M., Ramphul, U., Rodrigues, J., et al. (2014). In depth annotation of the *Anopheles gambiae* mosquito midgut transcriptome. *BMC Genomics* 15:636. doi: 10.1186/1471-2164-15-636

Pakpour, N., Akman-Anderson, L., Vodovotz, Y., and Luckhart, S. (2013a). The effects of ingested mammalian blood factors on vector arthropod immunity and physiology. *Microbes Infect.* 15, 243–254. doi: 10.1016/j.micinf.2013.01.003

Pakpour, N., Camp, L., Smithers, H. M., Wang, B., Tu, Z., Nadler, S. A., et al. (2013b). Protein kinase C-dependent signaling controls the midgut epithelial barrier to malaria parasite infection in anopheline mosquitoes. *PLoS One* 8:e76535. doi: 10.1371/journal.pone.0076535

Pakpour, N., Corby-Harris, V., Green, G. P., Smithers, H. M., Cheung, K. W., Riehle, M. A., et al. (2012). Ingested human insulin inhibits the mosquito NF-κB-dependent immune response to *Plasmodium falciparum*. *Infect. Immun.* 80, 2141–2149. doi: 10.1128/IAI.00024-12

Pakpour, N., Riehle, M. A., and Luckhart, S. (2014). Effects of ingested vertebrate-derived factors on insect immune responses. *Curr. Opin. Insect Sci.* 3, 1–5. doi: 10.1016/j.cois.2014.07.001

Park, J., Stanley, D., and Kim, Y. (2014). Roles of peroxinectin in PGE2-mediated cellular immunity in *Spodoptera exigua*. *PLoS One* 9:e105717. doi: 10.1371/journal.pone.0105717

Pascoa, V., Oliveira, P. L., Dansa-Petretski, M., Silva, J. R., Alvarenga, P. H., Jacobs-Lorena, M., et al. (2002). *Aedes aegypti* peritrophic matrix and its interaction with heme during blood digestion. *Insect Biochem. Mol. Biol.* 32, 517–523. doi: 10.1016/S0965-1748(01)00130-8

Pereira, M. G., Visbal, G., Salgado, L. T., Vidal, J. C., Godinho, J. L. P., De Cicco, N. N. T., et al. (2015). *Trypanosoma cruzi* epimastigotes are able to manage internal cholesterol levels under nutritional lipid stress conditions. *PLoS One* 10:e0128949. doi: 10.1371/journal.pone.0128949

Pereira-Chioccola, V. L., Acosta-Serrano, A., Correia de Almeida, I., Ferguson, M. A. J., Souto-Padron, T., Rodrigues, M. M., et al. (2000). Mucin-like molecules form a negatively charged coat that protects *Trypanosoma cruzi* trypomastigotes from killing by human anti-alpha-galactosyl antibodies. *J. Cell Sci.* 113(Pt 7), 1299–1307.

Perera, R., Riley, C., Isaac, G., Hopf-Jannasch, A. S., Moore, R. J., Weitz, K. W., et al. (2012). Dengue virus infection perturbs lipid homeostasis in infected mosquito cells. *PLoS Pathog.* 8:e1002584. doi: 10.1371/journal.ppat.1002584

Petersen, W., Stenzel, W., Silvie, O., Blanz, J., Saftig, P., Matuschewski, K., et al. (2017). Sequestration of cholesterol within the host late endocytic pathway restricts liver-stage *Plasmodium* development. *Mol. Biol. Cell* 28, 726–735. doi: 10.1091/mbc.E16-07-0531

Peterson, T. M. L., Gow, A. J., and Luckhart, S. (2007). Nitric oxide metabolites induced in *Anopheles stephensi* control malaria parasite infection. *Free Radic. Biol. Med.* 42, 132–142. doi: 10.1016/j.freeradbiomed.2006.10.037

Peterson, T. M. L., and Luckhart, S. (2006). A mosquito 2-Cys peroxiredoxin protects against nitrosative and oxidative stresses associated with malaria parasite infection. *Free Radic. Biol. Med.* 40, 1067–1082. doi: 10.1016/j.freeradbiomed.2005.10.059

Pietri, J. E., Pakpour, N., Napoli, E., Song, G., Pietri, E., Potts, R., et al. (2016). Two insulin-like peptides differentially regulate malaria parasite infection in the mosquito through effects on intermediary metabolism. *Biochem. J.* 473, 3487–3503. doi: 10.1042/BCJ20160271

Pietri, J. E., Pietri, E. J., Potts, R., Riehle, M. A., and Luckhart, S. (2015). *Plasmodium falciparum* suppresses the host immune response by inducing the synthesis of insulin-like peptides (ILPs) in the mosquito *Anopheles stephensi*. *Dev. Comp. Immunol.* 53, 134–144. doi: 10.1016/j.dci.2015.06.012

Pigeault, R., and Villa, M. (2018). Long-term pathogenic response to *Plasmodium relictum* infection in culex pipiens mosquito. *PLoS One* 13:e0192315. doi: 10.1371/journal.pone.0192315

Pimenta, P. F. P., Modi, G. B., Pereira, S. T., Shahabuddin, M., and Sacks, D. L. (1997). A novel role for the peritrophic matrix in protecting Leishmania from the hydrolytic activities of the sand fly midgut. *Parasitology* 115, 359–369. doi: 10.1017/S0031182097001510

Ponnudurai, T., Lensen, A. H. W., Van Gemert, G. J. A., Bensink, M. P. E., Bolmer, M., and Meuwissen, J. H. E. T. (1989). Sporozoite load of mosquitoes infected with *Plasmodium falciparum*. *Trans. R. Soc. Trop. Med. Hyg.* 83, 67–70. doi: 10.1016/0035-9203(89)90708-6

Powell, J. R. (2019). An evolutionary perspective on vector-borne diseases. *Front. Genet.* 10:1266. doi: 10.3389/fgene.2019.01266

Ramalho-Ortigao, M. (2010). Sand Fly-leishmania interactions: long relationships are not necessarily easy. *Open Parasitol. J.* 4, 195–204. doi: 10.2174/1874421401004010195

Ramirez, J. L., Souza-Neto, J., Torres Cosme, R., Rovira, J., Ortiz, A., Pascale, J. M., et al. (2012). Reciprocal tripartite interactions between the *Aedes aegypti* midgut microbiota, innate immune system and dengue virus influences vector competence. *PLoS Negl. Trop. Dis.* 6:e1561. doi: 10.1371/journal.pntd.0001561

Reiff, T., Jacobson, J., Cognigni, P., Antonello, Z., Ballesta, E., Tan, K. J., et al. (2015). Endocrine remodelling of the adult intestine sustains reproduction in *Drosophila*. *eLife* 4:e06930. doi: 10.7554/eLife.06930

Reth, M. (2002). Hydrogen peroxide as second messenger in lymphocyte activation. *Nat. Immunol.* 3, 1129–1134. doi: 10.1038/ni1202-1129

Reynolds, R. A., Kwon, H., and Smith, R. C. (2020). 20-hydroxyecdysone primes innate immune responses that limit bacterial and malarial parasite survival in *Anopheles gambiae*. *mSphere* 5:e00983-19. doi: 10.1128/mSphere.00983-19

Rodgers, F. H., Gendrin, M., Wyer, C. A. S., Christophides, G. K., Vilo, J., Yarza, P., et al. (2017). Microbiota-induced peritrophic matrix regulates midgut homeostasis and prevents systemic infection of malaria vector mosquitoes. *PLoS Pathog.* 13:e1006391. doi: 10.1371/journal.ppat.1006391

Romoli, O., and Gendrin, M. (2018). The tripartite interactions between the mosquito, its microbiota and *Plasmodium*. *Parasit. Vectors* 11:200. doi: 10.1186/s13071-018-2784-x

Rono, M. K., Whitten, M. M. A., Oulad-Abdelghani, M., Levashina, E. A., and Marois, E. (2010). The major yolk protein vitellogenin interferes with the anti-*Plasmodium* response in the malaria mosquito *Anopheles gambiae*. *PLoS Biol.* 8:e1000434. doi: 10.1371/journal.pbio.1000434

Rose, C., Casas-Sánchez, A., Dyer, N. A., Solórzano, C., Beckett, A. J., Middlehurst, B., et al. (2020). *Trypanosoma brucei* colonizes the tsetse gut via an immature peritrophic matrix in the proventriculus. *Nat. Microbiol.* 5, 909–916. doi: 10.1038/s41564-020-0707-z

Roy, S. G., and Raikhel, A. S. (2012). Nutritional and hormonal regulation of the TOR effector 4E-binding protein (4E-BP) in the mosquito *Aedes aegypti*. *FASEB J.* 26, 1334–1342. doi: 10.1096/fj.11-189969

Roy, S., Saha, T. T., Johnson, L., Zhao, B., Ha, J., White, K. P., et al. (2015). Regulation of gene expression patterns in mosquito reproduction. *PLoS Genet.* 11:1005450. doi: 10.1371/journal.pgen.1005450

Roy, S., Saha, T. T., Zou, Z., and Raikhel, A. S. (2018). Regulatory pathways controlling female insect reproduction. *Annu. Rev. Entomol.* 63, 489–511. doi: 10.1146/annurev-ento-020117-043258

Rus, F., Flatt, T., Tong, M., Aggarwal, K., Okuda, K., Kleino, A., et al. (2013). Ecdysone triggered PGRP-LC expression controls *Drosophila* innate immunity. *EMBO J.* 32, 1626–1638. doi: 10.1038/emboj.2013.100

Salcedo-Porras, N., and Lowenberger, C. (2019). The innate immune system of kissing bugs, vectors of chagas disease. *Dev. Comp. Immunol.* 98, 119–128. doi: 10.1016/j.dci.2019.04.007

Samaddar, S., Marnin, L., Butler, L. R., and Pedra, J. H. F. (2020). Immunometabolism in arthropod vectors: redefining interspecies relationships. *Trends Parasitol.* 36, 807–815. doi: 10.1016/j.pt.2020.07.010

Samsa, M. M., Mondotte, J. A., Iglesias, N. G., Assunção-Miranda, I., Barbosa-Lima, G., Da Poian, A. T., et al. (2009). Dengue virus capsid protein usurps lipid droplets for viral particle formation. *PLoS Pathog.* 5:e1000632. doi: 10.1371/journal.ppat.1000632

Sant'Anna, M. R., Diaz-Albiter, H., Aguiar-Martins, K., Al Salem, W. S., Cavalcante, R. R., Dillon, V. M., et al. (2014). Colonisation resistance in the sand fly gut: Leishmania protects *Lutzomyia longipalpis* from bacterial infection. *Parasit. Vectors* 7:329. doi: 10.1186/1756-3305-7-329

Sant'Anna, M. R., Diaz-Albiter, H., Mubaraki, M., Dillon, R. J., and Bates, P. A. (2009). Inhibition of trypsin expression in *Lutzomyia longipalpis* using RNAi enhances the survival of Leishmania. *Parasit. Vectors* 2, 1–10. doi: 10.1186/1756-3305-2-62

Santiago, P. B., de Araújo, C. N., Motta, F. N., Praça, Y. R., Charneau, S., Bastos, I. M. D., et al. (2017). Proteases of haematophagous arthropod vectors are involved in blood-feeding, yolk formation and immunity - a review. *Parasit. Vectors* 10:79. doi: 10.1186/s13071-017-2005-z

Santos-Araujo, S., Bomfim, L., Araripe, L. O., Bruno, R., Ramos, I., and Gondim, K. C. (2020). Silencing of ATG6 and ATG8 promotes increased levels of triacylglycerol (TAG) in the fat body during prolonged starvation periods in the Chagas disease vector *Rhodnius prolixus*. *Insect Biochem. Mol. Biol.* 127:103484. doi: 10.1016/j.ibmb.2020.103484

Saraiva, R. G., Kang, S., Simões, M. L., Angleró-Rodríguez, Y. I., and Dimopoulos, G. (2016). Mosquito gut antiparasitic and antiviral immunity. *Dev. Comp. Immunol.* 64, 53–64. doi: 10.1016/j.dci.2016.01.015

Schulze, R. J., Sathyanarayan, A., and Mashek, D. G. (2017). Breaking fat: the regulation and mechanisms of lipophagy. *Biochim. Biophys. Acta Mol. Cell Biol. Lipids* 1862, 1178–1187. doi: 10.1016/j.bbalip.2017.06.008

Schwartz, A., and Koella, J. C. (2001). Trade-offs, conflicts of interest and manipulation in *Plasmodium*-mosquito interactions. *Trends Parasitol.* 17, 189–194. doi: 10.1016/S1471-4922(00)01945-0

Schwenke, R. A., Lazzaro, B. P., and Wolfner, M. F. (2016). Reproduction–immunity trade-offs in insects. *Annu. Rev. Entomol.* 61, 239–256. doi: 10.1146/annurev-ento-010715-023924

Scott, T. W., Clark, G. G., Lorenz, L. H., Amerasinghe, P. H., Reiter, P., and Edman, J. D. (1993). Detection of multiple blood-feeding in *Aedes aegypti* (Diptera: Culicidae) during a single gonotrophic cycle using a histologic technique. *J. Med. Entomol.* 30, 94–99. doi: 10.1093/jmedent/30.1.94

Secundino, N. F. C., Eger-Mangrich, I., Braga, E. M., Santoro, M. M., and Pimenta, P. F. P. (2005). *Lutzomyia longipalpis* peritrophic matrix: Formation, structure, and chemical composition. *J. Med. Entomol.* 42, 928–938. doi: 10.1093/jmedent/42.6.928

Serafim, T. D., Coutinho-Abreu, I. V., Oliveira, F., Meneses, C., Kamhawi, S., and Valenzuela, J. G. (2018). Sequential blood meals promote Leishmania replication and reverse metacyclogenesis augmenting vector infectivity. *Nat. Microbiol.* 3, 548–555. doi: 10.1038/s41564-018-0125-7

Shahabuddin, M., Kaidoh, T., Aikawa, M., and Kaslow, D. C. (1995). *Plasmodium gallinaceum*: mosquito peritrophic matrix and the parasite-vector compatibility. *Exp. Parasitol.* 81, 386–393. doi: 10.1006/expr.1995.1129

Shahabuddin, M., Toyoshima, T., Aikawa, M., and Kaslow, D. C. (1993). Transmission-blocking activity of a chitinase inhibitor and activation of

malarial parasite chitinase by mosquito protease. *Proc. Natl. Acad. Sci. U.S.A.* 90, 4266–4270. doi: 10.1073/pnas.90.9.4266

Shao, L., Devenport, M., and Jacobs-lorena, M. (2001). The peritrophic matrix of hematophagous insects. *Arch. Insect Biochem. Physiol.* 47, 119–125. doi: 10.1002/arch.1042

Sharma, A., Nuss, A. B., and Gulia-Nuss, M. (2019). Insulin-like peptide signaling in mosquitoes: the road behind and the road ahead. *Front. Endocrinol.* 10:166. doi: 10.3389/fendo.2019.00166

Shaw, D. K., Tate, A. T., Schneider, D. S., Levashina, E. A., Kagan, J. C., Pal, U., et al. (2018). Vector immunity and evolutionary ecology: the harmonious dissonance. *Trends Immunol.* 39, 862–873. doi: 10.1016/j.it.2018.09.003

Shaw, W. R., and Catteruccia, F. (2019). Vector biology meets disease control: using basic research to fight vector-borne diseases. *Nat. Microbiol.* 4, 20–34. doi: 10.1038/s41564-018-0214-7

Shaw, W. R., Holmdahl, I. E., Itoe, M. A., Werling, K., Marquette, M., Paton, D. G., et al. (2020). Multiple blood feeding in mosquitoes shortens the *Plasmodium falciparum* incubation period and increases malaria transmission potential. *PLoS Pathog.* 16:e1009131. doi: 10.1371/journal.ppat.1009131

Short, S. M., Mongodin, E. F., MacLeod, H. J., Talyuli, O. A. C., and Dimopoulos, G. (2017). Amino acid metabolic signaling influences *Aedes aegypti* midgut microbiome variability. *PLoS Negl. Trop. Dis.* 11:e0005677. doi: 10.1371/journal.pntd.0005677

Sicard, J. F., Le Bihan, G., Vogeleer, P., Jacques, M., and Harel, J. (2017). Interactions of intestinal bacteria with components of the intestinal mucus. *Front. Cell. Infect. Microbiol.* 7:387. doi: 10.3389/fcimb.2017.00387

Sisterson, M. S. (2009). Transmission of insect-vectored pathogens: effects of vector fitness as a function of infectivity status. *Environ. Entomol.* 38, 345–355. doi: 10.1603/022.038.0206

Sojka, D., Franta, Z., Horn, M., Hajdušek, O., Caffrey, C. R., Mareš, M., et al. (2008). Profiling of proteolytic enzymes in the gut of the tick Ixodes ricinus reveals an evolutionarily conserved network of aspartic and cysteine peptidases. *Parasit. Vectors* 1:7. doi: 10.1186/1756-3305-1-7

Stanczyk, N. M., Brugman, V. A., Austin, V., Sanchez-Roman Teran, F., Gezan, S. A., Emery, M., et al. (2019). Species-specific alterations in *Anopheles mosquito* olfactory responses caused by *Plasmodium* infection. *Sci. Rep.* 9, 1–9. doi: 10.1038/s41598-019-40074-y

Sterkel, M., Oliveira, J. H. M., Bottino-Rojas, V., Paiva-Silva, G. O., and Oliveira, P. L. (2017). The dose makes the poison: nutritional overload determines the life traits of blood-feeding arthropods. *Trends Parasitol.* 20, 1–12. doi: 10.1016/j.pt.2017.04.008

Stiebler, R., Majerowicz, D., Knudsen, J., Gondim, K. C., Wright, D. W., Egan, T. J., et al. (2014). Unsaturated glycerophospholipids mediate heme crystallization: Biological implications for hemozoin formation in the kissing bug *Rhodnius prolixus*. *PLoS One* 9:e0088976. doi: 10.1371/journal.pone.0088976

Stierhof, Y. D., Bates, P. A., Jacobson, R. L., Rogers, M. E., Schlein, Y., Handman, E., et al. (1999). Filamentous proteophosphoglycan secreted by Leishmania promastigotes forms gel like three-dimensional networks that obstruct the digestive tract of infected sandfly vectors. *Eur. J. Cell Biol.* 78, 675–689. doi: 10.1016/S0171-9335(99)80036-3

Surachetpong, W., Pakpour, N., Cheung, K. W., and Luckhart, S. (2011). Reactive oxygen species-dependent cell signaling regulates the mosquito immune response to *Plasmodium falciparum*. *Antioxid. Redox Signal.* 14, 943–955. doi: 10.1089/ars.2010.3401

Surachetpong, W., Singh, N., Cheung, K. W., and Luckhart, S. (2009). MAPK ERK signaling regulates the TGF-β1-dependent mosquito response to *Plasmodium falciparum*. *PLoS Pathog* 5:e1000366. doi: 10.1371/journal.ppat.1000366

Tall, A. R., and Yvan-Charvet, L. (2015). Cholesterol, inflammation and innate immunity. *Nat. Rev. Immunol.* 15, 104–116. doi: 10.1038/nri3793

Taracena, M. L., Bottino-Rojas, V., Talyuli, O. A. C., Walter-Nuno, A. B., Oliveira, J. H. M., Angleró-Rodriguez, Y. I., et al. (2018). Regulation of midgut cell proliferation impacts *Aedes aegypti* susceptibility to dengue virus. *PLoS Negl. Trop. Dis.* 12:e0006498. doi: 10.1371/journal.pntd.0006498

Tedrow, R. E., Zimmerman, P. A., and Abbott, K. C. (2019). Multiple blood-feeding: a force multiplier for transmission. *Trends Parasitol.* 35, 949–952. doi: 10.1016/j.pt.2019.08.004

Telleria, E. L., Martins-Da-Silva, A., Tempone, A. J., and Traub-Cseko, Y. M. (2018). Leishmania, microbiota and sand fly immunity. *Parasitology* 145, 1336–1353. doi: 10.1017/S0031182018001014

Terra, W. R. (1988). Physiology and biochemistry of insect digestion: an evolutionary perspective. *Brazilian J. Med. Biol. Res.* 21, 675–734.

Terra, W. R. (2001). The origin and functions of the insect peritrophic membrane and peritrophic gel. *Arch. Insect Biochem. Physiol.* 47, 47–61. doi: 10.1002/arch.1036

Terra, W. R., Dias, R. O., Oliveira, P. L., Ferreira, C., and Venancio, T. M. (2018). Transcriptomic analyses uncover emerging roles of mucins, lysosome/secretory addressing and detoxification pathways in insect midguts. *Curr. Opin. Insect Sci.* 29, 34–40. doi: 10.1016/j.cois.2018.05.015

Thaker, S. K., Chapa, T., Garcia, G., Gong, D., Schmid, E. W., Arumugaswami, V., et al. (2019). Differential metabolic reprogramming by zika virus promotes cell death in human versus mosquito cells. *Cell Metab.* 29, 1206.e4–1216.e4. doi: 10.1016/j.cmet.2019.01.024

Tootle, T. L., Williams, D., Hubb, A., Frederick, R., and Spradling, A. (2011). *Drosophila* eggshell production: identification of new genes and coordination by Pxt. *PLoS One* 6:e19943. doi: 10.1371/journal.pone.0019943

Urbanski, A., and Rosinski, G. (2018). Role of neuropeptides in the regulation of the insect immune system – current knowledge and perspectives. *Curr. Protein Pept. Sci.* 19, 1201–1213. doi: 10.2174/1389203719666180809113706

Vallochi, A. L., Teixeira, L., Oliveira, K., da, S., Maya-Monteiro, C. M., and Bozza, P. T. (2018). Lipid droplet, a key player in host-parasite interactions. *Front. Immunol.* 9:1022. doi: 10.3389/fimmu.2018.01022

van den Abbeele, J., Caljon, G., de Ridder, K., de Baetselier, P., and Coosemans, M. (2010). *Trypanosoma brucei* modifies the tsetse salivary composition, altering the fly feeding behavior that favors parasite transmission. *PLoS Pathog.* 6:e1000926. doi: 10.1371/journal.ppat.1000926

Varvas, K., Kurg, R., Hansen, K., Järving, R., Järving, I., Valmsen, K., et al. (2009). Direct evidence of the cyclooxygenase pathway of prostaglandin synthesis in arthropods: Genetic and biochemical characterization of two crustacean cyclooxygenases. *Insect Biochem. Mol. Biol.* 39, 851–860. doi: 10.1016/j.ibmb.2009.10.002

Veal, E. A., Day, A. M., and Morgan, B. A. (2007). Hydrogen peroxide sensing and signaling. *Mol. Cell* 26, 1–14. doi: 10.1016/j.molcel.2007.03.016

Vial, T., Tan, W. L., Xiang, B. W. W., Missé, D., Deharo, E., Marti, G., et al. (2019). Dengue virus reduces AGPAT1 expression to alter phospholipids and enhance infection in *Aedes aegypti*. *PLoS Pathog.* 15:e1008199. doi: 10.1371/journal.ppat.1008199

Vieira, C. S., Figueiredo, M. B., Moraes, C., da, S., Pereira, S. B., Dyson, P., et al. (2021). Azadirachtin interferes with basal immunity and microbial homeostasis in the *Rhodnius prolixus* midgut. *Dev. Comp. Immunol.* 114:103864. doi: 10.1016/j.dci.2020.103864

Villalon, J. M., Ghosh, A., and Jacobs-Lorena, M. (2003). The peritrophic matrix limits the rate of digestion in adult *Anopheles stephensi* and *Aedes aegypti* mosquitoes. *J. Insect Physiol.* 49, 891–895. doi: 10.1016/S0022-1910(03)00135-5

Villarreal, S. M., Pitcher, S., Helinski, M. E. H., Johnson, L., Wolfner, M. F., and Harrington, L. C. (2018). Male contributions during mating increase female survival in the disease vector mosquito *Aedes aegypti*. *J. Insect Physiol.* 108, 1–9. doi: 10.1016/j.jinsphys.2018.05.001

Vivenes, A., Oviedo, M., Márquez, J. C., and Montoya-Lerma, J. (2001). Effect of a Second Bloodmeal on the Oesophagus Colonization by Leishmania mexicana Complex in *Lutzomyia evansi* (Diptera: Psychodidae). *Mem. Inst. Oswaldo Cruz* 96, 281–283. doi: 10.1590/S0074-02762001000300001

Wang, X., Hou, Y., Saha, T. T., Pei, G., Raikhel, A. S., and Zou, Z. (2017). Hormone and receptor interplay in the regulation of mosquito lipid metabolism. *Proc. Natl. Acad. Sci. U.S.A.* 114, E2709–E2718. doi: 10.1073/pnas.1619326114

Weiss, B. L., Savage, A. F., Griffith, B. C., Wu, Y., and Aksoy, S. (2014). The peritrophic matrix mediates differential infection outcomes in the tsetse fly gut following challenge with commensal, pathogenic, and parasitic microbes. *J. Immunol.* 193, 773–782. doi: 10.4049/jimmunol.1400163

Werling, K., Shaw, W. R., Itoe, M. A., Westervelt, K. A., Marcenac, P., Paton, D. G., et al. (2019). Steroid hormone function controls non-competitive *Plasmodium* development in *Anopheles*. *Cell* 177, 315.e14–325.e14. doi: 10.1016/j.cell.2019.02.036

Whiten, S. R., Keith Ray, W., Helm, R. F., and Adelman, Z. N. (2018). Characterization of the adult *Aedes aegypti* early midgut peritrophic matrix proteome using LC-MS. *PLoS One* 13:e0194734. doi: 10.1371/journal.pone.0194734

Whitten, M., Sun, F., Tew, I., Schaub, G., Soukou, C., Nappi, A., et al. (2007). Differential modulation of *Rhodnius prolixus* nitric oxide activities following challenge with *Trypanosoma rangeli*, *T. cruzi* and bacterial cell wall components. *Insect Biochem. Mol. Biol.* 37, 440–452. doi: 10.1016/j.ibmb.2007.02.001

Wigglesworth, V. (1965). The juvenile hormone. *Nature* 208, 522–524. doi: 10.1038/208522a0

Woolhouse, M. E. J., Dye, C., Etard, J.-F., Smith, T., Charlwood, J. D., Garnett, G. P., et al. (1997). Heterogeneities in the transmission of infectious agents: Implications for the design of control programs. *Proc. Natl. Acad. Sci. U.S.A.* 94, 338–342. doi: 10.1073/pnas.94.1.338

Wu, K., Li, S., Wang, J., Ni, Y., Huang, W., Liu, Q., et al. (2020). Peptide hormones in the insect midgut. *Front. Physiol.* 11:191. doi: 10.3389/fphys.2020.00191

Xiao, X., Yang, L., Pang, X., Zhang, R., Zhu, Y., Wang, P., et al. (2017). A Mesh-Duox pathway regulates homeostasis in the insect gut. *Nat. Microbiol.* 2:17020. doi: 10.1038/nmicrobiol.2017.20

Zande, D. (1967). Absence of cholesterol synthesis as contrasted with the presence of fatty acid synthesis in some arthropods. *Comp. Biochem. Physiol.* 20, 811–822. doi: 10.1016/0010-406X(67)90055-2

Zhang, G., Niu, G., Franca, C. M., Dong, Y., Wang, X., Butler, N. S., et al. (2015). *Anopheles* midgut FREP1 mediates *Plasmodium* invasion. *J. Biol. Chem.* 290, 16490–16501. doi: 10.1074/jbc.M114.623165

Zhu, Y., Tong, L., Nie, K., Wiwatanaratanabutr, I., Sun, P., Li, Q., et al. (2019). Host serum iron modulates dengue virus acquisition by mosquitoes. *Nat. Microbiol.* 4, 2405–2415. doi: 10.1038/s41564-019-0555-x

Zingales, B., Martin, N. F., De Lederkremer, R. M., and Colli, W. (1982). Endogenous and surface labeling of glycoconjugates from the three differentiation stages of *Trypanosoma cruzi*. *FEBS Lett.* 142, 238–242. doi: 10.1016/0014-5793(82)80143-9

Zou, Z., Saha, T. T., Roy, S., Shin, S. W., Backman, T. W. H., Girke, T., et al. (2013). Juvenile hormone and its receptor, methoprene-tolerant, control the dynamics of mosquito gene expression. *Proc. Natl. Acad. Sci. U.S.A.* 110, E2173–E2181. doi: 10.1073/pnas.1305293110.C

Conflict of Interest: The authors declare that the research was conducted in the absence of any commercial or financial relationships that could be construed as a potential conflict of interest.

frontiers in Physiology

ORIGINAL RESEARCH
published: 01 April 2021
doi: 10.3389/fphys.2021.654565

The Fate of Dietary Cholesterol in the Kissing Bug *Rhodnius prolixus*

Petter F. Entringer[1†], David Majerowicz[2] and Katia C. Gondim[1]*

[1] *Instituto de Bioquímica Médica Leopoldo de Meis, Universidade Federal do Rio de Janeiro, Rio de Janeiro, Brazil,*
[2] *Departamento de Biotecnologia Farmacêutica, Faculdade de Farmácia, Universidade Federal do Rio de Janeiro, Rio de Janeiro, Brazil*

Insects are unable to synthesize cholesterol and depend on the presence of sterols in the diet for cell membrane composition and hormone production. Thus, cholesterol absorption, transport, and metabolism are potential targets for vector and pest control strategies. Here, we investigate the dietary cholesterol absorption and tissue distribution in the kissing bug *Rhodnius prolixus* using radiolabeled cholesterol. Both the anterior and posterior midguts absorbed cholesterol from the ingested blood, although the anterior midgut absorbed more. We also observed esterified cholesterol labeling in the epithelium, indicating that midgut cells can metabolize and store cholesterol. Only a small amount of labeled cholesterol was found in the hemolymph, where it was mainly in the free form and associated with lipophorin (Lp). The fat body transiently accumulated cholesterol, showing a labeled cholesterol peak on the fifth day after the blood meal. The ovaries also incorporated cholesterol, but cumulatively. The insects did not absorb almost half of the ingested labeled cholesterol, and radioactivity was present in the feces. After injection of ^{3}H-cholesterol-labeled Lp into females, a half-life of 5.5 ± 0.7 h in the hemolymph was determined. Both the fat body and ovaries incorporated Lp-associated cholesterol, which was inhibited at low temperature, indicating the participation of active cholesterol transport. These results help describe an unexplored part of *R. prolixus* lipid metabolism.

Keywords: cholesterol, intestinal absorption, fat body, ovary, lipid transport

OPEN ACCESS

Edited by:
Jose Luis Ramirez, United States Department of Agriculture (USDA), United States

Reviewed by:
Marcos Sterkel, Consejo Nacional de Investigaciones Científicas y Técnicas (CONICET), Argentina
Marcelo Salabert Gonzalez, Fluminense Federal University, Brazil

****Correspondence:***
Katia C. Gondim
katia@bioqmed.ufrj.br

†Present address:
Petter F. Entringer, Laboratório Integrado de Bioquímica Hatisaburo Masuda, Instituto de Biodiversidade e Sustentabilidade/NUPEM, Universidade Federal do Rio de Janeiro, UFRJ, Macaé, Brazil

Specialty section:
This article was submitted to Invertebrate Physiology, a section of the journal Frontiers in Physiology

Received: *16 January 2021*
Accepted: *23 February 2021*
Published: *01 April 2021*

Citation:
Entringer PF, Majerowicz D and Gondim KC (2021) The Fate of Dietary Cholesterol in the Kissing Bug Rhodnius prolixus. Front. Physiol. 12:654565. doi: 10.3389/fphys.2021.654565

INTRODUCTION

Cholesterol and other sterols are lipid molecules fundamental for cell function, constituting membranes and regulating their fluidity (Yang et al., 2016). Besides, hormones produced from sterols are present in different phyla of the Animal Kingdom (Qu et al., 2015). Mammals absorb cholesterol from their diet, but their primary source of cholesterol is *de novo* synthesis from acetate (Alphonse and Jones, 2016). On the other hand, insects are auxotrophic for dietary sterols, as they can convert sterols into cholesterol (Behmer et al., 1999), but they do not synthesize cholesterol *de novo* due to the lack of essential enzymes in the biosynthetic pathway (Clark and Block, 1959; Li and Jing, 2020). Thus, inhibiting dietary cholesterol absorption may be an effective control action for insect pests and vectors.

Abbreviations: ApoLp-I, apolipophorin-I; ApoLp-II, apolipophorin-II; EDTA, ethylenediamine tetraacetic acid; HPTLC, high-performance thin-layer chromatography; Lp, lipophorin; LTP, lipid transfer particle; NPC, Niemann–Pick type C protein; PBS, phosphate-buffered saline; SCP, sterol carrier protein; TAG, triacylglycerol; Vg, vitellogenin.

Cholesterol metabolism in insects has been studied in a few species, especially in Lepidoptera, Orthoptera, and Diptera. The midgut is the leading site for the absorption of ingested cholesterol in *Manduca sexta* (Jouni et al., 2002b) and in the locusts *Schistocerca gregaria* and *Locusta migratoria* (Upadhyay et al., 2002). It was first shown in *Drosophila melanogaster* that the protein NPC1b (Niemann–Pick type C1b) acts at an early step in sterol incorporation by the insect midgut (Voght et al., 2007). Most insects, differently from vertebrates, have two *NPC1* homolog genes, which encode the plasma membrane protein (NPC1b) or one that is involved in intracellular sterol trafficking (NPC1a) (Jing and Behmer, 2020). Sterol carrier protein-2 (SCP-2) has also been implicated in dietary sterol absorption, although its role is not clear. The gut of the moth *Spodoptera litura* expresses some SCPs in large quantities, and knockdown of these genes reduced the amount of cholesterol present in the hemolymph (Guo et al., 2009). Similarly, the use of pharmacological SCP inhibitors in *M. sexta* reduced cholesterol uptake (Kim and Lan, 2010). Additionally, SCP overexpression in cultured *Aedes aegypti* cells increased cholesterol uptake (Lan and Wessely, 2004). These results indicate that SCPs also take part in cholesterol absorption control.

Intestinal cells esterify part of the absorbed cholesterol (Komnick and Giesa, 1994; Jouni et al., 2002b), although in the hemolymph cholesterol is mostly in the free form and only a very small proportion, if any, is found as cholesterol esters (Chino and Downer, 1982; Komnick and Wachtmann, 1994; Jouni et al., 2002b; Atella et al., 2006; Majerowicz et al., 2013). These results indicate the presence of cholesterol acyltransferase and cholesterol esterase activities in the intestinal cells. In fact, in *D. melanogaster*, the lipase magro, in addition to its luminal triacylglycerol (TAG) lipase activity, also has cholesterol esterase activity inside the midgut cells, being important to maintain cholesterol homeostasis (Sieber and Thummel, 2012). In the gut of the dragonfly *Aeshna cyanea*, a cholesterol esterase activity was also identified, but in that case, it was a luminal activity, probably for digestion of dietary esterified cholesterol (Komnick and Giesa, 1994).

Cholesterol, as other lipids, is transported in the insect hemolymph by lipophorin (Lp) (Chino and Downer, 1982; Dantuma et al., 1997; Jouni et al., 2002a,b, 2003; Yun et al., 2002; Atella et al., 2006; Majerowicz et al., 2013). In *M. sexta* larvae, Lp receives cholesterol from the intestine and delivers it to the fat body (Yun et al., 2002); a long (10 h) half-life was determined after injection of cholesterol-labeled Lp into larval hemolymph (Jouni et al., 2002b).

The presence of either antibodies against the lipid transfer particle (LTP) or suramin in the medium did not affect cholesterol delivery from the midgut to Lp and only partially inhibited cholesterol transfer to and from the fat body (Jouni et al., 2002a; Yun et al., 2002). LTP facilitates diacylglycerol transfer from the midgut to Lp and to the fat body (Canavoso and Wells, 2001; Canavoso et al., 2004b), and suramin affects Lp binding to its receptor (Gondim and Wells, 2000). Thus, based on these and some other results, these authors proposed a predominant role of aqueous diffusion in the cholesterol transfer between Lp and tissues, and that a receptor-mediated process, if present, had a smaller contribution. However, the mechanism involved in cholesterol transport between lipoprotein, other proteins, and cells in insects needs more study.

The fat body stores the hemolymph-derived cholesterol in both free and esterified forms; in larval *A. cyanea* and adult *M. sexta*, cholesterol esters may account for 60–75% of total cholesterol in this organ. On the other hand, in larvae and pupae of *M. sexta*, most of cholesterol found in the fat body is in the free form, unlike the adults of the same species (Komnick and Giesa, 1994; Jouni et al., 2002b). In the triatomines *Dipetalogaster maxima*, *Triatoma infestans*, and *Panstrongylus megistus*, free cholesterol stored in the fat body was consumed during fasting periods, as occurred to other neutral lipids (Canavoso et al., 1998).

Lipophorin also transfers cholesterol to developing oocytes, as shown in *M. sexta* and in the silkworm *Bombyx mori* (Jouni et al., 2002b, 2003). Maternal cholesterol is the major source of embryo sterol content; and, thus, the appropriate ingestion, absorption, and transport of cholesterol to the oocytes are required for successful reproduction (Behmer and Grebenok, 1998; Jing and Behmer, 2020).

Rhodnius prolixus is an important vector of Chagas disease in South and Central Americas (de Fuentes-Vicente et al., 2018), and it is a model for insect physiology and biochemistry studies (Nunes-da-Fonseca et al., 2017), including lipid metabolism (Gondim et al., 2018). Our group has already characterized various aspects of *R. prolixus* lipid metabolism, including TAG digestion, absorption, and distribution (Grillo et al., 2007); the interaction of Lp with different organs (Pontes et al., 2002; Grillo et al., 2003; Entringer et al., 2013); and the synthesis and dynamics of TAG in the fat body (Pontes et al., 2008; Alves-Bezerra and Gondim, 2012; Alves-Bezerra et al., 2017) and ovaries (Santos et al., 2011). However, cholesterol metabolism remains a gap in the knowledge of this insect physiology. *R. prolixus* is an exclusive hematophagous hemipteran, feeding on blood during the whole life cycle, nymphs and adults. Although blood contains significant amounts of cholesterol, there is no information about absorption and utilization of this lipid in any triatomine species. Thus, here, we used radiolabeled cholesterol to investigate the fate of dietary cholesterol ingested by *R. prolixus* during the blood meal.

MATERIALS AND METHODS

Insects

The experimental insects were adult mated females of *R. prolixus* taken from a colony kept at 28 ± 2°C, 75–85% relative humidity, and 12-h/12-h light and dark cycles. The insects were fed on the outer ears of live rabbits at 3-week intervals. All animal care and experimental protocols were conducted following the guidelines of the institutional animal care and use committee (Committee for Evaluation of Animal Use for Research from the Universidade Federal do Rio de Janeiro, CEUA-UFRJ), process number 01200.001568/2013-87, order number 149/19, and the NIH Guide for the Care and Use of Laboratory Animals (ISBN 0-309-05377-3).

Absorption and Distribution of ^{3}H-Cholesterol Added to a Blood Meal

Adult females of *R. prolixus* were fed in an artificial feeder (Garcia et al., 1975) on whole rabbit blood supplemented with ^{3}H-cholesterol, 10^6 disintegrations per minute (DPM)/ml of blood ([1,2-^{3}H(N)]-cholesterol, specific activity 51 Ci/mmol; PerkinElmer, Boston, MA, United States; 3 ng of ^{3}H-cholesterol/ml of blood). About 1 h after blood meal, insects were individually housed at 28°C. On the first, third, fifth, seventh, and 10th days after the ^{3}H-cholesterol-enriched blood meal, hemolymph was individually collected in the presence of phenylthiourea. Insects were dissected; and anterior midgut, posterior midgut, ovaries, and fat bodies were collected. The midgut tissue was separated from the luminal content, by individually placing the anterior and posterior midguts in 500 μl of cold water. The obtained organs were abundantly washed in phosphate-buffered saline (PBS; 10 mM of sodium phosphate, 0.15 M of NaCl, pH 7.4) and homogenized in 200 μl of the same buffer. The hemolymph, homogenates, and luminal contents were frozen for posterior analysis. When present (usually on the seventh and 10th days), total feces from the dissected insects were collected by washing the vial bottom with 500 μl of PBS.

Lipid Extraction and Cholesterol Analysis

Organ homogenates, hemolymph, and midgut luminal contents were subjected to lipid extraction (Blight and Dyer, 1959). The organic phases containing the lipids were dried under a stream of nitrogen, and lipids were resuspended in 30 μl of chloroform and analyzed by high-performance thin-layer chromatography (HPTLC) on Silica gel 60 plates (Merck, Darmstadt, Germany) developed in hexane:ethyl ether:acetic acid (60:40:1) as solvent (Kawooya and Law, 1988). The following commercial lipid standards were used: cholesterol, cholesteryl ester, free fatty acid, monoacylglycerol, diacylglycerol, and TAG (Sigma–Aldrich, St. Louis, MO, United States). Plates were stained with iodine vapor, the spots corresponding to free and esterified cholesterol were scraped, and the lipids were eluted three times from the silica with chloroform:methanol:water (1:2:1). The lipids were extracted from the supernatants in chloroform, and the radioactivity was determined by scintillation counting.

Identification of the Hemolymphatic Cholesterol Carrier

In order to follow cholesterol association with hemolymphatic lipoproteins, 40 adult females were fed on ^{3}H-cholesterol-supplemented blood as described in Section "Absorption and Distribution of ^{3}H-Cholesterol Added to a Blood Meal," and 6–7 days later, hemolymph was collected in the presence of 0.15 M of NaCl, 5 mM of ethylenediamine tetraacetic acid (EDTA), and protease inhibitor cocktail (Sigma–Aldrich). The hemolymph pool was centrifuged at 12,000 × *g* for 5 min at 4°C to remove cells. KBr was added to the supernatant to a final concentration of 44.5% in PBS, and this solution (10 ml) was overlaid with 10 ml of 11% KBr in PBS (Pontes et al., 2002). This material was centrifuged at 159,000 × *g* for 20 h at 4°C, in a Beckman Coulter (Fullerton, CA, United States) 70 Ti rotor. The gradient was fractionated from the top to the bottom; and the radioactivity associated with 10 μl of each fraction was determined by scintillation counting. To remove the KBr from the gradient fractions, Sephadex G-50 (Sigma–Aldrich) spin columns (Penefsky, 1977) equilibrated with PBS were used. Fractions were analyzed by sodium dodecyl sulfate–polyacrylamide gel electrophoresis (SDS-PAGE) (6–22%) (Laemmli, 1970) and stained with Coomassie blue.

In vitro Lipophorin Labeling With ^{3}H-Cholesterol

To obtain a purified ^{3}H-cholesterol-labeled Lp, an *in vitro* labeling protocol was adapted from one described for human low-density lipoprotein (LDL) (Coppens et al., 1995). Hemolymph was collected from adult females 4–5 days after a blood meal, in the presence of 0.15 M of NaCl, 5 mM of EDTA, and protease inhibitor cocktail (Sigma–Aldrich). After centrifugation to remove cells, 100 μCi of ^{3}H-cholesterol (0.7 μg) was added to the supernatant (5 ml). This material was incubated for 16 h at 28°C. Then, the ^{3}H-cholesterol-containing hemolymph was subjected to a KBr ultracentrifugation gradient, as described in Section "Identification of the Hemolymphatic Cholesterol Carrier." The gradient was fractionated from top to bottom. The radioactivity present in 10 μl of each fraction was determined by scintillation counting. ^{3}H-Cholesterol-Lp was localized in fractions 1–4, which were pooled, extensively dialyzed against PBS, concentrated using Centricon® (Millipore, Bedford, MA, United States), and stored under liquid nitrogen until use.

To confirm the association of ^{3}H-cholesterol with Lp, an aliquot of pooled fractions 1–4 was subjected to a second KBr ultracentrifugation gradient, where KBr concentration was adjusted to 44.5% in PBS (5 ml), and it was overlaid with 5 ml of PBS (0–44.5% KBr gradient). This material was centrifuged as described in Section "Identification of the Hemolymphatic Cholesterol Carrier," in a 70.1 Ti rotor. The gradient was fractionated from the top in 500-μl fractions; the radioactivity and absorbance at 280 nm were determined in each one. The density of fractions was determined by the refractive index of KBr at 25°C. To identify the fractions where the ^{3}H-cholesterol alone (non-associated with proteins) would localize, 100 μCi of ^{3}H-cholesterol was mixed with nonradioactive cholesterol (20 μg), and the mixture was subjected to an identical KBr gradient (0–44.5%). The gradient was fractionated in the same way, and the radioactivity present in each fraction was determined by scintillation counting.

^{3}H-Cholesterol-Lipophorin Injection

On the third day after a blood meal, *R. prolixus* adult females were injected with 5 μl of ^{3}H-cholesterol-Lp (∼10^5 DPM) into the hemocoel, using a 10-μl syringe (Hamilton, Reno, NV, United States), and kept at 28 or 4°C. At different times, 5 μl of hemolymph, ovaries, and fat bodies were collected. After being washed, the organs were homogenized in 0.15 M of NaCl, and radioactivity associated with the samples was determined by scintillation counting. Results obtained for hemolymph

were also used for the determination of ^{3}H-cholesterol-Lp half-life in adult female hemolymph, as described elsewhere (Soulages and Wells, 1994a).

RESULTS

Rhodnius prolixus feeds solely on blood, and although cholesterol is present in blood in considerable amounts, there is no information about its midgut traffic and absorption during digestion. Hemipteran midgut is composed of the anterior midgut (or stomach), where the blood meal is stored and digestion initiates, and the posterior midgut (or intestine), where blood components are mostly digested and absorbed (Billingsley, 1990). In this way, in order to investigate cholesterol metabolism in this triatomine, adult females were fed on blood enriched with labeled cholesterol, ^{3}H-cholesterol; and radioactivity was chased in midgut tissue and luminal contents, on the days after the blood meal. The amount of ^{3}H-cholesterol in the luminal contents of the anterior midgut progressively decreased; and by the fifth day after feeding, it was significantly lower than on the first day. A very small amount of radiolabeled esterified cholesterol could be detected (**Figure 1A**). The anterior midgut cells absorbed cholesterol from the diet, although this lipid did not seem to accumulate in the organ. A significant amount of labeled esterified cholesterol was also detected in these intestinal cells (**Figure 1B**). In the posterior midgut luminal content, the amount of labeled cholesterol increased as ingested blood moved from the anterior to the posterior midgut, and it reached higher levels on the fifth day after feeding. Significant levels of labeled esterified cholesterol also appeared during this period (**Figure 1C**). The cells of the posterior midgut also absorbed blood cholesterol and the lipid accumulated in the free form; its amount was higher on the 10th day after feeding, whereas labeled esterified cholesterol amounts remained low and constant (**Figure 1D**).

Labeled free and esterified cholesterol reached the hemolymph on the first day after feeding. However, hemolymphatic radioactivity levels always remained low and without significant changes; again, most of the labeling was found in free cholesterol (**Figure 2**). To identify the proteins that bound circulating cholesterol, the hemolymph was subjected to a KBr density gradient, and as expected, cholesterol was mostly associated with Lp, on the top of the gradient (**Figure 3**).

In order to understand cholesterol distribution by Lp after the lipoprotein received it from the midgut, other organs were dissected from the ^{3}H-cholesterol-fed females on the days after the blood meal. Both the fat body and ovaries showed incorporated dietary cholesterol on the first day after feeding. In the fat body, this cholesterol accumulation was dynamic, with a peak of accumulation on the fifth day after feeding (**Figure 4A**). In the ovaries, cholesterol accumulation progressively increased, in accordance with ovarian growth during vitellogenesis, with

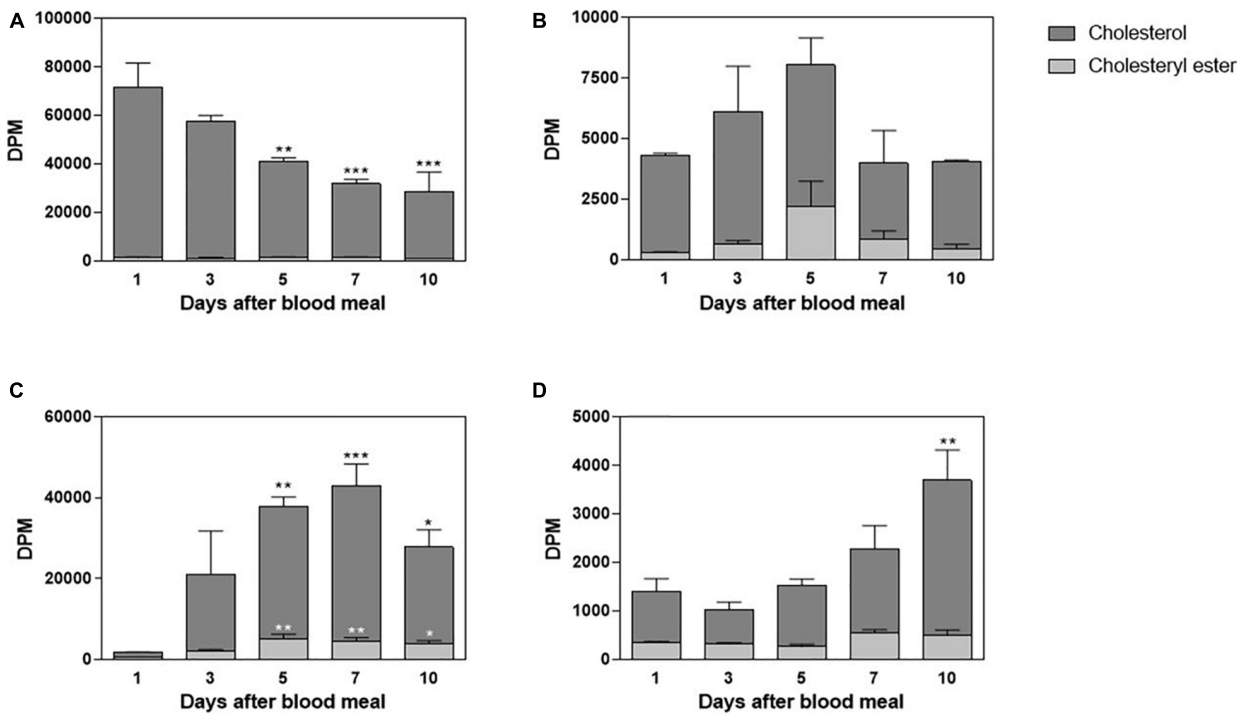

FIGURE 1 | Cholesterol absorption by the midgut. *Rhodnius prolixus* adult females were fed on ^{3}H-cholesterol-enriched blood and dissected on different days after the blood meal. Lipids from anterior midgut content **(A)** and tissue **(B)**, as well as from posterior midgut content **(C)** and tissue **(D)**, were extracted and analyzed by HPTLC. Radioactivity associated with free cholesterol (dark bars) and esterified cholesterol (light bars) was quantified and expressed as DPM/content or tissue ± SEM for three to four determinations. (*), (**), and (***): significantly different from day 1 after analysis by one-way ANOVA followed by Dunnett's posttest, $p < 0.05$, $p < 0.01$, and $p < 0.001$, respectively. HPTLC, high-performance thin-layer chromatography; DPM, disintegrations per minute.

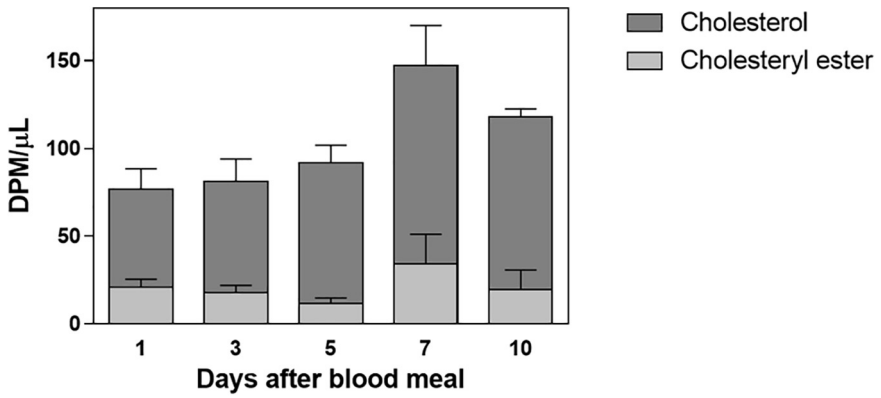

FIGURE 2 | Labeled cholesterol is found in the hemolymph after a blood meal. *Rhodnius prolixus* adult females were fed on ^{3}H-cholesterol-enriched blood, and on different days after the blood meal hemolymph was collected. Total lipids were extracted from the hemolymph and were analyzed by HPTLC. The radioactivity associated with free cholesterol (dark bars) and esterified cholesterol (light bars) was quantified and expressed as DPM/µl ± SEM for two to three determinations. $p > 0.05$ by one-way ANOVA. HPTLC, high-performance thin-layer chromatography; DPM, disintegrations per minute.

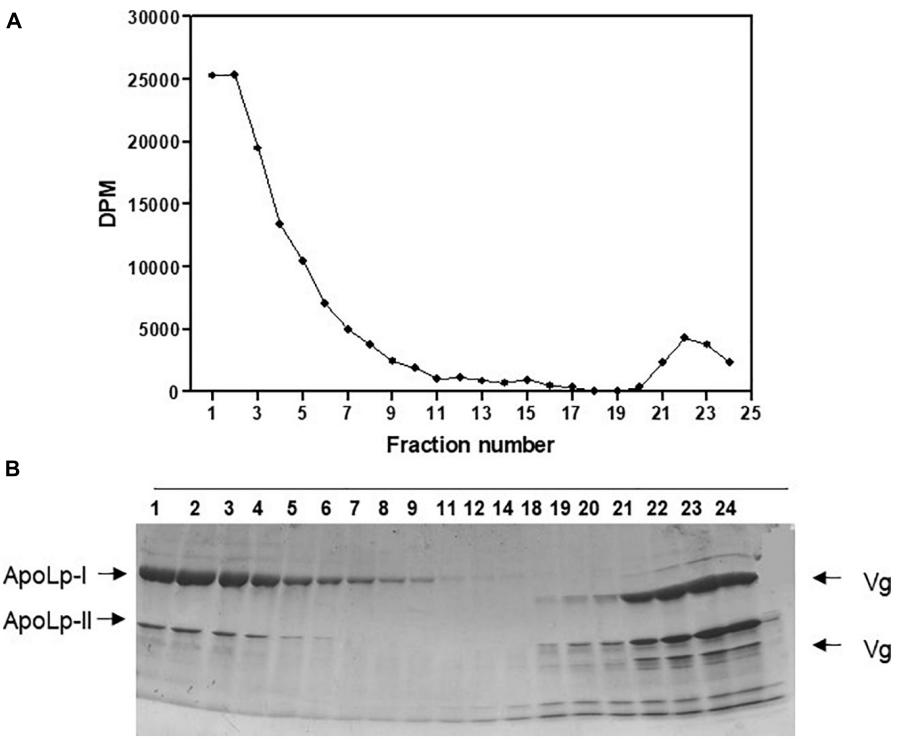

FIGURE 3 | Absorbed cholesterol associates with hemolymphatic lipophorin. *Rhodnius prolixus* adult females were fed on ^{3}H-cholesterol-enriched blood and on the sixth day after the blood meal hemolymph was collected and subjected to a density gradient ultracentrifugation. **(A)** Radioactivity present in gradient fractions was quantified and expressed as DPM/fraction. **(B)** Fractions were analyzed by SDS-PAGE (6–22%). Results shown are representative of four experiments. ApoLp-I, apolipophorin-I; ApoLp-II, apolipophorin-II; Vg, vitellogenin; DPM, disintegrations per minute; SDS-PAGE, sodium dodecyl sulfate–polyacrylamide gel electrophoresis.

higher levels of labeled lipid observed from the fifth to 10th days after feeding (**Figure 4B**). The esterified cholesterol was present in lower and constant proportions throughout the analyzed period in both organs.

Cholesterol absorption from the diet was not complete, and the insect feces contained a significant amount of labeled cholesterol (**Figure 5**). The presence of a small amount of the esterified lipid is noteworthy as well. Digestion in *R. prolixus* is very slow, and feces were present on the seventh and 10th days after feeding. Sometimes, there were feces on the fifth day, but this was not a general pattern, so we did not analyze fecal samples from the insects dissected at this day.

To investigate in more detail the cholesterol uptake by the organs, and to confirm that it was delivered by Lp, we established

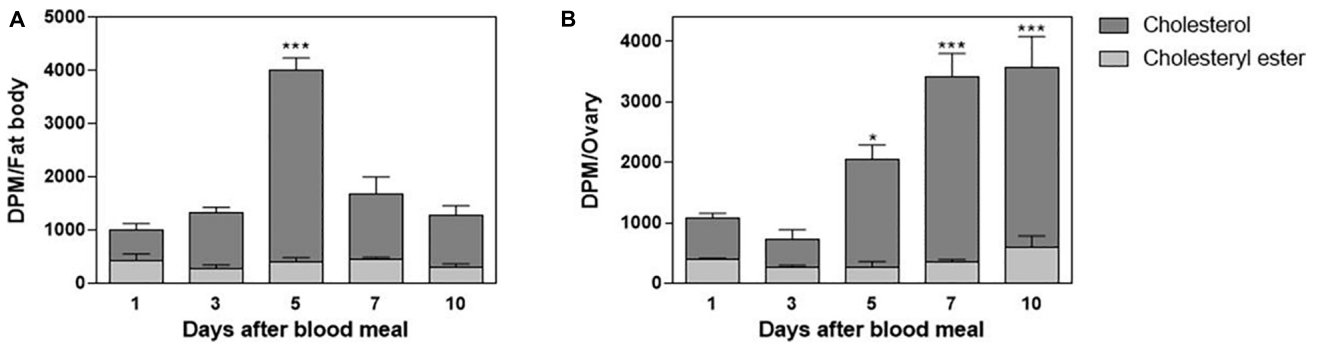

FIGURE 4 | The fat body and ovary incorporate cholesterol from the blood meal. *Rhodnius prolixus* adult females were fed on ^{3}H-cholesterol-enriched blood and dissected on different days after the blood meal. Total lipids from the fat body **(A)** or ovaries **(B)** were extracted and were analyzed by HPTLC. Radioactivity associated with free cholesterol (dark bars) and esterified cholesterol (light bars) was quantified and expressed as DPM/organ ± SEM for three to four determinations. (*) and (***): significantly different from 1 day after analysis by one-way ANOVA followed by Dunnett's posttest, $p < 0.05$ and $p < 0.001$, respectively. HPTLC, high-performance thin-layer chromatography; DPM, disintegrations per minute.

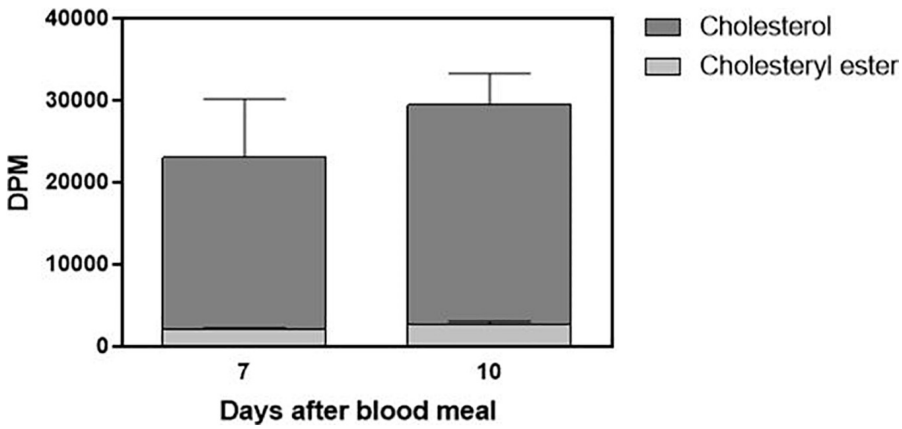

FIGURE 5 | Part of ingested cholesterol is excreted in feces. Feces (total amount produced after feeding) from *Rhodnius prolixus* adult females fed on ^{3}H-cholesterol-enriched blood were collected on the seventh and 10th days after the blood meal. Lipids were extracted from the feces and were analyzed by HPTLC. Radioactivity associated with free cholesterol (dark bars) and esterified cholesterol (light bars) was quantified and expressed as DPM/total feces ± SEM from three to four determinations. $p > 0.05$ by the Mann–Whitney test. HPTLC, high-performance thin-layer chromatography; DPM, disintegrations per minute.

a protocol for the *in vitro* association of ^{3}H-cholesterol with Lp. After incubation of the labeled lipid with non-radioactive hemolymph and analysis of the mixture by a KBr gradient, most of the radioactivity was present in the less dense fractions at the gradient top, where Lp was also located (**Figure 6A**). To verify whether the ^{3}H-cholesterol was associated with the lipoprotein, and not only floating on the gradient top, the four fractions from the top were pooled and analyzed on a second KBr gradient ultracentrifugation, where Lp located below the top, in accordance with its density as a high-density Lp (Coelho et al., 1997). The labeled cholesterol appeared associated with Lp, in the expected density range (**Figures 6B,C**). It is important to note that when ^{3}H-cholesterol was subjected to this same KBr gradient condition in the absence of Lp, it located on the lower-density fractions on the gradient top (**Figure 6D**).

The obtained purified radiolabeled Lp (fractions 1–4 of the 11–44.5% KBr gradient) was then injected into adult females on the third day after feeding. At this time point, the fat body was shown to synthesize and accumulate lipid stores very actively, and TAG contents are high; ovaries are rapidly growing, as oocytes are developing and accumulating yolk (Pontes et al., 2008; Santos et al., 2011). ^{3}H-Cholesterol was progressively cleared from the hemolymph, with a significant decrease after 3 h (**Figure 7A**) and a determined half-life of 5.5 ± 0.7 h. The fat body incorporated cholesterol rapidly, reaching maximal levels after 90 min (**Figure 7B**). Lp also transferred cholesterol to the ovaries, which reached maximal accumulation of radioactivity at 4 h 30 min after injection (**Figure 7C**). In both organs, radioactivity association was very fast and detected at the first time point (10 min), probably due to the binding of labeled Lp to cell surface, which is a very fast event (Gondim et al., 1989; Pontes et al., 2002; Entringer et al., 2013). As previously observed for diacylglycerol, phospholipids, and fatty acids (Gondim et al., 1989; Pontes et al., 2008; Santos et al., 2011), keeping the insects at 4°C inhibited cholesterol transfer from Lp to the tissues.

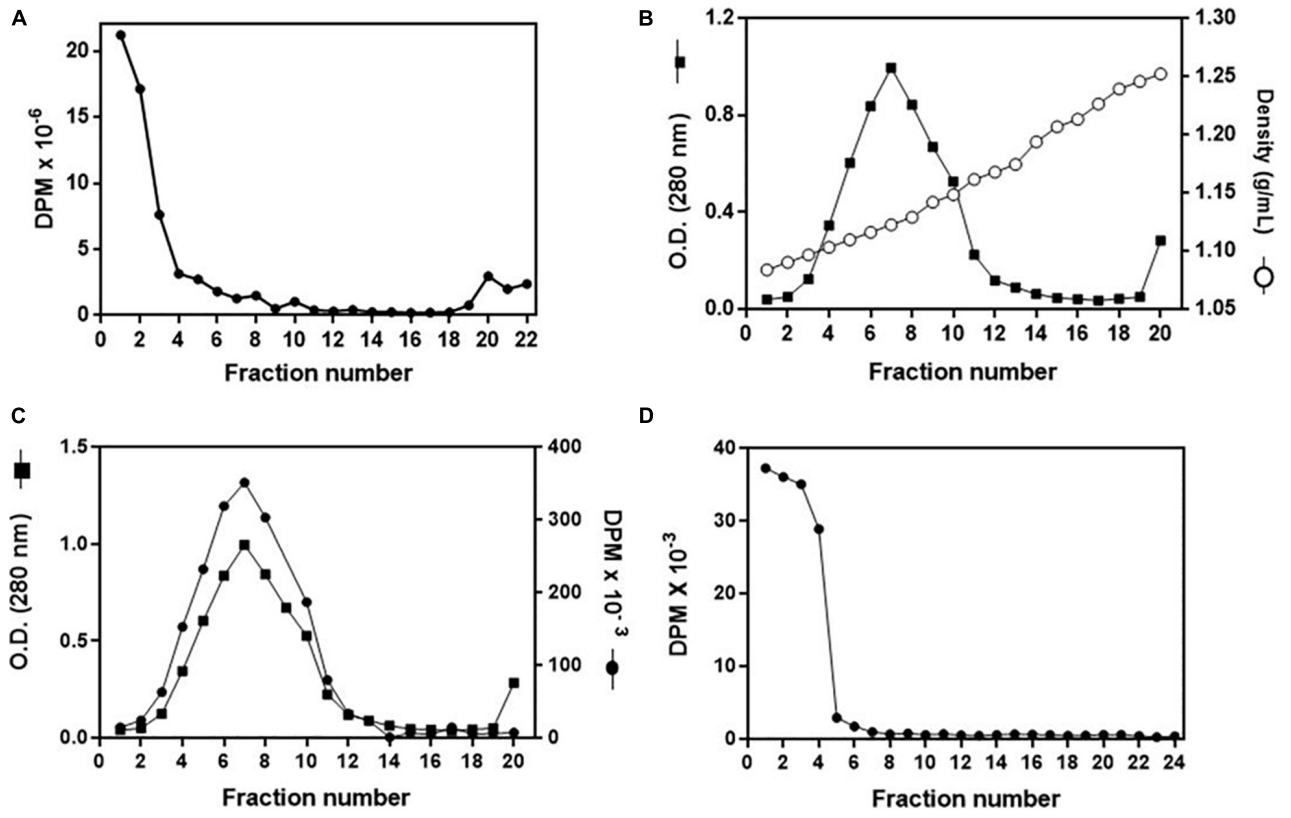

FIGURE 6 | Analysis of *in vitro* ^{3}H-cholesterol incorporation by lipophorin (Lp). **(A)** Non-radioactive hemolymph was incubated with ^{3}H-cholesterol for 16 h, and the mixture was analyzed by a KBr gradient ultracentrifugation (11–44.5% KBr). Radioactivity present in the gradient fractions was determined. **(B)** Fractions 1–3 from the gradient shown in **(A)** were pooled, and the sample was subjected to a second density gradient ultracentrifugation (0–44.5% KBr). The O.D. (280 nm) and density of each gradient fraction were determined. In **(C)**, values of O.D. are the same as in **(B)**, and the radioactivity present in each fraction was also determined. **(D)** ^{3}H-cholesterol (100 μCi + 20 μg non-radioactive cholesterol) was subjected to the same KBr gradient ultracentrifugation as in **(B,C)** in the absence of Lp, and the radioactivity present in the gradient fractions was determined. Results shown are representative of three experiments.

DISCUSSION

As in other insects already studied (Komnick and Giesa, 1994; Jouni et al., 2002b; Upadhyay et al., 2002), *R. prolixus* absorbed cholesterol from the diet, and this lipid accumulated in the fat body and ovaries, being associated with Lp in the hemolymph.

Our results showed that the anterior midgut absorbs cholesterol, as labeling could be found (in both free and esterified forms) in the tissue of this midgut portion. In hemipterans, the anterior midgut stores and concentrates the ingested blood and serves as a storage site for lipids (Billingsley, 1990). Generally, in triatomines, lipids are processed and absorbed in the posterior midgut (Rimoldi et al., 1985; Grillo et al., 2007), although in *P. megistus*, significant TAG digestion occurs in the anterior midgut (Canavoso et al., 2004a). Results from our group showed that the anterior midgut can also absorb free fatty acids present in blood (Majerowicz, unpublished results). These results indicate that the anterior midgut may have a more critical role in lipid metabolism than initially thought.

The presence of labeled esterified cholesterol in the midgut lumen is also an interesting finding. A simple hypothesis to explain this finding would be the presence of lecithin:cholesterol acyltransferase activity in the blood. This enzyme catalyzes the synthesis of esterified cholesterol and lysophosphatidylcholine from cholesterol and phosphatidylcholine (Ossoli et al., 2016), and it is present in the rabbit blood used for insect feeding (Carlucci et al., 2012). A recent proteomic analysis of *R. prolixus* midgut showed that enzymes involved with lipid utilization are highly expressed in this organ, confirming that it is very active in terms of lipid metabolism (Gumiel et al., 2020). Thus, an alternative explanation may be the excretion of esterified cholesterol synthesized by the intestinal cells. The intestines of *M. sexta* and *A. cyanea* esterify incorporated free cholesterol (Komnick and Giesa, 1994; Jouni et al., 2002b), and here, we showed that this is true for *R. prolixus* as well. In this way, the intestinal cells could excrete this esterified cholesterol back to the intestinal lumen. In mammals, two ATP-binding cassette transporters (ABCG5 and ABCG8) are responsible for this excretion activity (Patel et al., 2018). Orthologs of these genes are present in the genomes of moths, mosquitoes, and leafhoppers (Hull et al., 2014; Guo et al., 2015; Lu et al., 2016), but there is no information about their expression profile or biological activity. Future experiments of functional genomics in *R. prolixus* might help to investigate this hypothesis.

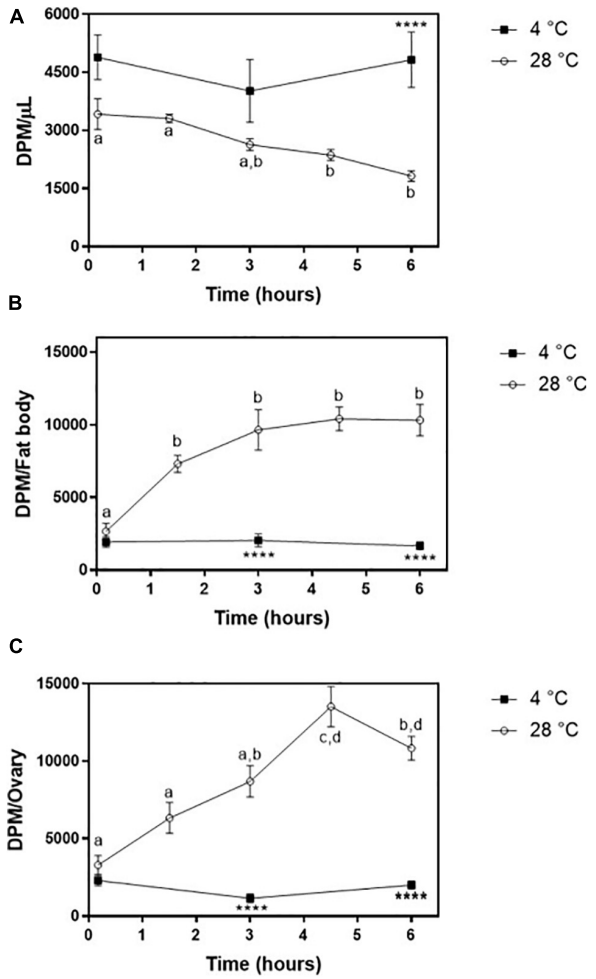

FIGURE 7 | Lipophorin transport of ^{3}H-cholesterol to the fat body and ovaries. *Rhodnius prolixus* adult females were injected with ^{3}H-cholesterol-Lp on the third day after the blood meal and maintained to 28°C (○) or 4°C (■). **(A)** At the indicated times, hemolymph was collected, and radioactivity was quantified and expressed as DPM/µl ± SEM for six to 12 determinations. The same insects were dissected, and fat body **(B)** and ovaries **(C)** were isolated. After homogenization, radioactivity in the organs was determined and expressed as DPM/organ ± SEM for 7–12 determinations. Different letters indicate statistical difference between the values of insects at 28°C by one-way ANOVA followed by Tukey's posttest. (****): significant difference between 4 and 28°C by two-way ANOVA followed by Sidak's multiple comparisons posttest, $p < 0.0001$. DPM, disintegrations per minute.

The observed increase in ^{3}H-cholesterol amount in posterior midgut tissue is possibly due to the incorporation of this lipid into newly synthesized microvillar and perimicrovillar membranes, where cholesterol seems to be abundant and important to maintain their spatial architecture (Albuquerque-Cunha et al., 2009).

Lipophorin transports cholesterol in the hemolymph, as expected, and the observed labeling ratio between free and esterified cholesterol reflects the ratio already described for *R. prolixus* Lp, which contains much smaller amounts of esterified cholesterol than of the free form (1.56 and 10.0% of total lipids, respectively) (Majerowicz et al., 2013). In the same way, in similar experiments where radioactive cholesterol was fed to the larvae of *M. sexta* and *A. cyanea*, in both cases, labeled cholesterol was found in the hemolymph in the free form, exclusively or almost. These results are in accordance with the fact that, unlike vertebrate lipoproteins, Lps of different insect species show a complete absence, or tiny amounts, of cholesterol esters (Soulages and Wells, 1994b; Majerowicz et al., 2013). The observed amount of labeled cholesterol in the hemolymph was always low despite its low decay rate in the hemolymph, as determined after injection of ^{3}H-cholesterol-labeled Lp.

Dietary cholesterol was incorporated by both the fat body and ovaries, but with different dynamics. In the fat body, the radioactivity levels peaked on the fifth day after feeding and on the seventh day had already returned to the initial levels. This profile indicated high uptake and outflow rates of cholesterol from the fat body. Accordingly, Lp binding to its receptors in the fat body membrane is maximal on the fifth day after feeding, and the uptake of fatty acids from the hemolymph by the fat body is also high around this time (Pontes et al., 2008). On the other hand, the delivery of phospholipids and diacylglycerol from the fat body to Lp is highest around the 10th day after feeding (Coelho et al., 1997). Since Lp also carries cholesterol, the dynamics of this transport can possibly follow a similar pattern as for other lipids. Interestingly, in other triatomines, the relative amounts of cholesterol in the fat body were constant during a long period after feeding, although the total lipid content varied (Canavoso et al., 1998), indicating that the cholesterol stock is dynamic and affected by the insect physiological condition. Most of fat body-incorporated cholesterol was in the free form, as observed for *M. sexta* larvae and pupae (Jouni et al., 2002b).

In the ovaries, cholesterol started to accumulate in the first day after feeding, and total incorporated radioactivity significantly increased at day 5. Differently from the fat body, cholesterol remained stored in the ovaries, as oocytes developed during this time. This is in accordance with the maternal origin of most of sterol content in embryos, accumulated during oogenesis (Jing and Behmer, 2020). The ovaries capture fatty acids, diacylglycerol, and phospholipids from Lp for oocyte growth during vitellogenesis (Gondim et al., 1989; Santos et al., 2011), and cholesterol is possibly simultaneously taken up. Similarly to the fat body, most of ^{3}H-cholesterol found in the ovaries was in the free form, unlike the observed in *M. sexta* oocytes, where the free and esterified forms were almost equally distributed (Jouni et al., 2002b). In *D. melanogaster*, high levels of esterified cholesterol were also found in early embryos (Guan et al., 2013).

Interestingly, the females did not absorb a great part of the labeled cholesterol added to the blood meal, which ended up excreted in feces. As insects are auxotrophic for cholesterol, we would expect high absorption efficiency. On the other hand, it is possible that, as the blood is very rich in cholesterol, it is more than enough to attend to the insects' demands, so that a significant part of the ingested cholesterol is not absorbed, with no impact on the insect physiology.

Both fat body and ovaries incorporated cholesterol associated with Lp with similar efficiency. However, incubation of insects at 4°C blocked this uptake, as also observed for other lipid classes,

as fatty acids, diacylglycerol, and phospholipids in *R. prolixus*, as well as for cholesterol in *M. sexta* (Gondim et al., 1989; Jouni et al., 2002a; Pontes et al., 2008; Santos et al., 2011), indicating that cholesterol incorporation by the organs depends on active metabolism and/or membrane properties. At 4°C, probably only Lp binding to cell surface occurred.

In summary, we showed here that *R. prolixus* adult females absorb cholesterol from the blood meal, that it is transferred to circulating Lp, and that it transports and delivers this lipid to the fat body and ovaries, where it is stored mostly as free cholesterol.

DATA AVAILABILITY STATEMENT

The raw data supporting the conclusions of this article will be made available by the authors, without undue reservation.

ETHICS STATEMENT

The animal study was reviewed and approved by the Committee for Evaluation of Animal Use for Research from the Universidade Federal do Rio de Janeiro, CEUA-UFRJ.

AUTHOR CONTRIBUTIONS

PE designed and conducted the experiments, analyzed the results, and revised the manuscript. DM analyzed the results and wrote the manuscript. KG designed the experiments and wrote the manuscript. All authors contributed to the article and approved the submitted version.

FUNDING

This work was supported by grants from Conselho Nacional de Desenvolvimento Científico e Tecnológico (CNPq), Fundação de Amparo à Pesquisa do Estado do Rio de Janeiro (FAPERJ), and Coordenação de Aperfeiçoamento de Pessoal de Nível Superior (CAPES; Finance Code 001). KG and DM are members of the Instituto Naciona de Ciência e Tecnologia em Entomologia Molecular (INCT-EM).

ACKNOWLEDGMENTS

We thank José de S. Lima Junior, Yan M. Araújo, and Mariana D. Martins for insect care.

REFERENCES

Albuquerque-Cunha, J. M., Gonzalez, M. S., Garcia, E. S., Mello, C. B., Azambuja, P., Almeida, J. C., et al. (2009). Cytochemical characterization of microvillar and perimicrovillar membranes in the posterior midgut epithelium of *Rhodnius prolixus*. *Arthropod. Struct. Dev.* 38, 31–44. doi: 10.1016/j.asd.2008.06.001

Alphonse, P. A., and Jones, P. J. (2016). Revisiting human cholesterol synthesis and absorption: the reciprocity paradigm and its key regulators. *Lipids* 51, 519–536. doi: 10.1007/s11745-015-4096-4097

Alves-Bezerra, M., and Gondim, K. C. (2012). Triacylglycerol biosynthesis occurs via the glycerol-3-phosphate pathway in the insect *Rhodnius prolixus*. *Biochim. Biophys. Acta Mol. Cell Biol. Lipids* 1821, 1462–1471. doi: 10.1016/j.bbalip.2012.08.002

Alves-Bezerra, M., Ramos, I. B., De Paula, I. F., Maya-Monteiro, C. M., Klett, E. L., Coleman, R. A., et al. (2017). Deficiency of glycerol-3-phosphate acyltransferase 1 decreases triacylglycerol storage and induces fatty acid oxidation in insect fat body. *Biochim. Biophys. Acta Mol. Cell Biol. Lipids* 1862, 324–336. doi: 10.1016/j.bbalip.2016.12.004

Atella, G. C., Silva-Neto, M. A. C., Golodne, D. M., Arefin, S., and Shahabuddin, M. (2006). Anopheles gambiae lipophorin: characterization and role in lipid transport to developing oocyte. *Insect. Biochem. Mol. Biol.* 36, 375–386. doi: 10.1016/j.ibmb.2006.01.019

Behmer, S. T., Elias, D. O., and Grebenok, R. J. (1999). Phytosterol metabolism and absorption in the generalist grasshopper, *Schistocerca americana* (Orthoptera: Acrididae). *Arch. Insect Biochem. Physiol.* 42, 13–25. doi: 10.1002/(sici)1520-6327(199909)42:1<13::aid-arch3>3.0.co;2-p

Behmer, S. T., and Grebenok, R. J. (1998). Impact of dietary sterols on life-history traits of a caterpillar. *Physiol. Entomol.* 23, 165–175. doi: 10.1046/j.1365-3032.1998.232074.x

Billingsley, P. F. (1990). The midgut ultrastructure of hematophagous insects. *Annu. Rev. Entomol.* 35, 219–248. doi: 10.1146/annurev.en.35.010190.001251

Blight, E. G., and Dyer, W. J. (1959). A rapid method of total lipid extraction and purification. *Can. J. Biochem. Physiol.* 37, 911–917. doi: 10.1139/o59-099

Canavoso, L. E., Bertello, L. E., de Lederkremer, R. M., and Rubiolo, E. R. (1998). Effect of fasting on the composition of the fat body lipid of Dipetalogaster maximus, Triatoma infestans and *Panstrongylus megistus* (Hemiptera: Reduviidae). *J. Comp. Physiol. B* 168, 549–554. doi: 10.1007/s003600050176

Canavoso, L. E., Frede, S., and Rubiolo, E. R. (2004a). Metabolic pathways for dietary lipids in the midgut of hematophagous *Panstrongylus megistus* (Hemiptera: Reduviidae). *Insect Biochem. Mol. Biol.* 34, 845–854. doi: 10.1016/j.ibmb.2004.05.008

Canavoso, L. E., Yun, H. K., Jouni, Z. E., and Wells, M. A. (2004b). Lipid transfer particle mediates the delivery of diacylglycerol from lipophorin to fat body in larval *Manduca sexta*. *J. Lipid Res.* 45, 456–465. doi: 10.1194/jlr.M300242-JLR200

Canavoso, L. E., and Wells, M. A. (2001). Role of lipid transfer particle in delivery of diacylglycerol from midgut to lipophorin in larval *Manduca sexta*. *Insect Biochem. Mol. Biol.* 31, 783–790. doi: 10.1016/s0965-1748(00)00183-1

Carlucci, A., Cigliano, L., Maresca, B., Spagnuolo, M. S., Di Salvo, G., Calabrò, R., et al. (2012). LCAT cholesterol esterification is associated with the increase of ApoE/ApoA-I ratio during atherosclerosis progression in rabbit. *J. Physiol. Biochem.* 68, 541–553. doi: 10.1007/s13105-012-0172-0

Chino, H., and Downer, R. G. H. (1982). Insect Hemolymph Lipophorin: a Mechanism of Lipid Transport in Insects. *Adv. Biophys.* 15, 67–92. doi: 10.1016/0065-227x(82)90005-3

Clark, A. J., and Block, K. (1959). The absence of sterol synthesis in insects. *J. Biol. Chem.* 234, 2578–2582. doi: 10.1016/s0021-9258(18)69741-8

Coelho, H. S. L., Atella, G. C., Moreira, M. F., Gondim, K. C., and Masuda, H. (1997). Lipophorin density variation during oogenesis in Rhodnius prolixus. *Arch. Insect Biochem. Physiol.* 35, 301–313. doi: 10.1002/(sici)1520-6327(199705)35:3<301::aid-arch4>3.0.co;2-w

Coppens, I., Levade, T., and Courtoy, P. J. (1995). Host plasma low density lipoprotein particles as an essential source of lipids for the bloodstream forms of Trypanosoma brucei. *J. Biol. Chem.* 270, 5736–5741. doi: 10.1074/jbc.270.11.5736

Dantuma, N. P., Pijnenburg, M. A., Diederen, J. H., and Van der Horst, D. J. (1997). Developmental down-regulation of receptor-mediated endocytosis of an insect lipoprotein. *J. Lipid Res.* 38, 254–265. doi: 10.1016/s0022-2275(20)37438-1

de Fuentes-Vicente, J. A., Gutiérrez-Cabrera, A. E., Flores-Villegas, A. L., Lowenberger, C., Benelli, G., Salazar-Schettino, P. M., et al. (2018). What makes an effective Chagas disease vector? Factors underlying *Trypanosoma cruzi-triatomine* interactions. *Acta Trop.* 183, 23–31. doi: 10.1016/j.actatropica.2018.04.008

Entringer, P. F., Grillo, L. A. M., Pontes, E. G., Machado, E. A., and Gondim, K. C. (2013). Interaction of lipophorin with *Rhodnius prolixus* oocytes: biochemical

properties and the importance of blood feeding. *Mem. Inst. Oswaldo Cruz* 108, 836–844. doi: 10.1590/0074-0276130129

Garcia, E. S., Maracarine, J. D., Garcia, M. L. M., and Ubatuba, F. B. (1975). Alimentação do Rhodnius prolixus no laboratório. *Acad. Bras. Cienc.* 47, 539–545.

Gondim, K. C., Atella, G. C., Pontes, E. G., and Majerowicz, D. (2018). Lipid metabolism in insect disease vectors. *Insect Biochem. Mol. Biol.* 101, 108–123. doi: 10.1016/j.ibmb.2018.08.005

Gondim, K. C., Oliveira, P. L., and Masuda, H. (1989). Lipophorin and oogenesis in Rhodnius prolixus: transfer of phospholipids. *J. Insect Physiol.* 35, 19–27. doi: 10.1016/0022-1910(89)90032-2

Gondim, K. C., and Wells, M. A. (2000). Characterization of lipophorin binding to the midgut of larval Manduca sexta. *Insect Biochem. Mol. Biol.* 30, 405–413. doi: 10.1016/S0965-1748(00)00014-X

Grillo, L. A., Majerowicz, D., and Gondim, K. C. (2007). Lipid metabolism in *Rhodnius prolixus* (Hemiptera: Reduviidae): role of a midgut triacylglycerol-lipase. *Insect Biochem. Mol. Biol.* 37, 579–588. doi: 10.1016/j.ibmb.2007.03.002

Grillo, L. A. M., Pontes, E. G., and Gondim, K. C. (2003). Lipophorin interaction with the midgut of *Rhodnius prolixus*: characterization and changes in binding capacity. *Insect Biochem. Mol. Biol.* 33, 429–438. doi: 10.1016/S0965-1748(03)00007-9

Guan, X. L., Cestra, G., Shui, G., Kuhrs, A., Schittenhelm, R. B., Hafen, E., et al. (2013). Biochemical membrane lipidomics during *Drosophila* development. *Dev. Cell* 24, 98–111. doi: 10.1016/j.devcel.2012.11.012

Gumiel, M., de Mattos, D. P., Vieira, C. S., Moraes, C. S., Moreira, C. J. C., Gonzalez, M. S., et al. (2020). Proteome of the triatomine digestive tract: from catalytic to immune pathways; focusing on annexin expression. *Front. Mol. Biosci. Dec.* 7:589435. doi: 10.3389/fmolb.2020.589435

Guo, X. R., Zheng, S. C., Liu, L., and Feng, Q. L. (2009). The sterol carrier protein 2/3-oxoacyl-CoA thiolase (SCPx) is involved in cholesterol uptake in the midgut of *Spodoptera litura*: gene cloning, expression, localization and functional analyses. *BMC Mol. Biol.* 10:102. doi: 10.1186/1471-2199-10-102

Guo, Z., Kang, S., Zhu, X., Xia, J., Wu, Q., Wang, S., et al. (2015). The novel ABC transporter ABCH1 is a potential target for RNAi-based insect pest control and resistance management. *Sci. Rep.* 5:13728. doi: 10.1038/srep13728

Hull, J. J., Chaney, K., Geib, S. M., Fabrick, J. A., Brent, C. S., Walsh, D., et al. (2014). Transcriptome-based identification of ABC transporters in the western tarnished plant bug *Lygus hesperus*. *PLoS One* 9:e113046. doi: 10.1371/journal.pone.0113046

Jing, X., and Behmer, S. T. (2020). Insect sterol nutrition: physiological mechanisms. *Ecology, and Applications. Annu. Rev. Entomol.* 65, 251–271. doi: 10.1146/annurev-ento-011019-025017

Jouni, Z. E., Takada, N., Gazard, J., Maekawa, H., Wells, M. A., and Tsuchida, K. (2003). Transfer of cholesterol and diacylglycerol from lipophorin to *Bombyx mori* ovarioles in vitro: role of the lipid transfer particle. *Insect Biochem. Mol. Biol.* 33, 145–153. doi: 10.1016/s0965-1748(02)00102-9

Jouni, Z. E., Yun, H. K., and Wells, M. A. (2002a). Cholesterol efflux from larval Manduca sexta fat body in vitro: high-density lipophorin as the acceptor. *J. Insect Physiol.* 48, 609–618. doi: 10.1016/s0022-1910(02)00081-1

Jouni, Z. E., Zamora, J., and Wells, M. A. (2002b). Absorption and tissue distribution of cholesterol in *Manduca sexta*. *Arch. Insect Biochem. Physiol.* 49, 167–175. doi: 10.1002/arch.10017

Kawooya, J. K., and Law, J. H. (1988). Role of lipophorin in lipid transport to the insect egg. *J. Biol. Chem.* 263, 8748–8753. doi: 10.1016/s0021-9258(18)68369-3

Kim, M. S., and Lan, Q. (2010). Sterol carrier protein-x gene and effects of sterol carrier protein-2 inhibitors on lipid uptake in *Manduca sexta*. *BMC Physiol.* 10:9. doi: 10.1186/1472-6793-10-9

Komnick, H., and Giesa, U. (1994). Intestinal absorption of cholesterol, transport in the hemolymph, and incorporation into the fat body and *Malpighian tubules* of the larval dragonfly *Aeshna cyanea*. *Comp. Biochem. Physiol. Comp. Physiol.* 107, 553–557. doi: 10.1016/0300-9629(94)90039-6

Komnick, H., and Wachtmann, D. (1994). Assimilation and esterification of dietary fatty alcohol by the nymphal dragonfly. Aeshna-Cyanea. *Insect Biochem. Mol. Biol.* 24, 319–328. doi: 10.1016/0965-1748(94)90012-4

Laemmli, U. K. (1970). Cleavage of structural proteins during the assembly of the head of bacteriophage T4. *Nature* 227, 680–685. doi: 10.1038/227680a0

Lan, Q., and Wessely, V. (2004). Expression of a sterol carrier protein-x gene in the yellow fever mosquito. *Aedes aegypti*. *Insect Mol. Biol.* 13, 519–529. doi: 10.1111/j.0962-1075.2004.00510.x

Li, S., and Jing, X. (2020). Fates of dietary sterols in the insect alimentary canal. *Curr. Opin. Insect Sci.* 41, 106–111. doi: 10.1016/j.cois.2020.08.001

Lu, H., Xu, Y., and Cui, F. (2016). Phylogenetic analysis of the ATP-binding cassette transporter family in three mosquito species. *Pestic. Biochem. Physiol.* 132, 118–124. doi: 10.1016/j.pestbp.2015.11.006

Majerowicz, D., Cezimbra, M. P., Alves-Bezerra, M., Entringer, P. F., Atella, G. C., Sola-Penna, M., et al. (2013). Rhodnius prolixus lipophorin: lipid composition and effect of high temperature on physiological role. *Arch. Insect Biochem. Physiol.* 82, 129–140. doi: 10.1002/arch.21080

Nunes-da-Fonseca, R., Berni, M., Tobias-Santos, V., Pane, A., and Araujo, H. M. (2017). *Rhodnius prolixus*: from classical physiology to modern developmental biology. *Genesis* 55:e22995. doi: 10.1002/dvg.22995

Ossoli, A., Pavanello, C., and Calabresi, L. (2016). High-Density lipoprotein, lecithin: cholesterol acyltransferase, and atherosclerosis. *Endocrinol. Metab. (Seoul, Korea)* 31, 223–229. doi: 10.3803/enm.2016.31.2.223

Patel, S. B., Graf, G. A., and Temel, R. E. (2018). ABCG5 and ABCG8: more than a defense against xenosterols. *J. Lipid Res.* 59, 1103–1113. doi: 10.1194/jlr.r084244

Penefsky, H. S. (1977). Reversible binding of Pi by beef heart mitochondrial adenosine triphosphatase. *J. Biol. Chem.* 252, 2891–2899. doi: 10.1016/s0021-9258(17)40446-7

Pontes, E. G., Grillo, L. A. M., and Gondim, K. C. (2002). Characterization of lipophorin binding to the fat body of *Rhodnius prolixus*. *Insect Biochem. Mol. Biol.* 32, 1409–1417. doi: 10.1016/S0965-1748(02)00061-69

Pontes, E. G., Leite, P., Majerowicz, D., Atella, G. C., and Gondim, K. C. (2008). Dynamics of lipid accumulation by the fat body of *Rhodnius prolixus*: the involvement of lipophorin binding sites. *J. Insect Physiol.* 54, 790–797. doi: 10.1016/j.jinsphys.2008.02.003

Qu, Z., Kenny, N. J., Lam, H. M., Chan, T. F., Chu, K. H., Bendena, W. G., et al. (2015). How did arthropod sesquiterpenoids and ecdysteroids arise? comparison of hormonal pathway genes in noninsect arthropod genomes. *Genome Biol. Evol.* 7, 1951–1959. doi: 10.1093/gbe/evv120

Rimoldi, O. J., Peluffo, R. O., González, S. M., and Brenner, R. R. (1985). Lipid digestion, absorption and transport in *Triatoma infestans*. *Comp. Biochem. Physiol.* 82, 187–190. doi: 10.1016/0305-0491(85)90150-6

Santos, R., Rosas-Oliveira, R., Saraiva, F. B., Majerowicz, D., and Gondim, K. C. (2011). Lipid accumulation and utilization by oocytes and eggs of *Rhodnius prolixus*. *Arch. Insect Biochem. Physiol.* 77, 1–16. doi: 10.1002/arch.20414

Sieber, M. H., and Thummel, C. S. (2012). Coordination of triacylglycerol and cholesterol homeostasis by DHR96 and the *Drosophila* lipA homolog magro. *Cell Metab.* 15, 122–127. doi: 10.1016/j.cmet.2011.11.011

Soulages, J. L., and Wells, M. A. (1994a). Metabolic fate and turnover rate of hemolymph free fatty acids in adult Manduca sexta. *Insect Biochem. Mol. Biol.* 24, 79–86. doi: 10.1016/0965-1748(94)90125-2

Soulages, J. L., and Wells, M. A. (1994b). Lipophorin: the structure of an insect lipoprotein and its role in lipid transport in insects. *Adv. Protein Chem.* 45, 371–415. doi: 10.1016/s0065-3233(08)60644-0

Upadhyay, R. K., Agarwal, H. C., and Dhar, R. (2002). Protein mediated cholesterol absorption in locusts *Schistocerca gregaria* (Forskal) and *Locusta migratoria* (Linn). *Ind. J. Exp. Biol.* 40, 151–161.

Voght, S. P., Fluegel, M. L., Andrews, L. A., and Pallanck, L. J. (2007). Drosophila NPC1b promotes an early step in sterol absorption from the midgut epithelium. *Cell Metab.* 5, 195–205. doi: 10.1016/j.cmet.2007.01.011

Yang, S. T., Kreutzberger, A. J. B., Lee, J., Kiessling, V., and Tamm, L. K. (2016). The role of cholesterol in membrane fusion. *Chem. Phys. Lipids* 199, 136–143. doi: 10.1016/j.chemphyslip.2016.05.003

Yun, H. K., Jouni, Z. E., and Wells, M. A. (2002). Characterization of cholesterol transport from midgut to fat body in *Manduca sexta* larvae. *Insect Biochem. Mol. Biol.* 32, 1151–1158. doi: 10.1016/s0965-1748(02)00051-6

Conflict of Interest: The authors declare that the research was conducted in the absence of any commercial or financial relationships that could be construed as a potential conflict of interest.

Advantages of publishing in Frontiers

OPEN ACCESS
Articles are free to read for greatest visibility and readership

FAST PUBLICATION
Around 90 days from submission to decision

HIGH QUALITY PEER-REVIEW
Rigorous, collaborative, and constructive peer-review

TRANSPARENT PEER-REVIEW
Editors and reviewers acknowledged by name on published articles

Frontiers
Avenue du Tribunal-Fédéral 34
1005 Lausanne | Switzerland

Visit us: www.frontiersin.org
Contact us: frontiersin.org/about/contact

REPRODUCIBILITY OF RESEARCH
Support open data and methods to enhance research reproducibility

DIGITAL PUBLISHING
Articles designed for optimal readership across devices

FOLLOW US
@frontiersin

IMPACT METRICS
Advanced article metrics track visibility across digital media

EXTENSIVE PROMOTION
Marketing and promotion of impactful research

LOOP RESEARCH NETWORK
Our network increases your article's readership